ECHOCARDIOGRAPHIC DEFORMATION CHARACTERISTICS IN ARRHYTHMOGENIC RIGHT VENTRICULAR CARDIOMYOPATHY

Thomas P. Mast

Financial support by the Dutch Heart Foundation for the publication of this thesis is gratefully acknowledged.

Financial support by **Corridor Care BV**, Chipsoft BV, St. Jude Medical Nederland BV, and Stichting Cardiovasculaire Biologie is gratefully acknowledged.

Cover: Bastiaan Mast & Koos Dekker
Lay-out: Gildeprint
ISBN: 978-94-6233-525-7

©T.P. Mast 2016

ECHOCARDIOGRAPHIC DEFORMATION CHARACTERISTICS IN ARRHYTHMOGENIC RIGHT VENTRICULAR CARDIOMYOPATHY

ECHOCARDIOGRAFISCHE DEFORMATIE KARAKTERISTIEKEN IN ARITMOGENE RECHTER VENTRIKEL CARDIOMYOPATHIE
(met een samenvatting in het Nederlands)

Proefschrift

ter verkrijging van de graad van doctor aan de Universiteit Utrecht op gezag van de rector magnificus, prof. dr. G.J. van der Zwaan, ingevolge het besluit van het college voor promoties in het openbaar te verdedigen op donderdag 2 februari 2017 des ochtends 10.30

door

Thomas Pieter Mast

geboren op 26 september 1986
te Utrecht

Promotor:	Prof. dr. P.A.F.M. Doevendans
Copromotoren:	Dr. M.J.M. Cramer
	Dr. A.J. Teske

Beoordelingscommissie: Prof. dr. F.W. Asselbergs
Prof. dr. M.P. van den Berg
Prof. dr. S.A.J. Chamuleau
Prof. dr. T. Leiner
Prof. dr. M.A. Vos

CONTENTS

INTRODUCTION

Chapter 1. **General Introduction and Thesis Outline** **9**

PART I **CURRENT AND FUTURE ROLE OF ECHOCARDIOGRAPHY IN ARVC**

Chapter 2. **Current and Future Role of Echocardiography in Arrhythmogenic Right Ventricular Dysplasia/Cardiomyopathy** **25**
Cardiol J. 2015;22(4):362-74 & book chapter: A. Abidov, I.B. Oliva, F.I. Marcus (editors). Cardiac MRI in the Diagnosis, Clinical Management, and Prognosis of Arrhythmogenic Right Ventricular Cardiomyopathy/Dysplasia. Elsevier 2016

PART II **THE ONGOING QUEST FOR EARLY DISEASE DETECTION IN ARVC**

Chapter 3. **Prolonged Electromechanical Interval Unmasks Arrhythmogenic Right Ventricular Dysplasia/Cardiomyopathy in the Subclinical stage** **49**
J Cardiovasc Electrophysiol. 2016 Mar;27(3):303-14

Chapter 4. **Right Ventricular Imaging and Computer Simulation for Electromechanical Substrate Characterization in Arrhythmogenic Right Ventricular Cardiomyopathy** **75**
J Am Coll Cardiol. 2016;68(20):2185-2197

Chapter 5. **Optimizing Family Screening Protocols: The Additional Value of Right Ventricle Deformation Imaging to Predict Disease Progression in Early Arrhythmogenic Right Ventricular Cardiomyopathy** **105**
Submitted

Chapter 6. **Left Ventricular Involvement in Arrhythmogenic Right Ventricular Dysplasia/Cardiomyopathy Assessed by Echocardiography Predicts AdverseClinical Outcome** **127**
J Am Soc Echocardiogr. 2015 Sep;28(9):1103-13

PART III **TOWARDS OPTIMAL ASSESSMENT OF STRUCTURAL DISEASE PROGRESSION IN ARVC**

Chapter 7. **Evaluation of Structural Progression in Arrhythmogenic Right Ventricular Dysplasia/Cardiomyopathy** **157**
JAMA Cardiol. In press 2017

Chapter 8. **Implementation of Echocardiographic Deformation Imaging for Optimal Assessment of Structural Disease Progression in Early ARVC** **177**
Submitted

DISCUSSION

Chapter 9. **Moving from multimodality diagnostic tests towards multimodality risk stratification in ARVC** **197**
JACC Cardiovasc Imaging. 2016 Oct 14

Chapter 10. **General discussion and Future Perspectives** **205**

APPENDIX

Nederlandse samenvatting 223
Contributing Authors 227
Curriculum Vitae 231
List of Publications 233
Dankwoord / Acknowledgments 235

CHAPTER 1

General Introduction and Thesis Outline

R1
R2
R3
R4
R5
R6
R7
R8
R9
R10
R11
R12
R13
R14
R15
R16
R17
R18
R19
R20
R21
R22
R23
R24
R25
R26
R27
R28
R29
R30
R31
R32
R33
R34
R35
R36
R37
R38
R39

R1 R2 R3 R4 R5 R6 R7 R8 R9 R10 R11 R12 R13 R14 R15 R16 R17 R18 R19 R20 R21 R22 R23 R24 R25 R26 R27 R28 R29 R30 R31 R32 R33 R34 R35 R36 R37 R38 R39

ARVC: Pathophysiology, Diagnosis, and Treatment Options

Arrhythmogenic right ventricular cardiomyopathy (ARVC) is a heart muscle disease which is clinically characterized by ventricular arrhythmias and right ventricular (RV) dysfunction.[1] Although ARVC is a relatively uncommon disorder, with an estimated prevalence of approximately 1:5000, it is recognized as an important cause of sudden cardiac death (SCD) among young people and athlethes.[2] The pathological hallmark of this disorder is classically described as fibro-fatty replacement of primarily the RV myocardium.[3] Since the first comprehensive description by Marcus *et al.* in 1982[1] remarkable progress has been made in the understanding of multiple aspects of this disease. A major breakthrough was the discovery that Naxos disease (a cardiocutaneous disorder) is caused by a plakoglobin deletion, which linked ARVC to desmosomal dysfunction.[4,5] The desmosome is a complex cell structure within the intercalated disc and plays an important role in maintaining mechanical integrity of myocardial cell-cell junctions (**Figure 1**).[6] Pathogenic mutation in genes encoding for desmosomal proteins are responsible for desmosomal dysfunction and causes disruptive myocardial cell-cell contact.[6]

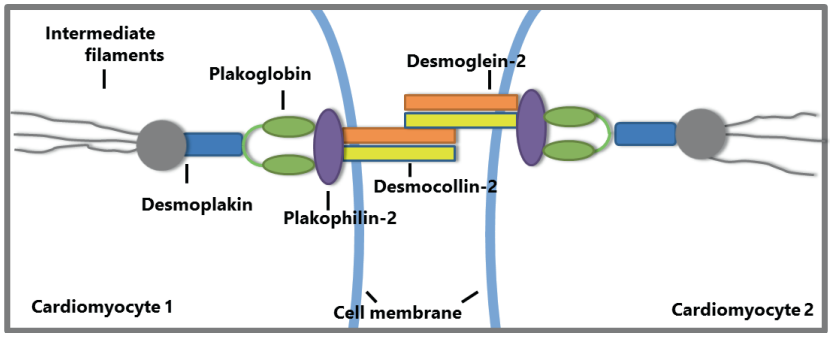

Figure 1. The cardiac desmosome
The cardiac desmosome provides mechanical cell-cell contact by connecting the cytoskeletons between cardiac myocytes.

This process is associated with myocardial cell-death that will eventually lead to fibro-fatty replacements of the myocardium.[3] In addition, the desmosome is known to interact with gap junctions and the sodium channel complex within the intercalated disc.[7,8] Therefore, the desmosomal dysfunction in ARVC causes cardiac abnormalities of both structural and electrical origin.[6,9] Although non-desmosomal and gene-elusive variants are also recognized in ARVC, pathogenic desmosomal mutations are currently found in the majority of ARVC index patients (approximately 60%), most commonly in the gene encoding for Plakophillin-2 protein (*PKP2*).[10-12]

Patients with ARVC usually present with symptoms due to a ventricular tachycardia (VT) originating from the RV between the second and fourth decade of live.[5,10] Sudden cardiac death (SCD) or aborted SCD is seen in approximately 10% of the index patients at presentation.[10] ARVC diagnosis remains a clinical challenge due to high variability of disease expression within and between families.[13] In 1994 and 2010, an international Task Force proposed a diagnostic guideline, the Task Force criteria (TFC), to standardize the diagnosis of ARVC.[14] The 1994 criteria relied solely on qualitative parameters, especially the non-invasive imaging criteria, and was consequently characterized by high specificity and low sensitivity.[15-17] Although the sensitivity increased after the modification in 2010, frequent false negatives findings still complicate early diagnosis in ARVC.[14,18-20] Therefore, early diagnosis is still one of the clinical challenges in ARVC. TFC encompasses a set of major and minor disease criteria defined on different subsets of disease expressions: 1) structural abnormalities by cardiac imaging, 2) tissue characterizations derived by endomyocardial biopsy, 3) depolarization abnormalities by electrocardiography (ECG), 4) repolarization abnormalities by ECG, 5) ventricular arrhythmias, and 6) family history of ARVC or presence of an ARVC related pathogenic mutation. **Table 1** shows the complete overview of the current 2010 TFC.

Table 1. 2010 Task Force criteria proposed by Marcus *et al.*[14]

Global or regional dysfunction and structural alterations	
2D-echo Major	Presence of a regional RV akinesia, dyskinesia, or aneurysm **and** 1 of the following (end-diastole): - PLAX RVOT ≥ 32 mm (corrected for BSA: PLAX RVOT/BSA ≥ 19 mm/m^2) **or** - PSAX RVOT ≥ 36 mm (corrected for BSA: PLAX RVOT/BSA ≥ 21 mm/m^2) **or** - RV-FAC ≤ 33%
Minor	Presence of a regional RV akinesia, dyskinesia, or aneurysm **and** 1 of the following (end-diastole): - PLAX RVOT ≥29 to < 32 mm (corrected for BSA: PLAX RVOT/BSA ≥16 to < 19 mm/m^2) **or** - PSAX RVOT ≥ 32 to < 36 mm (corrected for BSA: PSAX RVOT ≥ 18 to < 21 mm/m^2) **or** - RV-FAC > 33% to ≤ 40%
MRI Major	Presence of a regional RV akinesia or dyskinesia, or dyssynchronous RV contraction **and** 1 of the following: - Ratio of RV-EDV to BSA ≥ 110 ml/m^2 (male) ≥ 100 ml/m^2 (female) **or** - RVEF ≤ 40%
Minor	Presence of a regional RV akinesia or dyskinesia, or dyssynchronous RV contraction **and** 1 of the following: - Ratio of RV-EDV to BSA ≥100 < 110 ml/m^2 (male) ≥ 90 to < 100 ml/m^2 (female) **or** - RVEF > 40% ≤ 45%
RV angiography Major	Presence of regional RV akinesia, dyskinesia, or aneurysm
Tissue characterization	
Major	Residual myocytes < 60% by morphometric analysis (or < 50% if estimated), with fibrous replacement of the RV free wall myocardium in ≥1 sample, with or without fatty replacement of tissue on endomyocardial biopsy

Minor	Residual myocytes 60-75% by morphometric analysis (or 50% to 65% if estimated), with fibrous replacement of the RV free wall myocardium in ≥1 sample, with or without fatty replacement of tissue on endomyocardial biopsy
Depolarization abnormalities (ECG)	
Major	Epsilon wave (reproducible low-amplitude signals between end of QRS complex to onset of the T wave) in the right precordial leads (V_1-V_3)
Minor	Late potentials by SA-ECG in ≥ 1 of 3 parameters in the absence of a QRS duration of 110 ms on the standard ECG • Filtered QRS duration (fQRS) ≥ 114 ms • Duration of terminal QRS < 40 µV (low-amplitude signal duration) ≥ 38 ms • Root-mean-square voltage of terminal 40 ms ≤ 20 µV
Minor	Terminal activation duration of QRS ≥ 55 ms measured from the nadir of the S wave to the end of the QRS, including R', in V_1, V_2, or V_3, in the absence of complete RBBB
Repolarization abnormalities (ECG)	
Major	Inverted T waves in right precordial leads (V_1, V_2, and V_3) or beyond in individuals >14 years of age (in the absence of complete RBBB QRS ≥ 120 ms)
Minor	Inverted T waves in leads V_1 and V_2 in individuals >14 years of age (in the absence of complete RBBB) **or** Inverted T waves in leads in V_4-V_6 **or** Inverted T waves in leads V_1,-V_4 in individuals >14 years of age in the presence of complete RBBB
Ventricular arrhythmias	
Major	Nonsustained or sustained ventricular tachycardia of LBBB morphology with superior axis (negative or indeterminate QRS in leads II, III, and aVF and positive in lead aVL)
Minor	Nonsustained or sustained ventricular tachycardia of RV outflow configuration, LBBB morphology with inferior axis (positive QRS in leads II, III, and aVF and negative in lead aVL) **or** of unknown axis
Minor	>500 premature ventricular complexes/ 24 hours (Holter)
Family history	
Major	ARVC definite diagnosis confirmed in a first-degree relative who meets current 2010 Task Force criteria
Major	ARVC definite diagnosis confirmed pathologically at autopsy or surgery in a first-degree relative
Major	Identification of a pathogenic ARVC related mutation categorized as associated or probably associated with ARVC. Plakoglobin (*JUP*), Desmoplakin (*DSP*), Plakophilin-2 (*PKP2*), Desmoglein-2 (*DSG2*), Desmocollin-2 (*DSC2*), transforming growth factor beta-3 (*TGFβ3*), and transmembrane protein 43 (*TMEM43)*
Minor	History of ARVC in a first-degree relative in whom it is not possible or practical to determine whether the family member meets current Task Force criteria
Minor	ARVC confirmed pathologically or by current Task Force Criteria in second-degree relative
Minor	Premature sudden death (35 years of age) due to suspected ARVC/D in a first-degree relative

Definite ARVC diagnosis is fulfilled by the presence of 2 major, or 1 major plus 2 minor criteria, or 4 minor criteria from different subsets of criteria. *Abbreviations*: ARVC = arrhythmogenic right ventricular cardiomyopathy; ECG = electrocardiography; PLAX/PSAX = parasternal long/short axis view; RVOT = RV outflow tract; BSA = body surface area; RBBB/LBBB = right/left bundle branch block.

Therapeutic strategies of ARVC are predominantly focused on preventing both sustained ventricular arrhythmias and SCD. In approximately 75% of the ARVC index patients, a sustained ventricular arrhythmia was observed during 7 years of follow-up.[10] Therefore, the cornerstone of the management of ARVC patients is to prevent the incidence of potentially life-threatening ventricular arrhythmias.[21] The most invasive therapeutic strategy is the implantable cardioverter defibrillator (ICD) to intervene during episodes of sustained ventricular arrhythmia.[22] Several studies showed the importance of ICDs in ARVC, since 50-70% of the patients received appropriate ICD therapy during a mean follow-up period of 5–7 years.[23,24] Therefore, ICDs are recommended in ARVC patients by the current guideline on treatment in ARVC in case they already suffered from a hemodynamically unstable sustained ventricular arrhythmia, and in ARVC patients with severe systolic dysfunction.[21] In addition, ICDs should be considered in patients with a hemodynamically stable sustained VT or symptomatic patients when the complaints are probably due to ventricular arrhythmias.[21] Adrenergic stimulation has been increasingly associated to the onset of ventricular arrhythmias in ARVC.[25] Therefore, beta-blocker therapy is recommended in patients with recurrent VT's.[21] In addition, catheter ablation (preferably by an epicardial approach) could be of incremental value in incessant VT or frequent ICD interventions despite maximal pharmacological therapy.[26,27] In addition to the frequent occurrence of ventricular arrhythmias in ARVC, this disease is also known to cause heart failure. In a large longitudinal study, progression of ARVC led to symptomatic heart failure in 13% during 7 years of follow-up.[10] Heart failure is usually treated by standard pharmacological heart failure treatment such as beta-blockers and angiotensin-converting-enzyme inhibitors.[21] Whether this treatment strategy also has influence on disease progression itself is currently unknown.[21] On the contrary, a well-established modifier of disease progression in ARVC is exercise.[28,29] In ARVC mutation carriers, vigorous exercise increases the risk of adverse arrhythmic outcome and is more likely to contribute to the development of heart failure.[28] In gene-elusive ARVC, without any known disease causing mutation, exercise seems to play a disproportional major role in developing the ARVC phenotype.[30] Therefore, exercise restriction in ARVC is certainly recommended.[21,31]

THE ONGOING QUEST FOR EARLY DISEASE DETECTION IN ARVC

"What are we looking for? Where to find it?"

During the last decades, studies on genetics in ARVC has started to unravel the underlying pathological mechanisms underlying ARVC.[4,32,33] This has probably been the most important step towards the full understanding of the different existing disease mechanisms that play a role in ARVC. The increasing knowledge on the relationship between genetics and ARVC has led to the introduction of genetic testing in clinical practice.[5] This has been a major step

R1 R2 R3 R4 R5 R6 R7 R8 R9 R10 R11 R12 R13 R14 R15 R16 R17 R18 R19 R20 R21 R22 R23 R24 R25 R26 R27 R28 R29 R30 R31 R32 R33 R34 R35 R36 R37 R38 R39

forward in the identification of at-risk family members, and this subsequently led to guiding and counselling asymptomatic family members of index ARVC patients. Indeed, a significant part of the family members will also develop ARVC during life, the largest study (n = 274 relatives) performed on this topic showed that 28% already fulfilled definite diagnosis during first cardiac evaluation.[34] By following these family members for another 7 years, this number raised to 38%.[10,34]

Definite ARVC is associated to a low annual mortality rate of approximately 1-3%.[10,35] In family members, this appears to be even lower with an annual mortality rate of <0.5%, and ARVC in family members should be overall considered as benign.[10] Despite this overall favorable prognosis, SCD may occur during all stages of ARVC, even at presentation.[10] While SCD is obviously an event with high emotional impact for the family, SCD related to ARVC disproportional occurs in young apparently healthy individuals, which makes it even a more devastating event.[10,36] This well-known disease feature has fueled the urge for early disease detection to optimize the use of anti-arrhythmic drug therapy and the implantation of ICDs.[21] Therefore, the current guidelines suggest to perform serial cardiac evaluation in these subjects every 2-3 years.[21] Cardiac evaluation in ARVC family members encompasses ECG, Holter monitoring, and cardiac imaging to detect established phenotypic disease expressions, all according to current diagnostic TFC.[14,21] Early detection has been an important research topic with several major achievements during the last 5 years.[34,37-40] A key-finding was the discovery that the subtricuspid area, the RV basal region, was identified as the hotspot region where the first disease expression appears.[37] Therefore, in order to design new early detection strategies, this seemed to be the preferred region to detect early ARVC disease. Another important breakthrough was that electrical abnormalities seem to precede detectable structural alterations in ARVC, and this finding was supported by several clinical studies as well as experimental data derived from murine studies.[8,9,34,38-41] Accumulating evidence of the link between sodium channel dysfunction secondary to desmosomal changes raised the hypothesis that sodium channel dysfunction must be an important contributor to the ARVC phenotype.[6] Indeed, results from desmosomal mouse models learned us that sodium channel dysfunction was associated to detectable electrical abnormalities and ventricular arrhythmias in absence of any histopathological changes such as replacement fibrosis or necrosis.[9,41] These interesting experimental findings were also supported by the fact that reduced sodium channel function was found in myocardial specimens of ARVC patients.[8] The experimental evidence that electrical abnormalities precede structural abnormalities appears to be numerous and very convincing.[6,8,9,41] Moreover, this hypothesis was further supported by clinical data in men recently.[38-40] These clinical studies, by mainly describing the yield of serial evaluation in ARVC family members, showed that both ECG abnormalities and arrhythmias (electrical disease) occur before structural abnormalities do appear on conventional imaging such as cardiac magnetic resonance (CMR) imaging and conventional echocardiography.[38-40]

Therefore, the historical recognition of consecutive clinical stages in ARVC: 1) a concealed stage, 2) an electrical stage, and 3) an overt structural stage seems to be supported by firm evidence (**Figure 2**).[5,39] These important findings, predominantly gathered during the last 5 years, provided a well-directed framework for new approaches of early disease detection: we were supposed to look for electrical abnormalities in the subtricuspid area.

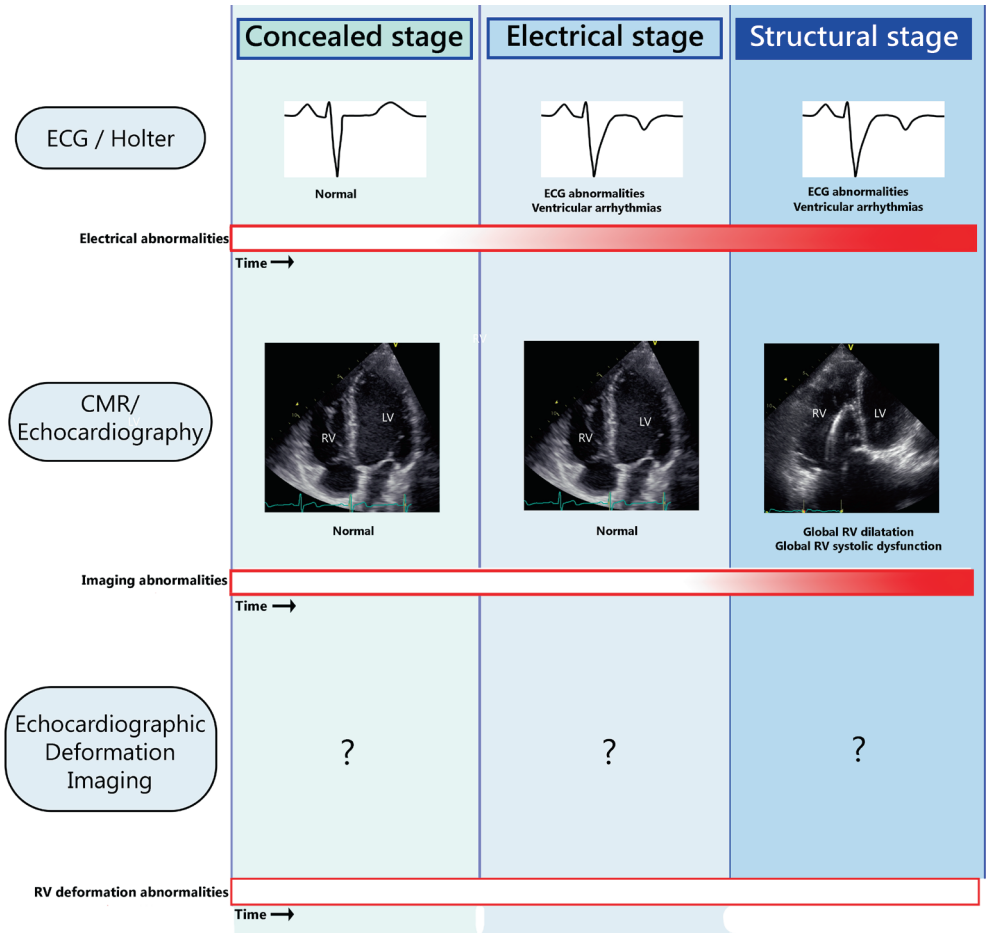

Figure 2. Consecutive clinical stages in ARVC. What is the role of deformation imaging in early detection?

ARVC is classically divided into three consecutive stages: 1) the concealed stage with no detectable abnormalities, 2) electrical stage with electrical abnormities but with no structural abnormalities, and 3) structural stage with overt structural abnormalities. *Abbreviations:* ARVC = Arrhythmogenic right ventricular cardiomyopathy, CMR = cardiac magnetic resonance imaging; RV/LV = right/left ventricle; ECG =electrocardiography

R1 R2 R3 R4 R5 R6 R7 R8 R9 R10 R11 R12 R13 R14 R15 R16 R17 R18 R19 R20 R21 R22 R23 R24 R25 R26 R27 R28 R29 R30 R31 R32 R33 R34 R35 R36 R37 R38 R39

Echocardiographic deformation imaging, is a technique that enables the assessment of both local and global mechanical function in the RV, including the subtricuspid area.[42,43] Previous studies, including some performed in our center, already showed that this technique was able to show clear RV abnormalities in definite ARVC patients.[44-46] Due to the advantages of local mechanical function assessment, especially in the subtricuspid area, this technique might be able to detect early signs of disease in ARVC family members even before abnormalities on conventional non-invasive imaging become apparent. However, as discussed before, it was clear that electrical abnormalities precede structural abnormalities in ARVC. Therefore, measuring electrical activation delay, a hallmark of ARVC, in the subtricuspid area could be of importance for early detection and arrhythmic risk stratification in early ARVC. Echocardiographic deformation imaging, as an imaging technique, is unable to measure electrical abnormalities itself. However, due to electrical-mechanical contraction coupling, local mechanical deformation could be potentially used as a surrogate of electrical abnormalities.[47] Previous preliminary studies already showed that heterogeneous contraction, probably secondary to heterogeneous electrical activation, could be identified in ARVC family members.[42,45] In the next chapter (***Chapter 2***) we discuss the current and potential role of echocardiographic deformation imaging in ARVC. Both the encouraging results of preliminary studies on RV deformation imaging in ARVC family members, and the advantage to obtain mechanical function of the subtricuspid area, merits further investigation of echocardiographic deformation imaging for early detection of ARVC. Therefore, in this thesis we aimed to address the following question:

- Is echocardiographic deformation imaging of incremental value in early ARVC diagnosis by the detection of abnormalities prior to conventional diagnostic approaches?

TOWARDS OPTIMAL ASSESSMENT OF STRUCTURAL DISEASE PROGRESSION IN ARVC

ARVC is generally considered as a progressive disease, this is most notable due to the fact that symptoms related to ARVC arise around 30 years of age while symptoms of heart failure (due to progressive RV failure and LV dysfunction) are typically seen at older age at advanced or end-stages of the disease.[5,10] Although much progress has been made in understanding the genetic basis of ARVC, identifying arrhythmic risk factors, and optimizing family screening protocols, little is known about structural disease progression in ARVC.[5] Optimal assessment of structural disease progression could nevertheless be of utmost importance in order to predict arrhythmic events and to guide future therapeutic approaches. During the last decades, cardiac magnetic resonance imaging (CMR) has become increasingly important in ARVC.[48] CMR enables functional evaluation of both ventricles, provides morphological

information, as well as tissue characterization.[48] Although CMR is the gold standard in RV imaging, this technique is not capable to track structural disease progression during the total disease course in an ARVC patient. The majority of ARVC patients received an ICD device which hampers serial evaluation by CMR.[10] Therefore, echocardiography seems the preferred technique to track structural disease progression in advanced ARVC. It is currently unknown if conventional echocardiography is capable to detect structural disease progression in ARVC. In early ARVC patients, who typically do not carry an ICD device, CMR is able to measure structural disease abnormalities during follow-up.[18] From studies aiming to measure structural progression by CMR and conventional echocardiography we have learned that the yield of abnormal findings is very low in early ARVC.[38,39] A possible explanation is that conventional imaging approaches (both CMR and conventional echocardiography) suffer from insufficient sensitivity.[14] For CMR, the capability to identify myocardial fibrosis by delayed gadolinium enhancement is hampered by the thin RV wall.[48] For both echocardiography and CMR, the detection of minor RV regional wall motion abnormalities, such as RV hypokinesia, is not reliable due to a high amount of false-positive findings in controls.[14,42] Another limitation of CMR is the low temporal resolution of this technique.[48] Therefore, subtle dyssynchronous wall motion during the early ARVC stages could be missed by CMR. Echocardiographic RV deformation imaging benefits from high temporal resolutions and provides insight in mechanical dyssynchrony.[43] Therefore, this technique could be of incremental value in monitoring structural disease progression in early ARVC. However, the role of echocardiographic deformation imaging in assessing structural disease progression is currently unclear. Therefore, this thesis aimed to address the following questions regarding this topic:

- Is conventional echocardiography capable to assess structural disease progression in a broad clinical spectrum of ARVC?
- Could echocardiographic deformation imaging optimize the assessment of structural disease progression in early ARVC?

Thesis Outline

This thesis is divided into three parts: ***Part I*** provides an overview of the current value of echocardiography in ARVC and a further elaboration on the possible clinical value of echocardiographic deformation imaging in ARVC is provided. ***Part II*** focuses on early detection of ARVC and shows the capability of echocardiographic RV deformation imaging to detect early pathological changes in absence of established disease criteria. While activation delay is one of the hallmarks of ARVC, we explored the value of measuring activation delay by RV deformation imaging. We defined a new deformation imaging derived parameter: time to onset of myocardial contraction (or electromechanical interval (EMI)), as a surrogate marker for activation delay. In ***Chapter 3***, the hypothesis was tested whether this parameter

could identify signs of activation delay in both ARVC patients and family members during early disease stages. Previously, several other deformation parameters were described with potential value for early detection of ARVC. In ***Chapter 4*** we described a new pattern-based approach that combines multiple deformation parameters into deformation patterns, including those described in *chapter 3,* and were correlated to disease severity. In the same chapter, we aimed to characterize the underlying substrate causing these patterns by a computer model to determine the underlying disease substrate. Based on current literature, we hypothesized that abnormal deformation patterns in the early stages of ARVC were caused by an underlying electrical substrate consisting of activation delay. In ***Chapter 5*****,** we further explored the clinical value of RV deformation patterns, as proposed in *chapter 4,* in early ARVC. In this chapter we tested the hypothesis that the presence of abnormal RV deformation patterns predicts disease progression in early ARVC. Although ARVC preferentially affects the RV, early LV abnormalities are now more frequently recognized in ARVC.[49-51] ***Chapter 6*** explores the capability of echocardiographic deformation imaging to detect early subtle LV pathology in ARVC and tested the hypothesis that the presence of LV involvement has prognostic implications with respect to the occurrence of arrhythmic events, heart failure, and death.

In ***Part III****,* we explored the role of both conventional echocardiography and RV deformation imaging for the optimal assessment of structural disease. In ***Chapter 7*** we aimed to gain insight in the capability of conventional echocardiography to detect progressive RV dysfunction in advanced ARVC during long-term follow-up. Previous studies showed that structural disease progression detected by conventional imaging approaches is rare in early ARVC. In the last chapter of this part (***chapter 8***), we explored the value of echocardiographic deformation imaging to detect structural disease progression in early ARVC. Our hypothesis was that echocardiographic deformation imaging detects signs of structural disease progression in absence of disease progression by conventional imaging approaches.

All parts are discussed further in ***Chapter 9*** and ***Chapter 10***. In these chapters we summarize our findings and look at the future perspective of echocardiographic deformation imaging and ARVC.

REFERENCES

R1 1. Marcus FI, Fontaine GH, Guiraudon G, et al. Right ventricular dysplasia: a report of 24 adult cases. *Circulation.* 1982;65(2):384-398.

R2 2. Romero J, Mejia-Lopez E, Manrique C, Lucariello R. Arrhythmogenic Right Ventricular Cardiomyopathy (ARVC/D): A Systematic Literature Review. *Clin Med Insights Cardiol.* 2013;7:97-114.

R3 3. Basso C, Thiene G, Corrado D, Angelini A, Nava A, Valente M. Arrhythmogenic right ventricular cardiomyopathy. Dysplasia, dystrophy, or myocarditis? *Circulation.* 1996;94(5):983-991.

R4 4. McKoy G, Protonotarios N, Crosby A, et al. Identification of a deletion in plakoglobin in arrhythmogenic right ventricular cardiomyopathy with palmoplantar keratoderma and woolly hair (Naxos disease). *Lancet.* 2000;355(9221):2119-2124.

R5 5. Basso C, Corrado D, Marcus FI, Nava A, Thiene G. Arrhythmogenic right ventricular cardiomyopathy. *Lancet.* 2009;373(9671):1289-1300.

R6 6. Noorman M, van der Heyden MA, van Veen TA, et al. Cardiac cell-cell junctions in health and disease: Electrical versus mechanical coupling. *J Mol Cell Cardiol.* 2009;47(1):23-31.

R7 7. Delmar M, McKenna WJ. The cardiac desmosome and arrhythmogenic cardiomyopathies: from gene to disease. *Circ Res.* 2010;107(6):700-714.

R8 8. Noorman M, Hakim S, Kessler E, et al. Remodeling of the cardiac sodium channel, connexin43, and plakoglobin at the intercalated disk in patients with arrhythmogenic cardiomyopathy. *Heart Rhythm.* 2013;10(3):412-419.

R9 9. Cerrone M, Noorman M, Lin X, et al. Sodium current deficit and arrhythmogenesis in a murine model of plakophilin-2 haploinsufficiency. *Cardiovasc Res.* 2012;95(4):460-468.

R10 10. Groeneweg JA, Bhonsale A, James CA, et al. Clinical Presentation, Long-Term Follow-Up, and Outcomes of 1001 Arrhythmogenic Right Ventricular Dysplasia/Cardiomyopathy Patients and Family Members. *Circ Cardiovasc Genet.* 2015;8(3):437-446.

R11 11. Cox MG, van der Zwaag PA, van der Werf C, et al. Arrhythmogenic right ventricular dysplasia/cardiomyopathy: pathogenic desmosome mutations in index-patients predict outcome of family screening: Dutch arrhythmogenic right ventricular dysplasia/cardiomyopathy genotype-phenotype follow-up study. *Circulation.* 2011;123(23):2690-2700.

R12 12. Groeneweg JA, van der Zwaag PA, Olde Nordkamp LR, et al. Arrhythmogenic right ventricular dysplasia/cardiomyopathy according to revised 2010 task force criteria with inclusion of non-desmosomal phospholamban mutation carriers. *Am J Cardiol.* 2013;112(8):1197-1206.

R13 13. Sen-Chowdhry S, Syrris P, Pantazis A, Quarta G, McKenna WJ, Chambers JC. Mutational heterogeneity, modifier genes, and environmental influences contribute to phenotypic diversity of arrhythmogenic cardiomyopathy. *Circ Cardiovasc Genet.* 2010;3(4):323-330.

R14 14. Marcus FI, McKenna WJ, Sherrill D, et al. Diagnosis of arrhythmogenic right ventricular cardiomyopathy/dysplasia: proposed modification of the task force criteria. *Circulation.* 2010;121(13):1533-1541.

R15 15. McKenna WJ, Thiene G, Nava A, et al. Diagnosis of arrhythmogenic right ventricular dysplasia/cardiomyopathy. Task Force of the Working Group Myocardial and Pericardial Disease of the European Society of Cardiology and of the Scientific Council on Cardiomyopathies of the International Society and Federation of Cardiology. *Br Heart J.* 1994;71(3):215-218.

R16 16. Hamid MS, Norman M, Quraishi A, et al. Prospective evaluation of relatives for familial arrhythmogenic right ventricular cardiomyopathy/dysplasia reveals a need to broaden diagnostic criteria. *J Am Coll Cardiol.* 2002;40(8):1445-1450.

R17 17. Nasir K, Bomma C, Tandri H, et al. Electrocardiographic features of arrhythmogenic right ventricular dysplasia/cardiomyopathy according to disease severity: a need to broaden diagnostic criteria. *Circulation.* 2004;110(12):1527-1534.

R18 R19 R20 R21 R22 R23 R24 R25 R26 R27 R28 R29 R30 R31 R32 R33 R34 R35 R36 R37 R38 R39

18. Borgquist R, Haugaa KH, Gilljam T, et al. The diagnostic performance of imaging methods in ARVC using the 2010 Task Force criteria. *Eur Heart J Cardiovasc Imaging.* 2014;15(11):1219-1225.
19. Femia G, Hsu C, Singarayar S, et al. Impact of new task force criteria in the diagnosis of arrhythmogenic right ventricular cardiomyopathy. *Int J Cardiol.* 2014;171(2):179-183.
20. Cox MG, van der Smagt JJ, Noorman M, et al. Arrhythmogenic right ventricular dysplasia/cardiomyopathy diagnostic task force criteria: impact of new task force criteria. *Circ Arrhythm Electrophysiol.* 2010;3(2):126-133.
21. Corrado D, Wichter T, Link MS, et al. Treatment of Arrhythmogenic Right Ventricular Cardiomyopathy/Dysplasia: An International Task Force Consensus Statement. *Circulation.* 2015;132(5):441-453.
22. Roguin A, Bomma CS, Nasir K, et al. Implantable cardioverter-defibrillators in patients with arrhythmogenic right ventricular dysplasia/cardiomyopathy. *J Am Coll Cardiol.* 2004;43(10):1843-1852.
23. Wichter T, Paul M, Wollmann C, et al. Implantable cardioverter/defibrillator therapy in arrhythmogenic right ventricular cardiomyopathy: single-center experience of long-term follow-up and complications in 60 patients. *Circulation.* 2004;109(12):1503-1508.
24. Bhonsale A, James CA, Tichnell C, et al. Incidence and predictors of implantable cardioverter-defibrillator therapy in patients with arrhythmogenic right ventricular dysplasia/cardiomyopathy undergoing implantable cardioverter-defibrillator implantation for primary prevention. *J Am Coll Cardiol.* 2011;58(14):1485-1496.
25. Dalal D, Nasir K, Bomma C, et al. Arrhythmogenic right ventricular dysplasia: a United States experience. *Circulation.* 2005;112(25):3823-3832.
26. Haqqani HM, Tschabrunn CM, Betensky BP, et al. Layered activation of epicardial scar in arrhythmogenic right ventricular dysplasia: possible substrate for confined epicardial circuits. *Circ Arrhythm Electrophysiol.* 2012;5(4):796-803.
27. Philips B, Madhavan S, James C, et al. Outcomes of catheter ablation of ventricular tachycardia in arrhythmogenic right ventricular dysplasia/cardiomyopathy. *Circ Arrhythm Electrophysiol.* 2012;5(3):499-505.
28. James CA, Bhonsale A, Tichnell C, et al. Exercise increases age-related penetrance and arrhythmic risk in arrhythmogenic right ventricular dysplasia/cardiomyopathy-associated desmosomal mutation carriers. *J Am Coll Cardiol.* 2013;62(14):1290-1297.
29. Heidbuchel H, La Gerche A. The right heart in athletes. Evidence for exercise-induced arrhythmogenic right ventricular cardiomyopathy. *Herzschrittmacherther Elektrophysiol.* 2012;23(2):82-86.
30. Sawant AC, Bhonsale A, Te Riele AS, et al. Exercise has a Disproportionate Role in the Pathogenesis of Arrhythmogenic Right Ventricular Dysplasia/Cardiomyopathy in Patients Without Desmosomal Mutations. *J Am Heart Assoc.* 2014;3(6).
31. Sawant AC, Te Riele AS, Tichnell C, et al. Safety of American Heart Association-recommended minimum exercise for desmosomal mutation carriers. *Heart Rhythm.* 2016;13(1):199-207.
32. Protonotarios N, Tsatsopoulou A, Anastasakis A, et al. Genotype-phenotype assessment in autosomal recessive arrhythmogenic right ventricular cardiomyopathy (Naxos disease) caused by a deletion in plakoglobin. *J Am Coll Cardiol.* 2001;38(5):1477-1484.
33. Gerull B, Heuser A, Wichter T, et al. Mutations in the desmosomal protein plakophilin-2 are common in arrhythmogenic right ventricular cardiomyopathy. *Nat Genet.* 2004;36(11):1162-1164.
34. Te Riele AS, James CA, Groeneweg JA, et al. Approach to family screening in arrhythmogenic right ventricular dysplasia/cardiomyopathy. *Eur Heart J.* 2016;37(9):755-763.
35. Hulot JS, Jouven X, Empana JP, Frank R, Fontaine G. Natural history and risk stratification of arrhythmogenic right ventricular dysplasia/cardiomyopathy. *Circulation.* 2004;110(14):1879-1884.

36. Bhonsale A, Groeneweg JA, James CA, et al. Impact of genotype on clinical course in arrhythmogenic right ventricular dysplasia/cardiomyopathy-associated mutation carriers. *Eur Heart J.* 2015;36(14):847-855.
37. Te Riele AS, James CA, Philips B, et al. Mutation-positive arrhythmogenic right ventricular dysplasia/cardiomyopathy: the triangle of dysplasia displaced. *J Cardiovasc Electrophysiol.* 2013;24(12):1311-1320.
38. Te Riele AS, Bhonsale A, James CA, et al. Incremental value of cardiac magnetic resonance imaging in arrhythmic risk stratification of arrhythmogenic right ventricular dysplasia/cardiomyopathy-associated desmosomal mutation carriers. *J Am Coll Cardiol.* 2013;62(19):1761-1769.
39. Te Riele AS, James CA, Rastegar N, et al. Yield of serial evaluation in at-risk family members of patients with ARVD/C. *J Am Coll Cardiol.* 2014;64(3):293-301.
40. Gomes J, Finlay M, Ahmed AK, et al. Electrophysiological abnormalities precede overt structural changes in arrhythmogenic right ventricular cardiomyopathy due to mutations in desmoplakin-A combined murine and human study. *Eur Heart J.* 2012;33(15):1942-1953.
41. Rizzo S, Lodder EM, Verkerk AO, et al. Intercalated disc abnormalities, reduced Na(+) current density, and conduction slowing in desmoglein-2 mutant mice prior to cardiomyopathic changes. *Cardiovasc Res.* 2012;95(4):409-418.
42. Teske AJ, Cox MG, Te Riele AS, et al. Early detection of regional functional abnormalities in asymptomatic ARVD/C gene carriers. *J Am Soc Echocardiogr.* 2012;25(9):997-1006.
43. Teske AJ, De Boeck BW, Melman PG, Sieswerda GT, Doevendans PA, Cramer MJ. Echocardiographic quantification of myocardial function using tissue deformation imaging, a guide to image acquisition and analysis using tissue Doppler and speckle tracking. *Cardiovasc Ultrasound.* 2007;5:27.
44. Prakasa KR, Wang J, Tandri H, et al. Utility of tissue Doppler and strain echocardiography in arrhythmogenic right ventricular dysplasia/cardiomyopathy. *Am J Cardiol.* 2007;100(3):507-512.
45. Sarvari SI, Haugaa KH, Anfinsen OG, et al. Right ventricular mechanical dispersion is related to malignant arrhythmias: a study of patients with arrhythmogenic right ventricular cardiomyopathy and subclinical right ventricular dysfunction. *Eur Heart J.* 2011;32(9):1089-1096.
46. Teske AJ, Cox MG, De Boeck BW, Doevendans PA, Hauer RN, Cramer MJ. Echocardiographic tissue deformation imaging quantifies abnormal regional right ventricular function in arrhythmogenic right ventricular dysplasia/cardiomyopathy. *J Am Soc Echocardiogr.* 2009;22(8):920-927.
47. De Boeck BW, Teske AJ, Leenders GE, et al. Detection and quantification by deformation imaging of the functional impact of septal compared to free wall preexcitation in the Wolff-Parkinson-White syndrome. *Am J Cardiol.* 2010;106(4):539-546 e532.
48. Te Riele AS, Tandri H, Bluemke DA. Arrhythmogenic right ventricular cardiomyopathy (ARVC): cardiovascular magnetic resonance update. *J Cardiovasc Magn Reson.* 2014;16:50.
49. Te Riele AS, James CA, Philips B, et al. Mutation-Positive Arrhyhmogenic Right Ventricular Dysplasia/Cardiomyopathy: The Triangle of Dysplasia Displaced. *J Cardiovasc Electrophysiol.* 2013;24(12):1311-1320.
50. Teske AJ, Cox MG, Peterse MC, Cramer MJ, Hauer RN. Case report: echocardiographic deformation imaging detects left ventricular involvement in a young boy with arrhythmogenic right ventricular dysplasia/cardiomyopathy. *Int J Cardiol.* 2009;135(1):e24-26.
51. Lindstrom L, Nylander E, Larsson H, Wranne B. Left ventricular involvement in arrhythmogenic right ventricular cardiomyopathy- a scintigraphic and echocardiographic study. *Clin Physiol Funct Imaging.* 2005;25(3):171-177.

PART I

CURRENT AND FUTURE ROLE OF ECHOCARDIOGRAPHY IN ARVC

CHAPTER 2

Current and Future Role of Echocardiography in Arrhythmogenic Right Ventricular Dysplasia/Cardiomyopathy

Thomas P Mast, Arco J Teske, Pieter A Doevendans, Maarten J Cramer

Cardiol J. 2015;22(4):362-74
Book chapter: A. Abidov, I.B. Oliva, F.I. Marcus (editors). Cardiac MRI in the Diagnosis, Clinical Management, and Prognosis of Arrhythmogenic Right Ventricular Cardiomyopathy/Dysplasia. Elsevier 2016

ABSTRACT

Arrhythmogenic right ventricular dysplasia/cardiomyopathy (ARVD/C) is an inherited progressive cardiomyopathy, clinically characterized by ventricular arrhythmias and increased risk of sudden cardiac death. Echocardiography has a role in the diagnosis and prognosis of ARVD/C. However, in the current era of magnetic resonance imaging (MRI), the role of echocardiography in ARVD/C patients and family member screening is subject to debate. Relatively novel echocardiographic techniques, such as three-dimensional right ventricular (3D-RV) imaging and tissue deformation imaging, may improve the diagnostic and prognostic performance of echocardiography in these patients.

3D-RV imaging provides more insights on RV anatomy and global function compared to conventional echocardiography. Subtle RV regional wall motion abnormalities, and mechanical dyssynchrony, are accurately measured by tissue deformation imaging.

Several studies suggest an incremental value of novel echocardiographic parameters in addition to conventional measurements. Moreover, new parameters indicating subtle RV dysfunction, and mechanical dyssynchrony, are of predictive value and could help in risk stratification of ARVD/C patients.

New robust parameters, derived from 3D-RV echocardiography and RV tissue deformation imaging, in combination with established conventional parameters, suggest that there is a current and future role for echocardiography in ARVD/C supplementing MRI.

INTRODUCTION

Arrhythmogenic right ventricular dysplasia/cardiomyopathy (ARVD/C) is an inherited progressive cardiomyopathy, clinically characterized by life-threatening ventricular arrhythmias and, in advanced stages, heart failure [1]. In up to 60% of ARVD/C patients, genetic mutations are found in genes encoding for desmosomal proteins [2, 3]. Desmosomes are located in the intercalated disc and provide structural and functional integrity between cardiac myocytes [4]. Desmosomal dysfunction leads to both mechanical and electrical uncoupling [4, 5]. This mechanical uncoupling is associated with fibro-fatty replacement of the myocardium and right ventricular (RV) dysfunction [6]. Electrical uncoupling of cardiac myocytes and the presence of surviving myocardial bundles within the fibrofatty tissue promote activation delay, therefore providing a substrate (macro re-entry) for ventricular arrhythmias [5, 7].

In Europe and North America, desmosomal mutations are predominantly found in the plakophilin-2 (*PKP2*) gene [3, 8, 9]. However, pathogenic ARVD/C mutations show incomplete penetrance and wide variable phenotypic expression [3]. Therefore, risk stratification remains challenging. Although desmosomes are expressed in all cardiac myocytes, a typical distribution of disease expression is observed. Typical involved areas are the subtricuspid region, the right ventricular outflow tract (RVOT), and the left ventricular (LV) posterolateral wall [10]. Traditionally, the RV apex was seen as an important region which was involved in this disease and was included in the so called “triangle of dysplasia” [1]. However, recent studies have shown that the RV apex is only involved in advanced stages of the disease [10]. Secondly, LV involvement is more common than previously thought, with a clear predilection site in the LV posterolateral region (**Figure 1**) [10, 11].

ARVD/C is diagnosed according to major and minor criteria stated in the 2010 revised Task Force criteria (TFC) [12]. The 2010 TFC include different categories: (1) structural RV alterations, (2) tissue characterization, (3) depolarization and repolarization abnormalities, (4) ventricular arrhythmias, and (5) family history and genetic data [12]. The diagnostic criteria are fulfilled by the presence of 2 major, or 1 major plus 2 minor criteria or, 4 minor criteria from different groups. RV functional and structural alterations are visualized by using different imaging modalities such as echocardiography, magnetic resonance imaging (MRI), and angiography. Diagnostic imaging criteria are scored if a regional RV wall motion abnormality is present in combination with RV dilatation or global RV systolic dysfunction [12]. Modality-specific cut-off values concerning global RV dysfunction and RV dilatation are provided in the 2010 TFC (**Table 1**) [12].

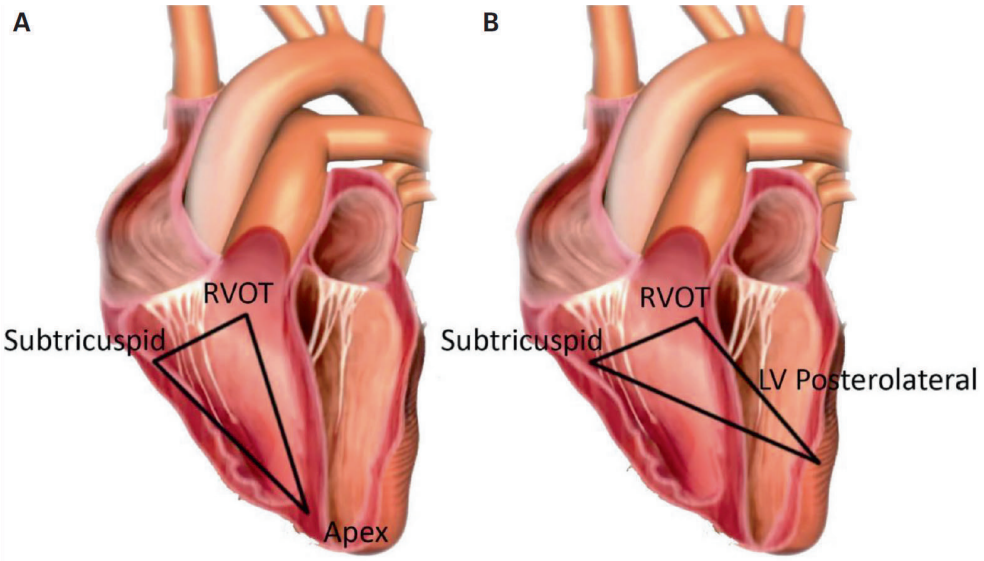

Figure 1. Triangle of dysplasia
A. Original triangle of dysplasia consisting of the following regions: 1) subtricuspid region, 2) right ventricular outflow tract (RVOT), and 3) apical region; B. Revised triangle of dysplasia. The left ventricular (LV) posterolateral wall seems to be a clear predilection site of arrhythmogenic right ventricular dysplasia/cardio-myopathy and is more commonly involved compared to the apical region.

Echocardiography is a noninvasive, and widely available imaging tool to evaluate patients with known or suspected ARVD/C. However, complete and accurate RV echocardiography is difficult due to the retrosternal position and complex geometry of the RV. MRI is not hampered by these limitations and has therefore taken a prominent role in imaging for ARVD/C [13]. Recently, MRI was found to be of superior value for the diagnosis of ARVC compared to conventional echocardiography [14]. Nevertheless, MRI is also prone to false-positive findings if there is an overreliance on detection of intramyocardial fat and wall thinning [15]. In addition, determination of normal RV wall motion around the moderator band insertions remains difficult by MRI [15, 16].

Emerging new echocardiographic techniques, specifically three dimensional (3D) RV echocardiography and tissue deformation imaging, may increase the performance of echocardiography, overcoming the previously mentioned shortcoming of conventional RV echocardiography [17, 18]. 3D imaging enables more accurate RV volumetric measurements compared to conventional echocardiography [19, 20]. Regional deformation imaging, another relatively new technique, quantifies regional RV wall motion and provides timing of regional motion [18, 21].

Table 1. 2010 Task Force criteria. Global or regional dysfunction and structural alterations

2D-echo	
Major	Presence of a regional RV akinesia, dyskinesia, or aneurysm **and** 1 of the following (end-diastole): - PLAX RVOT ≥ 32 mm (corrected for BSA: PLAX RVOT/BSA ≥ 19 mm/m^2) **or** - PSAX RVOT ≥ 36 mm (corrected for BSA: PSAX RVOT/BSA ≥ 21 mm/m^2) **or** - RV-FAC ≤ 33%
Minor	Presence of a regional RV akinesia, dyskinesia, or aneurysm **and** 1 of the following (end-diastole): - PLAX RVOT ≥29 to < 32 mm (corrected for BSA: PLAX RVOT/BSA ≥16 to < 19 mm/m^2) **or** - PSAX RVOT ≥32 to <36 mm (corrected for BSA: PSAX RVOT ≥18 to <21 mm/m^2) **or** - RV-FAC >33% to ≤40%
MRI	
Major	Presence of a regional RV akinesia or dyskinesia, or dyssynchronous RV contraction **and** 1 of the following: - Ratio of RV-EDV to BSA ≥ 110 ml/m^2 (male) ≥ 100 ml/m^2 (female) **or** - RVEF ≤ 40%
Minor	Presence of a regional RV akinesia or dyskinesia, or dyssynchronous RV contraction **and** 1 of the following: - Ratio of RV-EDV to BSA ≥100 < 110 ml/m^2 (male) ≥ 90 to < 100 ml/m^2 (female) **or** - RVEF > 40% to ≤ 45%
RV angiography	
Major	Presence of regional RV akinesia, dyskinesia, or aneurysm
Minor	No minor criterion specified for this modality

Derived from the 2010 Task Force criteria. RV = right ventricle; PLAX/PSAX = parasternal long/shorts axis; BSA = body surface area; RV-FAC = right ventricular fractional area change; RV-EDV = right ventricular end-diastolic volume; RVEF = right ventricular ejection fraction mm = millimeter; ml = milliliter; m = meter; MRI = magnetic resonance imaging

Implantable cardioverter-defibrillators (ICD) are frequently implanted in ARVD/C patients to prevent sudden arrhythmic death. These metallic devices make MRI unsuitable for evaluation of ARVD/C patients. For the purpose of monitoring ARVD/C patients, echocardiography is the current preferred imaging technology [22]. Novel echocardiographic techniques could conceivably provide new predictors for the occurrence of cardiac events during follow-up in addition to conventional measures of RV and LV function.

In this review, we aim to evaluate the current and future role of both conventional and new echocardiographic parameters in ARVD/C with respect to the diagnosis of the disease as well as follow-up. We provide illustrative examples of this relatively rare disease entity and we have added our echocardiographic protocol as a guide for the clinician.

R1 R2 R3 R4 R5 R6 R7 R8 R9 R10 R11 R12 R13 R14 R15 R16 R17 R18 R19 R20 R21 R22 R23 R24 R25 R26 R27 R28 R29 R30 R31 R32 R33 R34 R35 R36 R37 R38 R39

Conventional echocardiography

Extensive fibrofatty replacement of the myocardium affects regional ventricular wall motion and global systolic function [1]. Impaired systolic function leads to structural RV remodeling and is detected by conventional echocardiography as both global RV dilatation and RV systolic dysfunction [23, 24].

Regional and global RV dilatation are well described phenotypic features in ARVD/C patients [24]. RV inflow tract, RVOT, and longitudinal dimensions have been found to be increased compared to healthy controls (**Figure 2**) [17, 23–26].

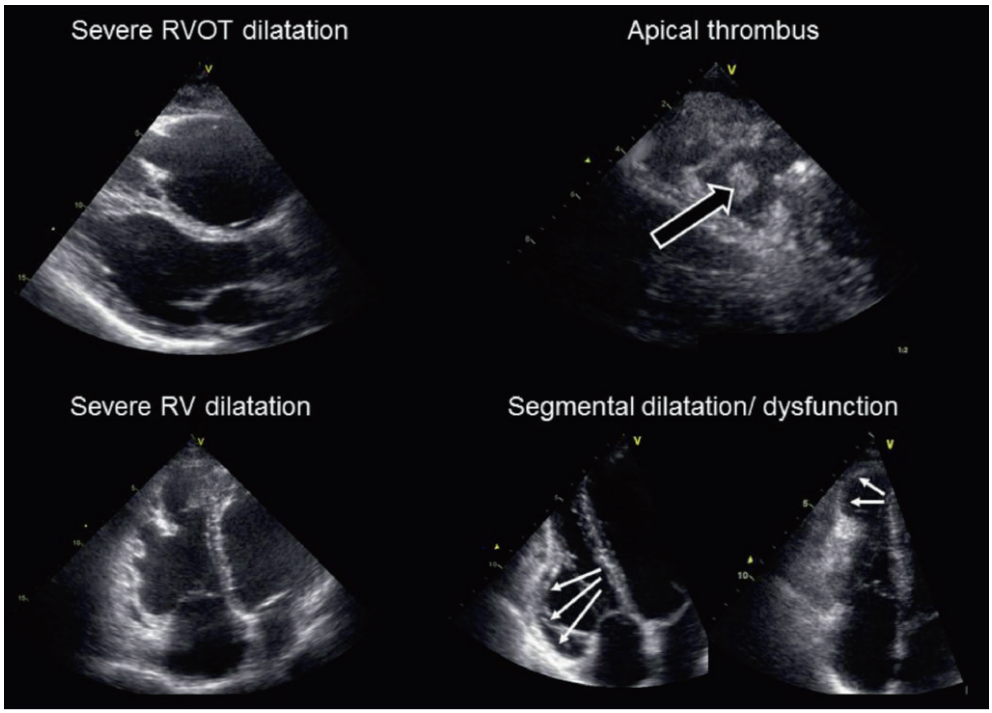

Figure 2. Conventional echocardiography in an arrhythmogenic right ventricular dysplasia/ cardiomyopathy (ARVD/C) patient

Left upper: PLAX, severe RVOT dilatation (57 mm, 27.4 mm/m^2) in 57-year-old ARVD/C patient; Right upper: RV SAX, apical thrombus in 16-year-old ARVD/C patient, RV-FAC was 29%; Left lower: AP4CH, severe dilatation of RV, RVIT = 49 mm, and hyperreflective moderator band; Right lower: AP4CH, apical aneurysm and segmental subtricuspid dilatation; PLAX = parasternal long axis view; RVOT = right ventricular outflow tract; RV = right ventricle; SAX = short axis view; RV-FAC = right ventricular-fractional area change; AP4CH = apical 4 chamber view; RVIT = right ventricular inflow tract.

Several robust parameters representing RV systolic function, such as the tricuspid annular plane systolic excursion (TAPSE), peak systolic RV annular velocity, and RV-fractional area change (RV-FAC), provide insight into global RV function and are generally decreased in ARVD/C (**Figure 3**) [17, 23–25, 27].

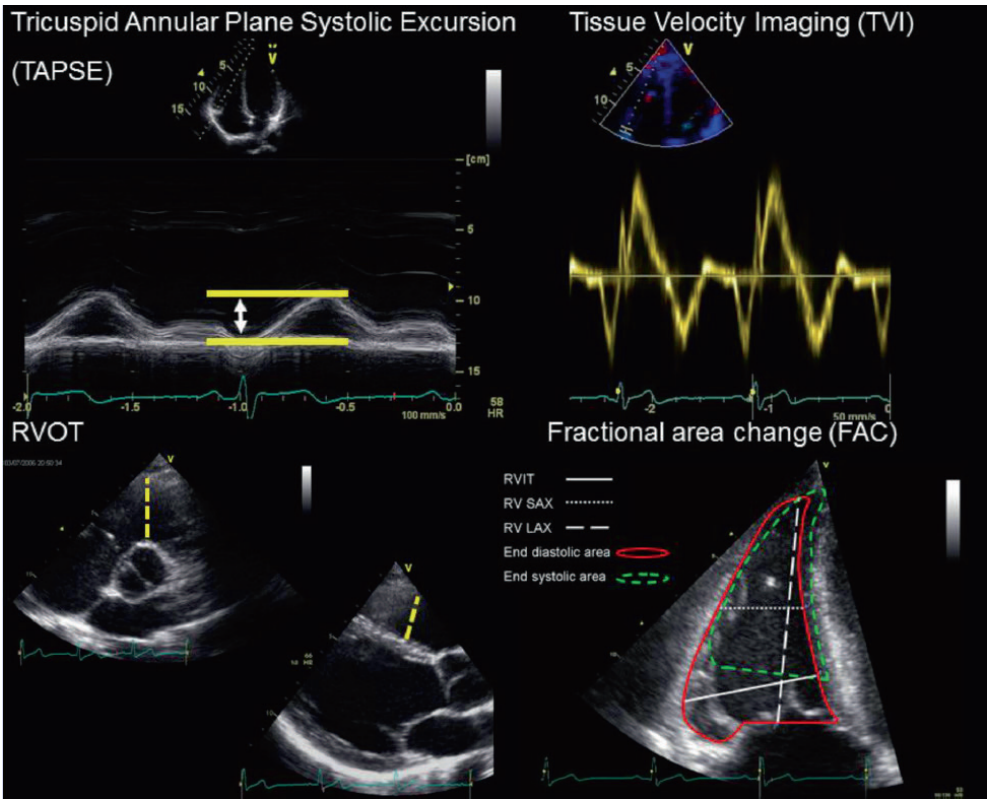

Figure 3. Conventional right ventricular measurements
Example of measurements of tricuspid annular plane systolic excursion (TAPSE) (upper left), peak annular systolic velocity (upper right), right ventricular outflow tract (RVOT) (lower left) and right ventricular-fractional area change (RV-FAC) (lower right).

Altered morphologic appearances, e.g. a hyper-reflective moderator band and excessive trabecular derangement, are also reported in ARVD/C (**Table 2**) [24]. However, these findings lack specificity and were not included in the 2010 TFC. A study performed by Yoerger *et al.* [24] in 2005 found that impaired RV-FAC and RVOT dilatation were the most common abnormal echocardiographic findings in ARVD/C patients. RVOT dilatation in the parasternal long-axis view was present in all ARVD/C patients and decreased RV-FAC was present in 62% of patients. Eventually, these parameters were chosen for the echocardiographic 2010 TFC [12]. TAPSE and peak systolic RV annular velocity were not evaluated in this study and could be the reason why these parameters are not part of the 2010 TFC.

Table 2. Wall motion abnormalities and morphological appearances in ARVD/C patients

Parameters	N = 29 [24] Percent of probands
RV global systolic function	
RV-FAC ≥32%	38
RV-FAC ≥26%- <32%	28
RV-FAC <26%	34
RV regional WMA	79
RVOT	45
Anteroseptal	55
Anterior	70
Apex	72
Septal	55
Inferior basal	59
Inferior apical	52
Hyperreflective moderator band	31
Excessive/abnormal trabeculations	54
Sacculations	17

RV-FAC = right ventricular – fractional area change; RVOT = right ventricular outflow tract; WMA = wall motion abnormalities

Conventional echocardiography is part of the current diagnostic 2010 TFC and consists of visual regional wall motion analyses, outflow tract dimensions and RV-FAC [12]. An echocardiographic TFC is assigned if RVOT dilatation or decreased RV-FAC is observed in combination with abnormal regional wall motion [12]. Akinetic, dyskinetic, or aneurysmatic RV wall segments are considered abnormal. Importantly, hypokinesis is not a part of the 2010 TFC [12]. In a study performed in our institution, we found that regional hypokinesia is a common finding in healthy individuals [28]. Depending on the degree of RVOT dilatation and reduction of RV-FAC, a major or minor criterion is assessed (**Table 1**) [12]. The presence of abnormal regional wall motion is mandatory for a major or minor criterion regardless of RVOT dilatation and/or systolic dysfunction. Therefore, optimal visual RV wall motion analysis is crucial and we suggest that all RV regions should be visualized during the examination (**Figure 4**) [26, 29]. Contrast enhanced echocardiography could be used to improve delineation of the RV free wall and enables more accurate RV wall motion analyses where there is suboptimal imaging quality [30]. Values for echocardiographic TFC were chosen for high specificity (76–95%) resulting in reduced sensitivity (55–87%) [12, 14]. Abnormal findings not fulfilling the current TFC should either be further assessed by MRI or these patients should undergo a follow-up echocardiogram after 1 year. This recommendation is based on our current practice and experience since there is currently no literature to support it. In addition to the diagnostic role of conventional echocardiography in ARVD/C, the prognostic value of echocardiography in ARVD/C has been extensively explored [22, 31, 32]. Both decreased TAPSE and RV-FAC are associated with the occurrence of major adverse cardiac events in ARVD/C [22, 32].

Both parameters are easily obtained and aid risk stratification of ARVD/C patients (**Figure 3**). Several studies have shown the clinical importance of LV involvement in ARVD/C [11, 31, 32]. Although, originally considered an end-stage phenomenon, LV involvement in a broad spectrum of ARVD/C patients has been shown [10, 33, 34]. Echocardiographic measured reduced LV ejection fraction has been found to be the strongest independent predictor of adverse outcome [31, 32].

Clinical data		**Length, weight, BSA**
View	**Remarks**	**Measurements**
Long axis (PLAX)	Zoom RVOT	RVOT PLAX dimension, RVOT-anterior wall motion analyses (green)
RV-2-chamber view		RV-anterior (blue) wall motion analyses, RV inferior (red) wall motion analyses
Short axis (PSAX)	Aortic valve level	RVOT PSAX dimension, RVOT-anterior wall motion analyses (green)
	RV midventricular and apical level	RV anterior wall motion analyses (blue), RV lateral wall motion analyses (yellow), and RV inferior wall motion analyses (red)
4-chamber view	RV focused apical position	RV lateral wall motion analyses (yellow), RV-FAC, TAPSE, RV peak annular velocity
RV inflow-outflow		RVOT wall motion analyses (green), RV-anterior wall motion analyses (blue), RV-inferior wall motion analyses (red)
RV subcostal view		RV inferior wall motion analyses (red)

Protocol is in addition to standard conventional echocardiography as provided by the American Society of echocardiography (ASE); BSA — body surface area; PLAX/PSAX — parasternal long/short axis view; RV — right ventricular; RVOT — right ventricular outflow tract; RV-FAC — right ventricular-fractional area change; TAPSE — tricuspid annular plane systolic excursion

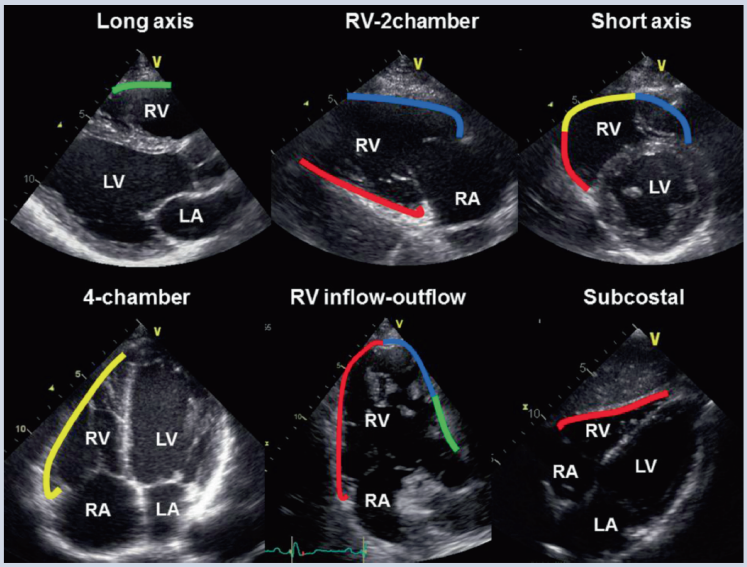

Figure 4. Echocardiographic arrhythmogenic right ventricular dysplasia/cardiomyopathy (ARVD/C) protocol and right ventricular (RV) view
Echocardiographic arrhythmogenic right ventricular dysplasia/cardiomyopathy (ARVD/C) protocol and right ventricular (RV) view; RA = right atrium; LV = left ventricle; LA = left atrium.

All aforementioned parameters are easily obtained by conventional echocardiography and provide useful information during diagnostic evaluation and follow-up in ARVD/C. The precise interval of repeated echocardiographic evaluation is unknown in patients diagnosed with ARVD/C. We advise echocardiographic interrogation in patients when clinical changes occur (e.g. heart failure, arrhythmias, and syncope). In stable patients with no change in any clinical parameter, an echocardiographic follow up every 4–5 years seems reasonable (unpublished data). We have provided the ARVD/C focused echocardiographic protocol which is currently in use in our institution (**Figure 4).**

Three-dimensional echocardiography

There is a marked difference between MRI and echocardiography in the 2010 TFC with respect to measuring RV dilatation and RV systolic dysfunction. Global RV dilatation by MRI is directly measured by RV end-diastolic volume (RVEDV), whereas conventional echocardiography only uses segmental outflow tract dilatation [12]. RVEDV and RV end-systolic volume (RVESV) leads to a 3D measurement of RV systolic function (ejection fraction) by MRI. Echocardiographic RV systolic function only contains a 2D measurement, by measuring the amount of RV area decrease during systole. This limited approach is due to the retrosternal location and complex crescent geometry of the RV. Therefore, the simple geometrical assumptions based on 2D acquisition that is frequently used in assessing LV dimensions, are invalid for the RV and prevents optimal volumetric calculation. These measurements by echocardiography are likely inferior to the 3D volumetric analysis performed by MRI. However, 3D-echocardiography is both feasible and comparable to MRI with respect to RV volumes and RV ejection fraction (RVEF) (**Figure 5**) [19, 20, 35]. With the implementation of 3D-echocardiography, subtle global RV systolic dysfunction can be seen in the early stages of ARVD/C, and can contribute to early diagnosis [36]. In ARVD/C patients, Prakasa *et al.* [19] found varying results by 2D-echocardiography compared to MRI for RVESV, RVEDV and RVEF with Pearson's correlations of 0.72, 0.50 and 0.88, respectively. 3D-echocardiography is hampered by acoustic dropout of the RV free wall and the anterior RV wall in patients with a dilated RV [19]. The current software algorithms may account for the frequently observed abnormal RV shape in ARVD/C patients with large saccular aneurysms. These two mechanisms likely explain the low yield of 3D-echocardiography in this subset of patients. A possible approach to overcome the limitation of acoustic dropout is to use 3D-based RV reconstruction to obtain RV volumes and function (**Figure 5**) [37, 38]. The reconstruction technique uses a magnetic field generator and a magnetic field sensor attached to the transducer to accurately localize 2D obtained RV anatomic landmarks within the magnetic field [37]. The reconstruction algorithm uses the distances between RV landmarks to match the landmarks to a catalog of subjects with similar RV anatomy. This 3D-based technique shows high correlation with MRI derived volumetric measurements in patients with pulmonary hypertension and congenital heart diseases. Inter-

method correlation was 0.87–1.00 (RVEDV), 0.88–1.00 (RVESV), and 0.75–0.88 (RVEF) [37, 38]. We currently lack studies with 3D-based RV reconstruction in ARVD/C patients.

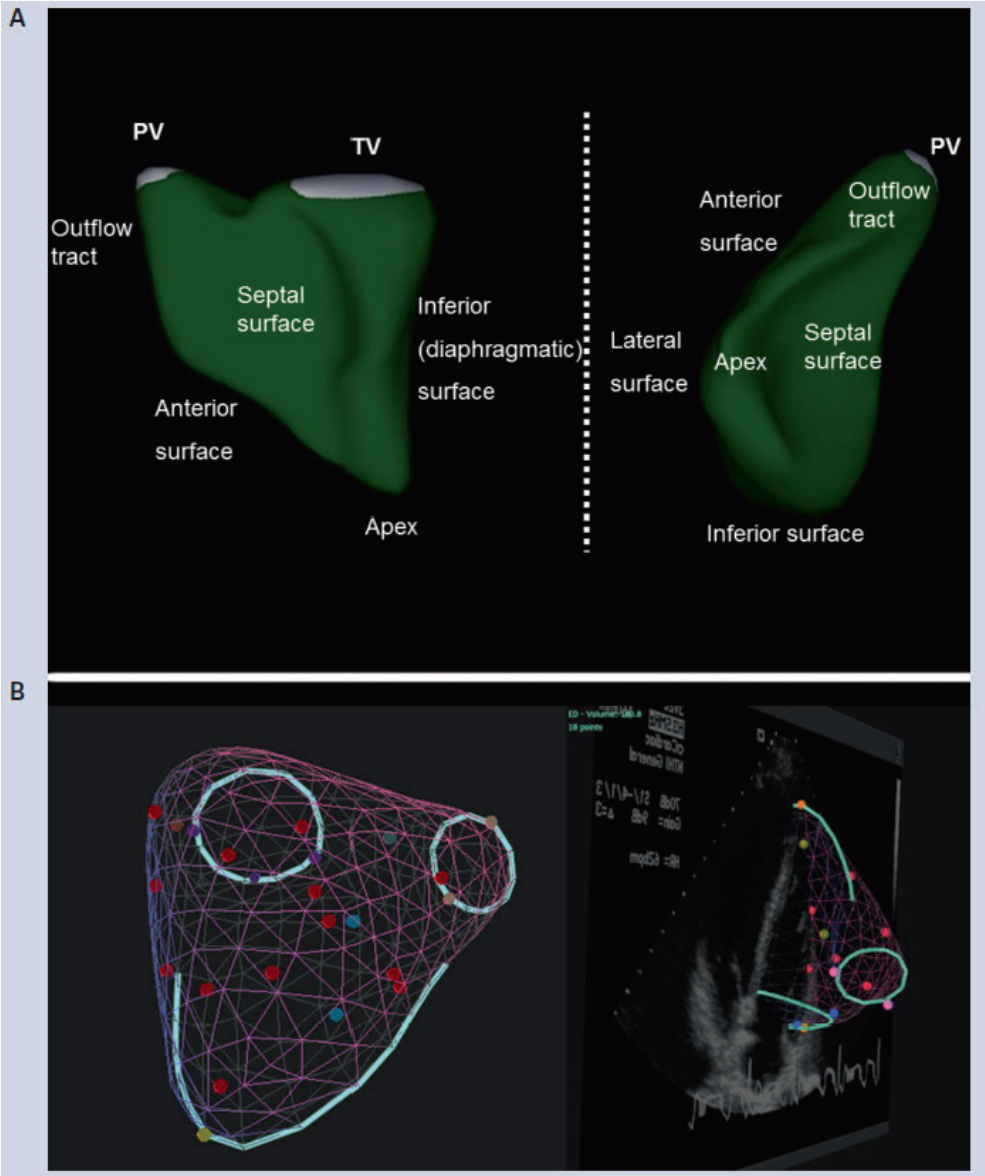

Figure 5. Perimeters of 3-dimensional-right ventricular (3D-RV) of imaging
A. 3D-RV echocardiographic imaging providing excellent insight in RV anatomy; B. 3D acquisition with knowledge based reconstruction. Multiple landmarks, chosen in 2D images, are used to reconstruct the RV anatomy; PV = pulmonary valve; TV = tricuspid valve

R1 R2 R3 R4 R5 R6 R7 R8 R9 R10 R11 R12 R13 R14 R15 R16 R17 R18 R19 R20 R21 R22 R23 R24 R25 R26 R27 R28 R29 R30 R31 R32 R33 R34 R35 R36 R37 R38 R39

Tissue deformation imaging

Echocardiographic tissue deformation imaging is a relatively new technique that provides quantitative regional wall motion analysis. Currently, two different techniques are commercially available: tissue Doppler imaging and speckle-tracking. Both techniques rely on different principles to calculate both regional and global deformation and deformation rate. We have previously shown that both techniques are feasible in the RV and that the calculated values are comparable to one another in ARVD/C patients [18].

Tissue Doppler imaging uses the differences between two velocity-time curves to measure the regional deformation of the myocardium. Velocity-time curves are derived from two points of known distance and encompass a region of interest. Deformation of the region of interest is absent if the difference between two velocity-time curves is zero, indicating this net resultant force on the myocardium is zero. However, differences in velocity-time curves indicate deformation, i.e. shortening or lengthening, of the myocardium. Deformation is plotted against time in a strain-time curve over the cardiac cycle (**Figure 6**).

Speckle tracking (or 2D-strain) uses natural acoustic echocardiographic reflection (speckles) in the B-mode image made within the myocardium to measure deformation. This speckle pattern is unique for each myocardial region and it is relatively stable throughout the cardiac cycle. The displacement of this speckled pattern is considered to follow myocardial movement and the change between speckles represents myocardial deformation. With dedicated software, it is possible to accurately track these speckle patterns throughout the cardiac cycle. The resulting data provide both regional and global deformation (rate) in the longitudinal direction. Radial strain in the thin walled RV is unreliable and we do not recommend its use in the RV [18, 39]. An in depth review on image acquisition, post processing, interpretation and implementation of both techniques has been published [18].

Due to the longitudinal fiber orientation of the RV cardiomyocytes, the resulting RV systolic wall motion is predominantly longitudinal [40]. Thus, the base of the ventricle (annular plane) moves apically, while the active inward motion is minimal and predominantly a result of tethering/traction at the LV insertion sites [41]. Consequently, RV myocardial tissue deformation results in longitudinal systolic shortening (**Figure 6**). The RV lateral free wall recordings, acquired in the apical 4 chamber view, are feasible for deformation imaging (> 90%) in ARVD/C patients [17, 42, 43]. Limitations in temporal resolution and angle dependency exclude the anterior, inferior, and RVOT for optimal deformation imaging analysis. However, Greiner *et al.* [43] explored multi-plane strain imaging to assess the antero- and infero-lateral side of the RV free wall and reported a high feasibility (84%). The role of 3D-speckle tracking has been investigated by Atsumi *et al.* [44]. 3D-speckle tracking records endocardial surface changes during the cardiac cycle and may provide more information than 2D longitudinal deformation. Both multiplane- and 3D-speckle measurement of tracking are promising new applications in RV deformation imaging. However, further validation is needed before recommendations for clinical implementations can be made.

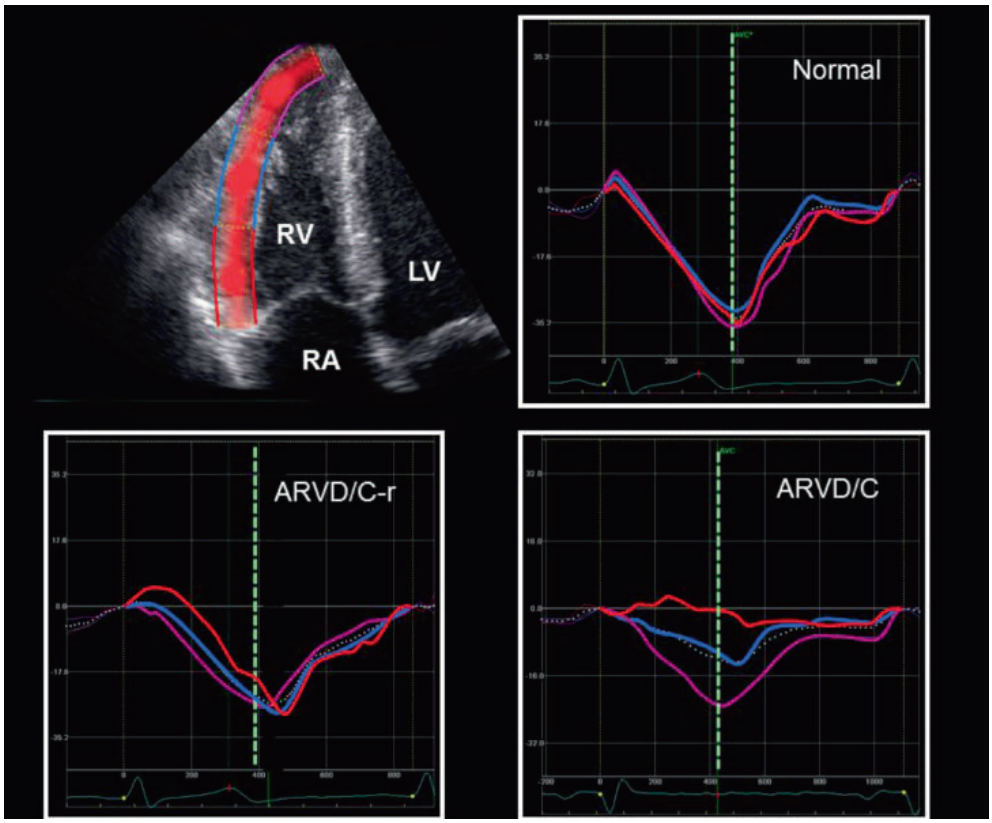

Figure 6. Tissue deformation imaging in arrhythmogenic right ventricular dysplasia/cardiomyopathy (ARVD/C)

Left upper: Tissue deformation imaging by speckle tracking. In the apical 4 chamber view the right ventricular (RV) lateral wall is traced and divided into the basal (red), mid (blue), and apical view (pink); Right upper: Normal RV deformation patterns with shortening during systole and stretching in diastole. All systolic strain values are approximately –30%. Cut off value is –18% to differentiate between normal and abnormal peak systolic strain; Left lower: RV deformation pattern in an ARVD/C relative. The apical (pink) and mid segment (blue) shows normal deformation. However, the basal (red) curve showed marked prestretch, delayed onset of shortening, and post-systolic shortening. In this patient, abnormal subtricuspid deformation was seen in absence of structural abnormalities according to the 2010 revised Task Force criteria; Right lower: RV deformation pattern in an ARVD/C patient. The apical segment (pink) shows normal deformation. Mid segment shows lower values of systolic peak strain (< –18%) and post-systolic shortening. The basal segment shows a dyskinetic pattern with stretching during systole; LV = left ventricular; RA = right atrium.

A major advantage of tissue deformation imaging compared to conventional echocardiographic wall motion analysis, is the ability to quantify regional wall motion rather than visual qualitative assessment. Quantifying wall motion facilitates the detection of subtle regional myocardial dysfunction. However, deformation imaging analysis is not hampered by visual misinterpretation of wall motion caused by tissue tethering. A third advantage is the ability to compare different myocardial segments over time to measure mechanical synchrony.

Systolic deformation

In this section, we provide the current published applications in deformation imaging. As previously mentioned, fibrofatty replacement of the myocardium subsequently impairs wall motion at specific sites in the RV. This is reflected by a reduced amount of peak systolic strain in the RV free wall in ARVD/C patients compared to controls (**Figure 6**) [20, 36, 45]. Peak systolic strain seems to be a reliable measurement of impaired wall motion and has high diagnostic value [17, 20, 42, 46, 47]. Moreover, deformation imaging reveals subtle wall motion abnormalities often in the absence of RV dilatation, global RV systolic function, and visual wall motion abnormalities [17]. Therefore, diagnostic performance of peak systolic strain was found to be superior to conventional measurements in ARVD/C patients [17, 42, 47]. A cut-off value of –18% peak systolic strain, to differentiate between normal and abnormal RV segments, seems to be a reliable parameter and was reported by Prakasa *et al.* [47]. Diagnostic performance was measured by Teske *et al.* [17] who found sensitivity of 97% and a specificity of 91%. Implementations of these findings (systolic peak strain and the presence of post-systolic shortening, in asymptomatic ARVD/C mutation carriers showed abnormalities in 71% of patients even though imaging criteria were not met by the 2010 TFC) [28]. While these measurements are very sensitive to detect regional contractility abnormalities, they lack specificity since other disease processes affecting the myocardium (ischemia, sarcoidosis, etc.) also produce a reduction of deformation parameters.

Beside regional wall motion analysis, deformation imaging also provides accurate measurements of global systolic RV function. In a (partial) ARVD/C cohort, mean RV free wall peak strain showed the strongest correlation with MRI obtained RVEF compared to other conventional 2D systolic parameters [48]. Several studies suggest an important role of exercise in the pathogenesis of ARVD/C [49, 50]. Extensive exercise seems to accelerate the course of disease. Acute effect of exercise on cardiac function was explored with stress echocardiography by Vitarelli *et al.* [42]. The normal increase in both RV and LV global longitudinal shortening was reduced after exercise in ARVD/C patients compared to controls. This is most likely explained by the fact that higher loading conditions in the RV during exercise unmask abnormal segments that have normal function in the normal (low pressure – low volume) resting situation. Diagnostic performance of these parameters exceeded both conventional measurements and regional longitudinal strain parameters. Both sensitivity and specificity were reported as greater than 90% [42].

Deformation after pulmonary valve closure

Post-systolic shortening (PSS) is an additional deformation imaging-derived parameter frequently detected in ARVD/C [28]. PSS is defined as the presence of longitudinal shortening after semilunar valve closure (i.e. pulmonary valve) [51]. It is a well described phenomenon in both ischemic- and non-ischemic cardiomyopathies [51–53]. The exact mechanism of PSS

is unclear. In a dyskinetic segment, PSS may originate as passive recoil by tissue interaction with surrounding contracting segments [45]. PSS could also be explained by local differences in electro-mechanical delay resulting in an out of phase active contraction [53]. Post-systolic shortening was found in 77.4% of the ARVD/C patients in the subtricuspid area [17]. Moreover, post-systolic shortening is proven to be an early sign of disease in asymptomatic *PKP2* mutation carriers (64%) without an established phenotypic expression of disease and could be of value in diagnosing ARVD/C (**Figure 6**) [28].

Dispersion of timing

Evidence is accumulating that electrical abnormalities precede structural alterations in ARVD/C [5, 54]. Consequently, early phenotypic expressions of ARVD/C would likely be of electrical-rather than structural origin. Due to the electro-mechanical contraction coupling, delay in myocardial electrical activation could be studied by mechanical activation patterns [55–57]. The high temporal resolution of echocardiography makes deformation imaging a suitable tool for measuring mechanical dyssynchrony. Measurements of dyssynchrony could provide evidence of early, subtle electrical disturbances in ARVD/C, and may further improve the diagnostic value of echocardiography [21, 58]. Moreover, due to the close relationship with electrical dyssynchrony, or electrical activation delay, mechanical dyssynchrony also contains possible prognostic information in predicting future arrhythmic events [21].

RV mechanical dyssynchrony in ARVD/C patients was first described by measuring time to peak velocity [58]. Tops *et al.* [58] showed marked delay in timing of septal and RV free wall peak velocity in ARVD/C compared to controls, indicating RV mechanical delay. Regional time to systolic peak data was analyzed by Sarvari *et al.* [21] and showed that dispersion of time to peak systolic value within the RV was markedly increased in ARVD/C patients compared to controls. They also found this effect in asymptomatic ARVD/C mutation carriers not fulfilling 2010 TFC, indicating early diagnostic value of mechanical dyssynchrony. Increased mechanical dispersion, probably due to the close correlation with electrical dyssynchrony, was also correlated with the occurrence of ventricular arrhythmias in ARVD/C patients [21].

DISCUSSION

Echocardiography is a non-invasive imaging tool that has an established role in both diagnosis and prognosis of ARVD/C patients [12, 24]. Early and accurate diagnosis of ARVD/C is pivotal, since lethal ventricular arrhythmias may occur in the very early stages of ARVD/C before overt structural alterations appear [59]. The current 2010 TFC echocardiographic measurements are not considered equally reliable as MRI based measurements [14]. Specifically, the difficult detection of regional wall abnormalities results in low sensitivity of echocardiography [14].

Several groups have shown the incremental diagnostic value of new echocardiographic tools such as 3D-echocardiography and tissue deformation imaging, and this could change the diagnostic role of echocardiography in ARVD/C.

Recent advances in 3D-echocardiography could improve assessment of RV volume and RV function and may prevent false-negative findings if performed together with other established conventional echocardiographic parameters [36]. Adding tissue deformation imaging derived parameters, especially peak systolic strain, could increase the yield of ARVD/C echocardiographic TFC [17, 20, 36, 46].

Recent insights into the pathophysiology of ARVD/C emphasize the importance of further exploring the parameters of mechanical dyssynchrony [5, 54]. Mechanical activation parameters derived from tissue deformation imaging could be of incremental value, especially the early detection of ARVD/C [55–57].

Risk stratification in ARVD/C mutation carriers is hampered by the large variability of both penetrance and disease severity (phenotypic expression) during the course of the disease. MRI is often not feasible for the periodical follow-up of ARVD/C patients due to the high rate of ICD implantation and the relative high cost. Thus, identifying reliable echocardiographic predictors in both early and advanced stages of disease is of utmost importance. Prognostic echocardiographic factors are already established in the more advanced disease stages [22, 32]. Both echocardiographic measured RV dysfunction and LV systolic dysfunction are known predictors for adverse outcome in ARVD/C [19, 31, 27]. However, life-threatening arrhythmic events may occur before extensive global systolic dysfunction. Future studies should focus on the correlation of subtle regional dysfunction and dyssynchrony with cardiac events [21, 59]. A study on the comparison between deformation imaging derived regional abnormalities and electrical abnormalities found during an electrophysiological study has to be performed to validate the current findings in electromechanical dyssynchrony. Validation is of particular importance since a recent study showed a weak correlation between late gadolinium contrast enhanced regions by MRI and the electro-anatomical scar a by electrophysiological study [60].

Finally, subtle changes in volumes and function over time could also have incremental value in predicting cardiac events compared to conventional measurements.

Conclusions

Conventional echocardiography has an established role in diagnosis and prognosis of ARVD/C. Novel echocardiographic parameters, derived from 3D-RV echocardiography and RV tissue deformation imaging, are promising to improve diagnostic sensitivity and specificity. Further validation is mandatory. Nevertheless, new echocardiographic parameters, combined with conventional parameters, enhances detection of phenotypic expressions of ARVD/C and indicates that there is a current and future role for echocardiography in ARVD/C.

In the ARVD/C patient, both echocardiography and MRI will remain complementary imaging modalities in the near future. Novel validated echocardiographic parameters will have the capability to detect subtle regional changes for the purpose of early diagnosis in absence of global RV structural alterations. Serial echocardiographic examination will provide insight in the progression of ARVD/C. Identification of robust predictors of adverse clinical outcome will guide therapeutic strategies and may prevent life threatening events.

Acknowledgements
We thank Dr. Folkert J. Meijboom and Bastiaan A. Mast for providing their figures and artwork.

R1 R2 R3 R4 R5 R6 R7 R8 R9 R10 R11 R12 R13 R14 R15 R16 R17 R18 R19 R20 R21 R22 R23 R24 R25 R26 R27 R28 R29 R30 R31 R32 R33 R34 R35 R36 R37 R38 R39

R1
R2
R3
R4
R5
R6
R7
R8
R9
R10
R11
R12
R13
R14
R15
R16
R17
R18
R19
R20
R21
R22
R23
R24
R25
R26
R27
R28
R29
R30
R31
R32
R33
R34
R35
R36
R37
R38
R39

REFERENCES

1. Marcus FI, Fontaine GH, Guiraudon G et al. Right ventricular dysplasia: A report of 24 adult cases. *Circulation*, 1982; 65: 384–398.
2. Sen-Chowdhry S, Syrris P, McKenna WJ. Role of genetic analysis in the management of patients with arrhythmogenic right ventricular dysplasia/cardiomyopathy. *J Am Coll Cardiol*, 2007; 50: 1813–1821.
3. Cox MG, van der Zwaag PA, van der Werf C et al. Arrhythmogenic right ventricular dysplasia/cardiomyopathy: Pathogenic desmosome mutations in index-patients predict outcome of family screening: Dutch arrhythmogenic right ventricular dysplasia/cardiomyopathy genotype-phenotype follow-up study. *Circulation*, 2011; 123: 2690–2700.
4. Noorman M, van der Heyden MA, van Veen TA et al. Cardiac cell-cell junctions in health and disease: Electrical versus mechanical coupling. *J Mol Cell Cardiol*, 2009; 47: 23–31.
5. Cerrone M, Noorman M, Lin X et al. Sodium current deficit and arrhythmogenesis in a murine model of plakophilin-2 haploinsufficiency. *Cardiovasc Res*, 2012; 95: 460–468.
6. Kim C, Wong J, Wen J et al. Studying arrhythmogenic right ventricular dysplasia with patient-specific iPSCs. *Nature*, 2013; 494: 105–110.
7. de Bakker JM, van Capelle FJ, Janse MJ et al. Slow conduction in the infarcted human heart. 'Zigzag' course of activation. *Circulation*, 1993; 88: 915–926.
8. Dalal D, Molin LH, Piccini J et al. Clinical features of arrhythmogenic right ventricular dysplasia/cardiomyopathy associated with mutations in plakophilin-2. *Circulation*, 2006; 113: 1641–1649.
9. Fressart V, Duthoit G, Donal E et al. Desmosomal gene analysis in arrhythmogenic right ventricular dysplasia/cardiomyopathy: Spectrum of mutations and clinical impact in practice. *Europace*, 2010; 12: 861–868.
10. Te Riele AS, James CA, Philips B, et al. Mutation-positive arrhythmogenic right ventricular dysplasia/cardiomyopathy: The triangle of dysplasia displaced. *J Cardiovasc Electrophysiol*, 2013; 24: 1311–1320.
11. Lindstrom L, Nylander E, Larsson H, Wranne B. Left ventricular involvement in arrhythmogenic right ventricular cardiomyopathy: A scintigraphic and echocardiographic study. *Clin Physiol Funct Imaging*, 2005; 25: 171–177.
12. Marcus FI, McKenna WJ, Sherrill D et al. Diagnosis of arrhythmogenic right ventricular cardiomyopathy/dysplasia: Proposed modification of the task force criteria. *Circulation*, 2010; 121: 1533–1541.
13. Tandri H, Macedo R, Calkins H et al. Role of magnetic resonance imaging in arrhythmogenic right ventricular dysplasia: Insights from the North American arrhythmogenic right ventricular dysplasia (ARVD/C) study. *Am Heart J*, 2008; 155: 147–153.
14. Borgquist R, Haugaa KH, Gilljam T et al. The diagnostic performance of imaging methods in ARVC using the 2010 Task Force criteria. *Eur Heart J Cardiovasc Imaging*, 2014; 15: 1219–1225.
15. Bomma C, Rutberg J, Tandri H et al. Misdiagnosis of arrhythmogenic right ventricular dysplasia/cardiomyopathy. *J Cardiovasc Electrophysiol*, 2004; 15: 300–306.
16. Sievers B, Addo M, Franken U, Trappe HJ. Right ventricular wall motion abnormalities found in healthy subjects by cardiovascular magnetic resonance imaging and characterized with a new segmental model. *J Cardiovasc Magn Reson*, 2004; 6: 601–608.
17. Teske AJ, Cox MG, De Boeck BW, Doevendans PA, Hauer RN, Cramer MJ. Echocardiographic tissue deformation imaging quantifies abnormal regional right ventricular function in arrhythmogenic right ventricular dysplasia/cardiomyopathy. *J Am Soc Echocardiogr*, 2009; 22: 920–927.
18. Teske AJ, De Boeck BW, Melman PG, Sieswerda GT, Doevendans PA, Cramer MJ. Echocardiographic quantification of myocardial function using tissue deformation imaging, a guide to image

acquisition and analysis using tissue Doppler and speckle tracking. *Cardiovasc Ultrasound*, 2007; 5: 27.

19. Prakasa KR, Dalal D, Wang J et al. Feasibility and variability of three dimensional echocardiography in arrhythmogenic right ventricular dysplasia/cardiomyopathy. *Am J Cardiol*, 2006; 97: 703–709.
20. Kjaergaard J, Hastrup Svendsen J, Sogaard P et al. Advanced quantitative echocardiography in arrhythmogenic right ventricular cardiomyopathy. *J Am Soc Echocardiogr*, 2007; 20: 27–35.
21. Sarvari SI, Haugaa KH, Anfinsen OG et al. Right ventricular mechanical dispersion is related to malignant arrhythmias: A study of patients with arrhythmogenic right ventricular cardiomyopathy and subclinical right ventricular dysfunction. *Eur Heart J*, 2011; 32: 1089–1096.
22. Saguner AM, Vecchiati A, Baldinger SH et al. Different prognostic value of functional right ventricular parameters in arrhythmogenic right ventricular cardiomyopathy/dysplasia. *Circ Cardiovasc Imaging* 2014; 7: 230–239.
23. Blomstrom-Lundqvist C, Beckman-Suurkula M, Wallentin I, Jonsson R, Olsson SB. Ventricular dimensions and wall motion assessed by echocardiography in patients with arrhythmogenic right ventricular dysplasia. *Eur Heart J*, 1988; 9: 1291–1302.
24. Yoerger DM, Marcus F, Sherrill D et al. Echocardiographic findings in patients meeting task force criteria for arrhythmogenic right ventricular dysplasia: new insights from the multidisciplinary study of right ventricular dysplasia. *J Am Coll Cardiol*, 2005; 45: 860–865.
25. Lindstrom L, Wilkenshoff UM, Larsson H, Wranne B. Echocardiographic assessment of arrhythmogenic right ventricular cardiomyopathy. *Heart*, 2001; 86: 31–38.
26. Rudski LG, Lai WW, Afilalo J et al. Guidelines for the echocardiographic assessment of the right heart in adults: a report from the American Society of Echocardiography endorsed by the European Association of Echocardiography, a registered branch of the European Society of Cardiology, and the Canadian Society of Echocardiography. *J Am Soc Echocardiog*, 2010; 23: 685–713.
27. Wang J, Prakasa K, Bomma C et al. Comparison of novel echocardiographic parameters of right ventricular function with ejection fraction by cardiac magnetic resonance. *J Am Soc Echocardiogr,* 2007; 20: 1058–1064.
28. Teske AJ, Cox MG, Te Riele AS et al. Early detection of regional functional abnormalities in asymptomatic ARVD/C gene carriers. *J Am Soc Echocardiogr*, 2012; 25: 997–1006.
29. Foale R, Nihoyannopoulos P, McKenna W et al. Echocardiographic measurement of the normal adult right ventricle. *Br Heart J*, 1986; 56: 33–44.
30. Tosoratti E, Badano LP, Gianfagna P et al. Improved delineation of morphological features of arrhythmogenic right ventricular cardiomyopathy with the use of contrast-enhanced echocardiography. *J Cardiovasc Med* (Hagerstown), 2006; 7: 566–568.
31. Lemola K, Brunckhorst C, Helfenstein U, Oechslin E, Jenni R, Duru F. Predictors of adverse outcome in patients with arrhythmogenic right ventricular dysplasia/cardiomyopathy: Long term experience of a tertiary care centre. *Heart*, 2005; 91: 1167–1172.
32. Pinamonti B, Dragos AM, Pyxaras SA et al. Prognostic predictors in arrhythmogenic right ventricular cardiomyopathy: Results from a 10-year registry. *Eur Heart J*, 2011; 32: 1105–1113.
33. Sen-Chowdhry S, Syrris P, Ward D, Asimaki A, Sevdalis E, McKenna WJ. Clinical and genetic characterization of families with arrhythmogenic right ventricular dysplasia/cardiomyopathy provides novel insights into patterns of disease expression. *Circulation*, 2007; 115: 1710–1720.
34. Teske AJ, Cox MG, Peterse MC, Cramer MJ, Hauer RN. Case report: Echocardiographic deformation imaging detects left ventricular involvement in a young boy with arrhythmogenic right ventricular dysplasia/cardiomyopathy. *Int J Cardiol*, 2009; 135: e24–e26.
35. Knight DS, Grasso AE, Quail MA et al. Accuracy and reproducibility of right ventricular quantification in patients with pressure and volume overload using single-beat three-dimensional echocardiography. *J Am Soc Echocardiogr*, 2015; 28: 363–374.

R1 R2 R3 R4 R5 R6 R7 R8 R9 R10 R11 R12 R13 R14 R15 R16 R17 R18 R19 R20 R21 R22 R23 R24 R25 R26 R27 R28 R29 R30 R31 R32 R33 R34 R35 R36 R37 R38 R39

36. Kjaergaard J. Assessment of right ventricular systolic function by tissue Doppler echocardiography. *Dan Med J*, 2012; 59: B4409.
37. Bhave NM, Patel AR, Weinert L et al. Three-dimensional modeling of the right ventricle from two-dimensional transthoracic echocardiographic images: Utility of knowledge-based reconstruction in pulmonary arterial hypertension. *J Am Soc Echocardiogr*, 2013; 26: 860–867.
38. Dragulescu A, Grosse-Wortmann L, Fackoury C, Mertens L. Echocardiographic assessment of right ventricular volumes: A comparison of different techniques in children after surgical repair of tetralogy of Fallot. *Eur Heart J Cardiovasc Imaging*, 2012; 13: 596–604.
39. Kannan A, Poongkunran C, Jayaraj M, Janardhanan R. Role of strain imaging in right heart disease: a comprehensive review. *J Clin Med Res*, 2014; 6: 309–313.
40. Carlsson M, Ugander M, Heiberg E, Arheden H. The quantitative relationship between longitudinal and radial function in left, right, and total heart pumping in humans. *Am J Physiol Heart Circ Physiol*, 2007; 293: H636–H644.
41. Gustafsson U, Lindqvist P, Waldenstrom A. Apical circumferential motion of the right and the left ventricles in healthy subjects described with speckle tracking. *J Am Soc Echocardiogr*, 2008; 21: 1326–1330.
42. Vitarelli A, Cortes Morichetti M, Capotosto L et al. Utility of strain echocardiography at rest and after stress testing in arrhythmogenic right ventricular dysplasia. *Am J Cardiol* 2013; 111: 1344–1350.
43. Greiner S, Heimisch M, Aurich M, Hess JA, Katus HA, Mereles D. Multiplane two-dimensional strain echocardiography for segmental analysis of right ventricular mechanics: New-RV study. *Clin Res Cardiol*, 2014; 103: 817–824.
44. Atsumi A, Ishizu T, Kameda Y et al. Application of 3-dimensional speckle tracking imaging to the assessment of right ventricular regional deformation. *Circ J*, 2013; 77: 1760–1768.
45. Herbots L, Kowalski M, Vanhaecke J, Hatle L, Sutherland GR. Characterizing abnormal regional longitudinal function in arrhythmogenic right ventricular dysplasia. The potential clinical role of ultrasonic myocardial deformation imaging. *Eur J Echocardiogr*, 2003; 4: 101–107.
46 Aneq MA, Engvall J, Brudin L, Nylander E. Evaluation of right and left ventricular function using speckle tracking echocardiography in patients with arrhythmogenic right ventricular cardiomyopathy and their first degree relatives. *Cardiovasc Ultrasound* 2012; 10: 37.
47. Prakasa KR, Wang J, Tandri H et al. Utility of tissue Doppler and strain echocardiography in arrhythmogenic right ventricular dysplasia/cardiomyopathy. *Am J Cardiol*, 2007; 100: 507–512.
48. Focardi M, Cameli M, Carbone SF et al. Traditional and innovative echocardiographic parameters for the analysis of right ventricular performance in comparison with cardiac magnetic resonance. *Eur Heart J Cardiovasc Imaging*, 2015; 16: 47–52.
49. Sawant AC, Bhonsale A, Te Riele AS et al. Exercise has a disproportionate role in the pathogenesis of arrhythmogenic right ventricular dysplasia/cardiomyopathy in patients without desmosomal mutations. *J Am Heart Assoc*, 2014; 3: e001471. doi: 10.1161/JAHA.114.001471.
50. James CA, Bhonsale A, Tichnell C et al. Exercise increases age-related penetrance and arrhythmic risk in arrhythmogenic right ventricular dysplasia/cardiomyopathy-associated desmosomal mutation carriers. *J Am Coll Cardiol*, 2013; 62: 1290–1297.
51. Weidemann F, Niemann M, Herrmann S et al. A new echocardiographic approach for the detection of non-ischaemic fibrosis in hypertrophic myocardium. *Eur Heart J*, 2007; 28: 3020–3026.
52. Skulstad H, Edvardsen T, Urheim S et al. Postsystolic shortening in ischemic myocardium: Active contraction or passive recoil? *Circulation*, 2002; 106: 718–724.
53. Hui W, Slorach C, Dragulescu A, Mertens L, Bijnens B, Friedberg MK. Mechanisms of right ventricular electromechanical dyssynchrony and mechanical inefficiency in children after repair of tetralogy of fallot. *Circ Cardiovasc Imaging*, 2014; 7: 610–618.

54. Te Riele AS, James CA, Rastegar N et al. Yield of serial evaluation in at-risk family members of patients with ARVD/C. *J Am Coll Cardiol*, 2014; 64: 293–301.

55. De Boeck BW, Teske AJ, Leenders GE et al. Detection and quantification by deformation imaging of the functional impact of septal compared to free wall preexcitation in the Wolff-Parkinson-White syndrome. *Am J Cardiol*, 2010; 106: 539–546.e532.

56. Prinzen FW, Augustijn CH, Allessie MA, Arts T, Delhaas T, Reneman RS. The time sequence of electrical and mechanical activation during spontaneous beating and ectopic stimulation. *Eur Heart J*, 1992; 13: 535–543.

57. Wyman BT, Hunter WC, Prinzen FW, McVeigh ER. Mapping propagation of mechanical activation in the paced heart with MRI tagging. *Am J Physiol*, 1999;276: H881–H891.

58. Tops LF, Prakasa K, Tandri H et al. Prevalence and pathophysiologic attributes of ventricular dyssynchrony in arrhythmogenic right ventricular dysplasia/cardiomyopathy. *J Am Coll Cardiol*, 2009; 54: 445–451.

59. Corrado D, Basso C, Thiene G. Sudden cardiac death in young people with apparently normal heart. *Cardiovasc Res*, 2001; 50: 399–408.

60. Marra MP, Leoni L, Bauce B et al. Imaging study of ventricular scar in arrhythmogenic right ventricular cardiomyopathy: comparison of 3D standard electroanatomical voltage mapping and contrast-enhanced cardiac magnetic resonance. *Circ Arrhythm Electrophysiol*, 2012; 5: 91–100.

R1
R2
R3
R4
R5
R6
R7
R8
R9
R10
R11
R12
R13
R14
R15
R16
R17
R18
R19
R20
R21
R22
R23
R24
R25
R26
R27
R28
R29
R30
R31
R32
R33
R34
R35
R36
R37
R38
R39

PART II

THE ONGOING QUEST FOR EARLY DISEASE DETECTION IN ARVC

CHAPTER 3

Prolonged Electromechanical Interval Unmasks Arrhythmogenic Right Ventricular Dysplasia/ Cardiomyopathy in the Subclinical Stage

Thomas P Mast, Arco J Teske, Anneline SJM Te Riele, Judith A Groeneweg, Jeroen F van der Heijden, Birgitta K Velthuis, Peter Loh, Pieter A Doevendans, Toon A van Veen, Dennis Dooijes, Jacques M de Bakker, Richard N Hauer [§], Maarten J Cramer [§]

§ contributed equally to this work.

J Cardiovasc Electrophysiol. 2016 Mar;27(3):303-14

ABSTRACT

Introduction: Arrhythmogenic right ventricular dysplasia/cardiomyopathy (ARVD/C) is characterized by high incidence of ventricular arrhythmias. Overt ARVD/C is preceded by a subclinical stage with lack of detectable ECG and structural abnormalities. Activation delay is present before structural abnormalities and is a hallmark of arrhythmogenesis. Deformation imaging may unmask activation delay in the subclinical stage.

Methods: Three groups were compared: (1) mutation-positive definite ARVD/C-patients fulfilling 2010 Task Force criteria (TFC) (n = 44); (2) asymptomatic mutation carriers not fulfilling TFC and without history of ventricular arrhythmias (n = 31); and (3) controls (n = 30). All underwent ECG and echocardiographic deformation imaging. As a surrogate for local activation delay the electromechanical interval (EMI) was measured, defined as time between onset-QRS and onset of shortening. Arrhythmic outcome (PVC-count, VT) of asymptomatic mutation carriers was correlated with EMI and ECG TFC.

Results: In definite ARVD/C-patients, EMI was prolonged in all lateral RV segments. In asymptomatic mutation carriers, prolonged EMI was detected in the subtricuspid area in 14/31. Terminal activation duration ≥55 milliseconds (definition: supporting information) was the only ECG abnormality in this group (8/31). After a mean follow-up of 4.2 ± 3.1 years 10/31 asymptomatic mutation carriers experienced arrhythmic outcome. Prolonged subtricuspid EMI was the only parameter significantly associated with arrhythmogenesis during follow-up.

Conclusion: In ARVD/C-patients, EMI prolongation was present throughout the RV. In asymptomatic mutation carriers, prolonged EMI in the subtricuspid area is often detected without any additional abnormalities. These preliminary results indicate that prolonged EMI is a new parameter unmasking activation delay in the subclinical stage and may contribute to risk stratification.

INTRODUCTION

Arrhythmogenic right ventricular dysplasia/cardiomyopathy (ARVD/C) is an inherited progressive cardiomyopathy clinically characterized by ventricular arrhythmias.[1] Sudden cardiac death (SCD) might be a first presentation of ARVD/C especially in young individuals.[2] Typically, affected individuals present with symptomatic ventricular arrhythmias predominantly originating from the right ventricle (RV), between the second and fourth decade of life, in the overt stage of disease.[3] At that stage ARVD/C is often undoubtedly diagnosed using the revised 2010 Task Force criteria (TFC).[4] However, overt disease is preceded by an asymptomatic subclinical stage with lack of detectable electrocardiographic (ECG) and structural abnormalities.[5] Early detection of subclinical ARVD/C might be of incremental value to risk stratify ARVD/C mutation carriers.

In 40–60% of ARVD/C-patients, pathogenic mutations are identified in genes predominantly encoding desmosomal proteins that may affect mechanical cell-cell coupling.[6-8] Accumulating evidence suggests that altered desmosomes are associated with redistribution of other intercalated disk proteins, including gap junctions (Connexin43) and ion channels (Nav1.5), resulting in electrical uncoupling and slow conduction, respectively.[9] Studies in mouse models have shown that these molecular alterations may occur in the absence of structural heart disease, giving rise to the hypothesis that these molecular changes precede cell death and fibrofatty replacement.[10] Tissue architecture will be modified by these late histopathologic alterations resulting in lengthened conduction pathways around fibrotic areas and load mismatch.[11, 12] Thus, in overt ARVD/C, both molecular and histopathologic changes promote electrical activation delay, providing substrates for reentry and ventricular arrhythmias.[11, 13, 14] However, in early ARVD/C stages activation delay may be predominantly due to the intercalated disk molecular protein redistribution.[10] Early detection of activation delay will facilitate ARVD/C recognition in the subclinical stage and may contribute to risk stratification.[15, 16]

Although activation delay can be assessed with invasive electrical activation mapping during an electrophysiologic study (EPS), this method is inappropriate for asymptomatic subjects.[17] Activation delay can also be detected on standard 12-lead ECG recordings derived from the right precordial leads (V_1–V_3) as epsilon waves and prolonged terminal activation duration (TAD).[4, 18] However, the anterior–superior positioning of these leads will predominantly detect electrical data from the RV outflow tract (RVOT). During normal sinus rhythm the RVOT is physiologically the latest activated part of the ventricular myocardium, facilitating ECG detection of even minor additional activation delay in ARVD/C.[19] In physiologically earlier activated parts minor activation delay may remain buried within the QRS complex, and thus invisible.[14] The signal averaged ECG is hampered by the same limitation.

Echocardiographic deformation imaging is an alternative noninvasive technique providing insight into local ventricular contraction patterns. This technique combined with ECG can be used to measure the electromechanical interval (EMI), defined as the interval between the onsets of QRS complex and local ventricular contraction, respectively.[20] Recently, our group provided evidence of subtricuspid involvement in the early phase of ARVD/C.[21] The present study tested the hypothesis that in ARVD/C EMI is prolonged at various physiologically relatively early activated RV sites, most pronounced in the subtricuspid area, and is associated with arrhythmic outcome during follow-up.

METHODS

Study Population

Between 2006 and 2014, 105 subjects (age>18 years old, 3 groups) were included and all underwent standard 12-lead surface ECG recording, 24-hour Holter monitoring, and echocardiography. The first group consisted of 44 definite (either 2 major, or 1 major and 2 minor, or 4 minor criteria) ARVD/C-patients according to 2010 TFC, and all carried pathogenic desmosomal mutations in *PKP2* (n = 39) or *DSG2* (n = 5) (*Supplementary Table A*).[2, 4] The second group consisted of 31 asymptomatic *PKP2* (n = 28) or *DSG2* (n = 3) mutation carriers not fulfilling ARVD/C diagnosis according to 2010 TFC; this was defined as the subclinical ARVD/C cohort. They were ascertained by family screening and were first-degree relatives of mutation-positive ARVD/C index-patients (probands). In this second group, history of ventricular tachycardia (VT), >500 premature ventricular complexes (PVC)/24 hours, or other symptoms related to ARVD/C were absent by definition. The 2010 TFC were applied in family members and not the Hamid criteria.[4, 22] The remaining control group consisted of healthy volunteers (n = 30) with no history of heart disease. Further details are depicted in **Figure 1**. A subgroup of 26 definite ARVD/C-patients, 19 asymptomatic mutation carriers, and all control subjects underwent cardiac magnetic resonance (CMR) imaging. The study was approved by the local institutional ethics review board.

Electrocardiography

All subjects underwent standard 12-lead ECG (recorded at rest, low pass filter of 100 Hz, 10 mm/mV at paper speed 25 mm/s), which was evaluated for depolarization (epsilon waves and terminal activation duration (TAD) ≥55 milliseconds), and repolarization (T-wave inversion in V_1 to V_2 or beyond) criteria according 2010 TFC.[4, 18] ECG analyses were performed by two experienced observers (R.N.H., J.A.G.) blinded for study group and echocardiographic measurements. For definitions, see *Supplementary Table B*.

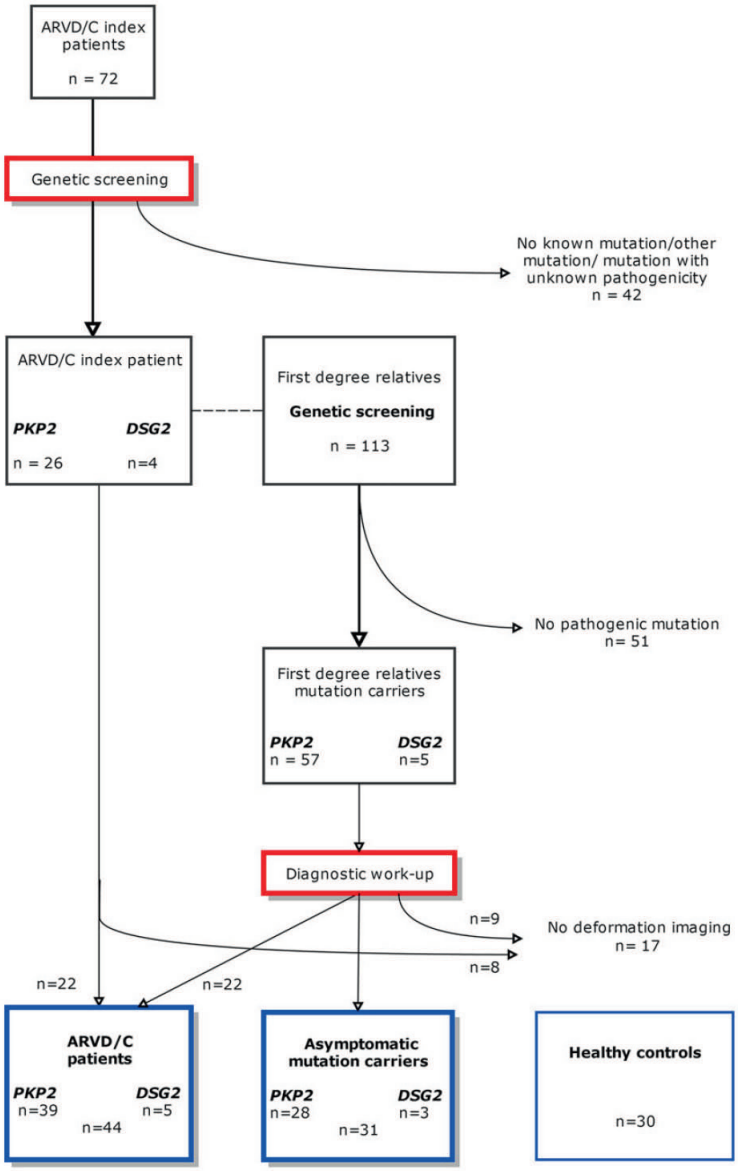

Figure 1. Flowchart of study groups
DSG2=desmoglein-2; *PKP2*=plakophilin-2.

Echocardiography

Echocardiography was performed on the same day as ECG recording with standard recordings as well as additional views of RV.[23-25] All examinations were analyzed for fulfillment of 2010 TFC, defined as akinesia, dyskinesia, or aneurysm, combined with RVOT enlargement

or decreased RV-fractional area change (RV-FAC).[4] RV-FAC≤33% was considered abnormal global RV systolic function.[4] Left ventricular (LV) global systolic function was measured as LV ejection fraction (LVEF) by the Simpson biplane method.[23] Global LV systolic function was considered abnormal if LVEF<50%.

Tissue deformation imaging

We described our protocol for analyzing RV deformation patterns by 2D-Speckle-Tracking previously.[26] In brief, real-time 2D (B-mode) small angle ultrasound data from the RV free wall were recorded in the (modified) apical four-chamber view.[25] Data were exported for offline analysis with dedicated software (EchoPAC version 11.2 revision 1.1; GE Vingmed Ultrasound AS). Doppler flow curves of the cardiac valves were used for timing cardiac events, and all timing information was aligned through ECG traces. A frame rate of 70–110 frames/s was implemented to ensure optimal tracking. Using a two step-tracking algorithm a region of interest was manually traced along the RV endocardial border from base to apex at the end of systole, with the width set to match the wall thickness. During post-processing only single wall recordings were available at the time of analysis to ensure optimal blinding. The RV free wall was divided into the basal (subtricuspid), mid-, and apical segment.

Electromechanical interval (EMI)

EMI was defined as the time interval between first electrical deflection of the QRS complex on the simultaneous ECG recording and onset of local myocardial shortening as measured by 2D-Speckle-Tracking (as shown in **Figure 2**). Measurement of EMI was performed by an experienced observer (T.P.M.), blinded for the study group. For definitions, see *Supplementary Table B*.

Cardiac Magnetic Resonance (CMR) Imaging

CMR-imaging was performed within 12 months of the ECG and echocardiogram, on a 1.5 Tesla MRI scanner (Achieva, Philips Healthcare, Best, The Netherlands), according to standard ARVD/C protocols.[27] CMR studies were analyzed for structural alterations fulfilling 2010 TFC, defined as akinesia or dyskinesia, combined with enlarged RV end-diastolic volume (RV-EDV) or reduced RV-ejection fraction (RVEF).[4] Structural alteration was considered to be present if detected by echocardiography or CMR.[4] RV function was considered abnormal if RV-EF≤40%.[4] LV global systolic function was measured as LVEF (LVEF<50% was considered abnormal). RV-EDV ≥110 mL/m^2 in males, and ≥100 mL/m^2 in females was considered as enlarged.[4] In addition, late enhancement of intravenously administered gadolinium was used to identify areas with myocardial fibrosis.

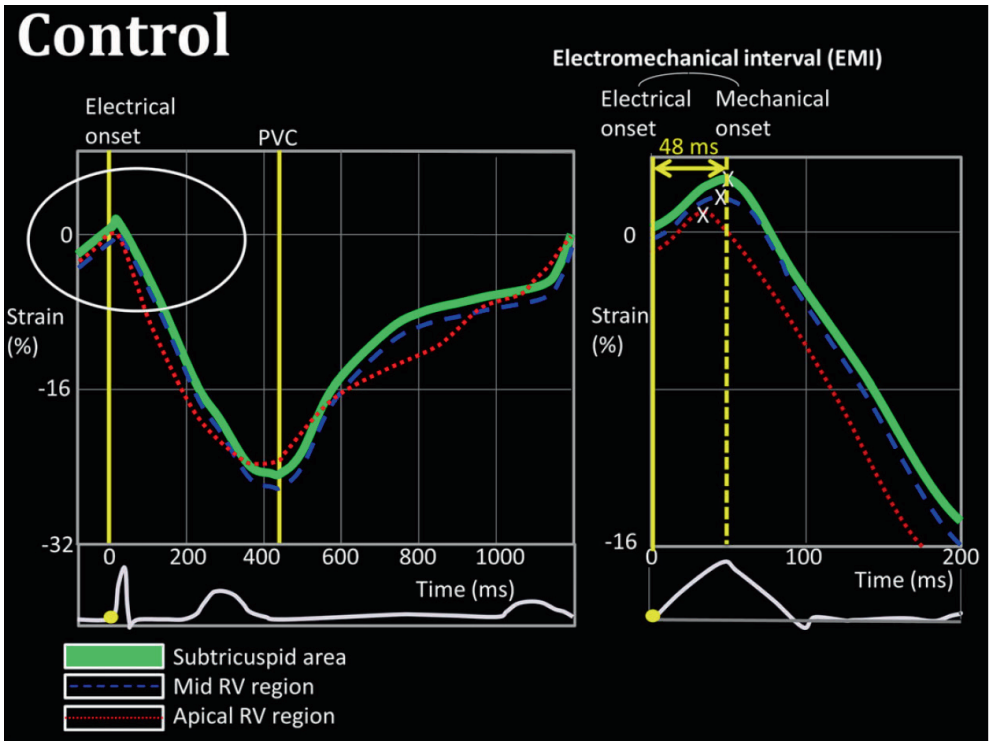

Figure 2. Measurement of the electro-mechanical interval
Deformation imaging derived myocardial shortening curve of the subtricuspid, mid-, and apical segment of the RV free wall in a normal subject. The electro-mechanical interval (EMI) is defined as the time between the first electrical deflection of QRS complex (electrical onset, yellow dot) and onset of local mechanical shortening (mechanical onset, white-X). Measurement of EMI is magnified on the right. Subtricuspid EMI was measured 48 milliseconds. ECG showed sinus rhythm with no signs of activation delay. PVC = pulmonary valve closure.

Follow-Up and Outcome Measure in Asymptomatic Mutation Carriers

All asymptomatic mutation carriers were prospectively followed at yearly intervals. Arrhythmic outcome was defined as the occurrence of non-sustained VT or an increase of PVC >500/24 hours during Holter monitoring (*Supplementary Table B*). Prolonged EMI and each element of 2010 TFC were tested as potential predictors for arrhythmic outcome in asymptomatic mutation carriers.[4]

Statistical Analyses

Continuous data are presented as mean ± standard deviation (SD) and categorical variables as numbers or percentages. Variables were tested for normal distribution using the Shapiro-Wilk test. Differences in continuous data between either ARVD/C-patients, asymptomatic mutation carriers, or controls were calculated using the independent Student t-test, ANOVA

in normally distributed data, and Mann-Whitney U-test or Kruskal-Wallis test in non-normally distributed data. For categorical data, Fisher's exact test or chi-square was used to compare differences between groups. P-values <0.05 were considered to indicate statistical significance. An optimal cut-off value for discriminating between prolonged and normal EMI was assessed by ROC-statistics. Freedom of arrhythmic outcome was analyzed by Kaplan-Meier statistics and log-rank test.

A second observer (A.J.T.) analyzed EMI in all three RV segments in a random sample of 25 subjects of the total population for calculation of interobserver variability. Reproducibility was measured by Cohen's Kappa-coefficient, coefficient of variations (SD of the difference between observers divided by the mean of measurements), and Bland–Altman plots. Statistical calculations were made using commercially available software (IBM SPSS Statistics for Windows, Version 21.0, IBM Corp, Armonk, NY, USA and GraphPad-Prism version 6.00 for Windows, GraphPad Software, La Jolla, CA, USA).

RESULTS

Baseline Characteristics

Baseline and clinical characteristics are summarized in **Table 1**. ARVD/C-patients were significantly older compared to controls (45.9 ± 15.5 and 36.7 ± 8.2 years, respectively). Most common first presentation in ARVD/C-patients was monomorphic sustained VT (n = 19).

In ARVD/C-patients, depolarization and repolarization abnormalities according to 2010 TFC were identified in 68% and 77%, respectively. In total, 93% of ARVD/C-patients fulfilled one or more ECG criteria. RV dimensions were enlarged and both RV and LV systolic function were decreased in ARVD/C-patients compared to controls. Abnormal RV function (RV-FAC≤33%) was detected in 59%, and abnormal LV function (LVEF<50%) in 11%. In ARVD/C-patients, structural alterations according to 2010 TFC detected by echocardiography and CMR were found in, respectively, 91% and 81% (**Table 1**). Late enhancement in the RV was present in 14/26 of the ARVD/C-patients, predominantly located in the basal RV free wall. LV late enhancement was detected in 5/26 patients, exclusively in the posterolateral wall. All ARVD/C-patients with late enhancement fulfilled 2010 TFC for structural alterations.

In asymptomatic mutation carriers prolonged TAD was the only ECG abnormality recorded in a minority (26%). Three subjects were identified with abnormal RV function (RV-FAC≤33%). However, none of the subjects fulfilled structural alterations according to 2010 TFC due to the absence of local RV dyskinesia or akinesia (**Table 1**). All asymptomatic mutation carriers had normal LV systolic function (LVEF≥50%). Late enhancement was not detected.

In controls, prolonged TAD was found in one subject. All conventional echocardiographic and CMR measurements were normal.

Table 1. Clinical characteristics

	ARVD/C patients (n=44)	Asymptomatic mutation carriers (n=31)	Controls (n=30)
Patient characteristics			
Age (y)	45.9±15.5*	29.7±14.1†	36.7±8.2
Male (%)	45%	39%	50%
ICD (n)	16	0	0
Proband – Family member	22 – 22	0 – 31	0 – 0
Pathogenic mutation	44	31	NA
Anti-arrhythmic drugs	31	0	0
Sotalol /Bisoprolol /Metoprolol /Disopyramide /Verapamil	24 / 2 / 2 / 2 / 1		
First presentation			
Ventricular fibrillation	1	0	NA
Sustained monomorphic VT	19	0	NA
Abnormal ECG	4	0	NA
Family screening	14	31	NA
Palpitations	6	0	NA
12-lead ECG			
Fulfillment of depolarization criteria (major- minor)	9 – 21	0 – 8	0 – 1
Epsilon wave	9	0	0
TAD ≥55ms	35	8	1
Fulfillment of repolarization criteria (major- minor)	27 – 7	0 – 0	0- 0
T-wave inversion V_1-V_3 or beyond	27		
T-wave inversion V_1-V_2	6		
T-wave inversion V_4-V_6	1		
T-wave inversion V_1-V_4 in presence of RBBB	0		
Structural alterations			
Fulfillment of structural criteria (major-minor)	34 – 6	0 – 0	0- 0
Echocardiography			
RV wall motion abnormalities	40	0	0
RVOT – PLAX (mm/m^2 ±SD)	18.5±3.8*	14.3±2.2	14.0±2.3
RVOT – PSAX (mm/m^2 ±SD)	19.1±4.0*	15.5±2.5	15.3±2.4
RV-FAC% (±SD)	32.1±9.3*	45.5±7.0	48.4±6.8
LVEF% (±SD)	57.3±6.9*	58.4±6.0†	62.6±3.4
CMR‡			
RV wall motion abnormalities	23/26	0	0
RV-EDV (ml/m^2 ±SD)	129.3±42.6*	86.1±17.6*	101.2±18.1
RVEF% (±SD)	37.7±11.3*	55.9±6.2	55.3±5.3
LVEF% (±SD)	54.8±11.9†	56.6±5.5	60.1±6.4
Arrhythmias (n)			
Fulfillment of arrhythmia criteria (major-minor)	16- 23	0 – 0	0- 0
PVC count / 24hrs - median (range)	2042 (43-11.180)	5 (0-124)	NA
Non-sustained VT	31	0	NA

Values are n/N, if not otherwise specified; *=P<0.01 compared to controls; †=P<0.05 compared to controls; NA=not applicable. All subjects were in sinus rhythm during ECG analyses. ‡=CMR was performed in a subgroup of 26 ARVD/C-patients, 19 asymptomatic mutation carriers, and all controls. RV wall motion abnormality was defined as the presence of a- or dyskinesia or aneurysm. ARVD/C = arrhythmogenic right ventricular dysplasia/cardiomyopathy; ICD = implantable cardioverter defibrillator; VT = ventricular tachycardia; ECG = electrocardiogram; ms = milliseconds; TAD = terminal activation duration; RBBB = right bundle branch block; RVOT = right ventricular outflow tract; PLAX/PSAX = parasternal long/short axis; mm = millimeter; RV-FAC = right ventricular–fractional area change; LVEF = left ventricular ejection fraction; CMR = cardiac magnetic resonance imaging; RV-EDV = right ventricular end-diastolic volume; RVEF = right ventricular ejection fraction; PVC = premature ventricular complex

R1 R2 R3 R4 R5 R6 R7 R8 R9 R10 R11 R12 R13 R14 R15 R16 R17 R18 R19 R20 R21 R22 R23 R24 R25 R26 R27 R28 R29 R30 R31 R32 R33 R34 R35 R36 R37 R38 R39

Electro-Mechanical Interval

ARVD/C-patients

EMI was significantly prolonged in the subtricuspid (basal), mid-, and apical RV free wall segments in ARVD/C-patients compared to controls (**Figs. 3A and 4**). Optimal cut-off values for discrimination between prolonged and normal EMI was 100 milliseconds for the subtricuspid area, whereas for both mid- and apical RV regions it was 65 milliseconds. Using the cut-off value for the subtricuspid area, 77% of ARVD/C-patients showed prolonged EMI in this area, being the most frequently involved area (**Figure 4**). The discriminative value of subtricuspid EMI was high with an area under the receiver–operating-curve of 0.94 (95CI:0.88–0.99) (**Figure 5**). By using 100 milliseconds as the cut-off value for prolonged subtricuspid EMI a sensitivity of 83% and specificity of 96% was reached. In the majority of ARVD/C-patients (71%) prolonged subtricuspid EMI was accompanied with ECG signs of activation delay or abnormal repolarization, and signs of structural alterations on echocardiography or CMR **(Figure 6, hatched bars**).

Asymptomatic mutation carriers

Asymptomatic mutation carriers showed prolonged EMI exclusively in the subtricuspid region, whereas other mean values were comparable to controls (**Figs. 3B and 4**). Forty-five percent of asymptomatic mutation carriers showed a prolonged EMI in the subtricuspid area using the 100-millisecond cut-off value and this was the most frequent abnormality compared to ECG or Holter abnormalities (electrical disease) (26%) and imaging parameters (0%) defined by 2010 TFC (**Figs. 4 and 6**). Prolonged EMI was the only sign of disease in 23% of this asymptomatic group in the absence of any ECG or structural abnormalities, other than mutation status. Signs of activation delay in the ECG and structural alterations were the first sign of disease in respectively 3% and 0% of asymptomatic mutation carriers (**Figure 6, solid bars**).

Feasibility and reproducibility

Measurement of EMI was feasible in 91% of the subjects and feasibility did not differ significantly between groups. Poor image quality and drop-out was the main reason for exclusion. Interobserver agreement for all EMI measurements was high with a Kappa value of 0.83. The coefficient of variation for measuring the subtricuspid EMI was 10.4%, with a perfect agreement (K = 1.0) in determining if subtricuspid EMI was prolonged. Bland–Altmann analyses showed no bias and good limits of agreement (*see Supplementary Table C*).

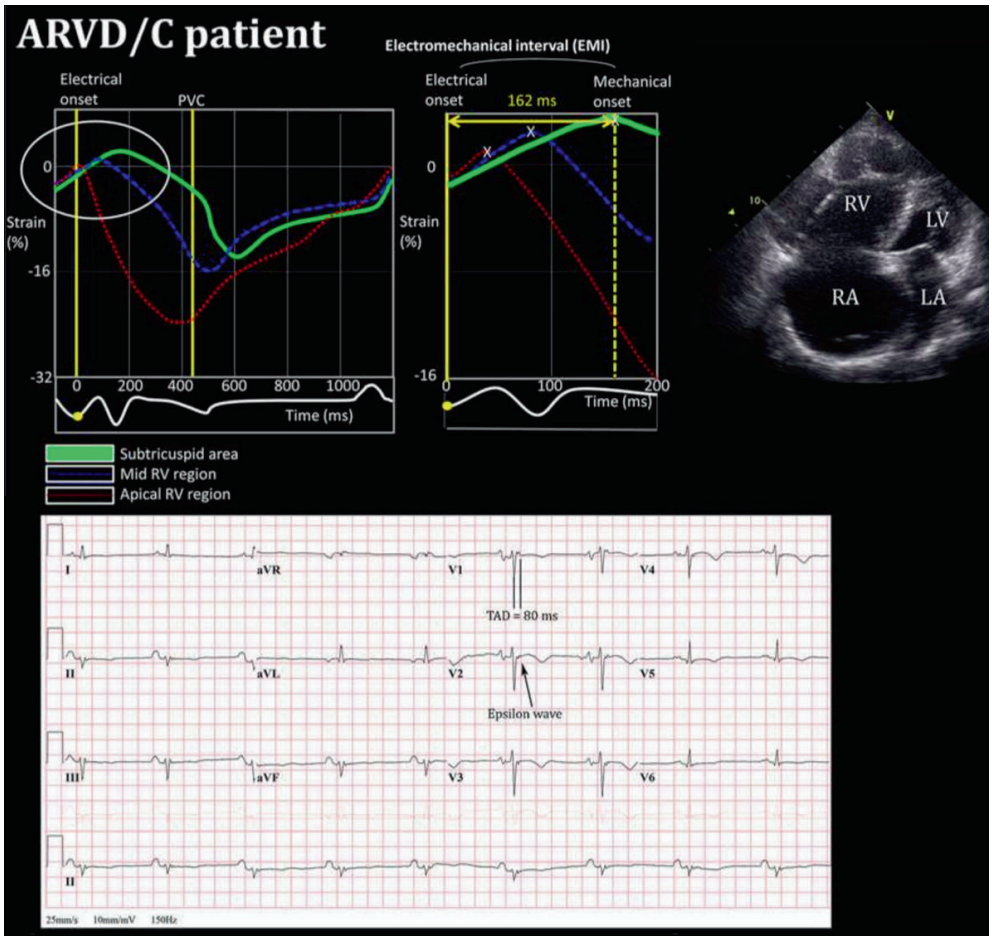

Figure 3A. Electrocardiogram, echocardiogram, and electro-mechanical interval—ARVD/C patient. Upper left: EMI measurements in a patient diagnosed with ARVD/C. The patient was identified with a pathogenic *PKP2* mutation (c.2386T>C,p.Cys796Arg). Prolonged EMI in the subtricuspid (green) and mid-RV region (blue), respectively, 162 and 74 milliseconds. In this patient, EMI was considered normal in the apical region, 41 milliseconds. PVC = pulmonary valve closure. Upper right: Echocardiographic apical four-chamber view with marked dilatation of the right ventricle (RV), and right atrium (RA). Multiple RV aneurysms are present. RV-fractional area change (RV-FAC%) is 15%. LV = left ventricle; LA = left atrium. Lower: ECG shows sinus rhythm, rate 52/min. Signs of enlarged right and left atrium. Ventricular left axis deviation. Signs of activation delay by prolonged terminal activation duration in V_1–V_3 and epsilon waves in V_2 (arrow). In addition, negative T waves in V_1–V_5 and slightly negative in II, III, and aVF

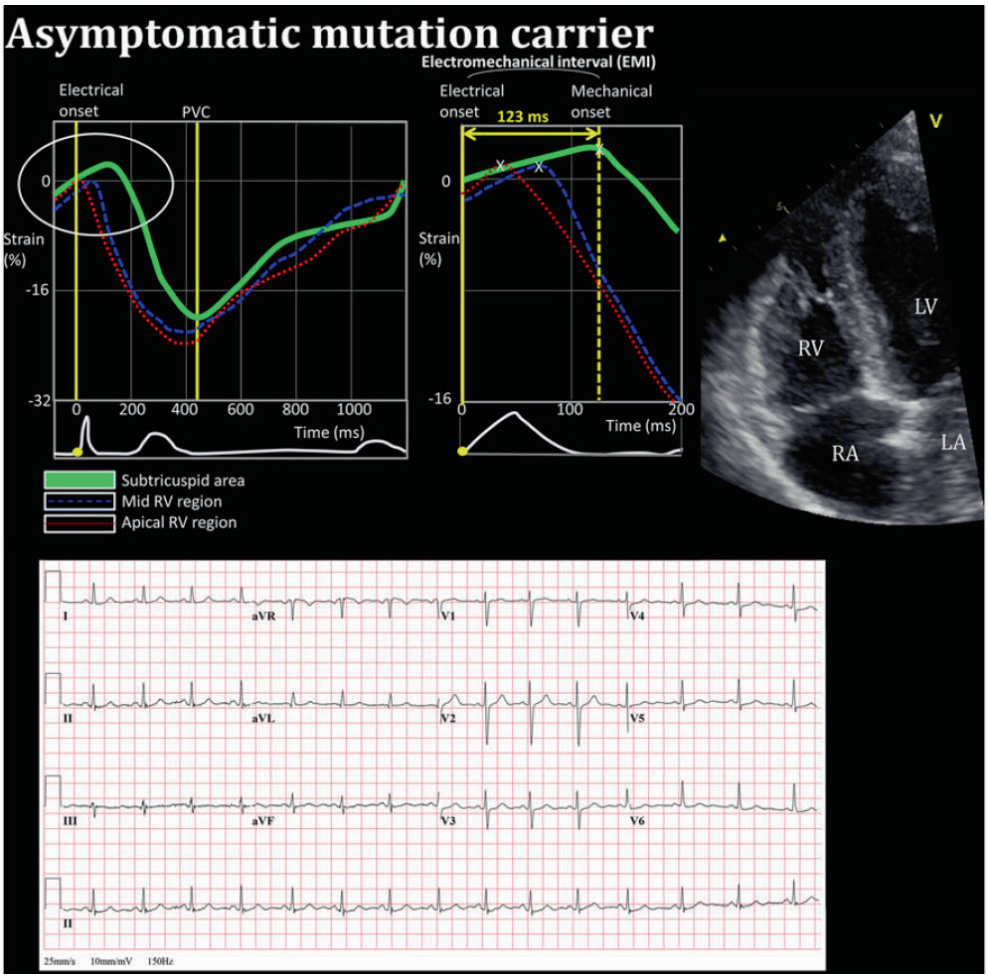

Figure 3B. Electrocardiogram, echocardiogram, and electro-mechanical interval—Asymptomatic mutation carrier

Electrocardiogram, echocardiogram, and electro-mechanical interval—asymptomatic mutation carrier. Upper left: EMI measurements in asymptomatic mutation carrier identified with a pathogenic *PKP2* mutation (c.397C>T,p.Gln133X). Upper right: Echocardiographic apical four-chamber view with normal dimensions of RV, RA, LV, and LA. No wall motion abnormalities. RV fractional area change (RV-FAC%) is 48%. Lower: ECG shows normal sinus rhythm, rate 90/min. Intermediate ventricular axis. No signs of ARVD/C and specifically no signs of activation delay. However, subtricuspid EMI is markedly prolonged (123 milliseconds).

Electro-mechanical interval (EMI)	ARVD/C patients (n = 44)	Asymptomatic mutation carriers (n=31)	Controls (n=30)	P-value Kruskal-Wallis
RV – subtricuspid – basal (ms)	183±107*	98±49*	56±29	P<0.0001
RV – mid (ms)	74±52*	53±28	39±23	P=0.001
RV – apex (ms)	61±63†	40±17	34±22	P=0.02

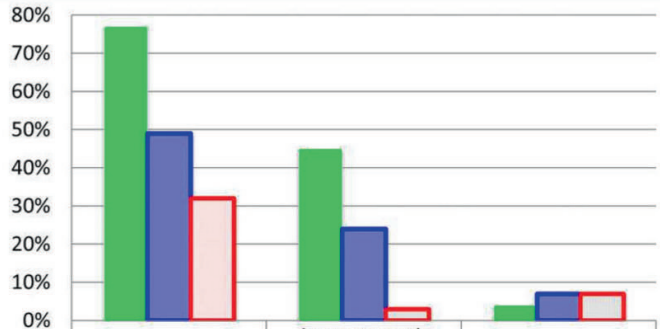

	ARVD/C	Asymptomatic mutation carriers	Controls
EMI - subtricuspid ≥ 100 ms	77%	45%	4%
EMI - mid ≥ 65 ms	49%	24%	7%
EMI - apex ≥ 65 ms	32%	3%	7%

Figure 4. Local electro-mechanical interval (EMI)
*P < 0.001 compared to controls; †P < 0.05 compared to controls. Upper table: Mean values of EMI in ARVD/C-patients, asymptomatic mutation carriers, and controls. EMI was prolonged in all RV segments for ARVD/C-patients compared to controls. In asymptomatic mutation carriers, mean EMI was only prolonged in the subtricuspid area. Lower figure: Prolongation of EMI was frequently present in the subtricuspid area in both ARVD/C-patients and asymptomatic mutation carriers. ARVD/C = arrhythmogenic right ventricular dysplasia/cardiomyopathy; EMI = electro-mechanical interval; ms = milliseconds.

Arrhythmic Outcome in Asymptomatic Mutation Carriers

Mean follow-up in asymptomatic mutation carriers was 4.2 ± 3.1 years. During follow-up, 10/31 asymptomatic mutation carriers experienced the arrhythmic outcome. Holter monitoring showed an increase of PVC >500/24 hours in eight subjects; in these eight subjects median PVC count was 890 (range: 504-6289). Nonsustained VT was recorded in two subjects.

In 14/31 asymptomatic mutation carriers prolonged subtricuspid EMI was detected at baseline. Of these 14, 8 asymptomatic mutation carriers experienced arrhythmic outcome. Subtricuspid EMI was significantly associated with arrhythmic outcome in the asymptomatic mutation carriers (P = 0.012) (**Figure 5**).

Besides carrying a pathogenic desmosomal mutation, the only established 2010 TFC present at baseline was prolonged TAD (n = 8). Prolonged TAD at baseline was also associated with an increased arrhythmic risk compared to normal TAD, 5/8 versus 5/23, respectively. However, this association was not significant (P = 0.09).

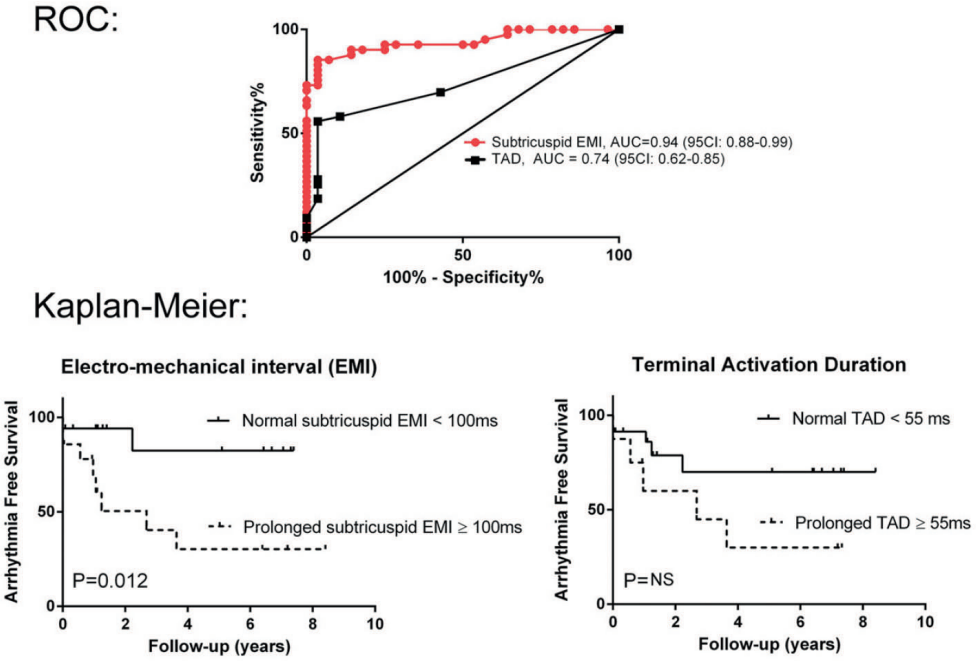

Figure 5. Diagnostic and predictive value of terminal activation duration and subtricuspid electro-mechanical interval.

Upper: ROC statistics showed statistically significant diagnostic value for subtricuspid EMI compared to terminal activation duration (TAD) ($P < 0.005$). Lower: In 10/31 asymptomatic mutation carriers an arrhythmic event occurred during follow-up and was significantly associated with prolonged subtricuspid EMI. ARVD/C = arrhythmogenic right ventricular dysplasia/cardiomyopathy; EMI = electro-mechanical interval; ms = milliseconds; NS = not statistically significant; ROC = receiver operator curve; TAD = terminal activation duration

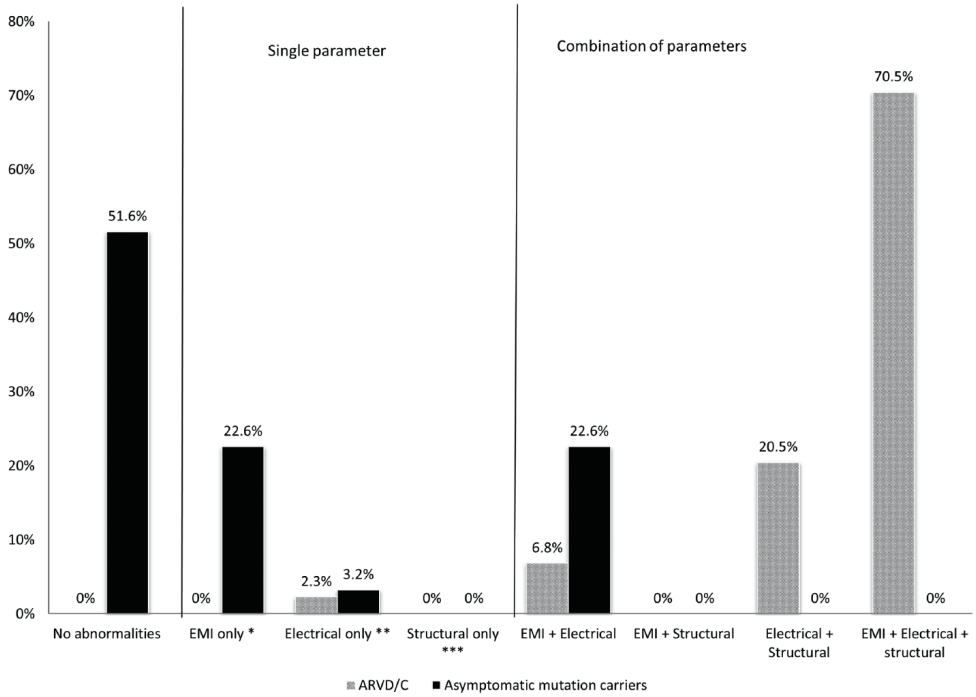

Figure 6. Distribution of parameters in ARVD/C and asymptomatic mutation carriers
Electro-mechanical interval (EMI) ≥ 100 milliseconds in the subtricuspid region. **Electrical disease was defined as the presence of ECG and/or arrhythmic 2010 TFC. ***The presence of structural 2010 TFC. In the majority (71%) of ARVD/C-patients prolonged EMI was detected with a combination of ECG or Holter abnormalities and structural abnormalities. In asymptomatic mutation carriers the most common single sign of disease was prolonged EMI in the subtricuspid area. Prolonged EMI seems to be the first abnormality in asymptomatic mutation carriers before electrical or structural disease. ARVD/C = arrhythmogenic right ventricular dysplasia/cardiomyopathy; ECG = electrocardiogram; EMI = electro-mechanical interval; TFC = 2010 Task Force Criteria.

DISCUSSION

In this study we analyzed EMI as a new noninvasive parameter for activation delay in ARVD/C. EMI was significantly prolonged throughout the RV free wall in ARVD/C-patients. More importantly, prolonged EMI in the subtricuspid region appeared to be a frequent first and most common phenotypic expression of disease in assumed unaffected asymptomatic mutation carriers.

Mechanism of prolonged EMI

EMI is defined as the interval between the time of first detectable electrical ventricular activation in the surface ECG and the time of local onset of myocardial shortening. In the

normal heart the onset of the QRS complex during sinus rhythm is due to earliest electrical activation of the myocardium at the mid-portion of the left side of the interventricular septum.[19] Because of the rapid conduction in the right bundle branch and Purkinje fibers, subendocardial RV activation starts shortly after the earliest LV septal activation in the mid–apical area of RV, and propagates toward the more basal area and finally the RVOT.[19] Epicardial activation follows the pattern of subendocardial activation after relatively slow myocardial conduction from endocardium to epicardium.[19] A few tens of milliseconds after electrical activation of the cardiomyocytes, sarcomeres shorten resulting in contraction of myocardium following the sequence of electrical activation.[28] The onset of regional longitudinal shortening marks the end of EMI.

The correlation between timing of local electrical activation and onset of shortening has been studied extensively.[28, 29] A clear linear correlation exists between the two events, justifying the use of the interval between onsets of electrical activity and myocardial shortening as a surrogate of electrical activation delay.[29] However, in the intact heart, in late electrically activated regions, delay in onset of myocardial shortening exceeds delay of local electrical activation.[28-31] This is due to the additional time needed to overcome the higher rise in cavity pressure during relatively late systole.[30, 31] However, importantly, the linear relationship between electrical and mechanical activation remains.[32]

In ARVD/C-patients, extensive histopathological changes, giving rise to altered tissue architecture, cause prolonged conduction pathways, load mismatch, and conduction slowing at pivotal points.[11, 14, 33] These changes in RV electrical conduction are reflected in the marked observed prolongation of EMI in ARVD/C-patients. As expected, prolonged EMI in ARVD/C-patients was frequently found in combination with electrocardiographic and structural abnormalities.

In asymptomatic mutation carriers, extensive histopathological changes may be less outspoken. Therefore, prolonged EMI may be not well explained by changes in tissue architecture. However, a recent finding in a *PKP2* mouse study shows altered distribution of gap junctions and Nav1.5 ion channels giving rise to activation delay and arrhythmogenesis in the absence of structural alterations.[10] These experimental findings support the existence of prolonged EMI in the early subclinical ARVD/C stage in man. Moreover, occurrence of prolonged EMI in the absence of structural alterations in humans supports the hypothesis that electrical abnormalities are present prior to histopathological changes.[10, 34]

Early involvement of the subtricuspid area

Our group recently reported evidence of early involvement of the subtricuspid area in ARVD/C.[21] Therefore, measuring the activation delay in this region is important to potentially unmask ARVD/C in the subclinical stage. Electrocardiography seems incapable in detecting minor activation delay in this often physiologically earlier activated part than

the RVOT.[13, 14] A study performed by Tandri *et al.* using 3D electroanatomical mapping during EPS showed a prolonged RV endocardial activation time in the absence of detectable prolonged depolarization on the surface ECG. This finding implies the superiority of invasively obtained local RV activation delay compared to both ECG and signal-averaged ECG activation delay markers.[13] However, an invasive approach such as EPS is not preferred since patients are frequently still asymptomatic. Echocardiographic deformation imaging is not hampered by these limitations and enables noninvasive measurements of activation delay in the subtricuspid area. EMI of the subtricuspid area seems of incremental value for early diagnosis in apparently unaffected asymptomatic mutation carriers.

Why this area is the first affected region in ARVD/C is still unknown. Enhanced mechanical shear stress may be involved since the subtricuspid area is facing higher cavity pressure at the moment of activation than apical/mid-ventricular regions. This hypothesis is supported by a recent study in an ARVD/C cell model, showing a correlation between shear stress and apoptosis.[35]

Potential role of EMI in risk stratification

This study primarily intended to provide insight into the extent of prolonged EMI in ARVD/C mutation carriers. However, as a parameter indicating activation delay, we also explored the potential value of EMI for risk stratification in asymptomatic mutation carriers. Cox *et al.* showed in a similar cohort with comparable duration of follow-up that the occurrence of sustained ventricular arrhythmias in genetically predisposed asymptomatic family members is very low (<2%).[7] Therefore, arrhythmic outcome was defined as the occurrence of nonsustained VT or an increase of PVC count on Holter monitoring. We demonstrated a significant correlation between subtricuspid EMI and an increase of ventricular ectopy in the asymptomatic mutation carrier group. Previous studies showed a relationship between the number of PVC and sustained ventricular arrhythmia outcome.[16, 36] However, the numbers in our study are small and the predictive role should be further evaluated in large studies with long-term follow-up.

We also assessed other previously described parameters concerning RV mechanical dyssynchrony (*Supplementary Table D*). A study by Sarvari *et al.* reported an increased dispersion of RV contraction duration in asymptomatic ARVD/C mutation carriers and seemed to be higher in the group that already experienced arrhythmic events.[37] We were able to test the potential diagnostic and predictive value of this parameter in our asymptomatic group. In our study, RV mechanical dispersion did not differ significantly between subjects experiencing an arrhythmic event and the group remaining free of event. However, the observed underperformance of this parameter in our asymptomatic group might be due to the differences in the asymptomatic group definition.

R1 R2 R3 R4 R5 R6 R7 R8 R9 R10 R11 R12 R13 R14 R15 R16 R17 R18 R19 R20 R21 R22 R23 R24 R25 R26 R27 R28 R29 R30 R31 R32 R33 R34 R35 R36 R37 R38 R39

Limitations

This study was limited by small population size as typical for ARVD/C research. Due to the low number of events and short duration of follow-up, the association between arrhythmic outcome and prolonged EMI remains weak and our observations should be considered preliminary.

We defined the measurement of EMI as the interval between the first detectable electrical ventricular activation on the simultaneous ECG recording and the time of local onset of myocardial shortening. Unfortunately, the choice of ECG lead during echocardiographic examination was not standardized in our echocardiographic protocol. This could have affected the determination of onset first electrical activation and consequential measurement of EMI.

Our cohort consisted of desmosomal *PKP2* or *DSG2* mutation carriers being common genes with ARVD/C-related mutations in The Netherlands.[38] Extrapolation to other ARVD/C subgroups is not warranted. We compared EMI with established criteria of ARVD/C including structural alteration detected by CMR.[4] Unfortunately, CMR was not available in all subjects resulting in a possible underestimation of structural abnormalities. Therefore, the conclusion that subtricuspid EMI was present in asymptomatic mutation carriers without additional structural abnormalities was not confirmed by CMR data in 12/31 subjects. In ARVD/C-patients, structural abnormalities were more often detected by echocardiography compared to CMR. This is not the general experience of the diagnostic performance of these modalities in ARVD/C.[39] This observed difference in our study should be attributed to the lack of CMR data in a significant amount of ARVD/C-patients (n = 18) with an ICD implanted. These patients are, almost by definition, the most severe affected in terms of functional and structural alterations on imaging.

The RVOT and posterolateral LV wall are commonly involved in ARVD/C.[1, 21, 40] Assessing EMI of RVOT and other RV segments besides the RV free lateral wall is difficult due to insufficient lateral resolution using echocardiography for Speckle-Tracking.[26] However, recent data suggest that the RVOT is only involved in more advanced stages and could be of lesser value in diagnosis and risk stratification in early ARVD/C.[21] The LV can be used for assessing EMI. However, dedicated single wall recordings are needed for reliable measurements. Unfortunately, these recordings were not made in the majority of our cohort.

A majority of ARVD/C-patients received antiarrhythmic drugs affecting activation delay during the echocardiographic examination that may lead to incorrect interpretation of EMI. However, sub-analysis of EMI in ARVD/C-patients with versus without anti-arrhythmic treatment did not affect the results (*Supplementary Table E*).

Conclusion

Prolonged EMI in the subtricuspid region is a novel marker of activation delay in ARVD/C and was found in a large number of asymptomatic mutation carriers. More importantly, EMI is often present in the absence of established criteria and should be considered as an early sign of disease. EMI as a surrogate for activation delay could help in risk stratification, depending on the outcome of future studies.

R1 R2 R3 R4 R5 R6 R7 R8 R9 R10 R11 R12 R13 R14 R15 R16 R17 R18 R19 R20 R21 R22 R23 R24 R25 R26 R27 R28 R29 R30 R31 R32 R33 R34 R35 R36 R37 R38 R39

R1
R2
R3
R4
R5
R6
R7
R8
R9
R10
R11
R12
R13
R14
R15
R16
R17
R18
R19
R20
R21
R22
R23
R24
R25
R26
R27
R28
R29
R30
R31
R32
R33
R34
R35
R36
R37
R38
R39

REFERENCES

1. Marcus FI, Fontaine GH, Guiraudon G, Frank R, Laurenceau JL, Malergue C, Grosgogeat Y: Right ventricular dysplasia: A report of 24 adult cases. *Circulation* 1982;65:384-398.
2. Bhonsale A, Groeneweg JA, James CA, Dooijes D, Tichnell C, Jongbloed JD, Murray B, te Riele AS, van den Berg MP, Bikker H, Atsma DE, de Groot NM, Houweling AC, van der Heijden JF, Russell SD, Doevendans PA, van Veen TA, Tandri H, Wilde AA, Judge DP, van Tintelen JP, Calkins H, Hauer RN: Impact of genotype on clinical course in arrhythmogenic right ventricular dysplasia/cardiomyopathy-associated mutation carriers. *Eur Heart J* 2015;36:847-855.
3. Sen-Chowdhry S, Syrris P, Ward D, Asimaki A, Sevdalis E, McKenna WJ: Clinical and genetic characterization of families with arrhythmogenic right ventricular dysplasia/cardiomyopathy provides novel insights into patterns of disease expression. *Circulation* 2007;115:1710-1720.
4. Marcus FI, McKenna WJ, Sherrill D, Basso C, Bauce B, Bluemke DA, Calkins H, Corrado D, Cox MG, Daubert JP, Fontaine G, Gear K, Hauer R, Nava A, Picard MH, Protonotarios N, Saffitz JE, Sanborn DM, Steinberg JS, Tandri H, Thiene G, Towbin JA, Tsatsopoulou A, Wichter T, Zareba W: Diagnosis of arrhythmogenic right ventricular cardiomyopathy/dysplasia: Proposed modification of the task force criteria. *Circulation* 2010;121:1533-1541.
5. Basso C, Corrado D, Marcus FI, Nava A, Thiene G: Arrhythmogenic right ventricular cardiomyopathy. *Lancet* 2009;373:1289-1300.
6. Sen-Chowdhry S, Syrris P, McKenna WJ: Genetics of right ventricular cardiomyopathy. *J Cardiovasc Electrophysiol* 2005;16:927-935.
7. Cox MG, van der Zwaag PA, van der Werf C, van der Smagt JJ, Noorman M, Bhuiyan ZA, Wiesfeld AC, Volders PG, van Langen IM, Atsma DE, Dooijes D, van den Wijngaard A, Houweling AC, Jongbloed JD, Jordaens L, Cramer MJ, Doevendans PA, de Bakker JM, Wilde AA, van Tintelen JP, Hauer RN: Arrhythmogenic right ventricular dysplasia/cardiomyopathy: Pathogenic desmosome mutations in index-patients predict outcome of family screening: Dutch arrhythmogenic right ventricular dysplasia/cardiomyopathy genotype-phenotype follow-up study. *Circulation* 2011;123:2690-2700.
8. Quarta G, Muir A, Pantazis A, Syrris P, Gehmlich K, Garcia-Pavia P, Ward D, Sen-Chowdhry S, Elliott PM, McKenna WJ: Familial evaluation in arrhythmogenic right ventricular cardiomyopathy: Impact of genetics and revised task force criteria. *Circulation* 2011;123:2701-2709.
9. Noorman M, Hakim S, Kessler E, Groeneweg JA, Cox MG, Asimaki A, van Rijen HV, van Stuijvenberg L, Chkourko H, van der Heyden MA, Vos MA, de Jonge N, van der Smagt JJ, Dooijes D, Vink A, de Weger RA, Varro A, de Bakker JM, Saffitz JE, Hund TJ, Mohler PJ, Delmar M, Hauer RN, van Veen TA: Remodeling of the cardiac sodium channel, connexin43, and plakoglobin at the intercalated disk in patients with arrhythmogenic cardiomyopathy. *Heart Rhythm* 2013;10:412-419.
10. Cerrone M, Noorman M, Lin X, Chkourko H, Liang FX, van der Nagel R, Hund T, Birchmeier W, Mohler P, van Veen TA, van Rijen HV, Delmar M: Sodium current deficit and arrhythmogenesis in a murine model of plakophilin-2 haploinsufficiency. *Cardiovasc Res* 2012;95:460-468.
11. de Bakker JM, van Capelle FJ, Janse MJ, Tasseron S, Vermeulen JT, de Jonge N, Lahpor JR: Slow conduction in the infarcted human heart. 'Zigzag' course of activation. *Circulation* 1993;88:915-926.
12. Fast VG, Kleber AG: Role of wavefront curvature in propagation of cardiac impulse. *Cardiovascular Research* 1997;33:258-271.
13. Tandri H, Asimaki A, Abraham T, Dalal D, Tops L, Jain R, Saffitz JE, Judge DP, Russell SD, Halushka M, Bluemke DA, Kass DA, Calkins H: Prolonged RV endocardial activation duration: A novel marker of arrhythmogenic right ventricular dysplasia/cardiomyopathy. *Heart Rhythm* 2009;6:769-775.
14. Haqqani HM, Tschabrunn CM, Betensky BP, Lavi N, Tzou WS, Zado ES, Marchlinski FE: Layered activation of epicardial scar in arrhythmogenic right ventricular dysplasia: Possible substrate for confined epicardial circuits. *Circ Arrhythm Electrophysiol* 2012;5:796-803.

15. Tops LF, Prakasa K, Tandri H, Dalal D, Jain R, Dimaano VL, Dombroski D, James C, Tichnell C, Daly A, Marcus F, Schalij MJ, Bax JJ, Bluemke D, Calkins H, Abraham TP: Prevalence and pathophysiologic attributes of ventricular dyssynchrony in arrhythmogenic right ventricular dysplasia/cardiomyopathy. *J Am Coll Cardiol* 2009;54:445-451.
16. Bhonsale A, James CA, Tichnell C, Murray B, Madhavan S, Philips B, Russell SD, Abraham T, Tandri H, Judge DP, Calkins H: Risk stratification in arrhythmogenic right ventricular dysplasia/cardiomyopathy-associated desmosomal mutation carriers. *Circ Arrhythm Electrophysiol* 2013;6:569-578.
17. Corrado D, Basso C, Leoni L, Tokajuk B, Bauce B, Frigo G, Tarantini G, Napodano M, Turrini P, Ramondo A, Daliento L, Nava A, Buja G, Iliceto S, Thiene G: Three-dimensional electroanatomic voltage mapping increases accuracy of diagnosing arrhythmogenic right ventricular cardiomyopathy/dysplasia. *Circulation* 2005;111:3042-3050.
18. Cox MG, Nelen MR, Wilde AA, Wiesfeld AC, van der Smagt JJ, Loh P, Cramer MJ, Doevendans PA, van Tintelen JP, de Bakker JM, Hauer RN: Activation delay and VT parameters in arrhythmogenic right ventricular dysplasia/cardiomyopathy: Toward improvement of diagnostic ECG criteria. *J Cardiovasc Electrophysiol* 2008;19:775-781.
19. Durrer D, van Dam RT, Freud GE, Janse MJ, Meijler FL, Arzbaecher RC: Total excitation of the isolated human heart. *Circulation* 1970;41:899-912.
20. De Boeck BW, Teske AJ, Leenders GE, Mohamed Hoesein FA, Loh P, van Driel VJ, Doevendans PA, Prinzen FW, Cramer MJ: Detection and quantification by deformation imaging of the functional impact of septal compared to free wall preexcitation in the Wolff-Parkinson-White syndrome. *Am J Cardiol* 2010;106:539-546 e532.
21. Te Riele AS, James CA, Philips B, Rastegar N, Bhonsale A, Groeneweg JA, Murray B, Tichnell C, Judge DP, Van Der Heijden JF, Cramer MJ, Velthuis BK, Bluemke DA, Zimmerman SL, Kamel IR, Hauer RN, Calkins H, Tandri H: Mutation-positive arrhyhmogenic right ventricular dysplasia/cardiomyopathy: The triangle of dysplasia displaced. *J Cardiovasc Electrophysiol* 2013;24:1311-1320.
22. Hamid MS, Norman M, Quraishi A, Firoozi S, Thaman R, Gimeno JR, Sachdev B, Rowland E, Elliott PM, McKenna WJ: Prospective evaluation of relatives for familial arrhythmogenic right ventricular cardiomyopathy/dysplasia reveals a need to broaden diagnostic criteria. *J Am Coll Cardiol* 2002;40:1445-1450.
23. Lang RM, Bierig M, Devereux RB, Flachskampf FA, Foster E, Pellikka PA, Picard MH, Roman MJ, Seward J, Shanewise JS, Solomon SD, Spencer KT, Sutton MS, Stewart WJ: Recommendations for chamber quantification: A report from the American Society of Echocardiography's Guidelines and Standards Committee and the Chamber Quantification Writing Group, developed in conjunction with the European Association of Echocardiography, a branch of the European Society of Cardiology. *J Am Soc Echocardiog* 2005;18:1440-1463.
24. Rudski LG, Lai WW, Afilalo J, Hua L, Handschumacher MD, Chandrasekaran K, Solomon SD, Louie EK, Schiller NB: Guidelines for the echocardiographic assessment of the right heart in adults: A report from the American Society of Echocardiography endorsed by the European Association of Echocardiography, a registered branch of the European Society of Cardiology, and the Canadian Society of Echocardiography. *J Am Soc Echocardiog* 2010;23:685-713.
25. Mast TP, Teske AJ, Doevendans PA, Cramer MJ: Current and future role of echocardiography in arrhythmogenic right ventricular dysplasia/cardiomyopathy. *Cardiol J* 2015;22:362-374.
26. Teske AJ, De Boeck BW, Melman PG, Sieswerda GT, Doevendans PA, Cramer MJ: Echocardiographic quantification of myocardial function using tissue deformation imaging, a guide to image acquisition and analysis using tissue Doppler and speckle tracking. *Cardiovasc Ultrasound* 2007;5:27.
27. Dalal D, Tandri H, Judge DP, Amat N, Macedo R, Jain R, Tichnell C, Daly A, James C, Russell SD, Abraham T, Bluemke DA, Calkins H: Morphologic variants of familial arrhythmogenic right ventricular dysplasia/cardiomyopathy a genetics-magnetic resonance imaging correlation study. *J Am Coll Cardiol* 2009;53:1289-1299.

28. Prinzen FW, Augustijn CH, Allessie MA, Arts T, Delhaas T, Reneman RS: The time sequence of electrical and mechanical activation during spontaneous beating and ectopic stimulation. *Eur Heart J* 1992;13:535-543.
29. Wyman BT, Hunter WC, Prinzen FW, McVeigh ER: Mapping propagation of mechanical activation in the paced heart with MRI tagging. *Am J Physiol* 1999;276:H881-H891.
30. Russell K, Opdahl A, Remme EW, Gjesdal O, Skulstad H, Kongsgaard E, Edvardsen T, Smiseth OA: Evaluation of left ventricular dyssynchrony by onset of active myocardial force generation: A novel method that differentiates between electrical and mechanical etiologies. *Circ Cardiovasc Imaging* 2010;3:405-414.
31. Russell K, Smiseth OA, Gjesdal O, Qvigstad E, Norseng PA, Sjaastad I, Opdahl A, Skulstad H, Edvardsen T, Remme EW: Mechanism of prolonged electromechanical delay in late activated myocardium during left bundle branch block. *Am J Physiol Heart Circ Physiol* 2011;301:H2334-H2343.
32. Suever JD, Hartlage GR, Magrath RP, Iravanian S, Lloyd MS, Oshinski JN: Relationship between mechanical dyssynchrony and intra-operative electrical delay times in patients undergoing cardiac resynchronization therapy. *J Cardiovasc Magn Reson* 2014;16:4.
33. Corrado D, Basso C, Leoni L, Tokajuk B, Turrini P, Bauce B, Migliore F, Pavei A, Tarantini G, Napodano M, Ramondo A, Buja G, Iliceto S, Thiene G: Three-dimensional electroanatomical voltage mapping and histologic evaluation of myocardial substrate in right ventricular outflow tract tachycardia. *J Am Coll Cardiol* 2008;51:731-739.
34. Te Riele AS, James CA, Rastegar N, Bhonsale A, Murray B, Tichnell C, Judge DP, Bluemke DA, Zimmerman SL, Kamel IR, Calkins H, Tandri H: Yield of serial evaluation in at-risk family members of patients with ARVD/C. *J Am Coll Cardiol* 2014;64:293-301.
35. Hariharan V, Asimaki A, Michaelson JE, Plovie E, MacRae CA, Saffitz JE, Huang H: Arrhythmogenic right ventricular cardiomyopathy mutations alter shear response without changes in cell-cell adhesion. *Cardiovasc Res* 2014;104:280-289.
36. Bhonsale A, James CA, Tichnell C, Murray B, Gagarin D, Philips B, Dalal D, Tedford R, Russell SD, Abraham T, Tandri H, Judge DP, Calkins H: Incidence and predictors of implantable cardioverter-defibrillator therapy in patients with arrhythmogenic right ventricular dysplasia/cardiomyopathy undergoing implantable cardioverter-defibrillator implantation for primary prevention. *J Am Coll Cardiol* 2011;58:1485-1496.
37. Sarvari SI, Haugaa KH, Anfinsen OG, Leren TP, Smiseth OA, Kongsgaard E, Amlie JP, Edvardsen T: Right ventricular mechanical dispersion is related to malignant arrhythmias: A study of patients with arrhythmogenic right ventricular cardiomyopathy and subclinical right ventricular dysfunction. *Eur Heart J* 2011;32:1089-1096.
38. van Tintelen JP, Entius MM, Bhuiyan ZA, Jongbloed R, Wiesfeld AC, Wilde AA, van der Smagt J, Boven LG, Mannens MM, van Langen IM, Hofstra RM, Otterspoor LC, Doevendans PA, Rodriguez LM, van Gelder IC, Hauer RN: Plakophilin-2 mutations are the major determinant of familial arrhythmogenic right ventricular dysplasia/cardiomyopathy. *Circulation* 2006;113:1650-1658.
39. Borgquist R, Haugaa KH, Gilljam T, Bundgaard H, Hansen J, Eschen O, Jensen HK, Holst AG, Edvardsen T, Svendsen JH, Platonov PG: The diagnostic performance of imaging methods in ARVC using the 2010 Task Force criteria. *Eur Heart J Cardiovasc Imaging* 2014;15:1219-1225
40. Mast TP, Teske AJ, Vd Heijden JF, Groeneweg JA, Te Riele AS, Velthuis BK, Hauer RN, Doevendans PA, Cramer MJ: Left ventricular involvement in arrhythmogenic right ventricular dysplasia/cardiomyopathy assessed by echocardiography predicts adverse clinical outcome. *J Am Soc Echocardiogr* 2015;28:1103-1113.

SUPPLEMENTARY FILES

Supplementary Table A. Mutations among study population

		ARVD/C patients (n = 44)	Asymptomatic mutation carriers (n = 31)
PKP2			
Nucleotide change	***Amino-Acid change***	*N*	*N*
1211-1212ins	Val406SerfsX4	10	3
2386T>C	Cys796Arg	4	5
235C>T	Arg79X	3	3
397C>T&2615C>T	Gln133X&Thr872Ile	5	3
2489+4A>C	IVS12+4A>C	3	2
397C>T	Gln133X	3	1
1369-1372CAAA	Gln457X	1	2
2146-1G>C	IVS10-1G>C	1	2
1848C>A	Tyr616X	0	1
917-918delCC	Pro318GlnfsX29	1	0
417C>T	Ser140Phe	1	0
148_151delACAG	Thr50SerfsX61	0	1
Deletion exon 1-14		4	2
Deletion exon 1-4		2	2
Deletion exon 10		1	0
Deletion exon 7-14		0	1
DSG2			
Nucleotide change	***Amino-Acid change***		
874C>T	Arg292Cys	2	2
137G>A&473T>G	Arg46Gln&Val158Gly	2	1
1003G>A	Thr335Ala	1	0

ARVD/C = arrhythmogenic right ventricular dysplasia/cardiomyopathy; *PKP2* = Plakophilin-2 gene; *DSG2* = Desmoglein-2 gene

R1 R2 R3 R4 R5 R6 R7 R8 R9 R10 R11 R12 R13 R14 R15 R16 R17 R18 R19 R20 R21 R22 R23 R24 R25 R26 R27 R28 R29 R30 R31 R32 R33 R34 R35 R36 R37 R38 R39

Supplementary Table B. Definition list

	Definition
ECG variables	
Epsilon wave	Distinct waves of small amplitude within the ST segment in the right precordial leads (V_{1-3}) and are distinct from the QRS complex.
Terminal activation duration	Longest value in lead V_{1-3}, from the nadir of the S wave to the end of all depolarization deflections, thereby including not only the S wave upstroke but also both late fractionated signals and epsilon waves. Terminal activation duration was only scored in absence of complete right bundle branch block. Each measurement was performed twice by two physicians independently. Per measurement, at least two consecutive QRS complexes in each lead were analyzed. A difference in measurement of ≤10 ms was accepted for agreement. In case of discrepancy agreement was reached by convention for final analyses.
T-wave inversion	T-wave was considered inverted if the voltage was ≥0.1 mV
Echocardiographic deformation imaging variables	
Electro-mechanical interval (EMI)	Time between first electrical deflection on the simultaneous ECG recording and first local onset of myocardial shortening.
Contraction duration	Time between first electrical deflection on the simultaneous ECG recording and peak strain timing
RV mechanical dispersion	Standard deviation of contraction duration in three RV and three septal segments
Arrhythmic variables	
Sustained ventricular tachycardia	Ventricular tachycardia which lasts 30 seconds or more, or less than 30 s when terminated electrically or pharmacologically.
Non-sustained ventricular tachycardia	≥3 consecutive premature ventricular complexes with a rate >100 / min, lasting <30 s, which was documented during exercise testing, loop monitoring, or 24hrs Holter monitoring.
Increase of premature ventricular complexes (PVC) >500/24Hrs	An increase in PVC count during Holter monitoring up to a previously absent value of >500/24Hrs.

ICD = implantable cardioverter defibrillator; ECG = electrocardiogram; RV = right ventricle

Supplementary Table C. Bland-Altman bias and limits of agreement for interobserver variability in measuring electro-mechanical interval

Electro-mechanical interval	Bias (ms)	95% limits of agreement (ms)
RV subtricuspid – basal	-2.7	-30 to 24
RV mid	-1.8	-34 to 30
RV apical	1.1	-24 to 26

RV = right ventricle.

Supplementary Table D. Measurement of RV mechanical dispersion.

	ARVD/C patients (n = 44)	Asymptomatic mutation carriers (n = 31)	Controls (n = 30)
RV mechanical dispersion (ms)	57±34*	25±13	25±14
	Event group (n=10)	**Asymptomatic mutation carriers – free of event (n = 21)**	**P-value**
RV mechanical dispersion (ms)	26±10	24±14	0.43

RV mechanical dispersion was defined as the standard deviation of contraction duration in three RV and three septal segments. * = P < 0.01 compared to controls. ARVD/C = arrhythmogenic right ventricular dysplasia/cardiomyopathy; RV = right ventricle; ms = milliseconds

Supplementary Table E. Electro-mechanical interval in patients with and without anti-arrhythmic drug therapy compared to controls

	ARVD/C patients Anti-arrhythmic drugs + (n = 31)	ARVD/C patients Anti-arrhythmic drugs – (n = 13)	Controls (n = 30)
Electro-mechanical interval (EMI)			
RV – subtricuspid- basal(ms)	158±119*	127±53*	48±32
RV – mid (ms)	94±101*	58±31*	29±21
RV – apex (ms)	53±44*	47±35†	27±24

* = P < 0.01 compared to controls ; † = P < 0.05 compared to controls + = with ;- = without. Mean values of EMI in ARVD/C patients with and without anti-arrhythmic drug therapy at the time of inclusion. Also in patients without medication interacting with the electrical activation significant prolongation exists compared to controls. ARVD/C = arrhythmogenic right ventricular dysplasia/cardiomyopathy ; RV = right ventricle ; ms = milliseconds

CHAPTER 4

Right Ventricular Imaging and Computer Simulation for Electromechanical Substrate Characterization in Arrhythmogenic Right Ventricular Cardiomyopathy

Thomas P Mast, Arco J Teske, John Walmsley, Jeroen F van der Heijden, René van Es, Frits W Prinzen, Tammo Delhaas, Toon A van Veen, Peter Loh, Pieter A Doevendans, Maarten J Cramer, § Joost Lumens §
§ contributed equally to this work.

J Am Coll Cardiol. 2016;68(20):2185-2197

ABSTRACT

Background: Previous studies suggested that electrical abnormalities precede overt structural disease in arrhythmogenic right ventricular cardiomyopathy (ARVC). Abnormal RV deformation has been reported in early ARVC without structural abnormalities. The pathophysiological mechanisms underlying these abnormalities remain unknown.

Objectives: The authors used imaging and computer simulation to differentiate electrical from mechanical tissue substrates among ARVC clinical stages.

Methods: ARVC desmosomal mutation carriers (n =84) were evaluated by electrocardiography (ECG), Holter monitoring, late-enhancement cardiac magnetic resonance imaging, and echocardiographic RV deformation imaging. Subjects were categorized based on the presence of 2010 International Task Force criteria: 1) subclinical stage (n = 21); 2) electrical stage (n = 15); and 3) structural stage (n = 48). Late enhancement was not present in any subclinical or electrical stage subjects.

Results: Three distinctive characteristic RV longitudinal deformation patterns were identified: type I: normal deformation (n = 12); type II: delayed onset of shortening, reduced systolic peak strain, and mild post-systolic shortening (n = 35); and type III: systolic stretching with large post-systolic shortening (n = 37). A majority (69%) of structural staged mutation carriers were type III, whereas a large proportion of both electrical and subclinical stage subjects (67% and 48%, respectively) were type II. Computer simulations demonstrated that the type II pattern can be explained by a combination of reduced contractility and mildly increased passive myocardial stiffness. This evolved into type III by aggravating both mechanical substrates. Electrical activation delay alone explained none of the patterns.

Conclusions: Different ARVC stages were characterized by distinct RV deformation patterns, all of which could be reproduced by simulating different degrees of mechanical substrates. Subclinical and electrical staged ARVC subjects already showed signs of local mechanical abnormalities. Our novel approach could lead to earlier disease detection and, thereby, influence current definitions of electrical and subclinical ARVC stages.

INTRODUCTION

Arrhythmogenic right ventricular (RV) cardiomyopathy (ARVC) is an inherited cardiomyopathy characterized by ventricular arrhythmias and progressive RV dysfunction (1,2). Presently, an ARVC-causing mutation can be identified in 60% of index patients (3). Familial ARVC is associated with reduced penetrance and variable disease expression (3), ranging from sudden cardiac death in young individuals to lifelong absence of any phenotype (4). ARVC is characterized histopathologically by fibrofatty replacement of the myocardium, forming a substrate for conduction delay as well as both regional and global RV dysfunction (1). Accumulating evidence suggests that this structural disease is preceded by electrical abnormalities (5–7). Therefore, ARVC is currently divided into 3 consecutive clinical stages: 1) *subclinical (concealed)*, with neither electrical nor structural abnormalities; 2) *electrical*, with only electrocardiographic (ECG) abnormalities; and 3) *structural*, with both electrical and structural abnormalities (7–9).

Echocardiographic deformation (or strain) imaging can quantify regional myocardial deformation and has been used to detect regional functional abnormalities in ARVC (10,11). Deformation imaging revealed abnormal deformation throughout all clinical ARVC stages, including the early subclinical stage in which conventional diagnostic techniques detected neither structural nor electrocardiographic abnormalities (12–15). The pathophysiological mechanisms underlying these regional functional abnormalities in the early stages of ARVC remain unknown.

We hypothesized that the observed abnormal deformation patterns in early ARVC stages are explained by an electrical substrate, such as activation delay, rather than regional contractile dysfunction; and the abnormal deformation patterns in the advanced structural stage result from regional contractile dysfunction and increased myocardial stiffness in addition to electrical activation delay.

To assess our hypotheses, we examined a cohort of desmosomal ARVC mutation carriers using both RV echocardiographic deformation imaging and conventional ARVC diagnostic criteria. After subdividing the cohort based on their RV deformation patterns, we examined the distribution of these patterns in each clinical ARVC stage. Finally, we used computer simulations to understand the electromechanical tissue abnormalities underlying these characteristic RV deformation patterns.

R1 R2 R3 R4 R5 R6 R7 R8 R9 R10 R11 R12 R13 R14 R15 R16 R17 R18 R19 R20 R21 R22 R23 R24 R25 R26 R27 R28 R29 R30 R31 R32 R33 R34 R35 R36 R37 R38 R39

METHODS

This retrospective study was conducted at the University Medical Center Utrecht in the Netherlands between 2006 and 2015, and approved by the local institutional ethics review board. During this period, 87 subjects carrying a pathogenic plakophillin-2 (*PKP2*) or desmoglein-2 (*DSG2*) mutation (54 index patients and 33 relatives) were sent for echocardiographic examination including RV deformation imaging; 3 were excluded due to inadequate image quality.

All mutation carriers underwent ECG, Holter monitoring, and cardiac imaging according to the diagnostic work-up as stated in the 2010 International Task Force criteria (TFC) (9). Definite diagnosis requires either 2 major, 1 major and 2 minor, or 4 minor criteria.

Eighty-four healthy unrelated age- and sexmatched controls were included to obtain normal RV deformation patterns.

ARVC stage classification was based on the presence of subsets of the 2010 TFC (7–9) (**Figure 1**). Subclinical ARVC stage was defined as the absence of any 2010 TFC, except for harboring a desmosomal ARVC pathogenic mutation. Electrical ARVC stage was defined as the presence of a major or minor criterion for depolarization, repolarization, or history of ventricular arrhythmias and the absence of structural abnormalities on imaging. Structural ARVC stage was defined as the presence of a major or minor TFC for structural abnormalities on noninvasive imaging, regardless of the history of ventricular arrhythmias or presence of ECG or Holter abnormalities.

Imaging protocols

Our echocardiographic protocol has been detailed elsewhere (10). Briefly, all data were obtained on a Vivid 7 or Vivid E9 ultrasound machine (General Electric, Milwaukee, Wisconsin) using a broadband M3S transducer. All echocardiographic studies were analyzed for fulfilling 2010 TFC for structural abnormalities (9). Conventional measurements included the end-diastolic diameter of the RV outflow tract in both the parasternal long- and short-axis view and RV fractional area change in the apical 4-chamber view (11). Left ventricular (LV) systolic function was measured by LV ejection fraction using Simpson's biplane measurement.

The RV focused apical 4-chamber view, after narrowing its sector width to optimize temporal resolution, was used to visualize the RV lateral free wall and stored for offline analysis (10).

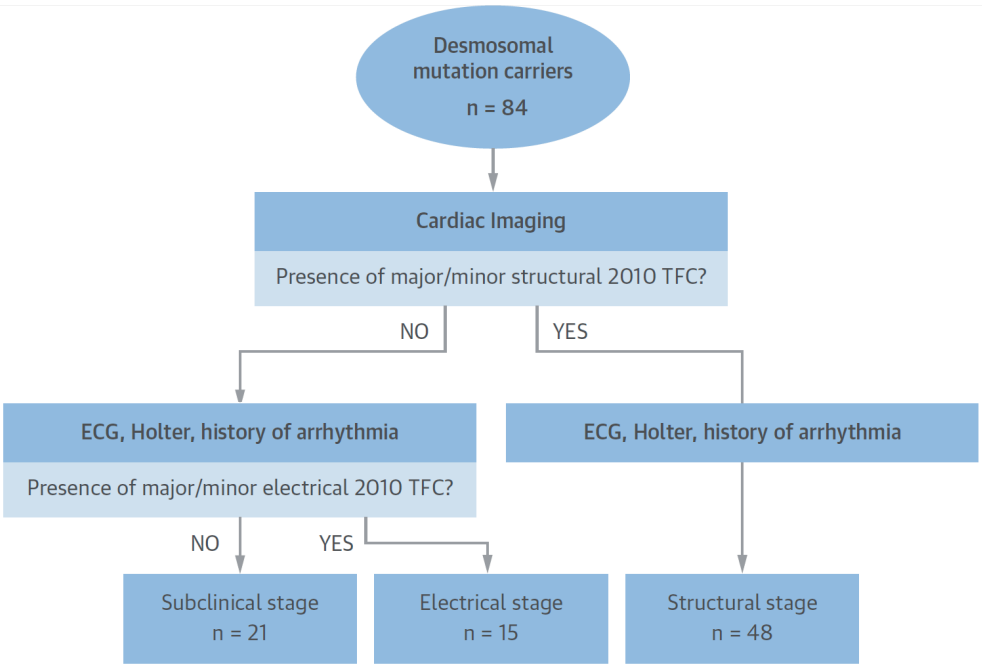

Figure 1. ARVC Stage Classification
Arrhythmogenic right ventricular cardiomyopathy (ARVC) stage classification was based on the presence of different subsets of 2010 International Task Force criteria (TFC) (9). ECG = electrocardiogram.

RV deformation patterns were classified based on the longitudinal strain curve of the RV basal lateral region (subtricuspid area). This region is known to be the earliest and most frequently involved area in ARVC (13,15,16). RV deformation patterns were classified based on previously determined criteria (defined in the *Supplementary Figure 1*): timing of onset shortening (15); timing of peak shortening (12); (systolic) peak strain (17,18); and post-systolic index (13). Two experienced operators examined the presence and degree of coexisting abnormal deformation parameters to obtain distinct patterns. After establishing 3 characteristic patterns, a decision tree was designed for final pattern classification (**Figure 2**). Operators blinded for clinical data performed the pattern classification.

Cardiac magnetic resonance imaging (CMR) was performed on a 1.5-T scanner (Achieva, Philips Healthcare, Best, the Netherlands), according to standard ARVC protocols (19). CMR studies were analyzed for structural abnormalities fulfilling 2010 TFC. Conventional CMR measurements included RV end-diastolic volume, RV ejection fraction, and LV ejection fraction. Late enhancement of intravenously administered gadolinium was used to identify areas with myocardial fibrosis in mutation carriers.

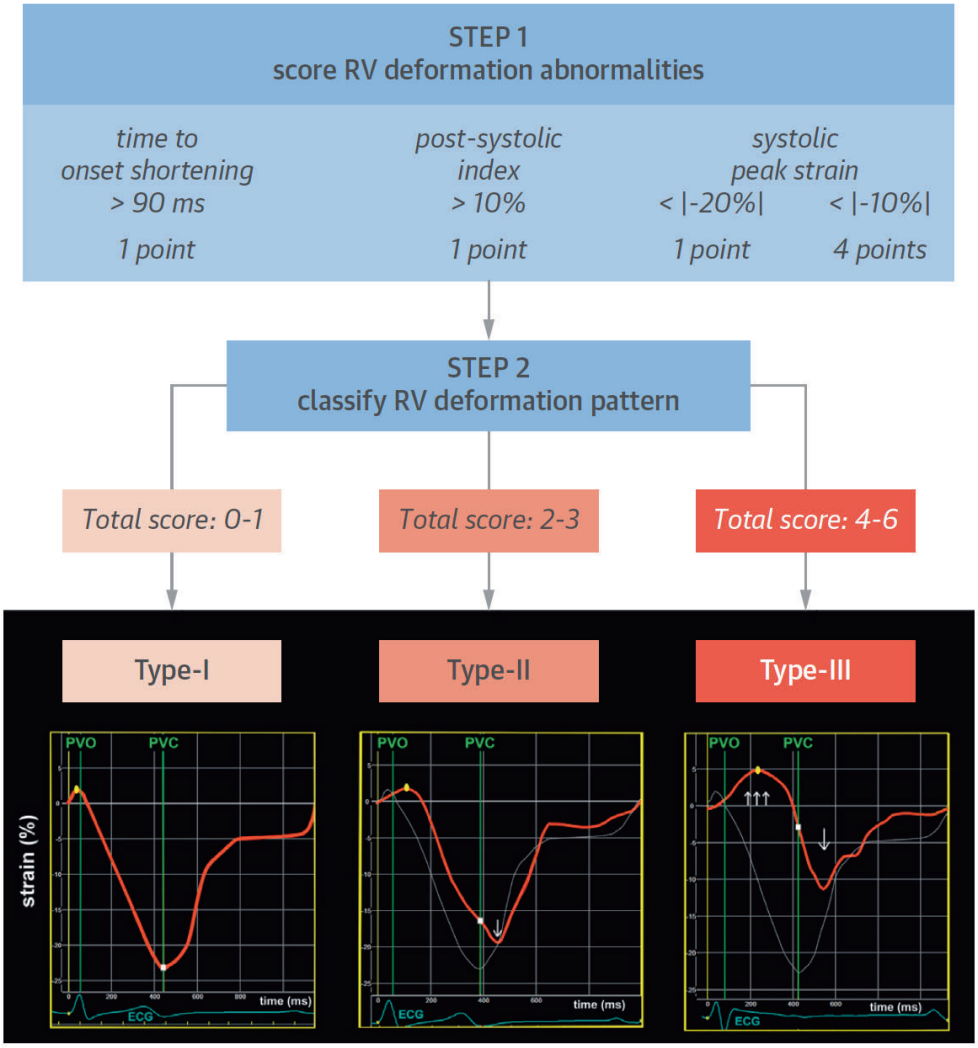

Figure 2. RV Deformation Pattern Classification
Based on the presence of different strain abnormalities in the right ventricular (RV) basal area, 3 distinct characteristic RV deformation patterns were identified: type I represents normal deformation; type II shows delayed onset of shortening (yellow dot) and reduced systolic peak strain (white square) compared with normal deformation, and presence of post-systolic shortening (arrow); and type III displays prominent systolic stretching (upward arrows) and passive recoil or shortening (downward arrow) during early diastole. Dotted white lines indicate type I deformation pattern for comparison. PVO/PVC = pulmonary valve opening/closure; other abbreviations as in Figure 1.

Model simulations

Computer simulations of regional RV myocardial deformation were performed to identify potential pathophysiological substrates underlying the mechanical discoordination in the RV free wall of ARVC patients. The open source CircAdapt model of the human heart and circulatory system was used (20).

A reference simulation representing the healthy adult cardiovascular system under baseline resting conditions was obtained as described previously (21). Realistic hemodynamic boundary conditions and tissue properties were obtained through structural adaptation of cardiac and vascular tissues to mechanical load (22).

The RV free wall was subdivided into 3 equally sized segments representing the basal, mid-ventricular, and apical regions, comparable to the segmentation used during echocardiographic deformation imaging in the patients. Stroke volume (97 ml) and heart rate (59 beats/min) were set to average values measured in the subset of healthy control subjects with CMR data available (n=35). A more detailed description of the methods used to obtain the healthy control simulation is in the Supplementary Files and *Supplementary Table 1*.

Simulation of Electrical and Mechanical Tissue Substrates

The following 3 RV tissue substrates that mimic pathophysiological changes, associated with ARVC were imposed to the RV basal segment to characterize their isolated effects on regional RV myocardial deformation (18,23,24):

1) *Electrical substrate:* onset of activation was delayed by 0, 30, and 60 ms relative to that of the apical and mid-ventricular segments.
2) *Mechanical hypocontractility substrate*: the ability of the myocardium to actively generate tension was reduced from 100% (normal contractility) to a minimum of 20% of its normal value, in steps of 10%. A value of 0% contractility would mean fully noncontractile myocardial tissue, which is assumed to be unlikely for the entire basal segment in ARVC mutation carriers.
3) *Mechanical stiffness substrate*: passive myocardial stiffness was increased from 100% (normal passive stiffness) to a maximum of 1000% of its normal value, in steps of 100%.

All combinations of the above substrates were simulated in addition to the isolated parameter variations, resulting in a total of 243 (3 x 9 x 9) ARVC substrate simulations. The 3 characteristic deformation indexes used to categorize the ARVC mutation carriers (i.e., time of onset shortening, post-systolic index, and systolic peak strain) were calculated for each from all simulated basal RV deformation curves. Additional information regarding study methods is in the Supplementary Files.

R1 R2 R3 R4 R5 R6 R7 R8 R9 R10 R11 R12 R13 R14 R15 R16 R17 R18 R19 R20 R21 R22 R23 R24 R25 R26 R27 R28 R29 R30 R31 R32 R33 R34 R35 R36 R37 R38 R39

Statistical Analysis

Values are presented as mean ± SD or median and interquartile range as appropriate. Normal distribution was tested by using the Shapiro-Wilk test. For continuous variables, comparison between subgroups was tested by 1-way analysis of variance, independent sample Student t, Kruskal-Wallis, or Mann-Whitney U test as appropriate. Categorical data were compared by the chisquare or Fisher exact test. Bonferroni correction was used to adjust for multiple comparisons. Interobserver and intraobserver agreement was determined by linear weighted Kappa statistics. A value of $p < 0.05$ was considered statistically significant. All statistical analyses were performed with SPSS Statistics for Windows, Version 21.0 (IBM Corp., Armonk, New York).

RESULTS

Our final study population consisted of 168 individuals: 53 subjects who fulfilled 2010 TFC for ARVC diagnosis, 31 family members (i.e., desmosomal mutation carriers by genetic screening) who did not meet 2010 TFC for diagnosis, and 84 healthy unrelated age- and sex-matched controls. Following TFC based ARVC stage classification (**Figure 1**), 48 (57%) mutation carriers were staged as structural, 15 (18%) electrical, and 21 (25%) as subclinical (**Table 1**). In the structural group, all subjects showed electrical abnormalities, most commonly T-wave inversion in the right precordial leads (V_1 to V_3) (n = 30; 63%). In the electrical group, prolonged terminal activation duration was the most common ECG abnormality (n = 12; 80%). None of the subjects in the electrical and subclinical stages had a history of sustained ventricular tachycardia.

Per conventional echocardiographic and CMR measurements (**Table 1**), RV dimensions were significantly enlarged and RV systolic function significantly decreased in the structural group versus controls. All structural parameters were comparable in the electrical stage, subclinical stage, and to controls. Due to the presence of implantable cardioverter defibrillators in this population, CMR was not available in 21 (25%) mutation carriers. CMR was available in 35 (42%) controls.

Table 1. Clinical characteristics for control subjects and mutation carriers categorized by TFC-based ARVC stage

	Controls (N=84)	Subclinical stage (N=21)	Electrical stage (N=15)	Structural stage (N=48)	P-value	
					All groups	Mutation carriers
Age (y)	40.5±14.9	27.2±13.9	39.9±17.4	44.6±19.4	P<.001	P<.001
Male	35 (42)	8 (38)	3 (20)	26 (54)	P=.114	P=.055
Proband	-	0 (0)	0 (0)	30 (63)	-	P<.001
ARVC diagnosis*	-	0 (0)	5 (33)	48 (100)	-	P<.001
2010 Task Force Criteria (major or minor)						
Structural criteria	0 (0)	0 (0)	0 (0)	48 (100)		
Depolarization criteria	0 (0)	0 (0)	12 (80)	33 (69)		
Repolarization criteria	0 (0)	0 (0)	5 (33)	39 (81)		
Arrhythmia criteria	-	0 (0)	5 (33)	43 (90)		
Pathogenic mutation	-	21 (100)	15 (100)	48 (100)		
CMR						
RV WMA**	0/35 (0)	0 (0)	1 (7)	35/35 (100)†	P<.001	P<.001
RV-EDV (ml/m^2)	98 [92,110]	88 [75,102]	96 [89,102]	130 [108,167]†	P<.001	P<.001
RVEF (%)	54 [51,56]	56 [50,63]	54 [48,57]	33 [26,41]†	P<.001	P<.001
LVEF (%)	57.7±5.3	58.1±4.0	57.1±7.1	54.5±9.0	P=.545	P=.314
Presence of LE	-	0 (0)	0 (0)	21/35 (60)	-	P<.001
Echocardiography						
RV WMA**	0	1 (5)	1 (7)	45 (94)†	P<.001	P<.001
PLAX RVOT (mm/m^2)	15.3±2.4	14.6±2.5	15.5±2.7	19.1±3.9†	P<.001	P<.001
PSAX RVOT (mm/m^2)	16.9±2.4	15.9±3.0	16.0±2.4	19.5±4.1†	P<.001	P<.001
RV-FAC (%)	44.1±6.7	47.0±7.0	43.1±6.3	30.8±8.9†	P<.001	P<.001
LVEF (%)	58.7±4.6	58.5±4.4	57.7±7.4	56.0±7.5†	P=.095	P=.001

Values are expressed by n (% of group size N), mean ± standard deviation, or median [interquartile range] if appropriate. †=P<0.05 versus age- and gender-matched controls (Bonferroni correction). *ARVC diagnosis was based on fulfilling either two major, one major and two minor, or four minor 2010 TFC. **Wall motion abnormality was noted if akinesia, dyskinesia, or aneurysm was present. ARVC = arrhythmogenic right ventricular cardiomyopathy; 2010 TFC = 2010 Task Force criteria; CMR = cardiac magnetic resonance imaging; RV = right ventricle; WMA = wall motion abnormality; EDV = end-diastolic volume; RVEF =right ventricular ejection fraction; LVEF = left ventricular ejection fraction; LE = late enhancement; mm = millimeter; PLAX/PSAX = parasternal long/short axis view; RVOT = RV outflow tract; RV-FAC = right ventricular fractional area change

R1 R2 R3 R4 R5 R6 R7 R8 R9 R10 R11 R12 R13 R14 R15 R16 R17 R18 R19 R20 R21 R22 R23 R24 R25 R26 R27 R28 R29 R30 R31 R32 R33 R34 R35 R36 R37 R38 R39

RV Deformation Patterns

Three distinct patterns of RV deformation could be discerned in the total study population (**Figure 2**).

- *Type I*: normal deformation of the RV basal area, a pattern similar to the one seen in the healthy controls.
- *Type II*: delayed onset of shortening and reduced systolic peak strain as compared with the normal deformation pattern, and post-systolic shortening.
- *Type III*: little or no systolic peak strain, more prominent post-systolic shortening, and often systolic stretching.

Type I pattern was found in 12 (14%), type II in 35 (42%), and type III in 37 (44%) of the ARVC mutation carriers; 81 (96%) controls had a type I pattern. RV deformation parameters categorized per type of RV deformation are depicted in **Table 2**. Combinations of lowered systolic peak strain, delayed onset of shortening, and post-systolic shortening were frequently seen in mutation carriers with type II and type III patterns.

The level of both interobserver and intraobserver agreement for classification of RV deformation patterns was excellent, kappa of 0.92 (0.83 to 1.00) and 0.96 (0.90 to 1.00), respectively. Further details on reproducibility are in *Supplementary Table 2*. RV deformation pattern distribution across the different clinical stages is shown in **Figure 3**. ARVC mutation carriers in the structural stage predominantly showed a type III pattern (69%). The electrical stage was predominantly associated with type II (67%). Almost one-half of the mutation carriers in the subclinical stage (48%) showed type II, whereas the remaining subjects in this group showed type I.

Simulations

Simulations of the 3 substrates introduced to the basal segment of the RV free wall demonstrated marked changes of this segment's strain pattern (**Figure 4**). The following basal strain signatures were identified:

1) *Electrical substrate*: delayed onset of activation characterized by fast stretch before onset of RV ejection followed by vigorous systolic shortening producing a larger peak strain.
2) *Mechanical hypocontractility substrate*: decreased myocardial contractility led to a pronounced delay of onset shortening, to systolic stretch, and to postsystolic shortening.
3) *Mechanical stiffness substrate:* the most notable strain signature of increasing passive stiffness was decrease of systolic peak strain. In contrast to the 2 mechanical substrates, introducing an electrical activation substrate in the RV basal area also affected the remaining RV free-wall tissue of the mid-ventricular and apical segments.

Table 2. Right ventricular deformation for control subjects and mutation carriers categorized by type of RV deformation

					P-value	
	Controls (N=84)	**Type-I (N=12)**	**Type-II (N=35)**	**Type-III (N=37)**	**All groups**	**Mutation carriers**
Deformation imaging						
Onset of shortening (ms)	52 [25,72]	60 [38,76]	119 [99,141]†	218 [128,293]†	P<.001	P<.001
Systolic peak strain (%)	-24.7±4.8	-23.9±5.3	-16.4±3.5†	-5.3±5.3†	P<.001	P<.001
Peak strain (%)	-25.4±4.9	-24.3±5.2	-19.4±4.1†	-9.6±6.8†	P<.001	P<.001
Post-systolic index (%)	2 [0,4]	1 [0,3]	15 [8,21]†	44 [22,78]†	P<.001	P<.001
Onset of shortening > 90 ms	5 (6)	1 (8)	30 (86)†	37 (100)†	P<.001	P<.001
Post-systolic index >10%	3 (4)	0	24 (69)†	32 (86)†	P<.001	P<.001
Systolic peak strain <-20%	4 (5)	0	29 (83)†	37 (100)†	P<.001	P<.001
Systolic peak strain <-10%	0	0	0	37 (100)†	P<.001	P<.001

Values are expressed by n (% of group size N), mean ± standard deviation, or median [interquartile range] if appropriate. †=P<0.05 versus age-and gender-matched controls (Bonferroni correction). ms=milliseconds

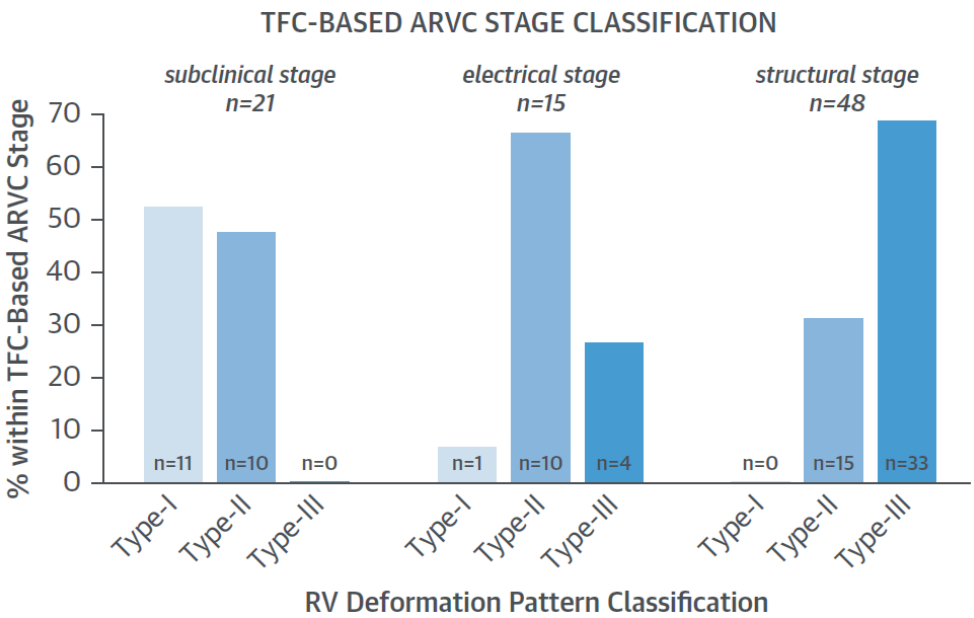

Figure 3. RV Deformation Pattern Distribution
The 3 characteristic RV deformation patterns were associated with different clinical stages of ARVC. Note that subclinical patients were nearly evenly divided between types I and II, whereas type II predominated in electrical patients and type III in structural patients. Abbreviations as in Figure 1.

This relatively early-activated normal tissue started shortening before onset of ejection and reached a lower value of systolic peak strain. The 3 characteristic types of RV deformation patterns observed in ARVC mutation carriers could be reproduced by simulating combinations of the aforementioned tissue substrates (**Central Illustration**). These deformation type-specific simulations were found to be the "best-match" simulations with time of onset shortening, post-systolic index, and systolic peak strain being closest to the average values measured in the patient subgroups. (More details on simulation selection are in *Supplementary Figure 2*). A side-by-side quantitative comparison between measured and simulated RV deformation indexes showed that adding an additional electrical substrate (activation delay) did not necessarily improve similarity between simulations and patient data (**Table 3**), suggesting that the different RV deformation patterns observed in the ARVC patient subgroups predominantly originate from differences in mechanical substrates. The type I pattern, as seen in 96% of the controls and 52% of the subclinical mutation carriers, was reproduced by simulating normal RV myocardial function (i.e., no local RV activation delay, normal contractility, and normal passive myocardial stiffness). The type II pattern was reproduced by reducing local contractility to 40% and increasing local passive stiffness to 200% of normal values.

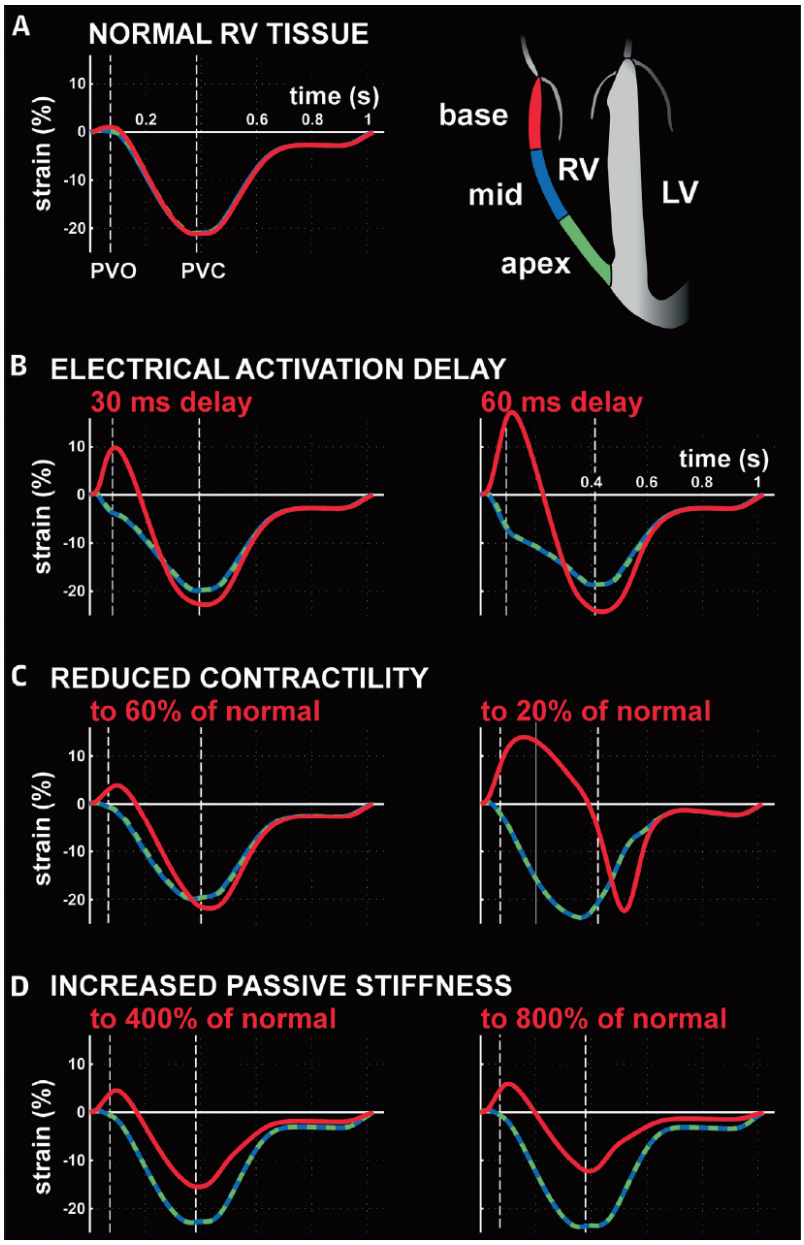

Figure 4. Simulations of Electrical and Mechanical RV Myocardial Substrates
Compared with (A) normal RV tissue, simulation ranges displayed the effects of (B) electrical substrate of delayed onset of activation, (C) mechanical substrate by decrease of myocardial contractility, and (D) mechanical substrate by increase of passive stiffness. LV = left ventricle; other abbreviations as in Figure 2.

The type III pattern was obtained by simulating a further reduction of contractility to 30% and an increase of passive stiffness to 800%. Besides regional RV myocardial deformation patterns, global RV geometry also changed as a result of the simulated type II and type III mechanical substrates; these changes followed the differences observed in the ARVC mutation carriers showing RV dilation with advancing ARVC disease (**Table 3**). A more detailed examination on the sensitivity of LV and RV systolic pump function and RV deformation parameters with respect to different degrees of hypocontractility, increased passive stiffness, and activation delay is available in *Supplementary Figures 3 to 5*. None of the observed RV deformation patterns of mutation carriers in the early electrical and subclinical ARVC stages was explained by (electrical) activation delay only. Adding activation delay had a negligible effect on the simulated patterns with severe mechanical hypocontractility and stiffness substrates (**Figure 5**).

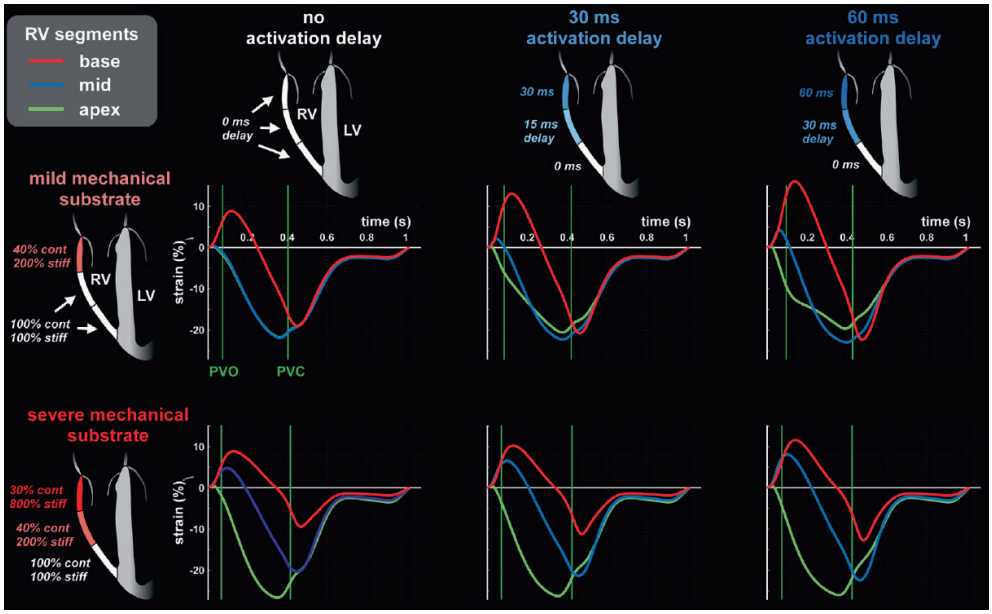

Figure 5. Effect of Electrical Activation Delay Added to Mechanical Substrates
Regional activation delay hardly changed the deformation patterns of RV segments in the type II and type III simulations with mild and severe mechanical hypocontractility and passive stiffness substrates, respectively. cont = contractility; stiff = stiffness; other abbreviations as in Figure 2.

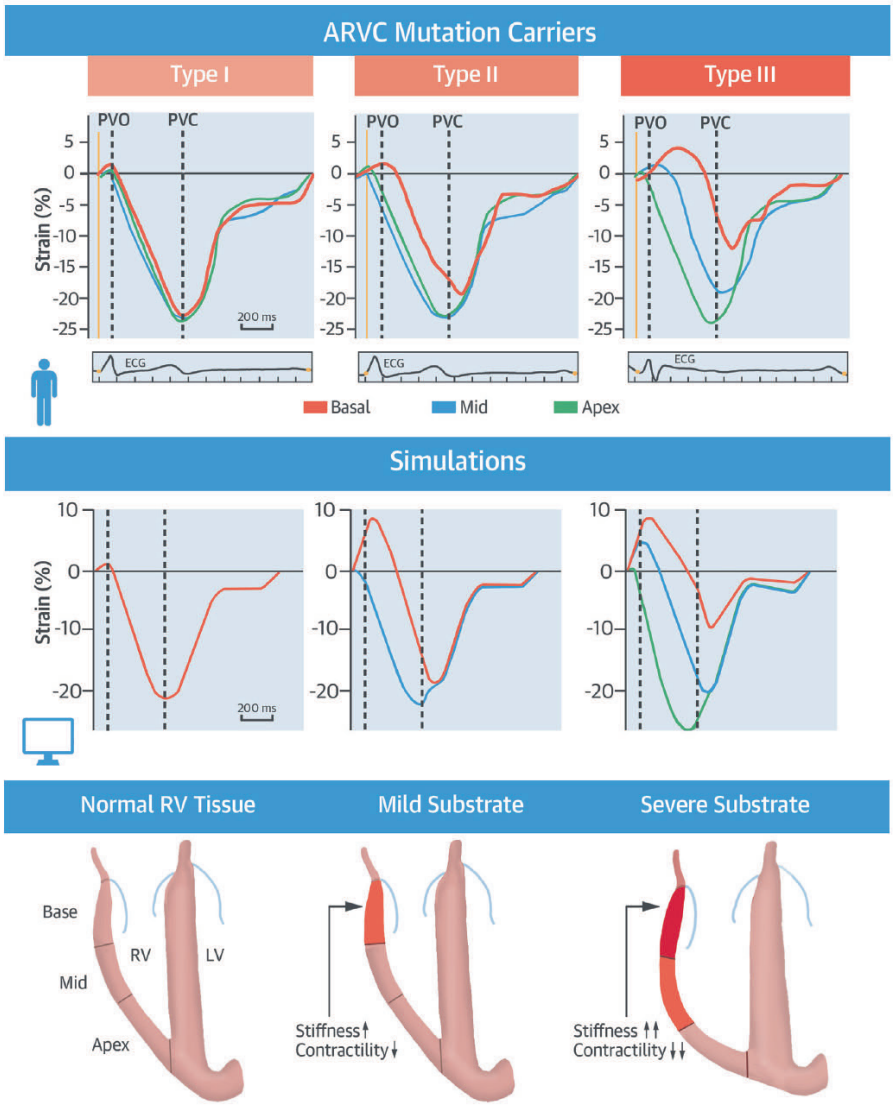

Mast, T.P. et al. J Am Coll Cardiol. 2016;68(20):2185–97.

Central Illustration. Strain Signatures in ARVC: Characteristic Types of RV Deformation
Using imaging and computer simulation to differentiate electrical from mechanical tissue substrates among arrhythmogenic right ventricular (RV) cardiomyopathy (ARVC) clinical stages, 3 distinctive characteristic RV longitudinal deformation patterns were identified. (Left) Type I normal deformation as seen in healthy controls, in 52% of the subclinical mutation carriers, and in CircAdapt model simulations of normal (healthy) RV tissue. (Middle) Type II, as seen in both subclinical and electrical stage mutation carriers, was reproduced by the computer simulation of severely reduced contractility and mildly increased passive stiffness in the basal (subtricuspid) RV segment. (Right) Type III, as mostly observed in the structural stage mutation carriers, was reproduced by the computer simulation of severely reduced contractility and severely increased passive stiffness in the basal (subtricuspid) RV segment. ECG = electrocardiogram; LV = left ventricular; PVO/PVC = pulmonary valve opening/closure

Table 3. Comparison of patients and simulations: RV geometry and basal deformation

	Controls	Type-I				Type-II				Type-III				P-value	
	(n=84)	Mutation carriers (n=12)	OPTIMAL SIMULATIONS *activation delay*			Mutation carriers (n=35)	OPTIMAL SIMULATIONS *activation delay*			Mutation carriers (n=37)	OPTIMAL SIMULATIONS *activation delay*			**All groups**	**Mutation carriers**
			none	30 ms	60 ms		none	30 ms	60 ms		none	30 ms	60 ms		
CMR* **															
RV-EDV (ml)	181±36	169±55	181*	183	188	208±86	197	200	206	247±85†	217	219	222	<.002	.039
RVEF (%)	54±4	55±8	54*	53	52	48±13	49	49	47	36±12†	45	44	44	<.001	<.001
SV (ml)	97±19	88±23	97**			95±17	97**			85±19	97**			.068	.154
HF (/min)	59±8	68±19	59**			63±11	59**			61±13	59**			.152	.374
Echocardiography															
Onset of shortening (ms)	52 [25,72]	60 [38,76]	62	92	114	119 [99,141]†	118	124	138	218 [128,293]†	130	132	142	<.001	<.001
Systolic peak strain (%)	-24.7±4.8	-23.9±5.3	-21.1	-22.6	-23.9	-16.4±3.5†	-17.2	-17.8	-16.7	-5.3±5.3†	-6.1	-6.5	-6.1	<.001	<.001
Post-systolic index (%)	2 [0,4]	1 [0,3]	0	0	1	15 [8,21]†	10	14	25	44 [22,78]†	35	42	52	<.001	<.001

Values are expressed by mean ± standard deviation, or median [interquartile range] if appropriate. P-values are for differences among mutation carriers and controls, or among mutation carriers only. †=P<0.05 versus age-and gender-matched controls (Bonferroni correction).
* RV-EDV and RVEF of the Type-I simulation without activation delay have been fitted to the average values measured in the controls.
** SV and HR in all Type-I, Type-II, and Type-III simulations were set to the average values measured in the controls.
*** Note that CMR data were available in a subgroup of 35 control subjects.

DISCUSSION

We used a combined echocardiographic deformation imaging and computer simulation approach to characterize pathophysiological RV tissue substrates in a broad spectrum of ARVC mutation carriers. First, we observed 3 characteristic deformation patterns within the RV free wall and showed they are clearly related to the different ARVC clinical stages. Second, computer simulations demonstrated that the RV deformation patterns typically observed in both the advanced structural and early electrical stages in ARVC mutation carriers can be explained by a combination of underlying reduced contractility and increased passive stiffness rather than electrical activation delay. The third and most striking finding was the existence of clearly abnormal type II RV deformation in mutation carriers in the subclinical and electrical stages that cannot be explained by exclusively electrical activation abnormalities. Instead, a severe degree of mechanical dysfunction is required to explain this type II pattern. Interestingly, according to the 2010 TFC, the subclinical stage subjects had normal ECGs and neither subclinical nor electrical stage subjects demonstrated structural abnormalities by conventional imaging.

Previous studies have shown numerous RV deformation characteristics, such as reduced systolic peak strain and differences in timing of onset and peak deformation, to be associated with ARVC in a broad spectrum of ARVC patients (12,15,18,25). To our knowledge, our study presented the first approach that combined all these observations into a set of characteristic RV deformation patterns. In clinical practice, strain parameter values are often just within normal range or mildly abnormal, whereas the shape of the deformation curve is clearly abnormal. A pattern-based approach might be more reliable, reproducible, and independent of loading conditions than individual timing- or amplitude-based strain measurements. Our pattern-based approach led to 3 distinct characteristic RV deformation patterns, the definitions of which allowed a more in-depth characterization of the underlying electromechanical substrate using a computer model. The severity of these substrates correlated well with ARVC severity.

Stages

By definition, all ARVC mutation carriers in the structural group fulfilled the 2010 TFC for structural abnormalities. This implied that a wall motion abnormality such as akinesia, dyskinesia, or aneurysm is present in combination with RV dilation or impaired RV systolic function measured by either CMR or echocardiography (9). These structural alterations result from fibrofatty replacements of the RV myocardium that affect regional wall motion and eventually global RV systolic function (1,8). Type III pattern predominates in structural stage patients and can, as hypothesized, be explained by model simulations representing RV mechanical substrate, that is, regional hypocontractility combined with increased passive

stiffness. Other studies using electroanatomic mapping and histopathology have found extensive electrical delay, low-voltage areas suggesting myocardial scar and fibrosis, and regional fibrous replacement of myocardium in this clearly affected group (16,24,26). These established findings corresponded well to the electromechanical substrates evaluated in our model simulations. Although an electrical activation delay clearly exists in the advanced structural ARVC stage, we demonstrated that it is unlikely to be the main determinant of the mechanical discoordination observed in these subjects (**Figure 5**).

Several clinical ARVC studies have suggested that electrical abnormalities precede structural abnormalities (6,7,27). These results are supported by experimental findings in mice carrying a *PKP2* mutation that revealed crosstalk between the desmosome and sodium channels (28,29). Sodium channel dysfunction was present before structural abnormalities developed, and these mice suffered ventricular arrhythmias before structural alterations became apparent (27,28). Therefore, we hypothesized that the abnormal deformation pattern in the electrical stage resulted from local electrical activation delay. However, type II RV deformation is present in most ARVC mutation carriers in the early electrical stage. This pattern can only be reproduced by simulating pronounced hypocontractility and a mild increase of passive stiffness in the RV basal area. The simulation with a substrate consisting of exclusively electrical activation delay (**Figure 4**) was not similar to any of the deformation patterns in our study cohort. Therefore, our results suggest that mechanical abnormalities throughout systole are already present in the so-called electrical stage, and that these abnormalities are not solely due to a delay in activation or repolarization. Our results illustrated a potential lack of sensitivity of the 2010 TFC for mechanical dysfunction and may suggest a potential role for deformation imaging in early ARVC detection (9,13–15). Nevertheless, our findings did not entirely exclude the theory of an electrical stage before structural disease as supported by murine studies (28,29). The sodium channel dysfunction could also be present in humans; however, it may not lead to detectable local mechanical discoordination.

Another important novel finding in our study was the presence of the clearly abnormal type II RV deformation pattern in almost one-half of the subclinical ARVC subjects. Remarkably, these subjects had a normal 12-lead ECG and lacked abnormalities on either CMR or conventional echocardiography, suggesting that both the conventional imaging modalities and 12-lead surface ECG lack sensitivity to detect early ARVC disease. The latter is supported by a study performed by Tandri *et al.* (24), who showed that prolonged total RV endocardial activation duration measured during an electrophysiological study did not correlate with surface ECG measurements.

The current study also extended our previous findings that the subtricuspid area (RV basal free wall) is an early affected region in ARVC (13,15,16). Why there is a predilection for the basal area to be the earliest-affected site in ARVC remains unresolved and beyond this study's scope. During sinus rhythm, the basal areas are activated slightly later than the mid and apical

regions (30). Consequently, the basal RV area faces higher regional wall stress compared with other RV regions, which might contribute to early disease expression (31). This effect may be exacerbated by the large increase in wall stress the RV experiences during exercise (32). Additionally, other studies have reported an apex–base gradient in action potential behavior and ion channel expression in the ventricular myocardium (33). It is therefore possible that functional differences between base and apex render the RV basal area more susceptible for disease expression. Further research is needed to mechanistically address these hypotheses.

Clinical implications

This study used a novel noninvasive approach combining echocardiographic deformation imaging and computer model simulations to characterize abnormal RV deformation in ARVC. Importantly, subjects in the subclinical phase of ARVC exhibited an abnormal RV deformation pattern that required mechanical abnormalities. RV deformation imaging by echocardiography may therefore be supplemental to current definitions of both electrical and subclinical ARVC stages for detecting early-stage ARVC pathology. Moreover, given that the combination of electrical and structural abnormalities is associated with a high arrhythmic propensity (6), accurate detection of both electrical and structural abnormalities is pivotal for optimal risk stratification. Our approach may play an important role in the noninvasive identification of high-risk ARVC family members and the noninvasive monitoring of disease progression. In that other RV pathologies such as ischemia, local infiltrative disease (sarcoidosis, myocarditis), or severe pulmonary hypertension could also produce regional loss of contractility and/or myocardial stiffening, the abnormal RV deformation patterns we reported are not necessarily ARVC-specific and should only be explained as ARVC disease expression if other conditions are ruled out or considered unlikely by conventional diagnostic approaches.

Study limitations

Our simulations evaluated only 3 pathophysiological variables known to contribute to the ARVC phenotype. Although more electromechanical tissue properties are likely to be changed during ARVC disease progression, these 3 parameter variations sufficed to reproduce the actual regional RV deformation abnormalities measured in ARVC patients experiencing different disease stages. Stroke volume and heart rate were set to the average values measured in the control subjects for all simulations. Furthermore, chronic RV dilation as a result of eccentric remodeling was not accounted for in our simulations. The combination of these 2 factors might explain the fact that the decline of RV function predicted by the type III simulation was smaller than that measured in the patients with type III RV deformation. CMR was not available in all subjects, primarily due to implantable cardioverter-defibrillator implantations. In these cases, the presence of structural 2010 TFC was determined solely from echocardiography. This modality is known to have a lower

diagnostic performance compared with CMR (34). Nevertheless, in 13 of 21 subjects with missing CMRs, structural criteria were indisputably met because echocardiography showed multiple clear RV wall motion abnormalities and severe RV systolic dysfunction. Moreover, in almost all of the subclinical and electrical stage subjects, a CMR was available, and therefore, regional wall motion abnormalities were likely to be detected. Our findings are limited to subjects carrying a pathogenic desmosomal mutation. Future prospective verification studies are needed to confirm our findings and determine whether our results can be extrapolated to nondesmosomal mutation carriers or gene-elusive ARVC patients.

Conclusions

We described 3 characteristic RV deformation patterns in ARVC mutation carriers that are confined to different ARVC disease stages. Computer simulations demonstrated that these abnormal patterns are not explained by electrical activation delay only and require at least some degree of local mechanical dysfunction. The substrate severity correlated well to ARVC disease severity. Both subclinical and electrical staged mutation carriers showed signs of underlying local subtricuspid mechanical dysfunction in absence of established clinical disease criteria.

Perspectives

Competency in Medical Knowledge: Patients with early-stage ARVC exhibit mechanical abnormalities before development of detectable electrical abnormalities, challenging the current staging criteria for this disease.

Translational Outlook: Prospective clinical studies are needed to clarify the role of echocardiographic deformation imaging in risk stratification for patients with ARVC.

REFERENCES

1. Marcus FI, Fontaine GH, Guiraudon G, et al. Right ventricular dysplasia: a report of 24 adult cases. *Circulation* 1982;65:384–98.
2. Dalal D, Nasir K, Bomma C, et al. Arrhythmogenic right ventricular dysplasia: a United States experience. *Circulation* 2005;112:3823–32.
3. Groeneweg JA, Bhonsale A, James CA, et al. Clinical presentation, long-term follow-up, and outcomes of 1001 arrhythmogenic right ventricular dysplasia/cardiomyopathy patients and family members. *Circ Cardiovasc Genet* 2015;8:437–46.
4. Bhonsale A, Groeneweg JA, James CA, et al. Impact of genotype on clinical course in arrhythmogenic right ventricular dysplasia/cardiomyopathy-associated mutation carriers. *Eur Heart J* 2015;36:847–55.
5. Protonotarios N, Anastasakis A, Antoniades L, et al. Arrhythmogenic right ventricular cardiomyopathy/dysplasia on the basis of the revised diagnostic criteria in affected families with desmosomal mutations. *Eur Heart J* 2011;32:1097–104.
6. Te Riele AS, Bhonsale A, James CA, et al. Incremental value of cardiac magnetic resonance imaging in arrhythmic risk stratification of arrhythmogenic right ventricular dysplasia/cardiomyopathy-associated desmosomal mutation carriers. *J Am Coll Cardiol* 2013;62:1761–9.
7. Te Riele AS, James CA, Rastegar N, et al. Yield of serial evaluation in at-risk family members of patients with ARVD/C. *J Am Coll Cardiol* 2014;64: 293–301.
8. Basso C, Corrado D, Marcus FI, et al. Arrhythmogenic right ventricular cardiomyopathy. *Lancet* 2009;373:1289–300.
9. Marcus FI, McKenna WJ, Sherrill D, et al. Diagnosis of arrhythmogenic right ventricular cardiomyopathy/dysplasia: proposed modification of the task force criteria. *Circulation* 2010;121:1533–41.
10. Teske AJ, De Boeck BW, Melman PG, et al. Echocardiographic quantification of myocardial function using tissue deformation imaging, a guide to image acquisition and analysis using tissue Doppler and speckle tracking. *Cardiovasc Ultrasound* 2007;5:27.
11. Mast TP, Teske AJ, Doevendans PA, Cramer MJ. Current and future role of echocardiography in arrhythmogenic right ventricular dysplasia/cardiomyopathy. *Cardiol J* 2015;22:362–74.
12. Sarvari SI, Haugaa KH, Anfinsen OG, et al. Right ventricular mechanical dispersion is related to malignant arrhythmias: a study of patients with arrhythmogenic right ventricular cardiomyopathy and subclinical right ventricular dysfunction. *Eur Heart J* 2011;32:1089–96.
13. Teske AJ, Cox MG, te Riele AS, et al. Early detection of regional functional abnormalities in asymptomatic ARVD/C gene carriers. *J Am Soc Echocardiogr* 2012;25:997–1006.
14. Mast TP, Teske AJ, vd Heijden JF, et al. Left ventricular involvement in arrhythmogenic right ventricular dysplasia/cardiomyopathy assessed by echocardiography predicts adverse clinical outcome. *J Am Soc Echocardiogr* 2015;28:1103–13.
15. Mast TP, Teske AJ, te Riele AS, et al. Prolonged electromechanical interval unmasks arrhythmogenic right ventricular dysplasia/cardiomyopathy in the subclinical stage. *J Cardiovasc Electrophysiol* 2016;27:303–14.
16. Te Riele AS, James CA, Philips B, et al. Mutation-positive arrhythmogenic right ventricular dysplasia/cardiomyopathy: the triangle of dysplasia displaced. *J Cardiovasc Electrophysiol* 2013;24:1311–20.
17. Prakasa KR, Wang J, Tandri H, et al. Utility of tissue Doppler and strain echocardiography in arrhythmogenic right ventricular dysplasia/cardiomyopathy. *Am J Cardiol* 2007;100:507–12.

R1 R2 R3 R4 R5 R6 R7 R8 R9 R10 R11 R12 R13 R14 R15 R16 R17 R18 R19 R20 R21 R22 R23 R24 R25 R26 R27 R28 R29 R30 R31 R32 R33 R34 R35 R36 R37 R38 R39

R1 R2 R3 R4 R5 R6 R7 R8 R9 R10 R11 R12 R13 R14 R15 R16 R17 R18 R19 R20 R21 R22 R23 R24 R25 R26 R27 R28 R29 R30 R31 R32 R33 R34 R35 R36 R37 R38 R39

18. Teske AJ, Cox MG, De Boeck BW, et al. Echocardiographic tissue deformation imaging quantifies abnormal regional right ventricular function in arrhythmogenic right ventricular dysplasia/cardiomyopathy. *J Am Soc Echocardiogr* 2009;22: 920–7.
19. Dalal D, Tandri H, Judge DP, et al. Morphologic variants of familial arrhythmogenic right ventricular dysplasia/cardiomyopathy a genetics magnetic resonance imaging correlation study. *J Am Coll Cardiol* 2009;53:1289–99.
20. Walmsley J, Arts T, Derval N, et al. Fast simulation of mechanical heterogeneity in the electrically asynchronous heart using the MultiPatch module. *PLoS Comput Biol* 2015;11:e1004284.
21. Lumens J, Arts T, Marcus JT, et al. Early-diastolic left ventricular lengthening implies pulmonary hypertension-induced right ventricular decompensation. *Cardiovasc Res* 2012;96:286–95.
22. Arts T, Lumens J, Kroon W, Delhaas T. Control of whole heart geometry by intramyocardial mechano-feedback: a model study. *PLoS Comput Biol* 2012;8:e1002369.
23. Lumens J, Tayal B, Walmsley J, et al. Differentiating electromechanical from nonelectrical substrates of mechanical discoordination to identify responders to cardiac resynchronization therapy. *Circ Cardiovasc Imaging* 2015;8:e003744.
24. Tandri H, Asimaki A, AbrahamT, et al. Prolonged RV endocardial activation duration: a novel marker of arrhythmogenic right ventricular dysplasia/cardiomyopathy. Heart Rhythm 2009;6:769–75. 25. Vigneault DM, te Riele AS, James CA, et al. Right ventricular strain by MR quantitatively identifies regional dysfunction in patients with arrhythmogenic right ventricular cardiomyopathy. *J Magn Reson Imaging* 2016;43:1132–9.
26. Haqqani HM, Tschabrunn CM, Betensky BP, et al. Layered activation of epicardial scar in arrhythmogenic right ventricular dysplasia: possible substrate for confined epicardial circuits. *Circ Arrhythm Electrophysiol* 2012;5:796–803.
27. Gomes J, Finlay M, Ahmed AK, et al. Electrophysiological abnormalities precede overt structural changes in arrhythmogenic right ventricular cardiomyopathy due to mutations in desmoplakin. A combined murine and human study. *Eur Heart J* 2012;33:1942–53.
28. Cerrone M, Noorman M, Lin X, et al. Sodium current deficit and arrhythmogenesis in a murine model of plakophilin-2 haploinsufficiency. *Cardiovasc Res* 2012;95:460–8.
29. Noorman M, van der Heyden MA, van Veen TA, et al. Cardiac cell-cell junctions in health and disease: electrical versus mechanical coupling. *J Mol Cell Cardiol* 2009;47:23–31.
30. Durrer D, van Dam RT, Freud GE, et al. Total excitation of the isolated human heart. *Circulation* 1970;41:899–912.
31. Prinzen FW, Hunter WC, Wyman BT, McVeigh ER. Mapping of regional myocardial strain and work during ventricular pacing: experimental study using magnetic resonance imaging tagging. *J Am Coll Cardiol* 1999;33:1735–42.
32. La Gerche A, Roberts T, Claessen G. The response of the pulmonary circulation and right ventricle to exercise: exercise-induced right ventricular dysfunction and structural remodeling in endurance athletes (2013 Grover Conference series). *Pulm Circ* 2014;4:407–16.
33. Szentadrassy N, Banyasz T, Biro T, et al. Apicobasal inhomogeneity in distribution of ion channels in canine and human ventricular myocardium. *Cardiovasc Res* 2005;65:851–60.
34. Borgquist R, Haugaa KH, Gilljam T, et al. The diagnostic performance of imaging methods in ARVC using the 2010 Task Force criteria. *Eur Heart J Cardiovasc Imaging* 2014;15:1219–25.

SUPPLEMENTARY FILES

Deformation parameters – definitions:

RV deformation patterns were classified based on the longitudinal strain curve of the RV basal lateral region (subtricuspid area). Classification was based on criteria that have previously been associated with ARVC: timing of onset shortening, timing of peak shortening, systolic peak strain, peak strain, and post-systolic shortening. Time to onset shortening was defined as time between onset-QRS and onset of mechanical shortening. Time to peak shortening was defined as time between onset-QRS and peak strain. Timing was expressed in milliseconds. Systolic peak strain (%) was defined as maximal negative value between pulmonary valve opening (PVO) and closure (PVC). In case of positive strain during systole, the value at PVC was taken. Peak strain (%) was defined as maximal negative value during entire cardiac cycle. Post-systolic index (%) was defined as:

$$Post\ systolic\ index = 100 \bullet \frac{\text{peak strain} - \text{systolic peak strain}}{\text{peak strain}}.$$

Timing of valve opening/closure was determined by Doppler flow curves. For example measurements of the used parameters in the RV deformation patterns see **Supplemental Figure 1**.

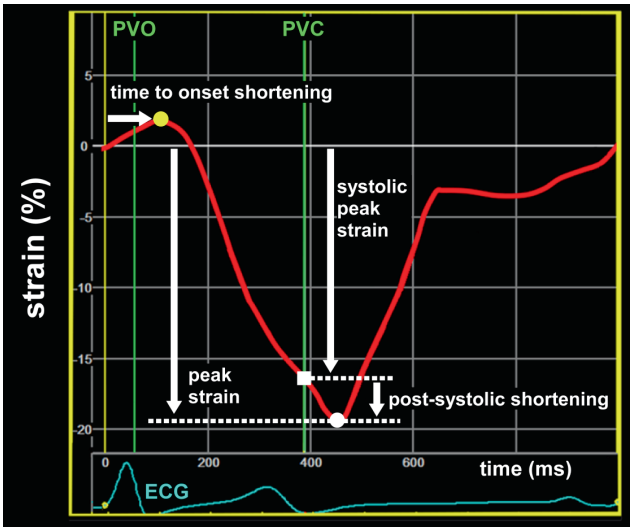

Supplemental Figure 1. Example of RV deformation characteristics in a Type-II pattern.

R1 R2 R3 R4 R5 R6 R7 R8 R9 R10 R11 R12 R13 R14 R15 R16 R17 R18 R19 R20 R21 R22 R23 R24 R25 R26 R27 R28 R29 R30 R31 R32 R33 R34 R35 R36 R37 R38 R39

Additional Information from the Methods Section

B-mode images from 1 cardiac cycle were analyzed with dedicated software (EchoPAC PC version 12, GE Vingmed Ultrasound AS) to perform two-dimensional (2D) speckle-tracking on the RV lateral free wall as previously described (1). Separate longitudinal strain curves were obtained for the basal, mid-ventricular, and apical RV regions. RVOT spectral Doppler measurements were used to determine times of pulmonary valve opening (PVO) and pulmonary valve closure (PVC).

To determine the interobserver variability of pattern classification, a second observer re-performed 2D speckle tracking and subsequently analyzed the strain curves in a random sample (n = 30) of our total study population. Intra-observer variability was determined 3 months after initial evaluation and blinded for previous classification results in the same random sample.

CircAdapt (www.circadapt.org) enables realistic and real-time simulation of beat-to-beat cardiovascular mechanics and hemodynamics under a wide range of physiological and pathophysiological conditions. Simulations of mechanical and hemodynamic ventricular interaction as well as RV myocardial deformation in the normal heart and during RV failure have been validated in previous studies (2,3). The CircAdapt model also enables realistic simulation of regional myocardial deformation in failing hearts with heterogeneous electromechanical tissue properties in the ventricular walls (4,5).

In all simulations, circulating blood volume and systemic peripheral vascular resistance were adjusted so that venous return (cardiac output) and mean arterial blood pressure (LV afterload) were maintained at 5.7 l/min and 91 mm Hg, respectively. Mean pulmonary arterial pressure (RV afterload) was 19 mm Hg in the healthy control simulation and arises from a previously published non-linear transpulmonary pressure-flow relationship mimicking the flow-dependent resistive behavior of the pulmonary vascular bed (6). Since cardiac output was similar for all simulations, RV afterload hardly varied between the simulations (mean ± SD: 20.0 ± 0.8 mm Hg).

Mechanical stiffness substrate: passive myocardial stiffness was increased from 100% (normal passive stiffness) to a maximum of 1000% of its normal value, in steps of 100%. These changes of passive stiffness were based on serial measurements of passive material properties of infarcted sheep LV myocardium (7). These experimental data reported increases of passive myocardial stiffness of 200% after 4-h ligation up to 1500% after 2-week ligation.

Supplemental Table 1: Control subjects versus simulation: cardiac function data

	Control subjects (n=35)	Control simulation
Echocardiography		
PVO (ms)	68 ± 10	74
PVC (ms)	397 ± 25	383
CMR		
HR (beats/min)	59 ± 8	59
SV (ml)	97 ± 19	97
RV-EDV (ml)	181 ± 36	181
RVEF (%)	54 ± 4	54
LV-EDV (ml)	170 ± 35	170
LVEF (%)	58 ± 5	57

Values are expressed as mean ± standard deviation. CMR = cardiac magnetic resonance imaging; EDV = end-diastolic volume; HR = heart rate; LV = left ventricle; LVEF = LV ejection fraction; PVC = time from onset QRS to pulmonary valve closure; PVO = time from onset QRS to pulmonary valve opening; RV = right ventricle; RVEF = RV ejection fraction; SV = stroke volume;

CircAdapt simulation protocol: healthy control simulation

The open access version of the CircAdapt model, which has previously been published by Walmsley *et al.* and is freely downloadable from www.circadapt.org, has been used for all simulations performed in this study. (8) We created a reference simulation matched to the control subjects in our current study as follows. We began our simulations with the model's default reference simulation (*PRef.mat*), which represents a generalized healthy adult cardiovascular system under baseline resting conditions. In the current study, the LV free wall and interventricular septum were synchronously activated 150 ms after right atrial activation. The RV free wall was activated after an additional 15 ms delay in accordance with human electrophysiological mapping data.(9) Normal cardiac output (5 L/min) and mean arterial blood pressure (91 mmHg) at a fixed heart rate of 70 beats per minute were obtained by a homeostatic control mechanism regulating total circulatory blood volume and systemic vascular resistance. In the model, both rise and decay time of myofiber contractile force generation were scaled to obtain realistic timing of pulmonary valve opening and closure as measured relative to onset QRS in the healthy control subjects (**Supplemental Table 1**) using Doppler flow velocity imaging. Size, mass and passive tissue stiffness of the vascular and cardiac walls were then adapted so that the local mechanical load on the constituting tissues was normalized to tissue-specific physiological levels.(10) After this structural adaptation, stroke volume and heart rate were set to average values measured in the healthy controls (**Supplemental Table 1**), using the homeostatic control mechanism mentioned above. The mean arterial blood pressure of 91 mmHg was maintained as this was also the average value measured in the control subjects. Values of LV and RV end-diastolic volumes and ejection fractions consistent with the average values measured in the control population

(**Supplemental Table 1**) were obtained through adjustments to the areas of the ventricular walls assigned to non-contractile, non-compliant tissue such as the tricuspid and mitral annuli. The resulting simulation, representing our healthy control population, was used as the starting point for the electrical and mechanical tissue substrate simulations described in the Methods section of the main text.

Additional Information on Reproducibility

A random sample of 30 cases were selected from our total study population. This sample consisted of 5 subclinical staged subjects, 5 electrical staged subjects, 11 structural staged subjects and 9 healthy controls. Observers were blinded for clinical characteristics during deformation analysis.

Supplemental Table 2: inter- and intra-observer agreement for classification of RV deformation patterns

Inter-observer agreement

	Observer #1			
Observer #2		**Type-I**	**Type-II**	**Type-III**
	Type-I	12	1	0
	Type-II	0	6	0
	Type-III	0	1	10

Linear weighted kappa = 0.92 (0.83-1.00)

Intra-observer agreement

	Observer #1 - First			
Observer #1 – second		**Type-I**	**Type-II**	**Type-III**
	Type-I	12	0	0
	Type-II	0	7	0
	Type-III	0	1	10

Linear weighted kappa = 0.96 (0.90-1.00)

Selection of the "best-match" Type-I, Type-II and Type-III simulations

The three characteristic deformation indices that were used to categorize the ARVC mutation carriers, i.e., time of onset shortening (x), post-systolic index (y), and systolic peak strain (z), were quantified for all simulations without an electrical activation delay. For each simulation, these three basal RV deformation indices were compared with the average values measured in each patient subgroup. The simulations with the smallest *Relative Error* when compared to the average index values in subgroup I, II or III, respectively, were selected as the "best-

match" simulations and were assumed to be most representative for the average Type-I, Type-II or Type-III patients. *Relative Error* was defined as:

$$Relative\ Error\ (TYPE) = \frac{|x_{sim} - x_{pat}(TYPE)|}{x_{pat\ ALL}} + \frac{|y_{sim} - y_{pat}(TYPE)|}{y_{pat\ ALL}} + \frac{|z_{sim} - z_{pat}(TYPE)|}{z_{pat\ ALL}},$$

where *sim* indicates simulated index values, *pat* is used for average index values measured in the patient subgroups (indicated by *TYPE*), and *pat ALL* is used for the average values of the indices in all 84 ARVC mutation carriers. Figure S2 shows the Relative Errors for all simulation per RV deformation pattern type.

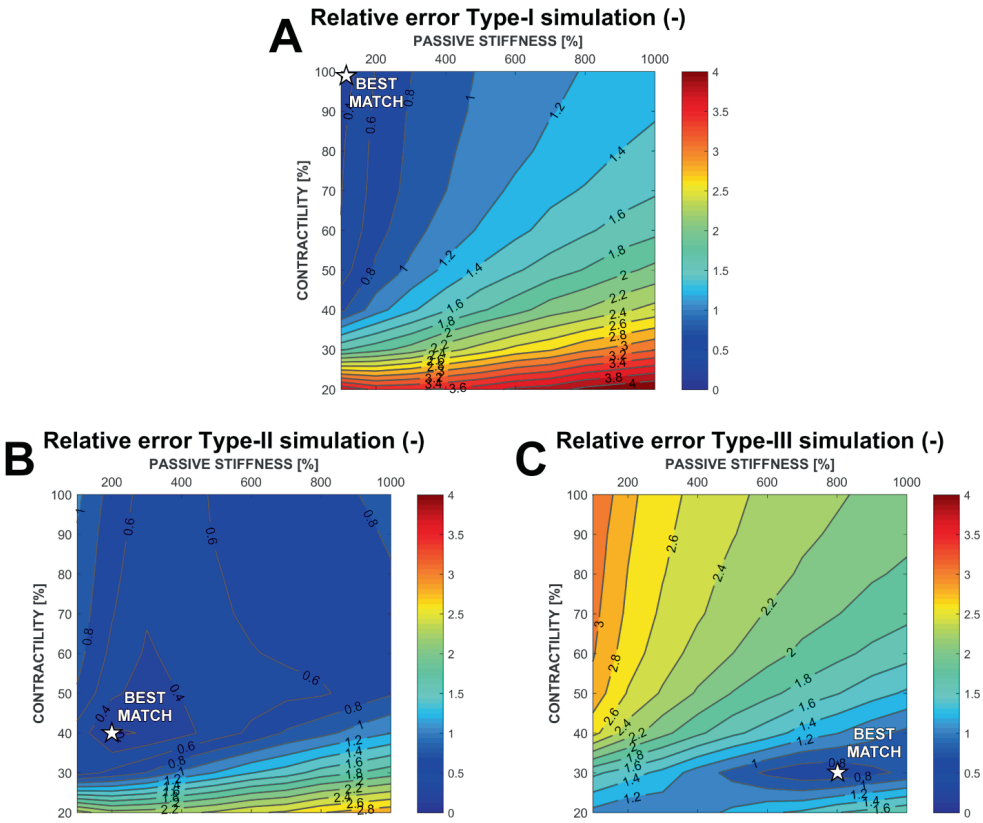

Supplemental Figure 2. Selection of "best-match" simulations based on smallest Relative Error per type of RV deformation.

The mechanical substrate combination giving the "best-match" simulation, i.e., with the smallest Relative Error, is indicated by a white star for the Type-I (A), Type-II (B) and Type-III (C) RV deformation patterns.

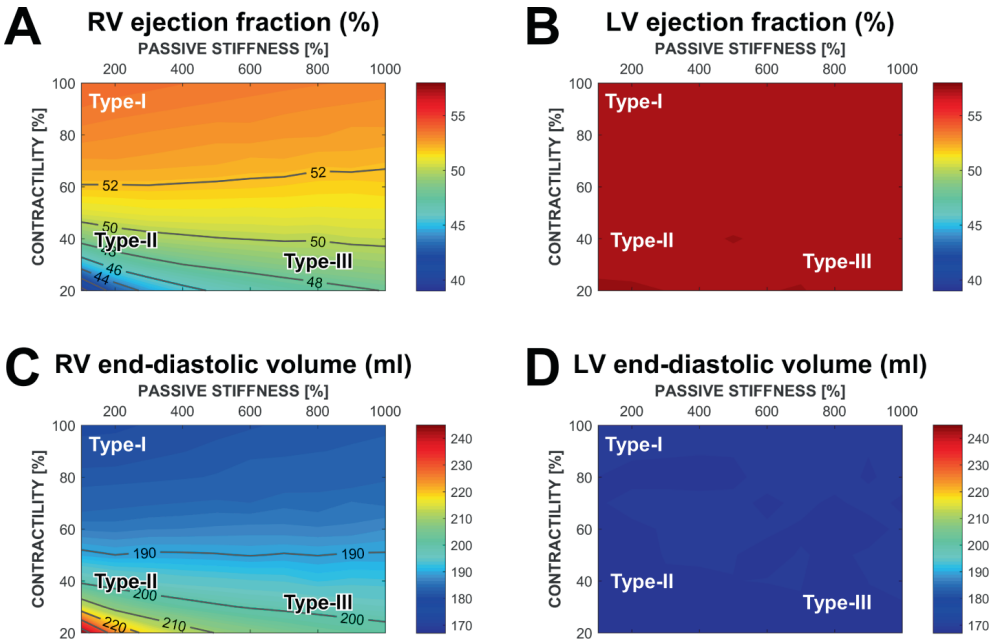

Supplemental Figure 3. Simulated effects of mechanical substrates on global right and left ventricular pump function.

Right ventricular (RV) ejection fraction (panel A) decreased due to increase of RV end-diastolic volume (panel C) with basal RV contractility, while both parameters were relative insensitive to changes of passive stiffness. Left ventricular (LV) ejection fraction and end-diastolic volume (panels B and D, respectively) were insensitive to changes of both basal RV contractility and passive stiffness. Note that it is indicated where in the parameter space the characteristic RV deformation patterns (Type-I, Type-II and Type-III), as observed in ARVC mutation carriers, were observed.

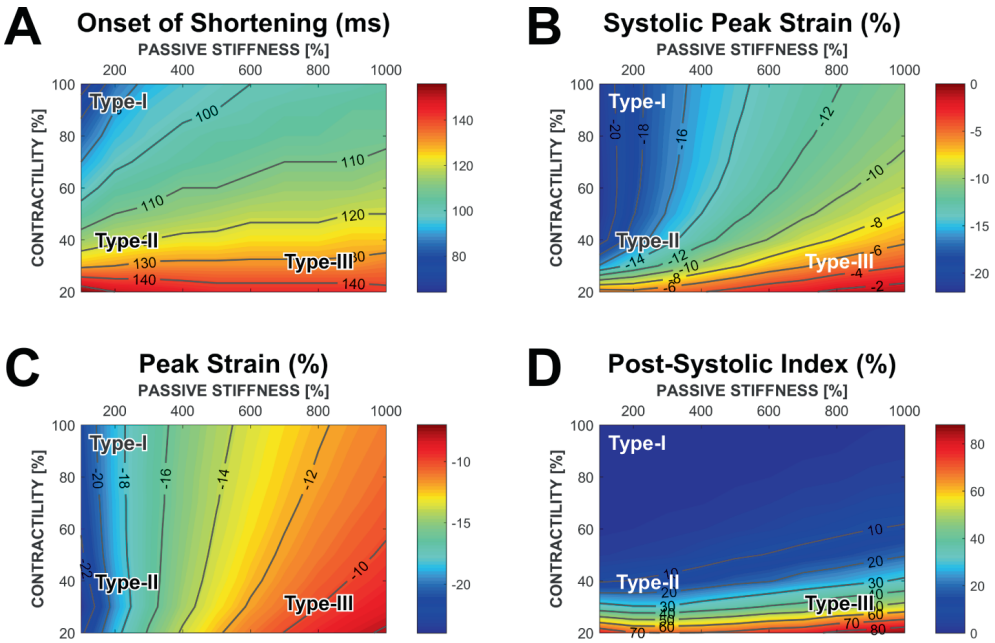

Supplemental Figure 4. Simulated effects of mechanical substrates on basal RV deformation indices. Sensitivities of A) onset of shortening, B) systolic peak strain, C) peak strain, and D) post-systolic index to changes of contractility and passive stiffness. Note that it is indicated where in the parameter space the characteristic RV deformation patterns (Type-I, Type-II and Type-III), as observed in ARVC mutation carriers, were observed. At low contractility, onset of shortening and systolic peak strain were mostly dependent on contractility. Both indices were also sensitive to changes of passive stiffness at higher contractility. Peak strain was most sensitive to changes of passive stiffness, whereas post-systolic index was most sensitive to contractility.

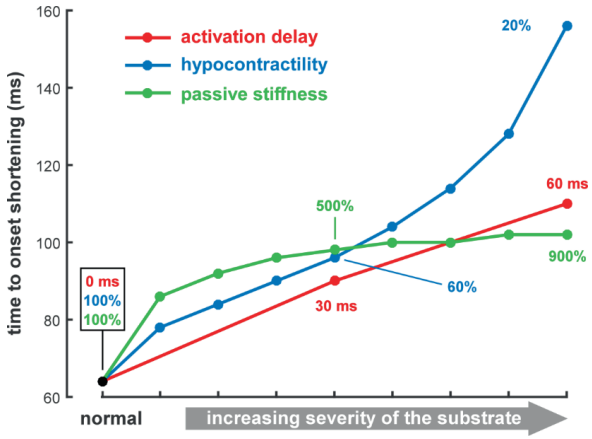

Supplemental Figure 5. Simulated effects of electrical and mechanical substrates on time to onset shortening.
Sensitivities to isolated changes of activation delay, contractility, and passive stiffness to time to onset of shortening. Note that onset of shortening is sensitive to all three tested tissue substrates.

R1
R2
R3
R4
R5
R6
R7
R8
R9
R10
R11
R12
R13
R14
R15
R16
R17
R18
R19
R20
R21
R22
R23
R24
R25
R26
R27
R28
R29
R30
R31
R32
R33
R34
R35
R36
R37
R38
R39

REFERENCES – SUPPLEMENTARY FILES

(1) Teske AJ, De Boeck BW, Melman PG, et al. Echocardiographic quantification of myocardial function using tissue deformation imaging, a guide to image acquisition and analysis using tissue Doppler and speckle tracking. *Cardiovasc Ultrasound* 2007;5:27.

(2) Walmsley J, Arts T, Derval N, et al. Fast Simulation of Mechanical Heterogeneity in the Electrically Asynchronous Heart Using the MultiPatch Module. *PLoS Comput Biol* 2015;11:e1004284.

(3) Arts T, Delhaas T, Bovendeerd P, et al. Adaptation to mechanical load determines shape and properties of heart and circulation: the CircAdapt model. *Am J Physiol Heart Circ Physiol* 2005;288:H1943-54.

(4) Lumens J, Delhaas T, Kirn B, Arts T. Three-wall segment (TriSeg) model describing mechanics and hemodynamics of ventricular interaction. *Ann Biomed Eng* 2009;37:2234-55.

(5) Lumens J, Arts T, Marcus JT, et al. Early-diastolic left ventricular lengthening implies pulmonary hypertension-induced right ventricular decompensation. *Cardiovasc Res* 2012;96:286-95.

(6) Lumens J, Blanchard DG, Arts T, et al. Left ventricular underfilling and not septal bulging dominates abnormal left ventricular filling hemodynamics in chronic thromboembolic pulmonary hypertension. *Am J Physiol Heart Circ Physiol* 2010;299:H1083-91.

(7) Gupta KB, Ratcliffe MB, Fallert MA, Edmunds LH, Jr., Bogen DK. Changes in passive mechanical stiffness of myocardial tissue with aneurysm formation. *Circulation* 1994;89:2315-26.

(8) Walmsley J, Arts T, Derval N et al. Fast Simulation of Mechanical Heterogeneity in the Electrically Asynchronous Heart Using the MultiPatch Module. *PLoS Comput Biol* 2015;11:e1004284.

(9) Durrer D, van Dam RT, Freud GE et al. Total excitation of the isolated human heart. *Circulation* 1970;41:899-912.

(10) Arts T, Delhaas T, Bovendeerd P et al. Adaptation to mechanical load determines shape and properties of heart and circulation: the CircAdapt model. *Am J Physiol Heart Circ Physiol* 2005;288:H1943-54.

CHAPTER 5

Optimizing Family Screening Protocols: The Additional Value of Right Ventricle Deformation Imaging to Predict Disease Progression in Early Arrhythmogenic Right Ventricular Cardiomyopathy

Thomas P Mast, Maarten J Cramer, Joost Lumens, Jeroen F van der Heijden, Karim Taha, Berto J Bouma, Maarten P van den Berg, Folkert W Asselbergs, Pieter A Doevendans, Arco J Teske

Submitted

ABSTRACT

Aims: Previous reports have shown that echocardiographic deformation imaging detects abnormal right ventricular (RV) deformation in absence of established disease expression in arrhythmogenic RV cardiomyopathy (ARVC). We aimed to explore if deformation imaging could be of incremental value in optimizing ARVC family screening protocols.

Methods and Results: First-degree relatives of ARVC patients (n=109, 82% pathogenic ARVC mutation carriers) without fulfilling structural Task-Force criteria (TFC) were serial evaluated according to 2010 TFC including RV deformation imaging. At baseline, 45 relatives (41%) had electrical abnormalities as defined by TFC, the remaining 64 relatives had no TFC abnormalities during clinical work-up. Deformation patterns of the subtricuspid region were scored by *Type-I*: normal deformation, *Type-II*: delayed onset, decreased systolic peak, and post-systolic shortening, or *Type-III*: systolic stretching and large post-systolic shortening. Type-I was seen in 50 (46%), Type-II in 53 (49%), and Type-III in 6 (5%) relatives. Sixty-five (60%) underwent a second evaluation after 3.7±2.1 years. Disease progression was defined as the development of a new 2010 TFC during follow-up that was absent at first evaluation. Deformation patterns Type-II/Type-III (n=37) at baseline were associated with disease progression during follow-up compared to relatives with normal deformation (Type-I, n=28); disease progression in: 43% vs. 4%, respectively, P<.001; positive and negative predictive values of abnormal deformation were 43% and 96%.

Conclusion: Normal RV deformation pattern is associated with an absence of disease progression during a 4-year follow-up in ARVC relatives. Echocardiographic deformation imaging identifies relatives that could benefit from a low-frequency follow-up strategy during ARVC family screening.

INTRODUCTION

Arrhythmogenic right ventricular cardiomyopathy (ARVC) is an inherited cardiomyopathy clinically characterized by ventricular arrhythmias and predominantly right ventricular (RV) dysfunction.[1] In the past decades, much progress has been made on defining the genetic basis of this condition.[2-5] Typical genetic features of ARVC are reduced penetrance and variable disease expressivity which complicates family screening.[6, 7] A recent consensus statement by an international Task Force recommends a repeated clinical assessment in all ARVC family members every 2-3 years, even in individuals without any morphological and/or functional abnormalities.[8] Comprehensive cardiac screening of ARVC family members is routinely performed by electrocardiography (ECG), Holter monitoring, and cardiac imaging for detecting established ARVC related abnormalities.[6, 9] However, early ARVC is characterized by the lack of overt structural abnormalities detected by conventional imaging approaches.[6, 10] Novel imaging techniques, such as echocardiographic deformation imaging, could be of incremental value in optimizing ARVC family screening protocols.

Echocardiographic deformation imaging is a technique that enables quantification of regional RV deformation and provides insight in mechanical dyssynchrony and regional contractility.[11-13] Previous reports suggest that this technique is capable to detect subtle local functional abnormalities in absence of structural abnormalities detected by conventional imaging.[13-15] Furthermore, we recently reported a new pattern-based approach that combines multiple deformation parameters into distinct deformation patterns. A clear correlation between abnormal deformation patterns and disease severity among ARVC desmosomal mutation carriers was found.[16] In addition, we were able to characterize the electromechanical substrate underlying these patterns.[16] Abnormal deformation was typically seen in the basal area of the RV free wall (or subtricuspid area) which is recognized as the one of the earliest affected area in ARVC.[14-17] Importantly, abnormal deformation in this specific area was seen during the earliest subclinical stage without any established phenotypic disease expression (Task Force criteria). Therefore, echocardiographic deformation imaging may play a pivotal role during ARVC family screening.

This longitudinal study was conducted to explore the value of deformation imaging in ARVC family member screening. Our hypothesis is that detectable RV deformation abnormalities precede the conventional signs of ARVC disease progression during the early ARVC stages and can therefore help to identify relatives at risk for disease progression.

R1
R2
R3
R4
R5
R6
R7
R8
R9
R10
R11
R12
R13
R14
R15
R16
R17
R18
R19
R20
R21
R22
R23
R24
R25
R26
R27
R28
R29
R30
R31
R32
R33
R34
R35
R36
R37
R38
R39

METHODS

Study population

During a 10-year observational period (2006-2016), we performed comprehensive echocardiographic examination according to our ARVC protocol including deformation imaging in probands and their relatives during their clinical work-up for ARVC.[11, 18] The study participants (n=194, age>18years) were derived from the Dutch National ARVC registry with patients from University Medical Center Utrecht (n=161), Academic Medical Center Amsterdam (n=18), and University Medical Center Groningen (n=15). In total, echocardiographic RV deformation imaging was available in 66 ARVC probands and 128 first-degree relatives. All probands were genetically tested for known ARVC related pathogenic mutations: plakophillin-2 (*PKP2*), desmoglein-2 (*DSG2*), desmocollin-2 (*DSC2*), desmoplakin (*DSP*) and plakoglobin (*JUP*).[9, 19] Non-desmosomal analysis included transmembrane protein 43 (*TMEM43*) and phospholamban (*PLN*).[20]

The following participants were eligible for this study: 1) first-degree relatives carrying the identical pathogenic ARVC mutation as identified in the probands, or 2) first-degree relatives of mutation-negative probands. These relatives (n=128) were classified by the presence of subsets of 2010 Task Force Criteria (TFC) during clinical work-up at baseline:[6, 9, 16]

- Relatives with structural abnormalities which fulfilled 2010 TFC detected by echocardiography or cardiac magnetic resonance imaging (CMR) were classified to the *structural stage*.
- Relatives without structural abnormalities fulfilling 2010 TFC but with the presence of ECG abnormalities (repolarization and/or depolarization) and/or history of ventricular arrhythmias as defined by the 2010 TFC were classified to the *electrical stage.*
- Relatives without any electrical or structural TFC were assigned to the *subclinical stage.*

To investigate the value of echocardiographic deformation imaging during the early clinical ARVC stages (i.e. subclinical and electrical stage), relatives fulfilling structural abnormalities by the TFC (i.e. structural stage) were excluded for further analysis (n=19). The final study population comprised 109 first-degree relatives with at least one echocardiographic exam with RV recordings suitable for RV deformation imaging (**Figure 1**).[11] The local medical ethical committees of each participating center approved this study.

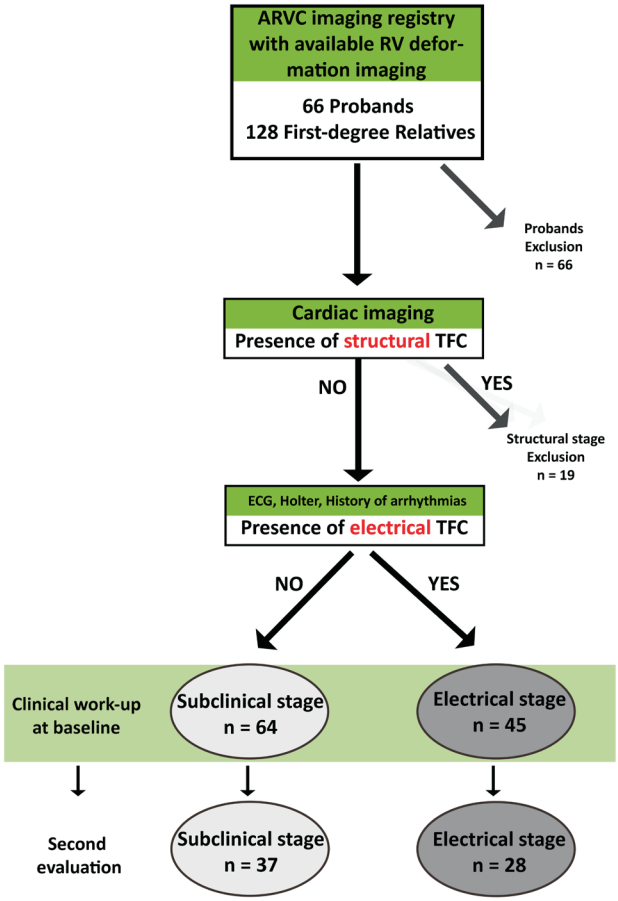

Figure 1. Study design
Relatives with right ventricular deformation imaging were eligible for this study. The presence of structural abnormalities (as defined by 2010 TFC) resulted in exclusion of the study. Only relatives in the early clinical stages (electrical stage and subclinical stage, n=109) were included in this study. Sixty-five relatives underwent a second cardiac evaluation. *Abbreviations*: ARVC = arrhythmogenic right ventricular cardiomyopathy; TFC = task force criteria; ECG = electrocardiography; RV = right ventricle

Cardiac evaluation

All subjects underwent standard 12-lead electrocardiography (ECG). ECGs were scored for the presence of epsilon waves and prolonged terminal activation duration (TAD≥55ms) (*ECG definition list, supplementary table 1)*.[9] Repolarization abnormalities were assessed in the precordial leads (V_1-V_6), T-waves of negative amplitude ≥0.1 mV were considered as inverted.[9] Holter recordings for 24 hours were analyzed for the presence of ventricular tachycardia's (VT) and premature ventricular complexes (PVC).[9] Structural abnormalities as defined by 2010 TFC were assessed by both cardiac magnetic resonance imaging (CMR)

and echocardiography following standard ARVC protocols.[9, 21] CMR studies were analyzed for fulfillment of TFC defined as RV regional wall motion abnormalities (akinesia, dyskinesia, or aneurysm) combined with RV dilatation by RV end-diastolic volume (RV-EDV) and RV systolic function (RVEF). Left ventricular (LV) systolic function was assessed by measurement of left ventricular ejection fraction (LVEF). Contrast enhanced images after administration of gadolinium were acquired to identify myocardial fibrosis. Echocardiographic exams were analyzed for fulfillment of 2010 TFC defined as RV regional wall motion abnormalities (akinesia, dyskinesia, or aneurysm) combined with RV outflow tract (RVOT) dimension in both the parasternal long/short axis view (PLAX/PSAX) and RV systolic function by RV- fractional area change (RV-FAC).[9, 22] LV systolic function was measured by LVEF using Simpson biplane method. ARVC definite diagnosis was based on the presence of subsets of 2010 TFC, which requires 2 major criteria, 1 major and 2 minor criteria, or 4 minor criteria.[9]

Echocardiographic RV deformation imaging

In addition to the standard clinical work-up, all subjects underwent RV echocardiographic deformation imaging with GE Vivid 7 or GE Vivid E9 (General Electric, Milwaukee, MN).[11] Details on image acquisition and post-processing were extensively described elsewhere.[11, 18] In brief, a focused modified narrow-angled 2D images in the apical 4 chamber view was recorded to assess the RV.[18] Frame rates between 55-110/s were accepted for RV deformation imaging. Echocardiographic images were analyzed by GE EchoPac 10.2 – PC software by GE Healthcare to perform 2D speckle tracking. After manual tracing, the RV lateral free wall was divided automatically into the basal, mid, and apical segment. The following deformation parameters were measured in the basal (or subtricuspid) area: time to onset shortening[23], systolic peak strain value[12, 24], and post-systolic index[14]. (For definition of echocardiographic deformation measurements see *Supplementary Figure S1*). These deformation parameters can be combined into specific distinct deformation patterns, as previously published (**Figure 2)**.[16]

- **Type-I:** defined as normal deformation characterized by onset shortening ≤90 ms, systolic peak strain ≥|-20%|, and ≤ 10% post-systolic shortening.[16]
- **Type-II:** characterized by delayed onset of shortening (>90ms), reduced systolic peak strain (<|-20%| ; >|- 10%|, and minor post-systolic shortening (>10%).[16]
- **Type-III** characterized by predominantly systolic stretching (systolic peak <|-10%|, and major post-systolic shortening.[16]

A single operator blinded for clinical data performed all deformation analyses. Inter-operator agreement was previously published.[16]

ARVC disease progression

A subset of 65 first-degree relatives (60%) underwent a second complete cardiac re-evaluation as defined by ECG, 24h-Holter monitoring, and cardiac imaging according to the TFC (**Figure 1**).[9] Disease progression was defined as the presence of a new TFC (structural, depolarization, repolarization, or arrhythmic TFC) that was absent at baseline. In detail, electrical disease progression was defined as the presence of a new depolarization, repolarization, or arrhythmic TFC at follow-up that was not present during first evaluation. Structural disease progression was defined as the presence of structural TFC as assessed by CMR/echocardiography during follow-up that was absent during first evaluation. RV deformation patterns in the basal area at baseline were evaluated for predictive value of disease progression.

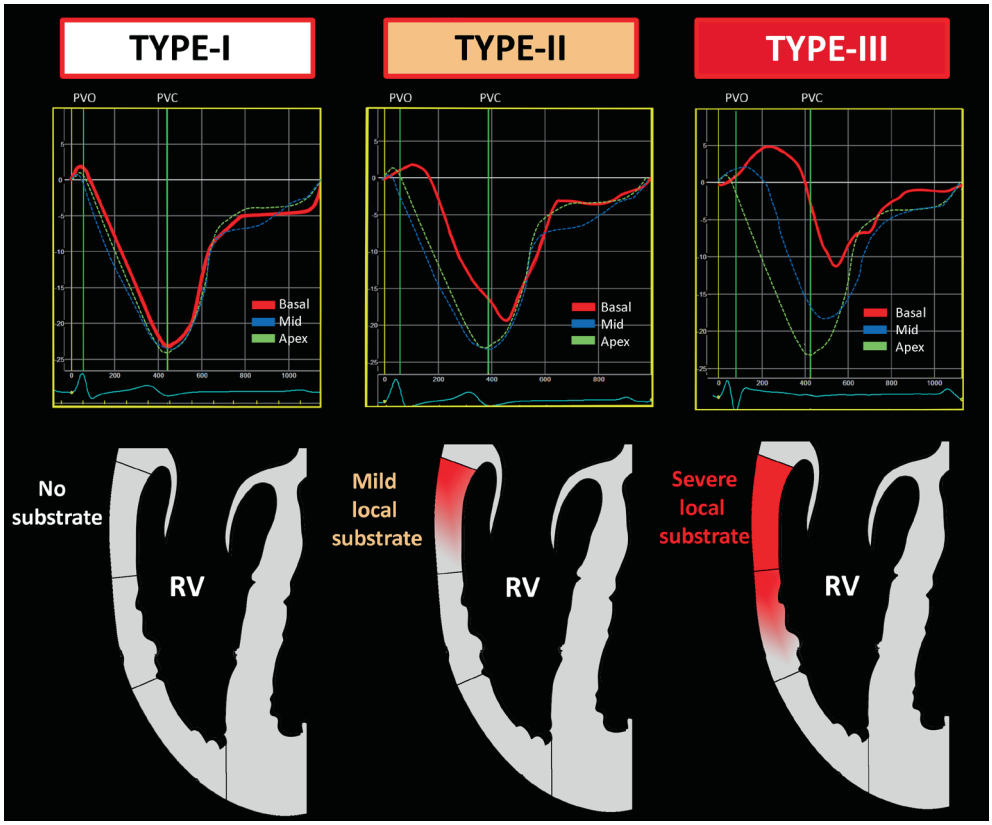

Figure 2. Right ventricular deformation patterns

Three distinct deformation patterns that are observed in arrhythmogenic right ventricular cardiomyopathy. In a previous report by our group, we used a computer model to simulate Type-II (middle panel) pattern by the introduction of a mechanical substrate consisting of hypocontractility and increased passive wall stiffness in the subtricusdid area.[16] Type-III (right panel) deformation pattern was simulated by aggravating this substrate. No local pathological electromechanical substrate was present in Type-I (normal deformation) (left panel). See Methods section for in depth explanation. *Abbreviations*: RV = right ventricle, PVO/PVC = timing of pulmonary valve opening/closure

R1 R2 R3 R4 R5 R6 R7 R8 R9 R10 R11 R12 R13 R14 R15 R16 R17 R18 R19 R20 R21 R22 R23 R24 R25 R26 R27 R28 R29 R30 R31 R32 R33 R34 R35 R36 R37 R38 R39

Statistical analysis

Means were expressed as mean ± standard deviation and median [inter-quartile range] if appropriate. Normal distribution was tested by the Shapiro-Wilk test. Mean group values were compared independent Student's *t*-test or Mann-Whitney-U test if appropriate. Distributions of proportions were performed by Fischer Exact test. Predictive values were expressed as positive/negative predictive value (PPV/NPV) with the 95% confidence interval (95CI). P-values were considered statically significance if P<.05 All statistical analyses were performed in commercially available software: IBM SPSS Statistics for Windows, Version 21.0. Armonk, NY: IBM Corp.

RESULTS

Clinical evaluation at baseline

The final study population comprised 109 subjects with a mean age of 33.7±17.4 years and 43 (39%) were men. The majority of our study participants were carriers of a pathogenic desmosomal mutation (n=76, 70%). Based on the baseline clinical evaluation, 64 subjects were assigned to the subclinical stage, and 45 to had electrical abnormalities as defined by the 2010 TFC (**Figure 1**). Subjects that showed electrical abnormalities at baseline, were significantly older compared to subjects in the subclinical stage (41.1±17.8 vs. 28.4±15.1, P<.001) and were significantly more often carriers of a pathogenic ARVC related mutation (**Table 1**). By study design, none of the subjects fulfilled 2010 TFC for structural abnormalities. All mean values of the structural parameters, including RV dimension and RV/LV systolic function, were comparable between subjects in the electrical and subclinical stage (**Table 1**). None of the included subjects had a history of sustained ventricular arrhythmias, none was on anti-arrhythmic medication, and 9 (8%) subjects had an implantable cardiac defibrillator (ICD) device implanted at baseline for primary prevention.

RV deformation patterns in relatives at baseline

The distribution of RV deformation patterns categorized by clinical stage is presented in **Figure 3**. The 64 subjects in the subclinical stage were characterized by normal deformation pattern Type-I (n=42, 66%), whereas deformation pattern Type-II was seen in the remaining 22 (34%) subjects. The electrical stage was characterized mainly by abnormal deformation pattern Type-II, which was seen in 31 (69%) subjects. In the remaining subjects in the electrical stage, Type-III was seen in 6 (13%), and Type-I was seen in 8 (18%).

In the subclinical stage, abnormal deformation pattern (Type-II) was relatively more frequently seen in older subjects (35.2±15.3 vs. 24.8±13.9 years, P=.008) and in pathogenic mutation carriers (43% vs. 12%, P=.035). Sex was equally distributed among Type-II versus Type-I (male sex: 36% vs. 33%, P=.510).

Table 1. Baseline characteristics of 109 first-degree relatives

Baseline characteristics	Subclinical stage N=64	Electrical stage N=45	P-value
Age (y)	28.4±15.1	41.1±17.8	*<.001*
Male	22 (34)	21 (47)	.234
Pathogenic ARVC mutation	47 (73)	42 (93)	*.011*
PKP2	37 (58)	34 (76)	.068
DSG2	3 (5)	1 (2)	.641
DSP	0 (0)	1 (2)	.413
PLN	7 (11)	6 (13)	.769
Symptomatic	5 (8)	8 (18)	.139
Palpitations	4 (6)	8 (18)	.070
Cardiac syncope	1 (2)	0 (0)	1.00
ARVC definite diagnosis	0 (0)	17 (38)	<.001
Follow up available	37 (58)	25 (56)	.846
Follow-up duration	3.7±2.2	3.8±1.9	.818
2010 Task Force Criteria			
Structural TFC (major/minor) (%)	0 (0)	0 (0)	1.00
Depolarization TFC (major/minor) (%)	0 (0)	27 (60)	<.001
TAD (%)	0 (0)	27 (60)	<.001
Epsilon wave (%)	0 (0)	0 (0)	1.00
Repolarization TFC (major/minor) (%)	0 (0)	17 (38)	<.001
T-wave inversion: V_1-V_3	0 (0)	9 (20)	<.001
T-wave inversion: V_1-V_2	0 (0)	6 (13)	<.001
T-wave inversion: V_1-V_4 with RBBB	0 (0)	0 (0)	1.00
T-wave inversion: V_4-V_6	0 (0)	2 (4)	.168
Arrhythmia TFC (major/minor) (%)	0 (0)	21 (47)	<.001
(Non-)sustained VT with superior axis	0 (0)	0 (0)	1.00
(Non-)sustained VT with inferior or unknown axis	0 (0)	3 (7)	.068
PVC>500/24h	0 (0)	20 (44)	<.001
Family history TFC (major) (%)	64 (100)	45 (100)	1.00
Echocardiography			
RV-WMA	0 (0)	1 (2)	.413
PLAX RVOT (mm/m^2)	15.5±2.5	16.0±2.3	.417
PSAX RVOT (mm/m^2)	16.5± 2.7	16.4±2.5	.767
RV-FAC (%)	47.7±6.7	45.2±6.9	.059
LVEF (%)	58.2±4.2	58.9±5.9	.519
CMR			
RV-WMA (%)	0 (0)	1 (2)	.413
RV-EDV (ml/m^2)	92.1±20.2	91.3±11.3	.876
RVEF (%)	55.4±7.8	51.9±6.6	.106
LVEF (%)	57.9±5.4	56.0±7.9	.317
LGE (%)	0 (0)	0 (0)	1.00

Values are, n (%),mean ± standard deviation. *Abbreviations*: ARVC = arrhythmogenic right ventricular cardiomyopathy; PKP2 = plakophillin-2; DSG2 = desmoglein-2; DSP = desmocollin; PLN = phospholamban; TFC = Task Force Criteria; TAD = terminal activation duration; RBBB = right bundle branch block; VT = ventricular tachycardia; PVC = premature ventricular complexes; CMR = cardiac magnetic resonance imaging; WMA = wall motion abnormality; PLAX/PSAX = parasternal long/short axis view; RVOT right ventricular outflow tract; RV-FAC = right ventricular fractional area change; LVEF/RVEF = left/right ventricular ejection fraction; RV-EDV = right ventricular end-diastolic volume; LGE = late gadolinium enhancement

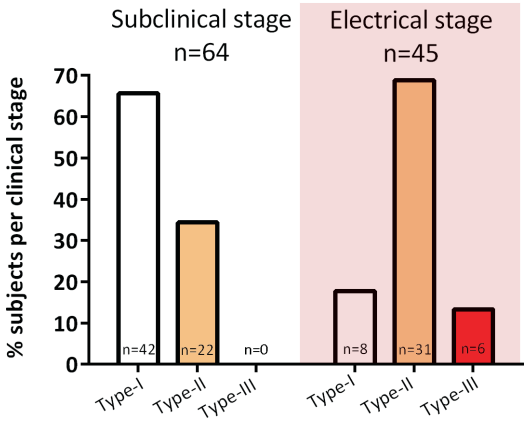

Figure 3. Distribution of RV deformation patterns categorized by clinical ARVC stage
Distribution of RV deformation patterns (horizontal axis) categorized by clinical ARVC stage; subclinical stage (left) and electrical stage (right). While normal deformation was most commonly seen (66%) in subclinical stage, a substantial amount of these relatives were identified with abnormal deformation pattern Type-II (34%). This patterns was also most frequently observed in electrical staged relatives (69%).

All six subjects in the electrical stage with Type-III carried a pathogenic desmosomal mutation. Age was comparable between normal deformation (Type-I) and abnormal deformation (Type-II/Type-III) at this stage (41.1±9.4 vs. 41.2±19.3 years, P=.989, respectively), as well as sex distribution (male gender: 46%, vs. 50%, P=.569, respectively). In four of the six (67%) subjects identified with a *PLN* mutation in the electrical stage we observed a normal RV deformation pattern (Type-I) in the RV basal area.

Disease Progression

Sixty-five (60%) subjects underwent a complete second re-evaluation after mean follow-up of 3.7±2.1 years. At baseline, 37 subjects of those were staged as relatives in the subclinical stage, the remaining 28 had already electrical abnormalities at baseline (**Figure 1**). In total, 17 (26%) subjects showed signs of ARVC disease progression, defined as a new TFC that was absent at baseline. Electrical progression occurred more frequently compared to structural disease progression: 11 showed only electrical progression, 4 showed electrical progression along with structural progression, and 2 showed structural progression on top of already existing electrical disease at baseline. None of the subjects suffered from a sustained arrhythmic event or appropriate ICD intervention during follow-up.

Predictive value of abnormal deformation in early ARVC

In the 65 subjects that underwent a second complete re-evaluation, a normal deformation pattern (Type-I) at baseline was seen in 28 (43%) subjects. In these 28 subjects with normal

deformation, disease progression occurred in only 1 subject (4%). Abnormal deformation was seen in the remaining 37 subjects (57%) (Type-II in 33, Type–III in 4) and in this group, disease progression was seen in 16 (43%) subjects. The negative predictive value (NPV) of normal deformation (Type-I) at baseline on disease progression was 96% (95CI: 80%-100%). The positive predictive value (PPV) of abnormal deformation at baseline on disease progression was 43% (95CI: 27%-60%) (**Figure 4**).

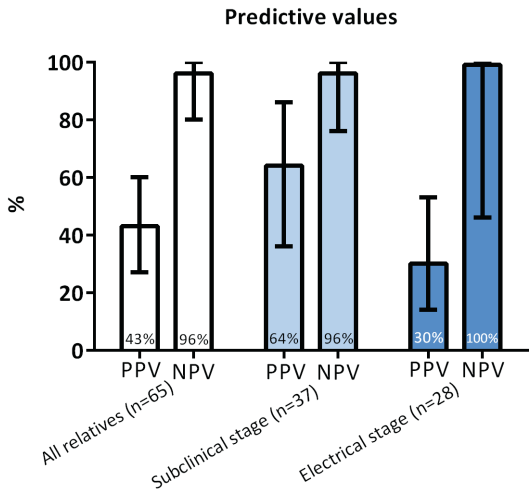

Figure 4. Predictive values of deformation results on disease progression
RV deformation imaging is a valuable tool to predict disease progression in ARVC relatives. The presence of Type-I (normal deformation) pattern is associated with a favorable short term prognosis. In other words, our results suggest that the first sign of established disease expression (by Task-Force criteria) by conventional techniques is not likely to be detected in the next 4 years. *Abbreviations*: PPV/NPV = positive/negative predictive value.

Figure 5 shows a flowchart of the rate of disease progression specified for both deformation pattern and clinical stage at baseline. The predictive value of deformation patterns differed between subjects in the subclinical stage and the electrical stage (**Figure 4***)*. In the 37 subjects in the subclinical stage that underwent a second clinical evaluation 23 (62%) showed a normal deformation pattern (Type-I) and only one (4%) of them showed disease progression; NPV: 96%, (95CI: 76%-100%). Type-II was seen in 14 (38%) at baseline, and disease progression occurred in 9 (64%) of them; PPV: 64% (95CI: 36%-86%).

In the electrical staged subjects (n=28), normal deformation (Type-I) was seen in 5, and none showed further disease progression; NPV: 100% (46%-100%). Type-II pattern was seen in 19 subjects and 5 (26%) showed signs of disease progression. Two of the four (50%) subjects in the electrical stage with an abnormal deformation pattern Type-III showed disease progression. The PPV of abnormal deformation on disease progression PPV was 30% (95CI:14%-53%) (**Figure 4***)*.

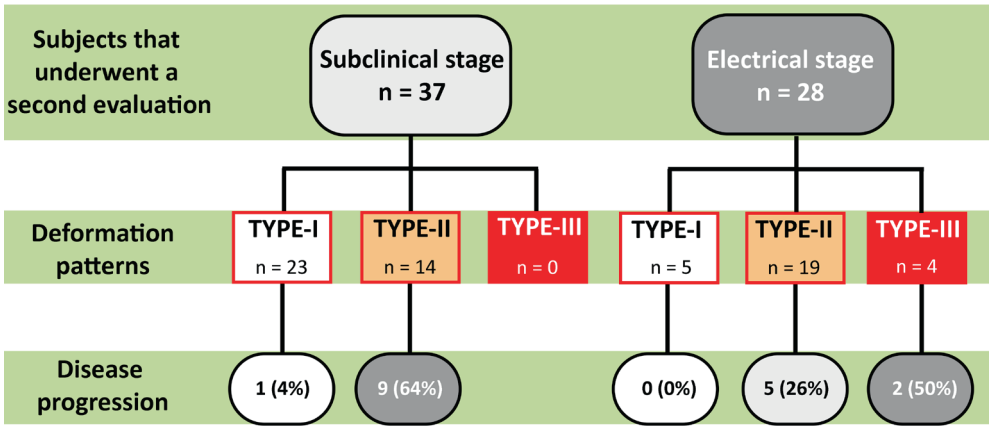

Figure 5. Rate of disease progression specified for deformation patterns and clinical stage at baseline
Normal subtricuspid deformation pattern (Type-I) at baseline indicates low risk on disease progression at follow-up.

DISCUSSION

ARVC is a cardiomyopathy which is recognized as a familial disease.[2, 3, 9, 19] Therefore, an international Task Force consensus statement recommends comprehensive cardiac screening in all relatives every 2-3 years.[8] However, it is well known that disease progression in family members does not behave uniformly and this warrants tailor-made cardiac screening intervals over time.[6, 7] Previous reports suggest that echocardiographic deformation imaging is capable to detect functional abnormalities prior to established indicators of TFC disease expression.[13, 14, 16, 23] The main finding of our study is that relatives with normal deformation in the RV basal area do not show any disease progression during a mean follow-up of almost 4 years. Therefore, the results of this study has implications for our follow-up strategy of relatives in clinical practice. Relatives with normal RV deformation on top of normal results during standard cardiac screening seem to have an excellent mid-term prognosis and less frequent cardiac screening might be equally effective.

Normal right ventricular deformation imaging in early ARVC

Our study shows that deformation imaging is able to identify relatives at low-risk for disease progression. This particularly holds true for relatives in the earliest stage without any established disease expression as defined by TFC. Normal deformation in the RV basal area in addition to the absence of abnormalities detected by ECG, Holter, and conventional cardiac imaging largely excludes disease progression during almost 4 years of follow-up. Previously, we demonstrated with computer modeling that deformation pattern Type-I represents

normal electromechanical properties of the RV myocardium such as seen in healthy individuals.[16] We focused on the RV basal area (subtricuspid region) since previous studies have suggested that this area is one of the first affected regions in ARVC.[14, 17, 23] Therefore, normal deformation in specifically this region on top of normal results by other diagnostic modalities should implicate the absence of overall disease expression. Our results suggest that these relatives without any disease expression (including normal deformation) are in a clinical stage that precedes the subclinical stage. Historically, a clinical stage without any disease expression in ARVC is often considered as the *concealed stage* (**Figure 6**).[25] Our data shows that deformation imaging helps to discriminate between relatives who are in a true concealed stage and relatives with already existing subtle local RV mechanical dysfunction not detected by conventional approaches (*subclinical stage*). Considering the progression rates in ARVC relatives observed in this study, we conclude that "truly" concealed staged relatives might benefit from a low-frequency follow-up strategy (4-5 years) instead of the currently 2-3 years routine follow-up.

Abnormal RV deformation imaging in early ARVC

By definition, relatives in the subclinical stage lack any established disease expression as defined by TFC. Interestingly, one third of the included subclinical staged subjects in this study were identified with an abnormal deformation pattern Type-II.[16] In a recent study, we already showed that this abnormal deformation pattern was present in almost half of desmosomal mutation carriers in the subclinical stage and the underlying electromechanical substrate was regional hypocontractility and mildly increased passive wall stiffness.[16] In the present study, we show that approximately half of the subjects in the subclinical stage with abnormal deformation showed unequivocal signs of disease progression during follow-up. This association between the presence of abnormal deformation and the occurrence of established disease expression during follow-up is interesting and supports our hypothesis that the observed deformation patterns are a functional representation of an underlying pathological electromechanical substrate.

The present study was performed in a larger cohort with a more heterogeneous genetic background compared to our previous explorative study using subtricuspid deformation patterns in ARVC.[16] In line with this study, we observed a high incidence of abnormal subtricuspid deformation in desmosomal mutation carriers without further disease expression. This present study also provided insight in the presence of RV deformation patterns in relatives without a desmosomal mutation such as gene-elusive relatives and *PLN* mutation carriers. First-degree relatives of gene-elusive index patients less frequently showed abnormal deformation compared to desmosomal mutation carriers. This could be explained by the fact that these family members are at an uncertain risk of developing ARVC since the presence of a genetic substrate in these individuals is unknown. Our results are in concordance with previous studies showing that approximately 20% of family members of

gene-elusive probands will develop ARVC compared to half of the family members harboring a pathogenic mutation.[7, 19] Another interesting finding was that a normal RV deformation pattern was detected in four out of six *PLN* mutation carriers with preexisting electrical abnormalities. Although the numbers are small, this may suggest that the subtricuspid area is a less common predilection site in *PLN* mediated ARVC as compared to desmosomal ARVC and this warrant further investigation.

Although the association between the presence of abnormal RV deformation and disease progression by fulfillment of TFC is interesting, these subjects did not suffer from any sustained ventricular arrhythmia or appropriate ICD intervention during follow-up. A previous large study performed by Te Riele *et al.* showed that the overall incidence of first life-threatening ventricular arrhythmias is 1 per 100 person-years in ARVC relatives.[7] If we apply this number to our study population one may expect that some relatives should have suffered from a first arrhythmic event during our study period. The apparent discrepancy could be explained by the fact that all relatives fulfilling structural TFC were excluded from our study, and precisely this form of advanced disease expression was seen in all relatives prior to sustained arrhythmic events.[6, 7, 10] Although we were not able to prove any association between abnormal deformation and sustained arrhythmias based on this study, we do speculate that abnormal deformation is an early sign of structural changes. However, considering the considerably low arrhythmic risk, cardiac screening every 2-3 years in accordance with the current Task Force consensus statement seems to be sufficient.[8] (**Figure 6**).

Towards optimization of family screening protocols

Since the first description of echocardiographic deformation imaging in ARVC patients almost 10 years ago several groups aimed to show the incremental value of this technique in ARVC.[11-16, 23, 24, 26, 27] The majority of these studies was of head-to-head design versus conventional diagnostic and prognostic approaches and used a cut-off value of a single deformation parameter. These studies, including some conducted in our own center, were often designed as feasibility studies with limited value for daily clinical practice. To our best knowledge, the present study is the first approach to optimize family screening protocols by using echocardiographic deformation imaging and thereby implementing deformation imaging results into daily practice. A recent paper by Leren *et al.* reported a multi-modality approach in identifying subjects at risk for ventricular arrhythmias during early ARVC and thereby aiming at the use of deformation imaging in addition to conventional techniques.[28] Our study is in line with their multi-modality design during family screening, yet we are convinced that a pattern-based approach is required to increase the added diagnostic value of RV deformation imaging. We may enter a new era in which echocardiographic deformation imaging enters the field of clinical decision making in ARVC.[29]

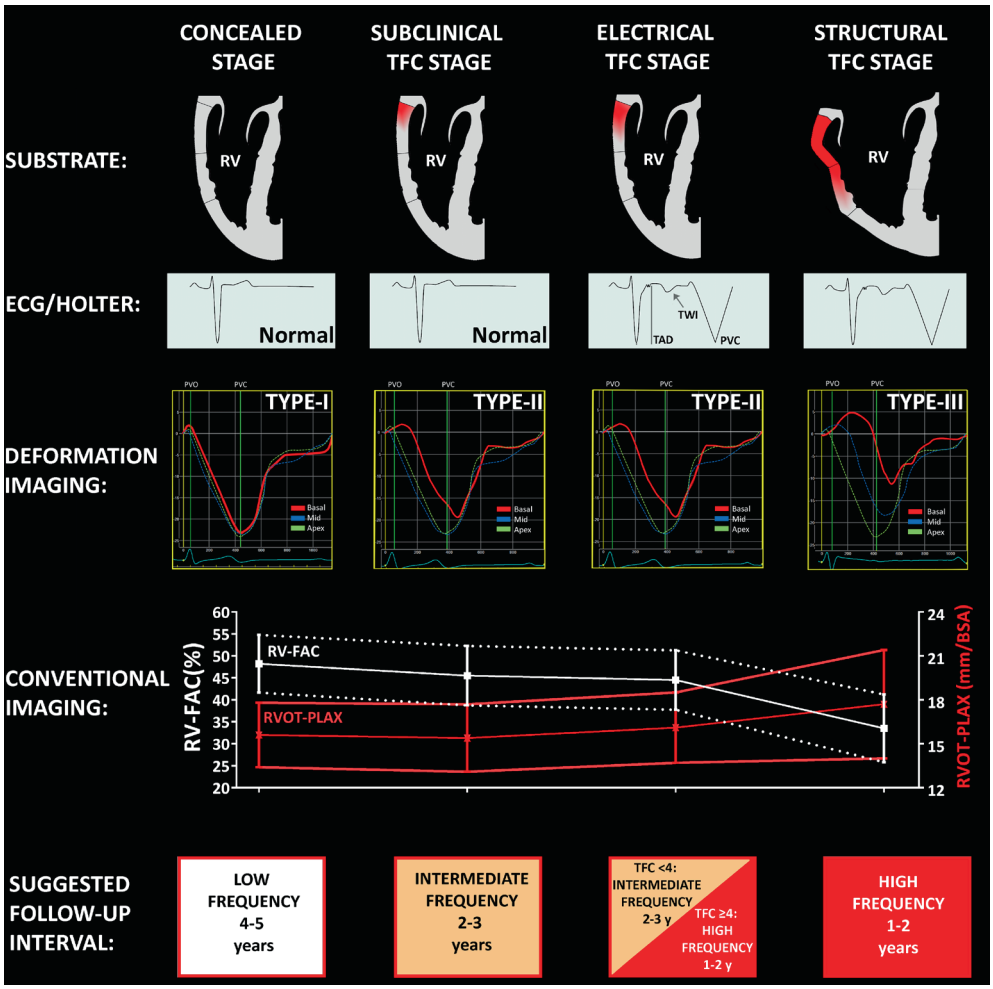

Figure 6. Follow-up strategies in relatives depends on the clinical ARVC stages
In the horizontal axis are the clinical stages, in the vertical axis the corresponding results during cardiac screening. The concealed stage (left) is the first stage in which no electrical- or structural were found. In this concealed stage RV deformation imaging shows normal deformation (Type-I) suggesting the absence of an electromechanical substrate. The subclinical TFC stage (middle left) is the second stage with again no detectable electrical and structural abnormalities. However, RV deformation imaging shows abnormal deformation pattern (Type-II) suggesting the presence of a local electromechanical substrate in the basal area. The electrical TFC stage (middle right) is characterized by electrical abnormalities in absence of structural abnormalities by conventional imaging. The structural stage (right) with both electrical and structural abnormalities as defined by the TFC. Deformation imaging shows pattern Type-III associated with a large RV electromechanical substrate. Normal deformation (Type-I) without any other detected abnormality excludes the presence of an electromechanical substrate, follow-up interval could be less frequent compared to the more advanced clinical stages in these relatives. *Abbreviations*: TFC = task force criteria; RV-FAC = right ventricular fractional area change, RVOT-PLAX = right ventricular outflow tract – parasternal long axis view; ECG = electrocardiogram; TAD = terminal activation duration; TWI = t-wave inversion PVC = premature ventricular complexes.

R1 R2 R3 R4 R5 R6 R7 R8 R9 R10 R11 R12 R13 R14 R15 R16 R17 R18 R19 R20 R21 R22 R23 R24 R25 R26 R27 R28 R29 R30 R31 R32 R33 R34 R35 R36 R37 R38 R39

Limitations

This study shows a clear association between abnormal deformation patterns and the occurrence of disease progression in early ARVC during family screening. Other RV pathologies could also produce similar abnormal RV deformation patterns and are not necessarily ARVC-specific. Therefore, this should only be explained as ARVC disease expression if other conditions are ruled out or considered unlikely by conventional diagnostic approaches.

A previous study also found that factors such as sex, cardiac symptoms, being a sibling, and mutation carrier status are associated with the development of ARVC diagnosis in relatives.[7] It would be interesting to know what the predictive value of deformation imaging is after correcting for these clinical factors. Unfortunately, due to relatively low size of this study, we were unable to perform such an analysis. Forty percent of our cohort did not underwent a second evaluation which is a potential source of selection bias. *Supplementary table 2* provides a baseline comparison between subjects with follow-up an without available follow-up. No significantly differences were seen except for a low representation of *PLN* mutation carriers in the group that underwent follow-up.

Other RV regions such as the RV outflow tract are not taken into account in our analysis due to the technical difficulties by echocardiographic deformation imaging in this specific region. Since this region could be of importance as being part of the triangle of dysplasia in ARVC, we might have overlooked some early disease expression.[9, 17] Another limitation is the use of single vendor post-processing software to analyze 2D echocardiographic images to assess regional RV deformation. It is currently unknown if our results remain valid when other software packages from different vendors will be used.

Conclusion

Echocardiographic deformation imaging is capable to identify relatives at low risk of disease progression during the early stages of ARVC. A normal RV deformation pattern at baseline is associated with an absence of disease progression during mid-term follow-up in relatives of ARVC patients, suggesting that a low-frequency follow-up strategy would suffice. Our data suggest that echocardiographic deformation imaging could be implemented in ARVC family screening.

Acknowledgements: We acknowledge the support from the Netherlands Cardiovascular Research Initiative: An initiative with support of the Dutch Heart Foundation, CVON2015-12 eDETECT Folkert W. Asselbergs is supported by a Dekker scholarship-Junior Staff Member 2014T001 – Netherlands Heart Foundation and UCL Hospitals NIHR Biomedical Research Centre.

REFERENCES

1. Marcus FI, Fontaine GH, Guiraudon G, Frank R, Laurenceau JL, Malergue C, Grosgogeat Y. Right ventricular dysplasia: a report of 24 adult cases. *Circulation* 1982;**65**(2):384-98.
2. Bhonsale A, Groeneweg JA, James CA, Dooijes D, Tichnell C, Jongbloed JD, Murray B, te Riele AS, van den Berg MP, Bikker H, Atsma DE, de Groot NM, Houweling AC, van der Heijden JF, Russell SD, Doevendans PA, van Veen TA, Tandri H, Wilde AA, Judge DP, van Tintelen JP, Calkins H, Hauer RN. Impact of genotype on clinical course in arrhythmogenic right ventricular dysplasia/cardiomyopathy-associated mutation carriers. *Eur Heart J* 2015;**36**(14):847-55.
3. McKoy G, Protonotarios N, Crosby A, Tsatsopoulou A, Anastasakis A, Coonar A, Norman M, Baboonian C, Jeffery S, McKenna WJ. Identification of a deletion in plakoglobin in arrhythmogenic right ventricular cardiomyopathy with palmoplantar keratoderma and woolly hair (Naxos disease). *Lancet* 2000;**355**(9221):2119-24.
4. Sen-Chowdhry S, Syrris P, Ward D, Asimaki A, Sevdalis E, McKenna WJ. Clinical and genetic characterization of families with arrhythmogenic right ventricular dysplasia/cardiomyopathy provides novel insights into patterns of disease expression. *Circulation* 2007;**115**(13):1710-20.
5. Dalal D, James C, Devanagondi R, Tichnell C, Tucker A, Prakasa K, Spevak PJ, Bluemke DA, Abraham T, Russell SD, Calkins H, Judge DP. Penetrance of mutations in plakophilin-2 among families with arrhythmogenic right ventricular dysplasia/cardiomyopathy. *J Am Coll Cardiol* 2006;**48**(7):1416-24.
6. Te Riele AS, James CA, Rastegar N, Bhonsale A, Murray B, Tichnell C, Judge DP, Bluemke DA, Zimmerman SL, Kamel IR, Calkins H, Tandri H. Yield of serial evaluation in at-risk family members of patients with ARVD/C. *J Am Coll Cardiol* 2014;**64**(3):293-301.
7. Te Riele AS, James CA, Groeneweg JA, Sawant AC, Kammers K, Murray B, Tichnell C, van der Heijden JF, Judge DP, Dooijes D, van Tintelen JP, Hauer RN, Calkins H, Tandri H. Approach to family screening in arrhythmogenic right ventricular dysplasia/cardiomyopathy. *Eur Heart J* 2016;**37**(9):755-63.
8. Corrado D, Wichter T, Link MS, Hauer R, Marchlinski F, Anastasakis A, Bauce B, Basso C, Brunckhorst C, Tsatsopoulou A, Tandri H, Paul M, Schmied C, Pelliccia A, Duru F, Protonotarios N, Estes NA, 3rd, McKenna WJ, Thiene G, Marcus FI, Calkins H. Treatment of arrhythmogenic right ventricular cardiomyopathy/dysplasia: an international task force consensus statement. *Eur Heart J* 2015;**36**(46):3227-37.
9. Marcus FI, McKenna WJ, Sherrill D, Basso C, Bauce B, Bluemke DA, Calkins H, Corrado D, Cox MG, Daubert JP, Fontaine G, Gear K, Hauer R, Nava A, Picard MH, Protonotarios N, Saffitz JE, Sanborn DM, Steinberg JS, Tandri H, Thiene G, Towbin JA, Tsatsopoulou A, Wichter T, Zareba W. Diagnosis of arrhythmogenic right ventricular cardiomyopathy/dysplasia: proposed modification of the task force criteria. *Circulation* 2010;**121**(13):1533-41.
10. Te Riele AS, Bhonsale A, James CA, Rastegar N, Murray B, Burt JR, Tichnell C, Madhavan S, Judge DP, Bluemke DA, Zimmerman SL, Kamel IR, Calkins H, Tandri H. Incremental value of cardiac magnetic resonance imaging in arrhythmic risk stratification of arrhythmogenic right ventricular dysplasia/cardiomyopathy-associated desmosomal mutation carriers. *J Am Coll Cardiol* 2013;**62**(19):1761-9.
11. Teske AJ, De Boeck BW, Melman PG, Sieswerda GT, Doevendans PA, Cramer MJ. Echocardiographic quantification of myocardial function using tissue deformation imaging, a guide to image acquisition and analysis using tissue Doppler and speckle tracking. *Cardiovasc Ultrasound* 2007;**5**:27.
12. Teske AJ, Cox MG, De Boeck BW, Doevendans PA, Hauer RN, Cramer MJ. Echocardiographic tissue deformation imaging quantifies abnormal regional right ventricular function in arrhythmogenic right ventricular dysplasia/cardiomyopathy. *J Am Soc Echocardiogr* 2009;**22**(8):920-7.
13. Sarvari SI, Haugaa KH, Anfinsen OG, Leren TP, Smiseth OA, Kongsgaard E, Amlie JP, Edvardsen T. Right ventricular mechanical dispersion is related to malignant arrhythmias: a study of patients with arrhythmogenic right ventricular cardiomyopathy and subclinical right ventricular dysfunction. *Eur Heart J* 2011;**32**(9):1089-96.

R1 R2 R3 R4 R5 R6 R7 R8 R9 R10 R11 R12 R13 R14 R15 R16 R17 R18 R19 R20 R21 R22 R23 R24 R25 R26 R27 R28 R29 R30 R31 R32 R33 R34 R35 R36 R37 R38 R39

14. Teske AJ, Cox MG, Te Riele AS, De Boeck BW, Doevendans PA, Hauer RN, Cramer MJ. Early detection of regional functional abnormalities in asymptomatic ARVD/C gene carriers. *J Am Soc Echocardiogr* 2012;**25**(9):997-1006.
15. Mast TP, Teske AJ, Te Riele AS, Groeneweg JA, Van Der Heijden JF, Velthuis BK, Loh P, Doevendans PA, Van Veen TA, Dooijes D, De Bakker JM, Hauer RN, Cramer MJ. Prolonged Electromechanical Interval Unmasks Arrhythmogenic Right Ventricular Dysplasia/Cardiomyopathy in the Subclinical Stage. *J Cardiovasc Electrophysiol* 2016;**27**(3):303-14.
16. Mast TP, Teske AJ, Walmsley J, Heijden JF, Es v R, Prinzen FW, Delhaas T, Veen TA, Loh P, Doevendans PA, Cramer MJ, Lumens J. Right ventricular deformation imaging and computer simulation for electromechanical substrate characterization in arrhythmogenic right ventricular cardiomyopathy (ARVC). *J Am Coll Cardiol* 2016;**68**(20):2185-2197.
17. Te Riele AS, James CA, Philips B, Rastegar N, Bhonsale A, Groeneweg JA, Murray B, Tichnell C, Judge DP, Van Der Heijden JF, Cramer MJ, Velthuis BK, Bluemke DA, Zimmerman SL, Kamel IR, Hauer RN, Calkins H, Tandri H. Mutation-positive arrhythmogenic right ventricular dysplasia/cardiomyopathy: the triangle of dysplasia displaced. *J Cardiovasc Electrophysiol* 2013;**24**(12):1311-20.
18. Mast TP, Teske AJ, Doevendans PA, Cramer MJ. Current and future role of echocardiography in arrhythmogenic right ventricular dysplasia/cardiomyopathy. *Cardiol J* 2015;**22**(4):362-74.
19. Groeneweg JA, Bhonsale A, James CA, te Riele AS, Dooijes D, Tichnell C, Murray B, Wiesfeld AC, Sawant AC, Kassamali B, Atsma DE, Volders PG, de Groot NM, de Boer K, Zimmerman SL, Kamel IR, van der Heijden JF, Russell SD, Jan Cramer M, Tedford RJ, Doevendans PA, van Veen TA, Tandri H, Wilde AA, Judge DP, van Tintelen JP, Hauer RN, Calkins H. Clinical Presentation, Long-Term Follow-Up, and Outcomes of 1001 Arrhythmogenic Right Ventricular Dysplasia/Cardiomyopathy Patients and Family Members. *Circ Cardiovasc Genet* 2015;**8**(3):437-46.
20. Groeneweg JA, van der Zwaag PA, Olde Nordkamp LR, Bikker H, Jongbloed JD, Jongbloed R, Wiesfeld AC, Cox MG, van der Heijden JF, Atsma DE, de Boer K, Doevendans PA, Vink A, van Veen TA, Dooijes D, van den Berg MP, Wilde AA, van Tintelen JP, Hauer RN. Arrhythmogenic right ventricular dysplasia/cardiomyopathy according to revised 2010 task force criteria with inclusion of non-desmosomal phospholamban mutation carriers. *Am J Cardiol* 2013;**112**(8):1197-206.
21. Tandri H, Calkins H, Nasir K, Bomma C, Castillo E, Rutberg J, Tichnell C, Lima JA, Bluemke DA. Magnetic resonance imaging findings in patients meeting task force criteria for arrhythmogenic right ventricular dysplasia. *J Cardiovasc Electrophysiol* 2003;**14**(5):476-82.
22. Rudski LG, Lai WW, Afilalo J, Hua L, Handschumacher MD, Chandrasekaran K, Solomon SD, Louie EK, Schiller NB. Guidelines for the echocardiographic assessment of the right heart in adults: a report from the American Society of Echocardiography endorsed by the European Association of Echocardiography, a registered branch of the European Society of Cardiology, and the Canadian Society of Echocardiography. *J Am Soc Echocardiogr* 2010;**23**(7):685-713.
23. Mast TP, Teske AJ, Riele AS, Groeneweg JA, Heijden JF, Velthuis BK, Loh P, Doevendans PA, Veen TA, Dooijes D, Bakker JM, Hauer RN, Cramer MJ. Prolonged electromechanical interval unmasks arrhythmogenic right ventricular dysplasia/cardiomyopathy in the subclinical stage. *J Cardiovasc Electrophysiol* 2015.
24. Prakasa KR, Wang J, Tandri H, Dalal D, Bomma C, Chojnowski R, James C, Tichnell C, Russell S, Judge D, Corretti M, Bluemke D, Calkins H, Abraham TP. Utility of tissue Doppler and strain echocardiography in arrhythmogenic right ventricular dysplasia/cardiomyopathy. *Am J Cardiol* 2007;**100**(3):507-12.
25. Basso C, Corrado D, Marcus FI, Nava A, Thiene G. Arrhythmogenic right ventricular cardiomyopathy. *Lancet* 2009;**373**(9671):1289-300.
26. Mast TP, Teske AJ, vd Heijden JF, Groeneweg JA, Te Riele AS, Velthuis BK, Hauer RN, Doevendans PA, Cramer MJ. Left Ventricular Involvement in Arrhythmogenic Right Ventricular Dysplasia/Cardiomyopathy Assessed by Echocardiography Predicts Adverse Clinical Outcome. *J Am Soc Echocardiogr* 2015;**28**(9):1103-13 e9.

27. Vitarelli A, Cortes Morichetti M, Capotosto L, De Cicco V, Ricci S, Caranci F, Vitarelli M. Utility of strain echocardiography at rest and after stress testing in arrhythmogenic right ventricular dysplasia. *Am J Cardiol* 2013;**111**(9):1344-50.
28. Leren IS, Saberniak J, Haland TF, Edvardsen T, Haugaa KH. Combination of ECG and Echocardiography for Identification of Arrhythmic Events in Early ARVC. *JACC Cardiovascular imaging* 2016;**In Press**.
29. Teske AJ, Mast TP. Moving From Multimodality Diagnostic Tests Toward Multimodality Risk Stratification in ARVC. *JACC Cardiovascular imaging* 2016;**Oct 14 - In press**.

SUPPLEMENTARY FILES

Supplementary table 1. Definitions of electrocardiographic parameters

Electrocardiographic definitions	
Epsilon waves	Distinct waves of small amplitude within the ST segment in the right precordial leads and are distinct from the QRS complex.
Terminal activation duration	The longest value in V_1–V_3, from the nadir of the S wave to the end of all depolarization deflections. Considered abnormal when ≥55 msec.
T-wave inversion	T-wave was considered inverted if the voltage was ≥0.1 mV

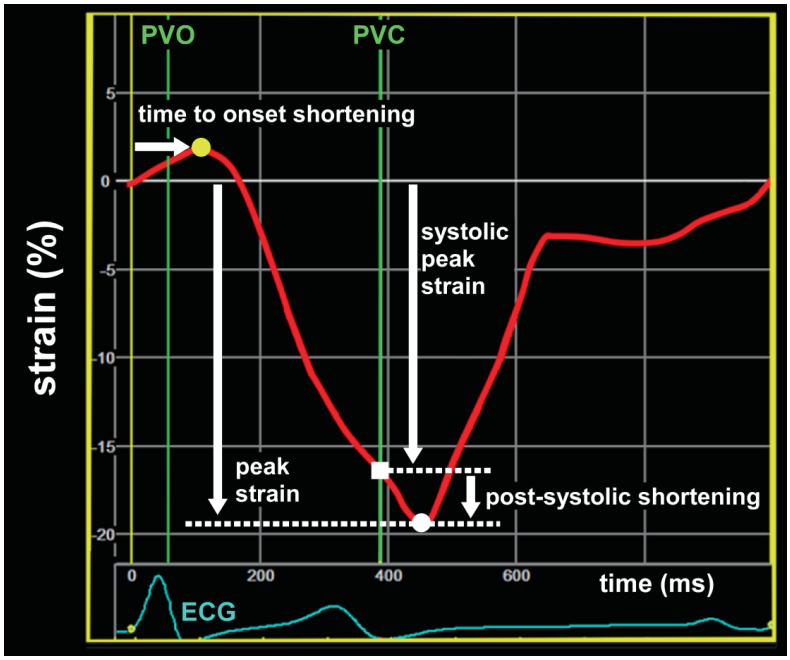

Supplementary figure 1. Definitions of Deformation imaging parameters

Deformation imaging definitions	
Time to onset shortening	time between onset-QRS and onset of mechanical shortening
Systolic peak strain	maximal negative value between pulmonary valve opening (PVO) and closure (PVC). In case of positive strain during systole, the value at PVC was taken
Peak strain	maximal negative value during entire cardiac cycle.
Post-systolic index	$100 * \frac{\text{peak strain} - \text{systolic peak strain}}{\text{peak strain}}$

Supplementary table 2. Comparison between relatives with and without a second evaluation

Baseline characteristics	Relatives without second evaluation N=44	Relatives with second evaluation N=65	P-value
Age (y)	36.4 ± 18.4	31.8 ± 16.6	*.178*
Male	24 (56)	41 (62)	.553
Pathogenic ARVC mutation	9 (20)	11 (17)	.801
PKP2	26 (59)	45 (69)	.310
DSG2	0 (0)	4 (6)	.146
DSP	0 (0)	1 (2)	1.00
PLN	9 (20)	4 (6)	*.034*
Symptomatic			
Palpitations	5 (11)	7 (17)	1.00
Cardiac syncope	0 (0)	1 (2)	1.00
ARVC definite diagnosis	6 (14)	11 (17)	.790
2010 Task Force Criteria			
Depolarization TFC (major/minor) (%)	7 (16)	20 (31)	.113
Repolarization TFC (major/minor) (%)	8 (18)	9 (14)	.596
Arrhythmia TFC (major/minor) (%)	8 (18)	13 (20)	1.00
Echocardiography			
RV-WMA	0 (0)	1 (2)	1.00
PLAX RVOT (mm/m^2)	16.3 ± 2.3	15.2 ± 2.3	*.034*
PSAX RVOT (mm/m^2)	17.0 ± 2.4	16.0 ± 2.6	.077
RV-FAC (%)	47.4 ± 7.3	46.1 ± 6.5	.325
LVEF (%)	57.5 ± 4.4	59.2 ± 5.3	.109
CMR			
RV-WMA (%)	0 (0)	1 (2)	1.00
RV-EDV (ml/m^2)	87.2 ± 21.7	94.1 ± 12.5	.136
RVEF (%)	56.0 ± 7.9	53.2 ± 7.3	.186
LVEF (%)	57.6 ± 6.1	56.6 ± 7.0	.569
LGE (%)	0 (0)	0 (0)	1.00

Values are, n (%),mean ± standard deviation. *Abbreviations*: ARVC = arrhythmogenic right ventricular cardiomyopathy; *PKP2* = plakophillin-2; *DSG2* = desmoglein-2; *DSP* = desmocollin; *PLN=phospholamban*; TFC = task force criteria; TAD = terminal activation duration; RBBB = right bundle branch block; VT = ventricular tachycardia; PVC = premature ventricular complexes; CMR = cardiac magnetic resonance imaging; WMA = wall motion abnormality; PLAX/PSAX = parasternal long/short axis view; RVOT right ventricular outflow tract; RV-FAC = right ventricular fractional area change; LVEF/RVEF = left/right ventricular ejection fraction; RV-EDV = right ventricular end-diastolic volume; LGE = late gadolinium enhancement

CHAPTER 6

Left Ventricular Involvement in Arrhythmogenic Right Ventricular Dysplasia/Cardiomyopathy Assessed by Echocardiography Predicts Adverse Clinical Outcome

Thomas P Mast,§ Arco J Teske,§ Jeroen F van der Heijden, Judith A Groeneweg,
Anneline SJM Te Riele, Birgitta Velthuis, Richard N Hauer,
Pieter A Doevendans, Maarten J Cramer
§ contributed equally to this work.

J Am Soc Echocardiogr. 2015 Sep;28(9):1103-13

ABSTRACT

Background: Among studies describing the phenotype of arrhythmogenic right ventricular dysplasia/cardiomyopathy (ARVD/C), significant discrepancy exists regarding the extent and impact of left ventricular (LV) involvement. The capability of conventional and new quantitative echocardiographic techniques to accurately detect LV involvement in ARVD/C remains unknown. The aim of this study was to test the hypothesis that accurate detection of LV involvement on echocardiography identifies patients at additional risk for cardiac events during follow-up.

Methods: Thirty-eight patients with ARVD/C, 16 pathogenic mutation–positive relatives, and 55 healthy control subjects were prospectively enrolled. Conventional echocardiography with additional deformation imaging was performed in all subjects to detect LV involvement. In a subgroup (n = 27), cardiac magnetic resonance imaging was performed with late enhancement. All patients and relatives were prospectively followed for events (sustained ventricular tachycardia, appropriate implantable cardioverter-defibrillator intervention, sudden cardiac death, and heart transplantation).

Results: Conventional echocardiography detected LV involvement in 32% of patients with ARVD/C and in none of the relatives. Deformation imaging revealed LV involvement in 68% of patients with ARVD/C and 25% of relatives and was correlated closely with late enhancement on cardiac magnetic resonance imaging. During a mean follow-up period of 5.9 ± 2.3 years, 20 patients with ARVD/C (53%) experienced events, and no events occurred in the relatives. LV involvement detected by deformation imaging (hazard ratio, 4.9; 95% CI, 1.7-14.2) and right ventricular outflow tract enlargement (hazard ratio, 1.2; 95% CI, 1.1-1.3) were the only independent predictors of outcomes.

Conclusions: Deformation imaging detected a high incidence of LV involvement in patients with ARVD/C and their relatives. Compared with conventional echocardiography, deformation imaging is superior in detecting minor LV involvement. LV involvement and an enlarged right ventricular outflow tract are independent prognostic markers of outcomes.

INTRODUCTION

Arrhythmogenic right ventricular (RV) dysplasia/cardiomyopathy (ARVD/C) is an inherited cardiomyopathy characterized by fibrofatty myocardial replacement, predominantly affecting the right ventricle.[1] However, left ventricular (LV) involvement has been demonstrated across a broad spectrum of disease severity.[2, 3 and 4] Detection of LV involvement is important because these patients seem to experience more potentially lethal ventricular arrhythmias than those with apparently isolated RV disease.[5 and 6] Noninvasive diagnostic modalities enabling the detection of LV involvement in patients with ARVD/C could therefore be of value in risk stratification in individual patients. Cardiac magnetic resonance (CMR) imaging has taken a prominent role, whereby late enhancement (LE) detects structural LV abnormalities (myocardial fibrosis) associated with ARVD/C.[7 and 8] Unfortunately, the limited availability, high cost, and inability to evaluate patients with implantable cardioverter-defibrillators (ICDs) render this technique unsuitable for serial evaluation in this specific patient population. Conventional echocardiography is often unable to detect minor LV pathology detected on CMR imaging, because these abnormalities are usually not associated with wall motion abnormalities.[7 and 9] However, echocardiographic deformation imaging enables the objective quantification of regional myocardial function,[10] which correlates closely with LE on CMR imaging with regard to fibrotic segments in patients with nonischemic heart disease, and can even detect regional abnormalities before the appearance of CMR LE in the left ventricle.[9 and 11] Previously, we reported a case in which deformation imaging was able to unmask LV involvement in a patient with ARVD/C with preserved LV systolic function and no regional wall motion abnormalities.[9] The capability of deformation imaging to detect LV involvement in a large cohort of patients with ARVD/C and their relatives remains unknown.

We hypothesized that echocardiographic deformation imaging is more sensitive than conventional echocardiographic parameters to detect LV wall motion abnormalities in patients with ARVD/C. The aim of this study therefore was to detect LV involvement in patients with ARVD/C and mutation-carrying relatives using echocardiographic deformation imaging and to explore the extent of LV dysfunction across a wide spectrum of ARVD/C severity. Second, we explored the predictive value of parameters derived from conventional and deformation imaging parameters in the occurrence of future cardiac events.

METHODS

Study Design

Between 2006 and 2008, consecutive individuals aged >18 years were prospectively enrolled for echocardiographic examination: 1) those with either known or suspected ARVD/C, 2)

family members of patients with ARVD/C, and 3) healthy control subjects. Group classification was established according to major and minor criteria as defined by the current 2010 ARVD/C diagnostic task force (12) and the results of deoxyribonucleic acid analysis of ARVD/C-associated genes, performed as described previously.(13 and 14) **Figure 1** demonstrates, in detail, the group classification on the basis of clinical assessment and genetic testing. Three groups were specified: (1) patients with ARVD/C (n = 38), (2) relatives of patients with ARVD/C carrying pathogenic mutations (n = 16), and (3) control subjects (n = 55) free of any cardiovascular disease.

End point data were obtained directly from patients or relatives during periodic evaluations at the outpatient clinic or hospital admissions until September 2014. The outcome measure was a composite of end points: spontaneous sustained monomorphic ventricular tachycardia, sudden cardiac death, aborted sudden cardiac death, appropriate ICD intervention for a ventricular arrhythmia, and heart transplantation. Outcome definitions are available in *Supplemental Table 1*. In case of reaching multiple clinical events during the follow-up period, the first event was considered the end point. Subsequent events were registered but were not included in further analysis. The study protocol was carried out with the approval of the Ethics Committee of the University Medical Center Utrecht, and all patients gave informed consent.

Standard Echocardiographic Study

The echocardiographic examination was performed with the subject at rest, in the left lateral decubitus position, using a Vivid 7 scanner (GE Vingmed Ultrasound AS, Horten, Norway) equipped with an M3S broadband transducer. A complete echocardiographic study was performed, with two-dimensional (B-mode) and Doppler tissue imaging recorded in both parasternal and apical views. Additional recordings of the three conventional apical views were recorded with the implementation of dual focus to optimize wall motion assessment. Special care was taken to avoid recording the right ventricle in any of these views for optimal blinding during postprocessing. According to the 16-segment model of the American Society of Echocardiography, regional LV wall motion was designated as normokinetic, hypokinetic, akinetic, dyskinetic, or not interpretable, after consensus was reached by two blinded experienced observers. From this the wall motion score index was calculated as the sum of scores divided by the total number of analyzed segments. Conventional echocardiographic measurement of both LV and RV dimensions was performed (see “Results”).[15] All dimensions were corrected for body surface area. RV function was measured by tricuspid annular plane systolic excursion (TAPSE) and RV fractional area change (FAC).16 Global LV function was measured by LV ejection fraction (LVEF) using the Simpson biplane method. Pulsed Doppler imaging was used to measure diastolic function.[17] A full description of the echocardiographic measurements is available as *Supplemental Data.*

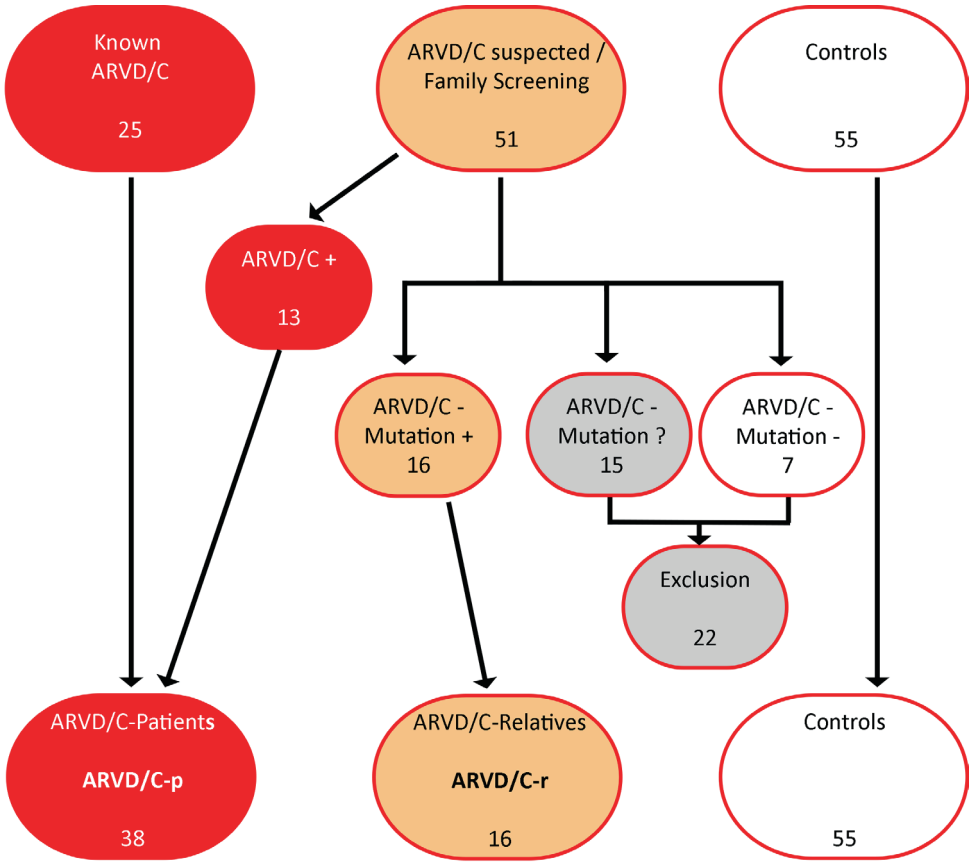

Figure 1. Flow chart of study group subdivisions
ARVD/C+/ARVD/C- = Presence/Absence of arrhythmogenic right ventricular cardiomyopathy according to the revised 2010 Task Force criteria. "Mutation+ or -" indicates presence of mutation associated with ARVD/C (from the index patient), "Mutation?" indicates that no genetic analysis was performed resulting in exclusion from the study. ARVD/C-p/ARVD/C-r = ARVD/C-patient/ARVD/C-relatives.

Deformation Imaging

We previously described our methods for image acquisition and postprocessing with commercially available software (EchoPAC PC version 11.2; GE Vingmed Ultrasound AS) for two-dimensional speckle-tracking analysis.[10 and 18] More details according to the acquisition and processing of tissue deformation imaging are available in the *Supplemental Files.* The following parameters were measured in the basal, middle, and apical segment of each wall (a total of 18 segments): systolic peak strain and strain rate, defined as the maximum negative value between aortic valve opening and closure (in case values were positive during systole, the end-systolic value was measured). Averaging systolic peak strain values over 18 LV segments resulted in the mean systolic peak strain. Postsystolic shortening was defined as 100 × [(peak strain value − end-systolic value)/end-systolic value].

R1 R2 R3 R4 R5 R6 R7 R8 R9 R10 R11 R12 R13 R14 R15 R16 R17 R18 R19 R20 R21 R22 R23 R24 R25 R26 R27 R28 R29 R30 R31 R32 R33 R34 R35 R36 R37 R38 R39

CMR Imaging

A subgroup of 19 patients with ARVD/C and eight relatives underwent CMR imaging as part of their clinical workup on a 1.5-T magnetic resonance imaging scanner (Achieva; Philips Healthcare, Best, The Netherlands) according to standard ARVD/C protocols.[19 and 20] All CMR examinations were performed within 12 months of the echocardiographic studies. LE of intravenously administered gadolinium was used to identify areas within the left ventricle with myocardial fibrosis using the 16-segment model of the American Society of Echocardiography. The presence of gadolinium LE on CMR imaging was determined by consensus reading of two blinded experienced observers and considered definite only if present in the same myocardial segment in two different imaging planes.

Definition of LV Involvement

To compare the presence of LV involvement between conventional echocardiography and deformation imaging, LV involvement according to conventional echocardiography was defined as LV dysfunction (LVEF <50%) and/or the presence of akinesia or dyskinesia *(LV involvement - conventional).* LV involvement according to deformation imaging was defined as the presence of abnormal systolic peak strain (<|−12.5%|) and/or postsystolic shortening >15% in two adjacent LV segments *LV involvement - deformation imaging.* Details concerning the cutoff values used for deformation imaging–derived parameters are stated in "Statistical Analysis."

Predictor Selection

All established phenotypic expressions of ARVD/C as described in the revised 2010 task force criteria[12] were chosen as potential predictors of outcomes, as well as both our parameters for LV involvement (*LV involvement–conventional and LV involvement–deformation imaging).* To increase the potential applicability of our definitions of LV involvement, only abnormalities in the LV posterolateral wall were used for correlation with clinical outcomes.[2 and 5] Other echocardiographic parameters were TAPSE, RV FAC, LVEF, abnormal diastolic function, and mean systolic peak strain. Although CMR imaging–derived parameters are part of the task force criteria, these were not used as potential predictors, because CMR was performed only in a subset of patients.

Statistical Analysis

Continuous data are presented as mean ± SD and categorical variables as numbers or percentages. Differences in continuous data between either patients with ARVD/C or their relatives and control subjects were calculated using the independent-samples Student's t test and $\chi 2$ or Fisher exact tests for categorical data. Bivariate correlations between continuous variables were determined using Pearson correlation coefficients. P values < .05 and 95% CIs of hazard ratios not including 1 were considered to indicate statistical significance.

Normal values for deformation imaging parameters are limited. Therefore, to correct for variability due to different observers and different echocardiographic vendors, we used our control group to identify normal values. In the control group, the 95% range of observed systolic peak values for strain and strain rate was evaluated to identify the normal values' lower limit. This resulted in single cutoff values of |−12.5%| for systolic peak strain and |−0.6%/sec| for peak strain rate, which were used to differentiate normal from abnormal regional deformation. Postsystolic shortening > 15% of the systolic peak strain value after aortic valve closure was considered abnormal.[21]

Categorical parameters derived from conventional and deformation echocardiographic imaging were correlated with clinical outcomes by Kaplan-Meier survival analysis and tested for significance with a log-rank test. Kaplan-Meier 3-year estimates of event risk were calculated for all categorical parameters. To calculate the magnitudes of both categorical and continuous single predictors, we performed univariate Cox proportional hazards analysis to obtain hazard ratios for each parameter individually. Parameters showing statistical significance ($P < .05$) were included in a multivariate Cox proportional hazards model to adjust for dependency relations between variables. If both the continuous and categorical variable of the same predictor were significantly related to clinical outcome, the continuous variable was selected. Multicollinearity was expected between different variables and was investigated by using correlation statistics and calculating variance inflation factors. Variables with correlation coefficients > 0.75 and/or variance inflation factors > 5 were not included simultaneously as predictors in a multivariate Cox regression model. Taking into account the small number of events, a backward elimination procedure was performed. Statistical calculations were made using commercially available software (SPSS version 20.0 for Windows; SPSS, Inc, Chicago, IL). All analyses of standard echocardiographic measurements, visual wall motion analysis, deformation imaging analysis, CMR imaging analysis were performed blinded to the other modality analyses and for clinical outcomes.

RESULTS

Study Population

The baseline characteristics of the study population are summarized in **Table 1**. No significant differences were seen between the two patient groups and the control subjects, other than age, which was higher in patients with ARVD/C, and more women among the relatives. At baseline, 84.2% of the patients with ARVD/C had already experienced episodes of (non) sustained ventricular tachycardia. Electrocardiographic abnormalities, as described in the task force criteria, were present in 92.1% of the patients with ARVD/C.[12] The mean duration of follow-up after the echocardiographic examination was 5.9 ± 2.3 years in the patients with ARVD/C and 6.7 ± 0.7 years in their relatives (P = NS).

Pathogenic mutations in the plakophilin-2 gene were most commonly identified: 71% in patients with ARVD/C and 75% in relatives (*Supplemental Table 2*). By study design, all 16 relatives of patients with ARVD/C carried pathogenic mutations associated with ARVD/C also identified in the index patients but did not fulfill the task force criteria.[12]

The control group consisted of 55 healthy volunteers unrelated to any of the patients with ARVD/C or their relatives.

Table 1. Baseline characteristics

	Patients (ARVD/C-p) (n=38)	Relatives (ARVD/C-r) (n=16)	Controls (n=55)
Patient characteristics			
Male (%)	57.9	25.0*	58.2
Age (years)	47.1±14.1*	31.9±13.8	37.9±12.8
Length (cm)	178.6±8.1	174.6±8.1	178.0±1.6
Weight (kg)	78.9±13.7	73.8±17.1	73.7±15.6
Body surface area (m^2)	1.98±0.19	1.88±0.22	1.91±0.25
Heart rate (/min)	60.6±10.6	59.9±7.1	57±10.9
ICD (%)	42.1	0	0
Mean follow-up (y)	5.9±2.3	6.7±0.7	0
Task Force criteria (major or minor) [12]			
Structural RV abnormalities (%)	89.5	18.8	0
Depolarization abnormalities (%)	71.1	18.8	0
Repolarization abnormalities (%)	81.6	18.8	0
History of ventricular arrhythmias (%)	94.7	6.3	0
Family history or pathogenic mutation † (%)	94.7	100	NA

* = p<0.01 vs. controls. † = Only mutations with known pathogenicity are included, no unclassified variants. ARVD/C = arrhythmogenic right ventricular dysplasia/cardiomyopathy. ICD = implantable cardioverter defibrillator. RV = right ventricle. Continuous data are presented as mean ± standard deviation

Conventional Echocardiographic Findings

All patients were in sinus rhythm during the echocardiographic examinations. All RV dimensions were significantly increased, and RV systolic function (TAPSE and RV FAC) was significantly reduced in patients with ARVD/C compared with control subjects (**Table 2**). No significant RV dilatation was seen in relatives, whereas TAPSE was moderately but significantly reduced in relatives compared with control subjects. Tricuspid regurgitation grade > 1 was present in 23.7% of the patients with ARVD/C and in none of the relatives or control subjects. LV end-diastolic volume was moderately reduced compared with control subjects in both ARVD/C groups. LV inflow tract diameter and end-diastolic LV posterior wall thickness in patients with ARVD/C were also found to be reduced (**Table 2**). LVEF were moderately but significantly reduced in patients with ARVD/C. Reduced LVEFs (<50%) were present in 15.8% of patients with ARVD/C and none of the relatives or control subjects. Both medial and lateral

annular peak velocities were found to be decreased in patients with ARVD/C compared with control subjects (*Supplemental Table 3).* LV diastolic dysfunction was present only in patients with ARVD/C in 31.6%. All diastolic parameters are listed in **Table 2**.
LV involvement according to conventional echocardiography was present in 31.6% of patients with ARVD/C and in none of the relatives or healthy control subjects (**Table 3**).

Table 2. Mean values of echocardiographic parameters

	Patients (ARVD/C-p) (n=38)	Relatives (ARVD/C-r) (n=16)	Controls (n=55)
Dimensions corrected for BSA			
RVOT-PLAX (mm/m^2)	19.4±4.8†	13.9±1.9	14.2±2.2
RVOT-SAX (mm/m^2)	20.2±4.7†	15.6±2.0	15.4±2.1
RVIT (mm/m^2)	23.4±4.5†	18.0±2.7	18.9±2.5
LVIT (mm/m^2)	21.1±2.5†	22.0±2.5	22.6±2.2
LVIT/RVIT ratio	0.93±0.21†	1.25±0.25	1.21±0.17
RA (cm^2/m^2)	10.9±3.9†	8.0±1.6	9.0±1.8
LA (cm^2/m^2)	8.8±1.7	8.3±1.1†	9.3±1.8
IVSd (mm/m^2)	5.2±0.8	5.1±0.7	5.4±0.6
LVPWd (mm/m^2)	4.3±0.8†	4.7±1.0	5.1±0.7
LVIDs (mm/m^2)	17.8±3.2	17.1±2.4	16.8±2.3
LVIDd (mm/m^2)	25.1±2.2	25.7±2.9	25.9±2.5
LV diastolic parameters			
Early diastolic filling velocity. E (cm/s)	59.3±14.5†	80.5±14.1	75.6±13.9
Late diastolic filling velocity. A (cm/s)	46.5±11.8	42.9±12.0	44.4±10.3
E/A-ratio	1.35±0.43†	2.05±0.76	1.78±0.48
Early diastolic TVI. E` (cm/s)	8.6±3.6†	13.9±3.0	13.5±3.2
E/E` ratio	8.26±4.95†	5.91±1.21	5.74±1.19
Abnormal diastolic function (%)	31.6†	0	0
RV systolic function			
TAPSE (mm)	17.1±4.0†	20.7±2.9†	24.0±2.7
RV-FAC (%)	30.8±9.4†	42.9±5.4	45.2±8.1
LV systolic parameters			
Ejection fraction (%)	55.5±10.6†	59.8±6.7	61.1±4.6
Abnormal systolic function, LVEF<50%, (%)	15.8†	0	0
End-diastolic volume (mL/m^2)	47.5±11.3*	47.5±7.4†	53.9±11.4
End-systolic volume (mL/m^2)	21.7±10.9	19.2±4.8	21.2±6.2
Wall motion score index	1.29±0.40†	1.08±0.12	1.08±0.12
Deformation imaging			
Mean systolic peak strain	-16.8±4.1†	-19.6±1.6	-20.0±2.2

Continuous data is presents as mean ± standard deviation. * = p<0.05, and † = p<0.01 vs. controls. BSA = body surface area. RVOT = right ventricular outflow tract. PLAX = parasternal long-axis view. PSAX = parasternal short-axis view. RVIT = right ventricular inflow tract. LVIT = left ventricular inflow tract. RA = right atrium. LA = left atrium. IVSd = end-diastolic interventricular septum dimension. LVPWd = left ventricular end-diastolic posterior wall dimension. LVIDs = systolic left ventricle internal dimension. LVIDd = diastolic left ventricle internal dimension. TVI = tissue velocity imaging. TAPSE = tricuspid annular plane systolic excursion. RV-FAC = right ventricular – fractional area change. LVEF = left ventricular ejection fraction.

Table 3. Percentage of patients with LV abnormalities and LV involvement among conventional echocardiography and deformation imaging.

Technique Parameter	Patients (ARVD/C-p) (n=38)	Relatives (ARVD/C-r) (n=16)	Controls (n=55)
Conventional			
LVEF < 50%	15.8	0	0
Presence of akinesia or dyskinesia (%)	26.3	0	0
Diastolic dysfunction (%)	31.5	0	0
***LV involvement - conventional* * (%)**	**31.6**	**0**	**0**
Deformation imaging			
Systolic peak strain ≤ |-12.5% | (%)	55.3	12.5	0
Systolic peak SR ≤|-0.6%| (%)	15.8	0	0
Post systolic shortening ≥ 15% (%)	63.2	18.8	0
LV involvement – deformation imaging ** (%)	**68.4**	**25.0**	**0**

* = LV involvement detected by conventional echocardiography was defined as the presence of akinesia or dyskinesia in the left ventricle or LVEF%<50%. ** =LV involvement detected by deformation imaging was defined as systolic peak strain |≤-12.5% | and/or post-systolic shortening > 15% in two adjacent LV segments. ARVD/C = arrhythmogenic right ventricular dysplasia/cardiomyopathy. LV = left ventricle. LVEF = left ventricular ejection fraction. SR = strain rate.

Deformation Imaging

Deformation imaging by speckle-tracking was feasible in 83% of all segments (n = 1,636 of 1,962). Feasibility did not differ significantly between patient groups. Mean values of systolic peak strain were significantly reduced in most LV segments (**Table 2** *and Supplemental Table 4*). Deformation imaging detected a high incidence of abnormal systolic peak strain and postsystolic shortening in two or more adjacent segments in patients with ARVD/C. The middle and apical regions of the posterolateral wall were clear predilection sites within the left ventricle (**Figure 2 and Figure 3**). LV involvement according to deformation imaging occurred in 68% of patients with ARVD/C (**Table 3**). LV involvement was associated with a higher incidence of tricuspid valve regurgitation, 60%, compared with 31% in patients with ARVD/C without LV involvement. RV systolic pressure did not differ between patients with or without LV involvement (*Supplemental Table 5*).

Among relatives of patients with ARVD/C, mean systolic peak strain values were also significantly reduced (**Table 2,** *Supplemental Table 4*). Only postsystolic shortening was detected in this group, and predilection sites were less apparent because of the smaller number of affected segments. LV involvement was detected in 25% of relatives (**Table 3**). No deformation imaging abnormalities were detected in control subjects.

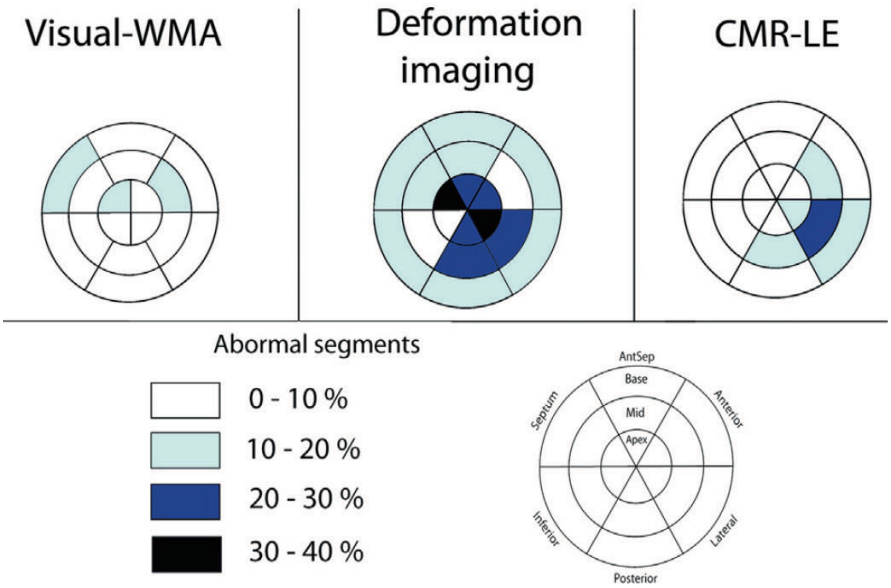

Figure 2. Graphical representation of abnormal segments by conventional echocardiography, deformation imaging (Speckle-Tracking) and CMR.
Distribution and frequency of LV wall motion abnormalities in ARVD/C patients (ARVD/C-p) detected with conventional echocardiography, deformation imaging (Speckle-Tracking) and CMR-LE. Note the agreement between CMR-LE and deformation imaging. Deformation imaging also detected wall motion abnormalities in 25 % of the ARVD/C-relatives, however a predilection site was less apparent due low numbers of affected segments. Visual-WMA = visual wall motion analyses. CMR-LE = cardiac magnetic resonance – late enhancement. ARVD/C = arrhythmogenic right ventricular dysplasia/cardiomyopathy. Note: CMR was only performed in a subgroup of ARVD/C patients (n=19).

CMR Imaging

CMR with LE was performed in a subgroup of 19 patients with ARVD/C and eight of their relatives. LE in the left ventricle was reported in four patients with ARVD/C; all others were negative. The distribution pattern of LE was subepicardial or midwall; no subjects had a subendocardial distribution pattern suggesting scar tissue due to coronary artery disease. In these four patients with ARVD/C, localization of LE corresponded well with the LV segments showing abnormal regional deformation. Less agreement regarding localization was seen between visual wall motion analyses and LE on CMR imaging. (**Figure 2 and Figure 3**). LV involvement according to deformation imaging was seen in nine patients without LE on CMR. Six of the 19 patients with ARVD/C who underwent CMR imaging reached clinical end points during follow-up. Only two of these patients showed LE on CMR imaging, while five of these six had deformation imaging abnormalities in two adjacent segments.

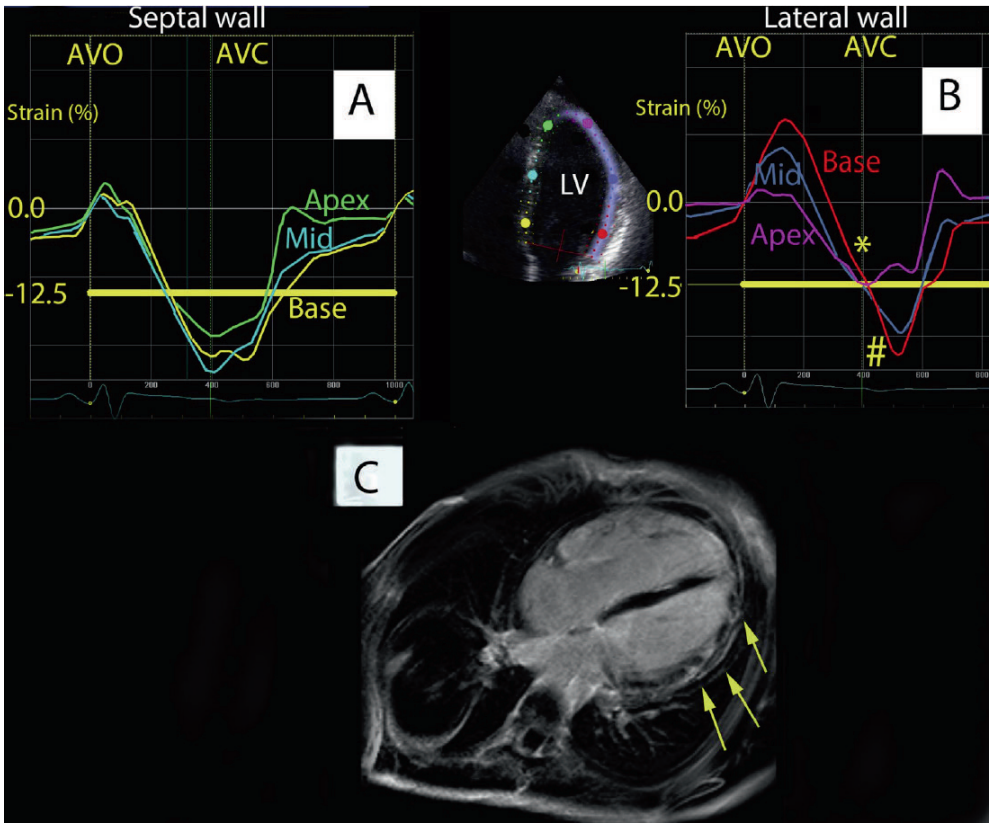

Figure 3. Left ventricular abnormalities in an ARVD/C patient
Example of a 16-year boy presenting with ventricular tachycardia. ECG and conventional echocardiography showed typical phenotypic signs of ARVD/C. LV visual wall motion, LVEF%, diastolic function and LV dimensions were considered normal indicating isolated RV disease. However, deformation imaging revealed abnormal deformation pattern of the LV lateral wall (A and B). CMR with late enhancement (LE) was performed afterwards and the pattern of LE was in concordance with this finding (C). A. Deformation imaging of the septal wall. Normal deformation pattern and peak systolic value. B. Deformation imaging of LV lateral wall. The lateral basal segment (red curve) shows (*) decreased peak (end)systolic-strain and (#) post-systolic-shortening. Lateral midsegment (blue-green) shows (#) post-systolic shortening. Apical (pink) segment shows normal deformation C. CMR-LE with late enhancement in the basal- and midlateral wall (yellow arrows) and a normal myocardium at the septal side. LV: left ventricle, AVO = aortic value opening, AVC = aortic valve closure, CMR-LE = cardiac magnetic resonance – late enhancement. ECG =electrocardiogram.

Clinical Outcomes

During a mean follow-up period of 5.9 ± 2.3 years, 20 patients with ARVD/C (53%) reached clinical end points. The most common end point was an appropriate ICD intervention for ventricular tachycardia. Five patients (12.5%) died of sudden cardiac death or refractory end-stage heart failure, and one patient (2.5%) underwent heart transplantation because of progressive heart failure symptoms due to progression of the disease. All six patients had already reached earlier end points before death or heart transplantation. All relatives of

patients with ARVD/C remained free of events during the follow-up period and were excluded from subsequent regression analysis.

Structural RV alteration and/or global RV dysfunction was the only established phenotypic expression, as mentioned in the task force criteria,12 that was significantly correlated with outcome. RV outflow tract (RVOT) end-diastolic dimension was the only conventional echocardiographic parameter indicating RV disease showing independent prognostic value (**Table 4**, *Supplemental Table 6).* The presence of electrocardiographic abnormalities and a history of ventricular arrhythmias did not differ between the event group and event-free survivors.

Table 4. Baseline characteristics related to clinical outcome

Parameter	**Event-free (n=18)**	**MACE (n=20)**	**P-value**	**Multivariate HR (95CI)**
Patient characteristics				
Age (years)	49.9±14.1	44.6±14.1	NS	NS
Gender (% male)	56%	60%	NS	NS
Task Force Criteria [12]				
Structural RV abnormalities	14 (78%)	20 (100%)	P<0.05	NS
Depolarization abnormalities	11 (61%)	16 (80%)	NS	NS
Repolarization abnormalities	15 (83%)	16 (80%)	NS	NS
History of ventricular arrhythmias	16 (89%)	20 (100%)	NS	NS
Pathogenic mutation or family history	17 (94.4%)	19 (95%)	NS	NS
Echocardiographic RV parameters				
*RVOT dimension**	*18.4±3.5*	*21.7±5.2*	*P<0.05*	*1.2 (1.1-1.3)*
RV-FAC%	34.3±9.9	27.4±7.9	P<0.05	NS
TAPSE (mm)	18.0±4.2	16.4±3.8	NS	NS
Echocardiographic LV parameters				
LVEF%	59.0±6.2	51.2±13.1	P<0.05	NS
LVEF<50%	0 (0%)	6 (30%)	P<0.01	NS
LV wall motion abnormalities	2 (11%)	8 (40%)	NS	NS
Abnormal diastolic function	6 (33%)	6 (30%)	NS	NS
LV involvement – conventional **	0 (0%)	7 (35%)	P<0.01	NS
Deformation imaging				
Mean systolic LV peak strain	18.8±2.5	15.1±4.4	P<0.01	NS
*LV involvement – deformation imaging **	*2 (11%)*	*11 (55%)*	*P<0.01*	*4.9 (1.7-14.2)*

Continuous data is presents as mean ± standard deviation. Several parameters indicating RV and LV structural abnormalities were correlated to adverse outcome. Remarkable, none of the ECG or arrhythmia criteria as described in the revised Task Force criteria contained prognostic value in ARVD/C patients. After multivariate regression analyses right ventricular outflow tract (RVOT) dimension and LV involvement measured by deformation imaging remained the only independent predictors for outcome. * right ventricular outflow tract dimension was measured in the parasternal short-axis view and corrected for body-surface area ** To increase the applicability of our definitions of LV involvement, these were limited to involvement of the posterolateral wall during regression analyses. *Abbreviations:* MACE = major adverse cardiac event, 95 CI = 95% confidence interval, NS = not significant, RV = right ventricle, LV = left ventricle, RVOT = right ventricular outflow tract, RV-FAC% = RV-FAC%= right ventricular – fractional area change %, LVEF% = left ventricular ejection fraction %

Conventional echocardiographic LV parameters, in particular LV dysfunction (LVEF < 50%), were also significantly correlated with outcomes. The presence of LV dysfunction (LVEF < 50%) at baseline (21.1% of patients with ARVD/C) was related to a significantly higher event rate during follow-up (**Figure 4**). The Kaplan-Meier estimate for 1-year event risk was 50% for the presence of LVEF < 50% at baseline versus 16.7% with normal LV function. Systolic medial and lateral peak annular velocity was lower in the event group compared with the group remaining free of events but did not reach statistical significance (*Supplemental Table 3*).

Both LV involvement–conventional and LV involvement–deformation imaging were significantly correlated with adverse outcomes. However, after multivariate regression, LV involvement–deformation imaging and RVOT dimension remained the only independent predictors of clinical outcomes, indicating the adverse aspect of biventricular disease in ARVD/C. The presence of LV involvement at baseline, measured by deformation imaging, decreased the mean event-free survival time by threefold, compared with isolated RV disease (2.2 vs 6.6 years) (**Table 4 and Figure 4**).

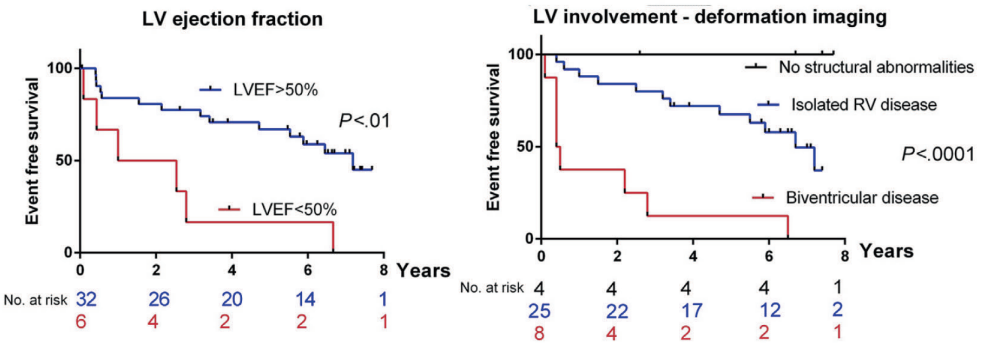

Figure 4. Clinical course of ARVD/C patients with left ventricular involvement versus isolated RV disease

Kaplan-Meier survival plots for left ventricular ejection fraction (LVEF%) (left), LV involvement – deformation imaging (right). Signs of LV involvement are associated with adverse outcome. LVEF = left ventricular ejection fraction. LV = left ventricle. RV = right ventricle.

DISCUSSION

In this prospective observational longitudinal study, we evaluated the occurrence and clinical impact of LV involvement in both phenotypic patients with ARVD/C and asymptomatic genetically predisposed relatives not meeting current 2010 task force criteria using both conventional and new quantitative echocardiographic parameters.

R1 R2 R3 R4 R5 R6 R7 R8 R9 R10 R11 R12 R13 R14 R15 R16 R17 R18 R19 R20 R21 R22 R23 R24 R25 R26 R27 R28 R29 R30 R31 R32 R33 R34 R35 R36 R37 R38 R39

Accurate Detection of LV Involvement

In our study, echocardiographic deformation imaging detected LV involvement in 68% of the patients with ARVD/C and 25% of their relatives. The distribution of regional deformation abnormalities matched the distribution of LE when LE was present. Moreover, deformation imaging also detected LV involvement in patients without LE on CMR imaging, and these patients seemed to be at higher risk for adverse clinical outcomes during follow-up. This supports the idea that deformation imaging can detect minor regional LV dysfunction in absence of myocardial fibrosis detected by CMR imaging.[11] LE patterns (midwall or subepicardial) were in concordance with the distribution seen on histopathology in an ARVD/C population.[22] Conventional echocardiography detected LV involvement in only 32% of the patients with ARVD/C, and the correlation with deformation imaging and LE on CMR imaging was low. We excluded hypokinesia as a visual wall motion abnormality in our analysis, and only akinesia and dyskinesia were taken into account as wall motion abnormalities. With the inclusion of hypokinesia, the percentage of wall motion abnormalities increased to similar levels as detected by deformation imaging. However, also with the inclusion of hypokinesia, the distribution pattern of conventional wall motion abnormalities remained not in agreement with CMR imaging or deformation imaging results. Moreover, hypokinesia was often scored as abnormal in our control group (22%), while deformation imaging revealed no abnormalities at all in healthy control subjects. Because of this high false-positive rate, conventional echocardiography seems unsuitable for detecting the often minor signs of LV involvement in patients with ARVD/C. Our data also extend prior findings indicating that deformation imaging is more able to detect regional wall motion abnormalities in ARVD/C mutation carriers than conventional echocardiography.[21]

Triangle of Dysplasia

In past decades, evidence has accumulated that challenges the concept of LV involvement as an "end-stage" phenomenon in ARVD/C.[4, 5 and 7] Recently, Te Riele *et al.* [1 and 2] proposed a new biventricular "triangle of dysplasia" consisting of the RV basal inferior and anterior wall and the LV posterolateral wall to replace the original RV triangle of dysplasia. [1 and 2] They found >40% LV involvement in a CMR study with 74 patients with ARVD/C with clear predilection site of the posterolateral midventricular region.[2] This region was also a clear common abnormal region in the left ventricle in our study population, which is in close concordance with this previous report.

Clinical Implications

Previous studies have highlighted the clinical relevance of LV dysfunction in patients with ARVD/C.[5, 6, 23, 24, 25, 26 and 27] Our results emphasize the prognostic relevancy of LV involvement in patients with ARVD/C. LV involvement measured by deformation imaging and RVOT

R1 R2 R3 R4 R5 R6 R7 R8 R9 R10 R11 R12 R13 R14 R15 R16 R17 R18 R19 R20 R21 R22 R23 R24 R25 R26 R27 R28 R29 R30 R31 R32 R33 R34 R35 R36 R37 R38 R39

dimension were the only independent predictors of adverse clinical outcomes, indicating the adverse aspect of biventricular involvement in ARVD/C. Importantly, the predictive value of LV involvement measured by deformation imaging is independent of LVEF reduction. This implies that minor structural LV involvement is already associated with the occurrence of events before global LV systolic dysfunction occurs.

In 40% to 60% of patients with ARVD/C, pathogenic mutations are identified in genes predominantly encoding for desmosomal proteins, which induces mechanical uncoupling.[14 and 28] This uncoupling leads to progressive myocardial cell loss, which is histopathological characterized by fibrofatty replacements of the myocardium.[1 and 29] Histopathologic changes promote electrical activation delay and provide substrates for reentry and ventricular arrhythmias.[30, 31, 32 and 33] Moreover, progressive loss of myocardium may eventually lead to heart failure in advanced stages of disease.[29] However, recent studies in mouse models have shown that altered desmosomes are associated with redistribution of several gap junction proteins resulting in electrical uncoupling before any histopathologic changes appear.[34] So both molecular and histopathologic changes could be responsible for the clinical adverse features of ARVD/C. LV involvement, as detected by deformation imaging, is an expression of myocardial cell loss and therefore explains the association with adverse clinical outcomes.6 However, in our study population, 45% of the patients with ARVD/C who experienced events during follow-up were identified to have normal LV systolic function (LVEF > 50%) and no signs of (minor) LV involvement at baseline. Therefore, it can be stated that solely the presence of structural LV alterations is not a complete explanation for the higher risk for clinical events. On the other hand, our data support the idea of a prominent role for molecular changes as the cause of clinical adverse events, particular in earlier stages of ARVD/C, in the absence of structural alteration.[34] Reliable predictors in patients with ARVD/C without extensive disease are still lacking and are mandatory to identify high-risk patients.

Besides the extent of structural alterations, several studies have shown the association between the presence of electrical abnormalities at baseline and clinical events.[19 and 35] Remarkably, electrical abnormalities were not significantly correlated with outcomes in our cohort. A possible explanation is the difference in disease severity, which was high in our population compared with other studies in this field.

Recently, echocardiographic RV systolic parameters were correlated with adverse clinical outcomes.[36] We also found single predictive value for these parameters. However, after adjusting for LV involvement, these parameters did not show independent predictive value. RVOT dimension, as part of the extent of RV structural alteration as mentioned in the task force criteria, was found to be an independent predictor of outcomes. This is consistent with a previous CMR study in a possible ARVD/C population, which correlated the extent of CMR imaging–measured RV abnormalities at baseline with adverse outcomes during follow-up.[37]

Our preliminary observations advocate for a potential prominent role for echocardiography

in the follow-up of patients with ARVD/C. Minor LV involvement, measured by deformation imaging in the posterolateral region, has prognostic value that is superior to conventional measurements of RV and LV function. Moreover, the frequent use of ICDs in this population suits echocardiography more than CMR imaging for the follow-up of patients with ARVD/C.
In this study, we determined LV involvement at baseline. It is possible that some patients developed LV abnormalities during their clinical courses. Monitoring LV involvement during follow-up might be of additional value in patients with ARVD/C. Visual wall motion analysis is not preferred for monitoring LV involvement because of high false-positive rates, whereas deformation imaging seems an accurate method for monitoring this minor pathology.

Limitations

The revised 2010 task force criteria were not available at the time of patient enrollment (2006–2008), so we were forced to apply the 2010 task force criteria in retrospect. Studies of ARVD/C are typically small in size. We performed both uni- and multivariate Cox regression analysis of 20 events that occurred in 38 patients with ARVD/C; because of these small numbers of patients with ARVD/C and events, our regression analysis suffers from lack of power. The likelihood of overfitting of our multivariate analyses is high. Our identification of independent predictors should be interpreted with this taken into account. Further validation of our results in studies that contain large numbers of patients and events is necessary. Therefore, the conclusions drawn from our data should be considered preliminary. Unfortunately, we were not able to perform an optimal comparison between CMR imaging and deformation imaging, because CMR imaging was not part of our prospective study protocol. Moreover, the frequent presence of ICDs also precluded CMR imaging in >40% of patients with ARVD/C. CMR imaging was available in only eight of 16 relatives of patients with ARVD/C, primarily because of a time difference between the moment of CMR imaging and echocardiographic examination of >12 months. Therefore, CMR imaging was performed only in a subset of patients. We performed a subanalysis to explore this potential bias (*Supplemental Table 7*). Event risk and baseline characteristics did not differ statistically significantly between the group that underwent CMR imaging and the group without CMR imaging data. We based the expected lower limit of normal values on our control population, an approach that may not be optimal to discriminate abnormal from normal because of the heterogeneity of deformation within the left ventricle. Larger studies in healthy control subjects may shed light on the range of normal values within specific regions of the left ventricle. Another approach in patients with ARVD/C could be to monitor changes in LV deformation during follow-up.

Conclusions

Deformation imaging detected LV involvement in 68% of patients with proven ARVD/C, and even in 25% of asymptomatic mutation carriers not fulfilling current 2010 task force criteria.

Additionally, our findings showed good agreement with LE on CMR imaging. The results of this study show that regional deformation imaging contains additional value in both detecting minor LV involvement in patients with confirmed or probable ARVD/C and invalidating false-positive results from visual assessment of wall motion abnormalities. This study underlines the clinical importance of LV involvement in patients with ARVD/C. On the basis of our preliminary data, we suggest measuring LVEF and establishing the peak systolic strain in the midventricular posterolateral wall in all patients with ARVC. If the LVEF is <50% and/or the peak systolic strain does not reach the −12.5% mark, the prognosis of these patients seems to be much worse compared with those with isolated RV disease and could be used to guide therapeutic strategies.

REFERENCES

1. F.I. Marcus, G.H. Fontaine, G. Guiraudon, R. Frank, J.L. Laurenceau, C. Malergue, et al. Right ventricular dysplasia: a report of 24 adult cases. *Circulation*, 65 (1982), pp. 384–398
2. A.S. Te Riele, C.A. James, B. Philips, N. Rastegar, A. Bhonsale, J.A. Groeneweg, et al. Mutation-Positive arrhythmogenic right ventricular dysplasia/cardiomyopathy: the triangle of dysplasia displaced. *J Cardiovasc Electrophysiol*, 24 (2013), pp. 1311–1320
3. 3 L. Lindstrom, E. Nylander, H. Larsson, B. Wranne. Left ventricular involvement in arrhythmogenic right ventricular cardiomyopathy—a scintigraphic and echocardiographic study. *Clin Physiol Funct Imaging*, 25 (2005), pp. 171–177
4. J. Kjaergaard, J. Hastrup Svendsen, P. Sogaard, X. Chen, H. Bay Nielsen, L. Kober, et al. Advanced quantitative echocardiography in arrhythmogenic right ventricular cardiomyopathy. *J Am Soc Echocardiogr*, 20 (2007), pp. 27–35
5. D. Corrado, C. Basso, G. Thiene, W.J. McKenna, M.J. Davies, F. Fontaliran, et al. Spectrum of clinicopathologic manifestations of arrhythmogenic right ventricular cardiomyopathy/dysplasia: a multicenter study. *J Am Coll Cardiol*, 30 (1997), pp. 1512–1520
6. B. Pinamonti, A.M. Dragos, S.A. Pyxaras, M. Merlo, A. Pivetta, G. Barbati, et al.Prognostic predictors in arrhythmogenic right ventricular cardiomyopathy: results from a 10-year registry. *Eur Heart J*, 32 (2011), pp. 1105–1113
7. S. Sen-Chowdhry, P. Syrris, D. Ward, A. Asimaki, E. Sevdalis, W.J. McKenna. Clinical and genetic characterization of families with arrhythmogenic right ventricular dysplasia/cardiomyopathy provides novel insights into patterns of disease expression. *Circulation*, 115 (2007), pp. 1710–1720
8. H. Tandri, H. Calkins. MR and CT imaging of arrhythmogenic cardiomyopathy. *Card Electrophysiol Clin*, 3 (2011), pp. 269–280
9. A.J. Teske, M.G. Cox, M.C. Peterse, M.J. Cramer, R.N. Hauer. Case report: echocardiographic deformation imaging detects left ventricular involvement in a young boy with arrhythmogenic right ventricular dysplasia/cardiomyopathy. *Int J Cardiol*, 135 (2009), pp. e24–e26
10. A.J. Teske, B.W. De Boeck, P.G. Melman, G.T. Sieswerda, P.A. Doevendans, M.J. Cramer. Echocardiographic quantification of myocardial function using tissue deformation imaging, a guide to image acquisition and analysis using tissue Doppler and speckle tracking. *Cardiovasc Ultrasound*, 5 (2007), p. 27.
11. F. Weidemann, M. Niemann, S. Herrmann, M. Kung, S. Stork, C. Waller, et al. A new echocardiographic approach for the detection of non-ischaemic fibrosis in hypertrophic myocardium. *Eur Heart J*, 28 (2007), pp. 3020–3026
12. F.I. Marcus, W.J. McKenna, D. Sherrill, C. Basso, B. Bauce, D.A. Bluemke, et al. Diagnosis of arrhythmogenic right ventricular cardiomyopathy/dysplasia: proposed modification of the task force criteria *Circulation*, 121 (2010), pp. 1533–1541
13. J.P. van Tintelen, M.M. Entius, Z.A. Bhuiyan, R. Jongbloed, A.C. Wiesfeld, A.A. Wilde, et al. Plakophilin-2 mutations are the major determinant of familial arrhythmogenic right ventricular dysplasia/cardiomyopathy. *Circulation*, 113 (2006), pp. 1650–1658
14. J.A. Groeneweg, P.A. van der Zwaag, L.R. Olde Nordkamp, H. Bikker, J.D. Jongbloed, R. Jongbloed, et al.Arrhythmogenic right ventricular dysplasia/cardiomyopathy according to revised 2010 task force criteria with inclusion of non-desmosomal phospholamban mutation carriers. *Am J Cardiol*, 112 (2013), pp. 1197–1206
15. R.M. Lang, L.P. Badano, V. Mor-Avi, J. Afilalo, A. Armstrong, L. Ernande, et al. Recommendations for cardiac chamber quantification by echocardiography in adults: an update from the American Society of Echocardiography and the European Association of Cardiovascular Imaging. *J Am Soc Echocardiogr*, 28 (2015), pp. 1–39

R1
R2
R3
R4
R5
R6
R7
R8
R9
R10
R11
R12
R13
R14
R15
R16
R17
R18
R19
R20
R21
R22
R23
R24
R25
R26
R27
R28
R29
R30
R31
R32
R33
R34
R35
R36
R37
R38
R39

16. L.G. Rudski, W.W. Lai, J. Afilalo, L. Hua, M.D. Handschumacher, K. Chandrasekaran, et al. Guidelines for the echocardiographic assessment of the right heart in adults: a report from the American Society of Echocardiography endorsed by the European Association of Echocardiography, a registered branch of the European Society of Cardiology, and the Canadian Society of Echocardiography. *J Am Soc Echocardiogr*, 23 (2010), pp. 685–713
17. S.F. Nagueh, C.P. Appleton, T.C. Gillebert, P.N. Marino, J.K. Oh, O.A. Smiseth, et al. Recommendations for the evaluation of left ventricular diastolic function by echocardiography. *Eur J Echocardiogr*, 10 (2009), pp. 165–193
18. A.J. Teske, B.W. De Boeck, M. Olimulder, N.H. Prakken, P.A. Doevendans, M.J. Cramer. Echocardiographic assessment of regional right ventricular function: a head-to-head comparison between 2-dimensional and tissue Doppler-derived strain analysis. *J Am Soc Echocardiogr*, 21 (2008), pp. 275–283.
19. A.S. te Riele, A. Bhonsale, C.A. James, N. Rastegar, B. Murray, J.R. Burt, et al. Incremental value of cardiac magnetic resonance imaging in arrhythmic risk stratification of arrhythmogenic right ventricular dysplasia/cardiomyopathy-associated desmosomal mutation carriers. *J Am Coll Cardiol*, 62 (2013), pp. 1761–1769
20. D. Dalal, H. Tandri, D.P. Judge, N. Amat, R. Macedo, R. Jain, et al. Morphologic variants of familial arrhythmogenic right ventricular dysplasia/cardiomyopathy a genetics-magnetic resonance imaging correlation study. *J Am Coll Cardiol*, 53 (2009), pp. 1289–1299
21. A.J. Teske, M.G. Cox, A.S. Te Riele, B.W. De Boeck, P.A. Doevendans, R.N. Hauer, et al. Early detection of regional functional abnormalities in asymptomatic ARVD/C gene carriers. *J Am Soc Echocardiogr*, 25 (2012), pp. 997–1006
22. D. Corrado, C. Basso, G. Thiene. Arrhythmogenic right ventricular cardiomyopathy: an update *Heart*, 95 (2009), pp. 766–773
23. D. Corrado, L. Leoni, M.S. Link, P. Della Bella, F. Gaita, A. Curnis, et al. Implantable cardioverter-defibrillator therapy for prevention of sudden death in patients with arrhythmogenic right ventricular cardiomyopathy/dysplasia. *Circulation*, 108 (2003), pp. 3084–3091
24. A. Nava, B. Bauce, C. Basso, M. Muriago, A. Rampazzo, C. Villanova, et al. Clinical profile and long-term follow-up of 37 families with arrhythmogenic right ventricular cardiomyopathy. *J Am Coll Cardiol*, 36 (2000), pp. 2226–2233
25. T. Pezawas, G. Stix, J. Kastner, B. Schneider, M. Wolzt, H. Schmidinger. Ventricular tachycardia in arrhythmogenic right ventricular dysplasia/cardiomyopathy: clinical presentation, risk stratification and results of long-term follow-up. *Int J Cardiol*, 107 (2006), pp. 360–368
26. T. Wichter, M. Paul, C. Wollmann, T. Acil, P. Gerdes, O. Ashraf, et al. Implantable cardioverter/defibrillator therapy in arrhythmogenic right ventricular cardiomyopathy: single-center experience of long-term follow-up and complications in 60 patients. *Circulation*, 109 (2004), pp. 1503–1508
27. P.K. Schuler, L.M. Haegeli, A.M. Saguner, T. Wolber, F.C. Tanner, R. Jenni, et al. Predictors of appropriate ICD therapy in patients with arrhythmogenic right ventricular cardiomyopathy: long term experience of a tertiary care center. *PLoS One*, 7 (2012), p. e39584
28. C. Basso, D. Corrado, B. Bauce, G. Thiene. Arrhythmogenic right ventricular cardiomyopathy. *Circ Arrhythm Electrophysiol*, 5 (2012), pp. 1233–1246
29. C. Basso, D. Corrado, F.I. Marcus, A. Nava, G. Thiene. Arrhythmogenic right ventricular cardiomyopathy. *Lancet*, 373 (2009), pp. 1289–1300
30. J.M. de Bakker, F.J. van Capelle, M.J. Janse, S. Tasseron, J.T. Vermeulen, N. de Jonge, et al. Slow conduction in the infarcted human heart. 'Zigzag' course of activation. *Circulation*, 88 (1993), pp. 915–926
31. H. Tandri, A. Asimaki, T. Abraham, D. Dalal, L. Tops, R. Jain, et al. Prolonged RV endocardial activation duration: a novel marker of arrhythmogenic right ventricular dysplasia/cardiomyopathy. *Heart Rhythm*, 6 (2009), pp. 769–775

32. L.F. Tops, K. Prakasa, H. Tandri, D. Dalal, R. Jain, V.L. Dimaano, et al. Prevalence and pathophysiologic attributes of ventricular dyssynchrony in arrhythmogenic right ventricular dysplasia/cardiomyopathy. *J Am Coll Cardiol*, 54 (2009), pp. 445–451
33. H.M. Haqqani, C.M. Tschabrunn, B.P. Betensky, N. Lavi, W.S. Tzou, E.S. Zado, et al. Layered activation of epicardial scar in arrhythmogenic right ventricular dysplasia: possible substrate for confined epicardial circuits. *Circ Arrhythm Electrophysiol*, 5 (2012), pp. 796–803
34. M. Cerrone, M. Noorman, X. Lin, H. Chkourko, F.X. Liang, R. van der Nagel, et al. Sodium current deficit and arrhythmogenesis in a murine model of plakophilin-2 haploinsufficiency. *Cardiovasc Res*, 95 (2012), pp. 460–468
35. S. Peters, H. Peters, L. Thierfelder. Risk stratification of sudden cardiac death and malignant ventricular arrhythmias in right ventricular dysplasia-cardiomyopathy. *Int J Cardiol*, 71 (1999), pp. 243–250
36. A.M. Saguner, A. Vecchiati, S.H. Baldinger, S. Rueger, A. Medeiros-Domingo, A.S. Mueller-Burri, et al.Different prognostic value of functional right ventricular parameters in arrhythmogenic right ventricular cardiomyopathy/dysplasia. *Circ Cardiovasc Imaging* (2014)
37. M. Deac, F. Alpendurada, F. Fanaie, R. Vimal, J.P. Carpenter, A. Dawson, et al. Prognostic value of cardiovascular magnetic resonance in patients with suspected arrhythmogenic right ventricular cardiomyopathy. *Int J Cardiol*, 168 (2013), pp. 3514–3521

R1
R2
R3
R4
R5
R6
R7
R8
R9
R10
R11
R12
R13
R14
R15
R16
R17
R18
R19
R20
R21
R22
R23
R24
R25
R26
R27
R28
R29
R30
R31
R32
R33
R34
R35
R36
R37
R38
R39

SUPPLEMENTARY FILES

Standard Echocardiographic Measurements

Conventional measurements included end-diastolic RVOT diameter in the parasternal long-axis and short-axis views. End-diastolic LV internal diameter, end-diastolic interventricular septal thickness and posterior wall thickness, and end-systolic LV internal diameter were measured in the parasternal long-axis view on M-mode imaging. In the apical four-chamber view, the LV and RV short-axis inflow tract diameters were measured at the level of the valve leaflet tips at end-diastole. Right and left atrial single-plane areas were measured at end-systole. All dimensions were corrected for body surface area. In the apical four-chamber view, TAPSE and RV end-systolic area and end-diastolic area were measured to acquire RV FAC. LVEF was measured using the biplane Simpson method. Pulsed Doppler imaging was used to interrogate transmitral as well as LV outflow tract flow (5-mm sample) at end-expiration during breath-hold for diastolic parameters (early [E] and atrial [A] peak velocities, the E/A ratio, and deceleration time) and the timing of cardiac events, respectively. In the apical four-chamber view, a pulsed tissue Doppler sample (6 mm) was placed at the lateral and septal mitral annulus (E′ peak velocity and the E/E′ ratio). Diastolic function was defined as either normal or abnormal (impaired relaxation, pseudonormal, or restrictive), corrected for age.17 LV involvement measured by conventional echocardiography was defined as the occurrence of LV dysfunction (LVEF < 50%) and/or visual wall motion abnormalities in two adjacent segments.

Deformation Imaging

We acquired wide-angle, real-time, two-dimensional ultrasound data from the LV walls in the three standard apical views (frame rate, ±40-60 frames/sec). Commercially available software (EchoPAC PC version 11.2) was used for offline analysis. Doppler flow curves of the cardiac valves were used for timing cardiac events, and all timing information was aligned through electrocardiographic traces.

Supplementary Table A. Definition of clinical outcome variables

Outcome variable	Definition
Sustained ventricular tachycardia	Ventricular tachycardia which lasts 30 seconds or more, or less than 30 s when terminated electrically or pharmacologically
Appropriate implantable cardioverter defibrillator (ICD) intervention	ICD shock or antitachycardia pacing in response to a ventricular tachyarrhythmia and documented by stored intracardiac ECG data
Sudden cardiac death	Death of cardiac origin that occurred unexpectedly within 1 hour of the onset of new symptoms or a death that was unwitnessed and unexpected
Aborted sudden cardiac death	Sudden cardiac death, as described above, reversed by cardiopulmonary resuscitation and/or defibrillation or cardioversion

ICD = implantable cardioverter defibrillator. ECG = electrocardiogram

Supplementary Table B. Percentage of identified pathogenic mutations among different groups

Genes	Patients (ARVD/C-p) (n=38)	Relatives (ARVD/C-r) (n=16)
Plakophilin-2 (*PKP2*) (%)	71.0	75.0
Phospholamban (*PLN*) (%)	10.5	12.5
Desmogleine-2 (*DSG2*) (%)	5.3	6.25
Desmocolline-2 (*DSC2*) (%)	2.6	6.25
Unclassified variant (%)	5.2	-
No genetic data (%)	5.2	-

Supplementary Table C. Systolic peak velocity in medial and lateral annulus among study groups and in relation to clinical outcome.

	Patients (ARVD/C-p) (n=38)	Relatives (ARVD/C-r) (n=16)	Controls (n=55)
TDI medial – systolic peak velocity (cm/s)	6.4±1.7*	7.5±0.7	7.9±1.2
TDI lateral – systolic peak velocity (cm/s)	6.9±2.0*	8.2±1.5	8.7±2.1

***** = P<0.01 vs. controls

	Event free (n=18)	MACE (n=20)	P-value
TDI medial – systolic peak velocity (cm/s)	6.8±1.3	6.0±1.9	NS
TDI lateral – systolic peak velocity (cm/s)	7.2±1.4	6.6±2.5	NS

NS = not significant. TDI = tissue Doppler imaging. MACE = major adverse clinical event

Supplementary Table D. Mean values of peak-strain and peak-SR for Speckle Tracking (upper) and Tissue Doppler imaging (lower)

Speckle-Tracking		**Controls (n=55)**		**ARVD/C-p (n=38)**		**ARVD/C-r (n=16)**	
		Peak Strain (mean±SD)	Peak SR (mean±SD)	Peak Strain (mean±SD)	Peak SR (mean±SD)	Peak Strain (mean±SD)	Peak SR (mean±SD)
Septum	Base	-17.4±2.7	-0.97±0.20	-15.7±4.3*	-0.92±0.30	-17.5±2.5	-0.94±0.13
	Mid	-19.6±2.6	-1.02±0.17	-17.0±4.4†	-0.90±0.20†	-19.6±2.2	-0.94±0.15
	Apex	-23.1±4.3	-1.36±0.31	-19.6±7.1†	-1.21±0.40	-21.5±4.2	-1.21±0.28
Lateral	Base	-18.9±3.8	-1.29±0.31	-18.8±5.9	-1.40±0.44	-18.1±3.5	-1.39±0.33
	Mid	-18.8±3.8	-1.02±0.25	-14.9±7.3†	-0.97±0.29	-17.1±3.1	-1.06±0.25
	Apex	-21.8±4.0	-1.31±0.32	-15.8±8.1†	-1.08±0.45*	-18.8±4.1*	-1.11±0.27*
Inferior	Base	-19.9±3.6	-1.19±0.27	-19.1±4.7	-1.24±0.40	-21.2±2.6	-1.32±0.31
	Mid	-20.5±3.1	-1.11±0.19	-18.7±4.3*	-0.98±0.30*	-20.4±2.1	-1.05±0.15
	Apex	-22.0±3.2	-1.30±0.24	-20.2±4.5	-1.16±0.26*	-22.0±3.8	-1.33±0.25
Anterior	Base	-19.9±4.5	-1.02±0.26	-18.9±5.7	-1.29±0.54*	-22.7±4.2	-1.26±0.28†
	Mid	-20.6±4.0	-1.03±0.27	-18.0±4.5*	-1.03±0.30	-22.4±2.9	-1.22±0.20*
	Apex	-21.0±3.8	-1.24±0.33	-16.3±6.1†	-1.06±0.34	-20.6±3.2	-1.21±0.21
Posterior	Base	-20.0±3.8	-1.38±0.28	-18.0±6.1	-1.42±0.48	-18.7±3.3	-1.57±0.47
	Mid	-19.5±3.1	-1.10±0.19	-15.2±8.2†	-0.95±0.47	-18.8±3.2	-1.10±0.22
	Apex	-20.1±4.4	-1.24±0.33	-15.6±7.3†	-1.11 ±0.51	-19.5±4.6	-1.34±0.45
AntSept	Base	-18.6±3.3	-0.96±0.18	-14.6±3.5†	-0.84±0.18†	-17.2±2.7	-0.87±0.12
	Mid	-20.4±2.8	-1.05±0.18	-15.6±4.5†	-0.93±0.23†	-20.9±3.6	-1.09±0.35
	Apex	-20.3±4.8	-1.24±0.36	-16.2±7.0†	-1.12±0.50	-16.1±13.7	-1.17±0.35
Mean systolic peak		-20.0±2.2	-1.15±0.15	-16.9±4.1†	-1.08±0.25	-19.6±1.6	-1.18±0.15
Tissue Doppler imaging		**Controls (n=29)**		**ARVD/C p (n=38)**		**ARVD/C-r (n=16)**	
Septum	Base	-19.2±3.4	-1.22±0.21	-15.5±5.6†	-0.93±0.30†	-20.1±3.6	-1.15±0.22
	Mid	-20.6±3.9	-1.21±0.32	-16.9±4.7†	-0.99±0.27†	-20.0±2.4	-1.22±0.26
	Apex	-24.4±3.5	-1.33±0.23	-18.9±6.8†	-1.05±0.46†	-22.3±3.9*	-1.24±0.28
Lateral	Base	-18.5±3.9	-1.28±0.31	-16.9±5.7	-1.17±0.37	-18.6±4.0	-1.36±0.43
	Mid	-19.7±3.8	-1.18±0.37	-13.8±8.9†	-0.95±0.39†	-19.0±4.7	-1.17±0.44
	Apex	-18.7±3.8	-1.41±0.45	-14.6±7.0*	-0.95±0.43†	-17.3±4.7	-1.17±0.36
Inferior	Base	-20.6±3.8	-1.24±0.26	-18.8±6.1	-1.17±0.47	-20.2±5.1	-1.27±0.39
	Mid	-20.0±3.8	-1.10±0.27	-17.5±5.0*	-0.95±0.36	-18.7±3.9	-1.02±0.30
	Apex	-24.9±3.4	-1.55±0.31	-20.8±5.7†	-1.18±0.38†	-22.3±3.3	-1.34±0.30
Anterior	Base	-21.5±4.5	-1.35±0.41	-17.4±5.9†	-1.01±0.34†	-21.5±5.7	-1.31±0.45
	Mid	-22.7±5.2	-1.36±0.34	-16.6±4.6†	-0.95±0.29†	-20.2±4.7	-1.45±0.63
	Apex	-19.3±3.8	-1.38±0.56	-14.8±6.6†	-0.92±0.40*	-15.3±4.8	-1.04±0.39
Posterior	Base	-19.4±4.2	-1.27±0.45	-16.9±4.7*	-1.18±0.32	-20.0±4.0	-1.33±0.40
	Mid	-20.4±3.8	-1.16±0.36	-13.9±9.7†	-0.93±0.41*	-18.1±3.3	-1.06±0.23
	Apex	-23.1±4.2	-1.45±0.43	-16.4±6.5†	-0.97±0.38†	-18.6±4.7*	-1.22±0.49
AntSept	Base	-15.8±3.8	-1.10±0.26	-12.2±5.5†	-0.88±0.35†	-18.4±5.3	-1.17±0.32
	Mid	-21.3±2.3	-1.41±0.36	-16.9±5.5†	-1.00±0.41†	-19.0±4.5	-1.13±0.37*
	Apex	-19.1±3.9	-1.12±0.33	-14.8±4.7†	-0.91±0.36*	-17.7±3.9	-1.04±0.26
Mean systolic peak		-20.6±1.7	-1.28±0.13	-16.5±4.0†	-1.02±0.25†	-19.4±1.8	-1.21±0.21

In this manuscript only the Speckle-Tracking data is presented. All analyses were also performed with Tissue Doppler imaging and gave similar results. Tissue Doppler imaging was only available in a subset of controls (n= 29). *= p<0.05. and †= p<0.01 vs. controls using unpaired students T-test. SR = strain rate. SD = standard deviation.

Supplementary Table E. Valve regurgitations and pulmonary artery pressure in ARVD/C patients

	LV involvement + (n= 26)	LV involvement – (n= 12)	RVOT PLAX/ BSA ≥16 mm/m^2 (n=29)	RVOT PLAX/ BSA <16 mm/m^2 (n=9)
Mitral valve regurgitations (%)	20.0	23.1	27.6	0
No regurgitations (%)	80.0	76.9	72.4	100.0
Grade I (%)	12.0	23.1	20.7	0.0
Grade II (%)	8	0	6.9	0.0
Grade III (%)	0.0	0.0	0.0	0.0
Tricuspid valve regurgitations (%)	60.0*	30.8	62.0*	11.1
No regurgitation	40.0	69.2	37.9	88.9
Grade I (%)	28.0	23.1	31.0	11.1
Grade II (%)	16.0	0.0	13.8	0.0
Grade III (%)	16.0	7.7	17.2	0.0
RV systolic pressure (mmHg)	30.7±6.5	28.7±8.4	29.1±7.7	32.8±4.4
Pulmonary acceleration time (ms)	167.73±4.0	158.5±25.0	163.4±28.1	167.4±39.8

*= P<0.05. Classification of valve regurgitations were based on guidelines provided by American Society of Echocardiography (ASE). RVSP was measured as RVSP (mmHg) = (4 * ((tricuspid valve regurgitation max velocity ^{2})) + estimated right atrial pressure). LV involvement was based on results derived from deformation imaging (see methods section).

Supplementary Table F. Specific overview of Task Force criteria in relation to clinical outcome

	Event free (n=18)	MACE (n=20)	P-value	Multivariate HR (95CI)
Global or regional RV dysfunction and structural alteration				
Fulfilment of TFC on echocardiography or CMR (TFC)	14 (78%)	20 (100%)	P<0.05	NS
Major criterion (TFC)	10 (56%)	18 (90%)	P<0.05	NS
Minor criterion (TFC)	4 (22%)	2 (10%)	NS	NS
RVOT-PLAX (mm/BSA)	17.8±3.8	20.8±5.3	P<0.05	-
RVOT-SAX (mm/BSA)	*18.4±3.5*	*21.7±5.2*	*P<0.05*	*1.2 (1.1-1.3)*
TAPSE (mm)	18.0±4.7	16.4±3.8	NS	NS
RV-FAC%	34.3±9.9	27.4±7.8	P<0.05	NS
Depolarization abnormalities				
Fulfilment of depolarization criterion (TFC)	11 (61%)	16 (80%)	NS	NS
Epsilon waves (% patients) (TFC)	2 (11%)	7 (35%)	NS	NS
TAD (% patients) (TFC)	9 (50%)	9 (45%)	NS	NS
Repolarization abnormalities				
Fulfilment of repolarization criterion (TFC)	15 (83%)	16 (80%)	NS	NS
T-wave inversion V_1-V_3 without RBBB (TFC)	10 (56%)	15 (75%)	NS	NS
T-wave inversion V_1-V_2 without RBBB or V_4-V_6 or V_1-V_4 with RBBB (TFC)	5 (27%)	1 (5%)	NS	NS
History of arrhythmias				
Fulfilment of arrhythmia criterion (TFC)	16 (89%)	20 (100%)	NS	NS
(Non-)sustained VT LBBB with superior axis (TFC)	9 (53%)	13 (59%)	NS	NS
(Non-)sustained VT LBBB with inferior axis or unknown axis (TFC)	13 (72%)	18 (90%)	NS	NS
>500 PVC/ 24 hour (TFC)	8 (44%)	9 (45%)	NS	NS
Family History				
Fulfilment of TFC family history criterion (TFC)	17 (94.4%)	19 (95%)	NS	NS

Continuous data is presents as mean ± standard deviation.
Abbreviations: MACE = major adverse cardiac event. 95 CI = 95% confidence interval. NS = not significant. RV = right ventricle. LV = left ventricle. TFC= (as defined as in) 2010 revised Task Force criteria[12]. RVOT = right ventricular outflow tract. PLAX = parasternal long axis view. SAX = short axis view. TAPSE = tricuspid annulus plane systolic excursion. RV-FAC%= right ventricular – fractional area change%. TAD = terminal activation duration. RBBB = right bundle branch block. VT = ventricular tachycardia. PVC = premature ventricular complexes

Supplementary Table G. Baseline and outcome differences between subjects with or without available CMR data.

	Patients (ARVD/C-p) with CMR data (n=19)	Patients (ARVD/C-p) without CMR data (n=19)	Relatives (ARVD/C-r) with CMR data (n=8)	Relatives (ARVD/C-r) without CMR data (n=8)
Patient characteristics				
Male (%)	52.6	63.2	50.0	50.0
Age (years)	47.2±7.0	47.0±11.9	31.6±12.4	32.3±15.9
Length (cm)	181.2±8.5	176.4±7.7	174.6±8.1	174.6±8.7
Weight (kg)	77.6±14.5	80.0±13.3	75.1±8.7	72.5±11.5
Body surface area (m^2)	1.99±0.2	1.97±0.2	1.89±0.28	1.86±0.18
Heart rate (/min)	61.2±10.7	59.5±10.7	61.0±6.5	58.8±8.0
ICD (%)	0	79.0	0.0	0.0
Mean follow-up (y)	5.6±2.5	5.7±2.2	6.5±0.5	6.9±0.8
Task Force criteria (major or minor)				
Structural RV abnormalities (%)	84.2	94.7	25.0	12.5
Depolarization abnormalities (%)	68.2	73.4	25.0	12.5
Repolarization abnormalities (%)	78.9	84.2	25.0	12.5
History of ventricular arrhythmias (%)	84.2	94.7	0	12.5
Family history or pathogenic mutation (%)	78.9	100.0	100.0	100.0
Outcome				
Events during follow-up	42.1	63.1	0	0

CMR data was not available in all subjects which could lead to potential bias. However, clinical characteristics were comparable between subjects with or without avaliable CMR data. † = Only mutations with known pathogenicity are included, no unclassified variants. ARVD/C = arrhythmogenic right ventricular dysplasia/cardiomyopathy. CMR = cardiac magnetic resonance. ICD = implantable cardioverter defibrillator. RV = right ventricle. Continuous data are presented as mean ± standard deviation.

R1. R2. R3. R4. R5. R6. R7. R8. R9. R10. R11. R12. R13. R14. R15. R16. R17. R18. R19. R20. R21. R22. R23. R24. R25. R26. R27. R28. R29. R30. R31. R32. R33. R34. R35. R36. R37. R38. R39.

PART III

TOWARDS OPTIMAL ASSESSMENT OF STRUCTURAL DISEASE PROGRESSION IN ARVC

CHAPTER 7

Evaluation of Structural Progression in Arrhythmogenic Right Ventricular Dysplasia/Cardiomyopathy

Thomas P Mast, Cynthia A James, Hugh Calkins, Arco J Teske, Crystal Tichnell, Brittney Murray, Peter Loh, Stuart D Russell, Birgitta K Velthuis, Daniel P Judge, Dennis Dooijes, Ryan J Tedford, Jeroen F van der Heijden, Harikrishna Tandri, Richard N Hauer, Theodore P Abraham, Pieter A Doevendans, Anneline SJM te Riele, Maarten J Cramer,

JAMA Cardiol. 2017 in press

ABSTRACT

Importance: Considerable research has described the arrhythmic course of arrhythmogenic right ventricular dysplasia/cardiomyopathy (ARVD/C). However, objective data characterizing structural progression such as ventricular enlargement and cardiac dysfunction in ARVD/C are relatively scarce.

Objectives: 1) To define the extent of structural progression, 2) identify predictors of structural progression, and 3) determine the association between structural progression and electrocardiographic (ECG) changes in ARVD/C patients.

Design, Setting, and Participants: First and last available echocardiograms of 85 ARVD/C patients fulfilling 2010 Task Force diagnostic criteria (TFC) from a Trans-Atlantic ARVD/C registry were retrospectively compared to assess structural disease progression.

Main Outcomes and Measures: To assess structural progression, we compared RV size and systolic function between baseline and last follow-up. RV size was determined by RV outflow tract (RVOT) dimension, RV/LV systolic function by RV fractional area change (RV-FAC) and LV ejection fraction (LVEF), respectively. Multivariable logistic regression was used to study associations between baseline characteristics and the occurrence of structural progression.

Results: After a mean follow-up of 6.4±2.5 years, RVOT dimension increased from 35 mm [inter-quartile range: 31,39] to 37 mm [33,41] (P<.001), RV-FAC decreased from 39% [33,44] to 34% [24,42] (P<.001), rate: -3.3%/5y,[-8.9,+1.2] indicating large inter-patient variability. LVEF decreased from 55% [52,60] to 54% [49,57] (P=.001), rate: -0.2%/5y,[-6.5,+1.7]. Forty exams were re-analyzed to establish the measurement error. Subjects exceeding the measurement error by ±2 standard deviations were identified with significant progressive disease, for RV: a decrease in RV-FAC>10% (n=21), for LV: decrease in LVEF>7% (n=23). RV progression was associated with depolarization criteria at baseline (Odds Ratio (OR): 9.0; 95CI:1.1-74.2, P=.041); whereas LV progression was associated with Phospholamban (*PLN*) mutation (OR: 8.8; 95CI:2.1-37.2, P=.003). There was no association between progressive RV/LV structural disease and newly developed ECG TFC.

Conclusions and Relevance: 1) Structural dysfunction in ARVD/C is progressive with substantial inter-patient variability. 2) Significant structural RV progression was associated with prior depolarization abnormalities, whereas LV progression is modified by genetic background. 3) Structural progression was not associated with development of new ECG TFC. The results of this study pave the way for designing and launching trials aimed at reducing structural progression in patients with ARVD/C.

INTRODUCTION

Arrhythmogenic right ventricular dysplasia/cardiomyopathy (ARVD/C) is an inherited cardiomyopathy clinically characterized by life-threatening ventricular arrhythmias and ventricular dysfunction.[1] The most characteristic histopathologic feature of the disease is fibro-fatty replacement of right ventricular (RV) myocardium, although left dominant forms of the disease are well-recognized.[2,3] Since the first major description of ARVD/C,[4] much has been learned about this condition. When viewed broadly, the majority of research efforts have focused on developing optimal approaches for diagnosis,[5] defining the genetic basis of this condition,[6,7] and describing, predicting, and treating ARVD/C-associated ventricular arrhythmias.[7,8]

In contrast to the intense research focus placed on diagnosis, genetics, and arrhythmic outcomes, remarkably relatively little attention has been given to defining and characterizing the progressive nature of the condition. This is particularly true for the question of the extent to which ventricular enlargement and cardiac dysfunction progress in ARVD/C. While it is widely acknowledged that ARVD/C is progressive, as evidenced by the fact that it is not present at birth and emerges decades later,[8] no large studies have been performed to define the extent and rate of structural progression over time. This is emerging as next critical research and clinical frontier in the field of ARVD/C. With increased awareness of this condition, better characterization of risk factors for SCD,[9] an increased use of implantable cardiac defibrillators (ICDs) for SCD prevention, and improvements in catheter ablation to achieve ventricular tachycardia (VT) control,[10] the remaining management question concerns whether structural progression occurs, in whom, and at what rate. Once defined, clinical trials can be designed to specifically test whether a variety of pharmacologic therapies or exercise restriction are useful in preventing progression.

Therefore, the main purpose of this study was to characterize the extent of structural progression of ARVD/C over time using data obtained from a unique transatlantic cohort of ARVD/C patients from the United States and The Netherlands. Additional goals of this study were to identify predictors of structural progression of ARVD/C, and to determine the association between structural progression and electrical progression as assessed by electrocardiograms (ECG) and Holter monitoring.

METHODS

Study population

The study population was comprised of 85 ARVD/C patients (22 from the Johns Hopkins ARVD/C Registry (http://ARVD.com) (JHU) and 63 from the University Medical Center Utrecht

ARVD/C registry, The Netherlands). All patients were diagnosed with ARVD/C based on the 2010 Task Force Criteria (TFC).[5] For the purpose of this study, we included subjects that underwent at least two separate echocardiographic evaluations a minimum of 2 years apart at their home institution (JHU/Utrecht). The first echocardiographic exam after fulfillment of definite 2010 TFC diagnosis was considered the baseline echocardiogram.[5] The last available clinical echocardiogram during follow-up was used as follow-up echocardiogram, which was performed at least 2 years after baseline echocardiogram. The study was approved by the local institutional ethics review boards.

Clinical characterization

Fulfillment of TFC at baseline and last follow-up was assessed for each participant. By study design, echocardiography was available in all subjects at baseline and at last follow-up. All echocardiographic exams were evaluated for the presence of regional RV wall motion abnormalities (akinesia, dyskinesia or aneurysm), RV outflow tract (RVOT) dimension, in both the parasternal long and short axis view (PLAX/PSAX), and RV-fractional area change (RV-FAC) as described in the TFC.[5,11] In addition, LV ejection fraction (LVEF) by Simpson biplane method was assessed.[12]

All subjects underwent routine 12-lead ECG recording at baseline and last follow-up. ECG was evaluated for the presence of depolarization criteria (epsilon waves and terminal activation duration (TAD) ≥55ms), and repolarization criteria (precordial T-wave inversion, V_1-V_6), as described in the TFC.[5] Definitions of ECG parameters are provided as *Supplementary Material, Table 1*). Signal-averaged ECG (SA-ECG) were evaluated for the presence of late potential as defined in the TFC.[5] Minor depolarization criteria (prolonged TAD and late potentials by SA-ECG) were grouped together since SA-ECG was not performed routinely in The Netherlands. minor criteria prolonged TAD and late potentials were grouped together since signal averaged ECG was not performed routinely in the Dutch individuals Holter monitoring was evaluated for premature ventricular complex (PVC) count, which according to the TFC was abnormal if > 500/24h were recorded.[5]

Genetic testing was performed in all index patients by molecular genetic screening of 5 ARVD/C-associated desmosomal genes: plakophillin-2 (*PKP2*), desmoglein-2 (*DSG2*), desmocollin-2 (*DSC2*), desmoplakin (*DSP*) and plakoglobin (*JUP*). Non-desmosomal analysis included transmembrane protein 43 (*TMEM43)* and phospholamban (*PLN).* Relatives were only included in this study that were genotyped and found to carry the same mutation as the probands or were a first degree family member of a mutation-negative probands.

Cardiac magnetic resonance (CMR) examinations were performed according to standard protocols for ARVD/C which are described elsewhere.[13] CMR examinations were used for initial diagnosis of ARVD/C and were analyzed for the presence of major and minor structural TFC.

Measurement of structural disease progression

To assess structural progression, we compared RV systolic function determined by RV-FAC, LV systolic function determined by LVEF, and RVOT dimension measured in the PLAX and PSAX views between baseline and follow-up for each patient. For each structural parameter, structural progression was normalized in absolute percentage change over a 5-year period in each of the 85 patients. All 170 (2x85) echocardiograms exams were analyzed by one operator to exclude inter-observer variability. Measurements were performed blinded for clinical data, as well as previous echocardiographic measurements.

We next characterized each patient based on presence or absence of significant structural RV/LV progression. To do so we used a cut-off value of differences in RV-FAC (for RV progression) and LVEF (for LV progression) between baseline and last follow-up. Cut-off values were established based on the measurement error, which we determined by re-analyzing RV-FAC and LVEF in a random sample of 40 subjects by the same observer. The mean difference between the two measurements ± 2 standard deviations was used to determine cut-off values indicating significant structural progression. By this method we aimed to correct for the measurement error inherent to the echocardiographic measurements.[14] The mean difference for RV-FAC measurements was 1.0±5.2% and 0.7±3.4 % for RV-FAC and LVEF, respectively. This resulted in a cut-off value for RV-FAC of 10% and LVEF of 7%. The difference between first and second measurement fulfilled definition for normal distribution implying non-systematic errors.

Thus, the definitions used to assign presence or absence of progressive LV and RV disease were as follows:

- *Significant RV structural progression* was defined as an absolute value decrease of >10% in RV-FAC.
- *Significant LV structural progression* was defined as an absolute value decrease of >7% in LVEF.

Determinants of significant structural progression

To explore the association of clinical characteristics with significant structural progression we studied the association between age, gender, genetic background, and proband status with the occurrence of significant structural progression. Baseline parameters were also tested for predictive value including: echocardiographic structural parameters, presence of arrhythmic TFC, presence of depolarization TFC, and presence of repolarization TFC abnormalities. In addition, follow-up duration was included as determinant to assess the potential influence of inter-patient differences in follow-up duration. All analyses were performed separately for significant RV structural progression and significant LV structural progression.

R1 R2 R3 R4 R5 R6 R7 R8 R9 R10 R11 R12 R13 R14 R15 R16 R17 R18 R19 R20 R21 R22 R23 R24 R25 R26 R27 R28 R29 R30 R31 R32 R33 R34 R35 R36 R37 R38 R39

Correlation with electrical progression

To study the association between electrical progression and structural progression we assessed the correlation between the fulfillment of new electrical TFC in follow-up and the occurrence of significant structural RV/LV progression. Electrical progression was defined by a newly developed depolarization, repolarization, or arrhythmic TFC (minor/major).

Statistics

Continuous data were presented as mean ± standard deviation (SD) or median [inter-quartile range] as appropriate. Categorical variables were presented as numbers (percentages). Comparison of continuous data between groups was performed by independent Student's *t*-test or Mann-Whitney-U test. Categorical data were compared by the Fisher-exact test. The paired Student's *t*-test or Wilcoxon Signed rank test was used to evaluate differences in continuous variables between baseline and last follow-up. McNemar's test without Yates' correction for continuity was used for paired proportional data. Differentiation between normally and non-normally distributed data was assessed by the Shapiro-Wilk test. A P-value < 0.05 was considered significant.

Univariable logistic regression was performed to identify predictors of progressive RV and LV disease. Univariable predictors with P-values < 0.10 were included in multivariable logistic regression analysis. A backward stepwise elimination selection procedure was used. Predictors with an odds ratio (OR) with a 95% confidence intervals (95CI) not including 1 were considered significant. All calculations were performed by a commercially available software package: IBM SPSS Statistics for Windows, Version 21.0.

RESULTS

Study population

The study population included 85 ARVD/C patients whose clinical characteristics are shown in **Table 1**. All subjects fulfilled TFC for definite ARVD/C diagnosis. The mean age at baseline was 42.8 ± 14.4 years, and 55% were men. Our cohort consisted predominantly of 61 (72%) probands, the remaining were 24 first-degree relatives from 21 families. Genetic testing was performed in all subjects except one relative of a mutation-negative proband. A pathogenic ARVD/C related mutation was found in the majority of the study population (n=64, 75%).[5,8,15] All mutation carriers, except one, were identified with a single heterozygous mutation carriers. An overview of the mutations represented in the study population is provided in *supplementary Table 2***.** Mutations in *PKP2* were most common (n=44, 52%). At baseline, 47 (55%) patients had a history of sustained ventricular tachycardia with left bundle branch block (LBBB) morphology. An ICD was implanted at baseline in 49 (58%) patients.

Table 1. Clinical characteristics

	Baseline (N=85)	Last follow-up (N=85)	P-value
Age (years)	42.8 ± 14.4	49.2 ± 14.1	
Male	47 (55)		
Ethnicity (Caucasian/Mongoloid)	83 (98) / 2 (2)		
Probands	61 (72)		
ICD	49 (58)	69 (81)	<.001
Follow-up duration (y)	6.4 ± 2.5		
Genetics			
Pathogenic mutation	64 (75)		
PKP2/DSG2/DSP/DSC2/PLN	44/3/2/1/14 (52/4/2/1/17)		
No pathogenic mutation	21 (25)		
Task Force criteria (TFC)			
Structural TFC			
Structural major TFC	57 (67)	64 (75)	.008
Structural minor TFC	7 (8)	9 (11)	NS
Depolarization TFC			
Epsilon waves (major)	9 (11)	15 (18)	.014
Depolarization minor TFC *	62 (73)	67 (78)	.025
Terminal activation duration ≥55ms	42 (49)	53 (62)	<.001
Repolarization TFC			
T-wave inversion V_1-V_3 (major)	52 (61)	55 (65)	NS
T-wave inversion V_1-V_2 (minor)	11 (13)	10 (12)	NS
T-wave inversion V_4-V_6 (minor)	5 (6)	6 (7)	NS
T-wave inversion V_1-V_4 in presence RBBB (minor)	1 (1)	2 (2)	NS
Arrhythmias TFC			
VT, superior axis (major)	29 (34)	30 (35)	NS
VT, inferior or unknown axis (minor)	48 (57)	52 (61)	.046
PVC count > 500/24h** (minor)	41 (54)	53 (70)	.001
Family history TFC			
Pathogenic ARVD/C mutation carrier (major)	50 (59)		-
ARVD/C confirmed in first-degree relative (major)	33 (39)		-
ARVD/C confirmed in second-degree relative (minor)	4 (5)		-
SCD < 35 in a first-degree relative due to suspected ARVD/C (minor)	8 (9)		-

Values are expressed n/N (%), or means ± standard deviations, or median [inter-quartile ranges].
* Depolarization minor criteria was scored if terminal activation duration > 55ms on ECG or late potentials by signal-averaged ECG (SA-ECG). SA-ECG is not regularly performed in The Netherlands and therefore not listed.
** Holter monitoring was only performed in 76 subjects at baseline. *Abbreviations:* NS = non-significant, ARVD/C = arrhythmogenic right ventricular dysplasia/cardiomyopathy; ICD = implantable cardioverter defibrillator; *PKP2* = Plakophillin-2; *DSG2* = Desmoglein-2; *DSC2* = Desmocollin-2; *DSP* = Desmoplakin; *PLN* =Phospholamban; TFC = 2010 Task Force criteria; VT = ventricular tachycardia; RBBB = right bundle branch block; PVC = premature ventricular complexes

R1 R2 R3 R4 R5 R6 R7 R8 R9 R10 R11 R12 R13 R14 R15 R16 R17 R18 R19 R20 R21 R22 R23 R24 R25 R26 R27 R28 R29 R30 R31 R32 R33 R34 R35 R36 R37 R38 R39

Structural progression

Shown in **Figure 1** are the changes in RV-FAC, LVEF, RVOT-PLAX, and RVOT-PSAX observed over time. During a mean follow-up of 6.4 ± 2.5 years, the RV-FAC fell from 39% [33,44] to 34% [24,42] (P<.001), while the LVEF decreased from 55% [52,60] to 54% [49,57] (P=.001). RVOT dimension measured in the PLAX view increased from 35 mm [31,39] to 37 mm [33,41] (P<.001) and in the PSAX view increased from 35 mm [31,39] to 37 mm [34,41] (P<.001).

Figure 2 shows the rate of change of each of the above parameters observed in each study participant. As shown, the rate of RV-FAC change normalized to a 5 year period was-3.3 %/5y [-8.9,+1.2]. An absolute decrease in RV-FAC was observed in 67% of patients. This decrease in RV-FAC met our pre-specified cut-off for a significant decrease in RV-FAC of ≥10% in 28% of the patients in this study. In contrast, the rate of LVEF change was modest: -0.2 %/5y [-6.5,+1.7] with an absolute decrease in LVEF observed in 50% of patients. This decrease in LVEF met our pre-specified cut-off for a significant decrease in LVEF of ≥7% in 29% of patients in this study. The rate of RVOT-PLAX change was 1.4 mm/5y [0.0,3.4]. An increase in RVOT-PLAX was observed 66%. The rate of RVOT-PSAX change was 1.4 mm/5y [0.0,3.9]. An increase in RVOT-PSAX was observed in 67%.

Predictors of significant structural progression

We next examined the association of demographic, genetic, and baseline clinical characteristics with the presence of significant RV and LV structural progression as defined by our prespecified cutoff values. As mentioned, 21 (28%) of patients met criteria for significant RV structural progression (absolute decrease in RV-FAC>10%). As shown in **Table 2A**, in univariable analysis, being a proband (p=0.039), fulfilling depolarization criteria (p=0.025), and RVOT dimension in the PSAX (p=.046) at baseline were predictive of RV structural disease progression during follow-up. In the fully adjusted model, correcting for proband status and RVOT dimension, fulfillment of depolarization criteria at baseline (OR: 9.0; 95CI, 1.1-74.2) remained significantly associated with significant RV progressive disease during follow-up.

Twenty-three (29%) ARVD/C patients showed structural progressive LV disease as defined by an absolute decrease in LVEF of >7%. As shown in **Table 2B**, in univariable analysis, age at first echocardiographic evaluation (P=.076), baseline LV systolic function (P=.014), and harboring a *PLN* mutation (P=.009) were associated with LV progressive disease during follow-up. After adjusting for age, being a carrier of a *PLN* mutation (OR: 8.8; 95CI, 2.1-37.1) and baseline LVEF (OR: 1.14; 95CI, 1.04-1.24) remained independent predictors of progressive LV disease.

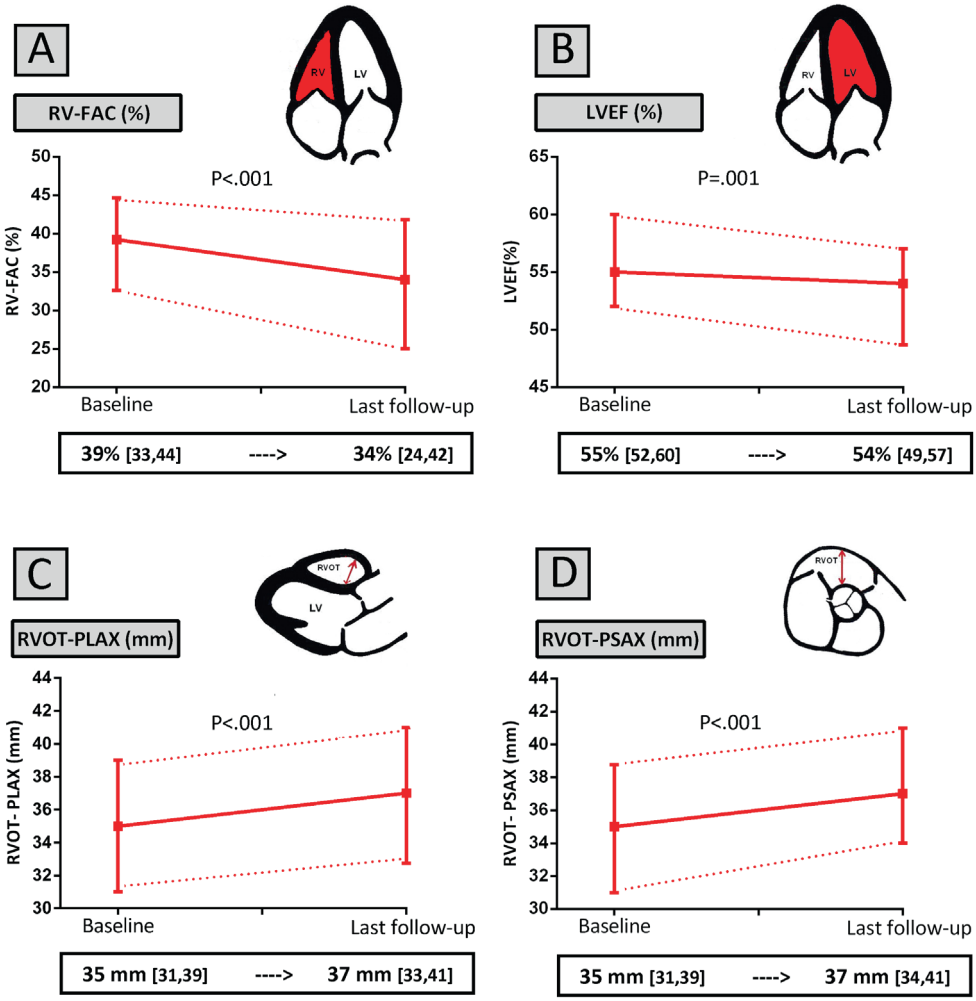

Figure 1. Structural progression in ARVD/C patients
Panel A-D. All panels show the structural parameter on the vertical axis. Median value at baseline and last follow-up on the horizontal axis. Mean follow-up = 6.4±2.5 years. ***Panel A:*** median RV-FAC decreased from 39% [33,44] at baseline to 34% [24,42] at follow-up (P<.001). ***Panel B***: median LVEF decreased from 55% [52,60] at baseline to 54% [49,57] at follow-up (P=.001). ***Panel C:*** median RVOT-PLAX increased from 35 mm [31,39] at baseline to 37 mm [33,41] at follow-up (P<.001). ***Panel D:*** median RVOT-PSAX increased from 35 mm [31,39] at baseline to 37 mm [34,41] at follow-up (P<.001). *Abbreviations:* RV-FAC = right ventricular fractional area change; LVEF = left ventricular ejection fraction; RVOT = right ventricular outflow tract; PLAX/PSAX=parasternal long/short axis; mm = millimeter

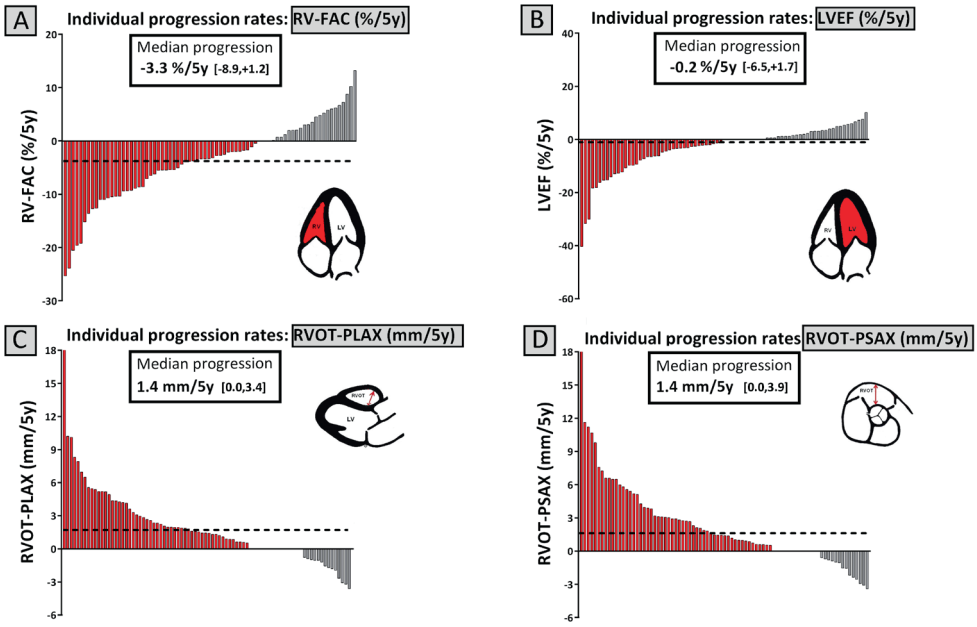

Figure 2. Distribution of progression rates for right ventricular outflow tract dimension and ventricular systolic function

Panel A-D are showing normalized % change in structural parameter over a 5-year period in each of the 85 patients in this study. In the horizontal axis, each bar represents individual progression rated ranked in ascending order. Vertical axis is showing the structural parameter as %/5y value. **Panel A:** RV-FAC decrease in 67%, the median fall in RV-FAC was -3.3%/5y (dotted line). **Panel B**: LVEF decrease in 50%, the median fall in LVEF was -0.2%/5y (dotted line). **Panel C**: RVOT-PLAX increase in 66%, the median rise in RVOT-PLAX dimension was 1.4 mm/5y (dotted line). **Panel D**: RVOT-PLAX increase in 68%, the median rise in RVOT-PLAX dimension was 1.4 mm/5y (dotted line). *Abbreviations:* RVOT = right ventricular outflow tract; PLAX/PSAX = parasternal long/short axis; RV-FAC = right ventricular fractional area change; LVEF = left ventricular ejection fraction; mm = millimeter; 5y = 5=year

Table 2. Predictors for significant RV structural progression based on univariable and multivariable logistic regression

A) significant RV structural progression: decrease in RV function (RV-FAC) by absolute value of 10%

Variable	Univariable OR (95CI)	P-value	Multivariable OR (95CI)	P-value
Age	1.02 (0.98-1.06)	NS	-	-
Male gender	1.59 (0.55-4.58)	NS	-	-
Proband	5.16 (1.08-24.6)	.039	4.1 (0.9-20.4)	NS
Follow-up duration (py)	1.12 (0.91-1.38)	. NS	-	-
Electrical Task Force criteria				
Depolarization criteria (major or minor)	**10.9 (1.35-87.3)**	**.025**	**9.0 (1.10-74.2)**	**.041**
Repolarization criteria (major or minor)	1.90 (0.48-7.50)	NS	-	
Arrhythmic criteria (major or minor)	1.42 (0.27-7.44)	NS	-	
Baseline structural measurements				
RVOT-PLAX (mm)	1.07 (0.99-1.14)	NS	-	-
RVOT-PSAX (mm)	1.07 (1.00-1.15)	.046	1.03 (0.96-1.11)	NS
RV-FAC (%)	0.98 (0.93-1.04)	NS	-	-
LVEF (%)	0.98 (0.91-1.05)	NS	-	-
Genetics				
Desmosomal mutation	Ref.		-	-
Gene elusive	1.69 (0.51-5.63)	NS	-	-
PLN	1.37 (0.35-5.35)	NS	-	-

B) Significant LV structural progression: decrease in LV systolic function (LVEF) by absolute value of 7%

Variable	Univariable OR (95CI)	P-value	Multivariable OR (95CI)	P-value
Age	**1.03 (1.00-1.07)**	**.076**	1.03 (0.99-1.08)	NS
Male gender	0.72 (0.27-1.92)	NS		
Proband	2.13 (0.63-7.20)	NS		
Follow-up duration (py)	0.95 (0.77-1.16)	NS		
Electrical Task Force criteria				
Depolarization criteria (major or minor)	1.16 (0.39-3.48)	NS		
Repolarization criteria (major or minor)	0.71 (0.23-2.22)	NS		
Arrhythmic criteria (major or minor)	1.29 (0.24-6.90)	NS		
Baseline structural measurements				
RVOT-PLAX (mm)	1.03 (0.97-1.10)	NS		
RVOT-PSAX (mm)	1.06 (0.99-1.13)	NS		
RV-FAC (%)	1.00 (0.95-1.05)	NS		
LVEF (%)	**1.11 (1.02-1.21)**	**.014**	**1.14 (1.04-1.24)**	**.005**
Genetics				
Desmosomal mutation	Ref.		Ref.	
Gene elusive	2.06 (0.61-6.97)	NS	2.39 (0.63-9.05)	NS
PLN	**5.48 (1.52-19.8)**	**.009**	**8.79 (2.08-37.16)**	**.003**

Panel A. Logistic regression was used to identify predictors for significant RV structural progression which was found in 21 (28%) of the ARVD/C patients. Fulfillment of depolarization criteria at baseline was associated with significant RV structural progression.
Panel B. LV structural progression which was found in 23 (29%) of the ARVD/C patients. Carriers of a Phospholamban (*PLN*) mutation showed more significant LV structural progression compared to desmosmal mutation carriers. High baseline values of LVEF at baseline was also associated with more decrease in LV systolic function during follow-up. *Abbreviations*: NS = non-significant; OR = odds ratio; 95CI = 95% confidence interval; py =per year; RVOT-PLAX/PSAX = right ventricular outflow tract – parasternal long/short axis; RV-FAC= right ventricular – fractional area change; LVEF = left ventricular ejection fraction; mm = millimeter

Table 3. Structural progression versus electrical progression by Task Force criteria

A	Progressive structural RV disease (n=21)			Stable RV disease (n=54)		
	Baseline	Follow-up	P-value	Baseline	Follow-up	P-value
Depolarization TFC						
Epsilon waves (major)	3 (14)	7 (33)	*.046*	4 (7)	6 (11)	.157
Depolarization minor TFC	20 (95)	20 (95)	1.00	*35 (65)*	*39 (72)*	*.046*
Repolarization TFC						
T-wave inversion V_1-V_3 (major)	16 (76)	18 (86)	.157	32 (59)	32 (59)	1.00
T-wave inversion V_1-V_2 (minor)	2 (10)	0 (0)	.157	8 (15)	9 (17)	.317
T-wave inversion V_4-V_6 (minor)	1 (5)	1 (5)	1.00	3 (6)	4 (7)	.317
T-wave inversion V_1-V_4 in presence RBBB (minor)	0 (0)	0 (0)	1.00	0 (0)	1 (2)	.317
Arrhythmias TFC						
VT, superior axis (major)	8 (38)	9 (43)	.317	18 (33)	18 (33)	1.00
VT, inferior or unknown axis (minor)	15 (71)	16 (76)	.317	28 (52)	30 (56)	.157
PVC count > 500/24h (minor)	12/19 (63)	14/19 (74)	.157	*24/49 (49)*	*33/49 (67)*	*.003*

Values are expressed n/N (%). Ten patients were excluded in this analysis due to insufficient image quality. Progressive RV disease was defined as > 10 % absolute decrease in RV-FAC. TFC= Task Force criteria; VT = ventricular tachycardia; PVC = premature ventricular complexes

B	Progressive structural LV disease (n=23)			Stable LV disease (n=55)		
	Baseline	Follow-up	P-value	Baseline	Follow-up	P-value
Depolarization TFC						
Epsilon waves (major)	3 (13)	4 (17)	.317	*4 (7)*	*9 (16)*	*.025*
Depolarization minor TFC	17 (74)	18 (78)	.317	39 (71)	43 (78)	*.046*
Repolarization TFC						
T-wave inversion V_1-V_3 (major)	14 (61)	15 (65)	.317	36 (65)	38 (69)	.157
T-wave inversion V_1-V_2 (minor)	1 (4)	0 (0)	.317	8 (15)	8 (15)	1.00
T-wave inversion V_4-V_6 (minor)	4 (17)	4 (17)	1.00	1 (2)	2 (4)	.317
T-wave inversion V_1-V_4 in presence RBBB (minor)	0 (0)	1 (4)	.317	0 (0)	0 (0)	1.00
Arrhythmias TFC						
VT, superior axis (major)	9 (39)	9 (39)	1.00	17 (31)	18 (33)	.317
VT, inferior or unknown axis (minor)	14 (61)	14 (61)	1.00	31 (56)	34 (62)	.083
PVC count > 500/24h (minor)	12/21 (57)	12/21 (57)	1.00	*27/50 (54)*	*37/50 (74)*	*.002*

Values are expressed n/N (%). Seven patients were excluded in this analysis due to insufficient image quality. Progressive LV disease was defined as > 7 % absolute decrease in LVEF. TFC= Task Force criteria; VT = ventricular tachycardia; PVC = premature ventricular complexes

Correlation between structural and electrical progression

We compared fulfillment of repolarization, depolarization, and arrhythmia TFC at baseline and follow-up and sought to establish whether these signs of electrical progression were associated with significant structural progression. As shown in **Table 1**, in the entire population an increased proportion of participants met not only structural TFC, but also depolarization TFC and arrhythmias TFC during follow-up. However, as shown in **Table 3**, changes in electrical TFC were not disproportionately likely to occur in patients with significant structural progression. Shown in **Table 3a** are changes in electrical TFC for subjects identified with significant structural RV progression compared to subjects without significant structural RV progression during follow-up. In patients with significant structural RV progression, fulfillment of major depolarization TFC significantly increased during follow-up, with major depolarization TFC seen in 3 out of 21 (14%) at baseline and in 7 out of 21 (33%) during follow-up (P=.046). However, new depolarization abnormalities also developed in patients without significant structural RV progression with minor depolarization TFC fulfilled in 35 out of 54 (65%) at baseline and in 39 out of 54 (72%) during follow-up (P=.046). Only patients with stable RV disease had a significant increase in likelihood of meeting arrhythmia TFC while repolarization TFC did not significantly increase in either the stable or progressive group during follow-up.

Similarly, as shown in **Table 3b,** patients with significant LV structural progression showed no increased likelihood of fulfilling depolarization TFC, repolarization TFC, and arrhythmic TFC during follow-up. In contrast, a greater proportion of patients with stable LV disease met major and minor depolarization TFC during follow-up (4 out of 55 (7%) at baseline and in 9 out of 55 (16%) during follow-up (P=.025), and 39 out of 55 (71%) at baseline and 43 out of 55 (78%) during follow-up (P=.046), respectively). Fulfillment of arrhythmic TFC also significantly increased only in the stable group (P=.002).

DISCUSSION

Overview and main findings

Since the first major description of ARVD/C more than 30 years ago, great progress has been made in elucidating the genetic basis of ARVD/C,[6,7] determining the natural history of this condition with a focus on cardiac arrhythmias,[8] defining optimal approaches for diagnosis,[5] developing approaches for risk stratification and the indications for ICD implantation,[16-18] and identifying the importance of exercise as an environmental trigger for this condition.[19,20] Despite this remarkable progress in understanding ARVD/C, little attention has been focused on identifying and characterizing the progressive nature of this condition. This is a critical issue both for patient management and also in determining the need for as well as the feasibility

of clinical trials designed to prevent progression. It was in this context that we designed this study. The main purpose of this study was to characterize the extent of structural progression of ARVD/C as assessed with echocardiographic imaging over time using data obtained from a unique transatlantic cohort of ARVD/C patients from the United States and The Netherlands. Additional goals of this study were to identify predictors of structural progression of ARVD/C, and to determine the association between structural progression and electrical progression as assessed by ECG and Holter monitoring.

There are three main findings of this study. First, the results of our study provide definitive evidence of the structural progression in patients with ARVD/C. This study also defines the proportion of patients in whom structural progression is observed over an average follow-up of 6 years, and determines the overall rate of progression. Second, we have identified several variables associated with structural progression including the severity ECG abnormalities at baseline and genetic background. And third, the results of this study reveal that structural disease progression is not reflected by the presence of new ECG TFC.

Prior studies

Physicians who longitudinally care for patients with ARVD/C recognize that ARVD/C is a progressive condition. Evidence for this can be derived from a number of sources and is reflected in the studies which have reported outcomes of ARVD/C patients in the past 3 decades.[7,21,22] Perhaps the most compelling line of evidence that ARVD/C is a progressive disease reflects the fact that the mean age of presentation in ARVD/C patients is 36 years of age with virtually no patients being diagnosed with this condition before puberty.[8] Additional evidence includes a previous study of 18 patients who underwent cardiac transplantation for ARVD/C.[23] The mean age of presentation of these patients was 24 years and the mean age of transplantation (72% for heart failure) was 16 years later.[23] Although no prior studies have specifically focused on defining structural progression, several studies contain within them evidence of progression based on serial echocardiograms.[24,25] For example, in 2000, Nava *et al.* reported serial echocardiographic data in 132 ARVD/C patients with 7% of them showing increasing RV dimensions and increased wall motion abnormalities during almost 9 years of follow-up.[22] Our data is in line with this study and extends their findings to a cohort fulfilling the current diagnostic criteria. A more recent study, that aimed to identify predictors of adverse outcomes in ARVD/C, also reported echocardiographic data in a cohort of ARVD/C patients, and reported signs of decreasing RV function and increasing RV dimensions over time.[25] Limitations of this study were the inclusion of subjects who did not meet the complete TFC, a small sample size, and a limited follow-up duration.

A number of studies have also examined ECG evidence of progression.[26-29] The largest of these by Saguner *et al.* reported that in 77 ARVD/C patients depolarization abnormalities increased during follow-up.[28] Another observation was that T-wave inversion may disappear during disease course.

Structural and Electrical Progression in ARVD /C patients

The results of this study confirm and extend the results of the prior studies reviewed above. In our study population of 85 patients each of whom met TFC for ARVD/C, we observed a significant decline in RV systolic function and an increase in dilatation of the RV dimensions during a follow-up period of more than 6 years. Overall, RV-FAC, which was selected as the primary indicator of RV systolic function, declined with more than 3% per 5 years. A significant decline in RV function, which was defined as a decline of > 10% was observed in nearly one-third of patients. A significant decline in LV function was also seen among ARVD/C patients. In our study population, LVEF, as indicator of LV systolic function, decreased with 0.2%/5y. Although statistically significant, the overall decline in LVEF is low and lacks clinical importance for the overall ARVC population. Nevertheless, almost one-third of our patients showed signs of a significant decline of more than 7% in LVEF. This underscores the presence of significant structural ARVD/C disease progression in both the RV and the LV. Previously, both decreased RV-FAC and LVEF were found to be associated with adverse outcome in ARVD/C, which stresses the clinical importance of careful analysis of structural progression.[9,25,30]

Another important finding of this study is that the declines in RV and LV function were not uniform. Progression is subject to high inter-patient variability in a large cohort and this proves the non-uniformity of ARVD/C disease progression. This finding, while perhaps not surprising, makes it clear that a number of clinical variables must be involved. Previous studies have proposed that environmental factors, such as exercise, might be mediators of the severity of ARVD/C phenotype.[19,20] Other studies have proposed that superimposed myocarditis or inflammation may play an important role.[31] One could hypothesize that these environmental and inflammatory factors are the origin of the large inter-patient variability in structural progression. It is notable that consistent with our recent research,[32,33] and in contrast to other cardiomyopathies,[34] age of onset does not appear to predict rate of progression.

Our data shows that fulfillment of depolarization criteria at baseline is associated with progressive structural RV disease during follow-up. All patients, except one, identified with significant RV structural progression showed abnormal depolarization ECG at baseline. Another finding of our study is that ARVD/C patients identified with a *PLN* mutation demonstrated more progressive LV dysfunction compared to non-*PLN*-mediated ARVD/C. Bhonsale *et al.* already showed a higher prevalence of LV dysfunction among *PLN* mutation carriers than carriers of desmosomal ARVD/C mutations and this careful analysis confirms the deterioration of LV function during the disease course in these patients.[7] Although these findings are intriguing, the limited statistical power of this study hampers to be conclusive about the moderator of structural disease progression. Larger studies, including exercise data, are needed to further elucidate the moderators of structural disease progression.

We observed no association between rapid structural disease progression and newly acquired ECG or arrhythmic TFC. Rather, fulfillment of new repolarization, depolarization, and

arrhythmia criteria are as common among those with stable structural disease. Therefore, both ECG and echocardiography are required to monitor overall disease progression in ARVD/C.

Limitations

Our study has a number of limitations which must be considered when interpreting the results of this study. These limitations include its retrospective design with the associated variable follow-up interval between echocardiograms. Furthermore, the use of echocardiography for the assessment of structural progression is associated with some limitations inherent to this technique. The complex RV geometry prevents volumetric assessment by echocardiography. Therefore, we used two-dimensional methods for estimating the changes in RV function and RV size which might be less sensitive to minor signs of structural progression. These limitation could be aggravated by the use of a single observer in this study. The modest sample size with 85 patients in which one-third showed the outcome definition also affects the reliability of our results derived during the regression analyzes. The likelihood of overfitting in this model is high and this should be taken into account by interpreting our results. Furthermore, detailed information concerning the exercise programs and medications taken by each of the subjects during the duration between echocardiograms was unavailable for many patients and hence not included in this analysis.

Conclusions

This study demonstrated that ARVD/C is a progressive cardiomyopathy with marked inter-patient variability in the rate of progression. These preliminary findings could have several important implications for patients and those who care for and carry out clinical trials on patients with ARVD/C. It is important to educate patients and physicians on the progressive nature of this condition. Due to the modest size of this study further studies are needed to elucidate the progressive nature of ARVD/C. Nevertheless, the results of this study pave the way for designing and launching trials to further study and ultimately reduce progression in patients with ARVD/C. We hope the information contained in this study will help trigger a new wave of research on this important and previously largely ignored aspect of ARVD/C.

Acknowledgments

The authors wish to acknowledge funding from the Dr. Francis P. Chiaramonte Private Foundation and the St. Jude Medical Foundation. The Johns Hopkins ARVD/C Program is supported by the Leyla Erkan Family Fund for ARVD Research, the Dr. Satish, Rupal, and Robin Shah ARVD Fund at Johns Hopkins, the Bogle Foundation, the Healing Hearts Foundation, the Campanella family, the Patrick J. Harrison Family, the Peter French Memorial Foundation, and the Wilmerding Endowments. We are grateful to the ARVD/C patients and families who have made this work possible.

REFERENCES

1. Basso C, Corrado D, Marcus FI, Nava A, Thiene G. Arrhythmogenic right ventricular cardiomyopathy. *Lancet.* 2009;373(9671):1289-1300.
2. Sen-Chowdhry S, Syrris P, Prasad SK, et al. Left-dominant arrhythmogenic cardiomyopathy: an under-recognized clinical entity. *J Am Coll Cardiol.* 2008;52(25):2175-2187.
3. Basso C, Thiene G, Corrado D, Angelini A, Nava A, Valente M. Arrhythmogenic right ventricular cardiomyopathy. Dysplasia, dystrophy, or myocarditis? *Circulation.* 1996;94(5):983-991.
4. Marcus FI, Fontaine GH, Guiraudon G, et al. Right ventricular dysplasia: a report of 24 adult cases. *Circulation.* 1982;65(2):384-398.
5. Marcus FI, McKenna WJ, Sherrill D, et al. Diagnosis of arrhythmogenic right ventricular cardiomyopathy/dysplasia: proposed modification of the task force criteria. *Circulation.* 2010;121(13):1533-1541.
6. McKoy G, Protonotarios N, Crosby A, et al. Identification of a deletion in plakoglobin in arrhythmogenic right ventricular cardiomyopathy with palmoplantar keratoderma and woolly hair (Naxos disease). *Lancet.* 2000;355(9221):2119-2124.
7. Bhonsale A, Groeneweg JA, James CA, et al. Impact of genotype on clinical course in arrhythmogenic right ventricular dysplasia/cardiomyopathy-associated mutation carriers. *Eur Heart J.* 2015;36(14):847-855.
8. Groeneweg JA, Bhonsale A, James CA, et al. Clinical Presentation, Long-Term Follow-Up, and Outcomes of 1001 Arrhythmogenic Right Ventricular Dysplasia/Cardiomyopathy Patients and Family Members. *Circ Cardiovasc Genet.* 2015;8(3):437-446.
9. Corrado D, Wichter T, Link MS, et al. Treatment of Arrhythmogenic Right Ventricular Cardiomyopathy/Dysplasia: An International Task Force Consensus Statement. *Circulation.* 2015;132(5):441-453.
10. Philips B, Madhavan S, James C, et al. Outcomes of catheter ablation of ventricular tachycardia in arrhythmogenic right ventricular dysplasia/cardiomyopathy. *Circ Arrhythm Electrophysiol.* 2012;5(3):499-505.
11. Rudski LG, Lai WW, Afilalo J, et al. Guidelines for the echocardiographic assessment of the right heart in adults: a report from the American Society of Echocardiography endorsed by the European Association of Echocardiography, a registered branch of the European Society of Cardiology, and the Canadian Society of Echocardiography. *J Am Soc Echocardiogr.* 2010;23(7):685-713.
12. Lang RM, Badano LP, Mor-Avi V, et al. Recommendations for cardiac chamber quantification by echocardiography in adults: an update from the American Society of Echocardiography and the European Association of Cardiovascular Imaging. *J Am Soc Echocardiogr.* 2015;28(1):1-39 e14.
13. Tandri H, Calkins H, Nasir K, et al. Magnetic resonance imaging findings in patients meeting task force criteria for arrhythmogenic right ventricular dysplasia. *J Cardiovasc Electrophysiol.* 2003;14(5):476-482.
14. Wang J, Prakasa K, Bomma C, et al. Comparison of novel echocardiographic parameters of right ventricular function with ejection fraction by cardiac magnetic resonance. *J Am Soc Echocardiogr.* 2007;20(9):1058-1064.
15. Groeneweg JA, van der Zwaag PA, Olde Nordkamp LR, et al. Arrhythmogenic right ventricular dysplasia/cardiomyopathy according to revised 2010 task force criteria with inclusion of non-desmosomal phospholamban mutation carriers. *Am J Cardiol.* 2013;112(8):1197-1206.
16. Bhonsale A, James CA, Tichnell C, et al. Risk stratification in arrhythmogenic right ventricular dysplasia/cardiomyopathy-associated desmosomal mutation carriers. *Circ Arrhythm Electrophysiol.* 2013;6(3):569-578.
17. te Riele AS, Bhonsale A, James CA, et al. Incremental value of cardiac magnetic resonance imaging in arrhythmic risk stratification of arrhythmogenic right ventricular dysplasia/cardiomyopathy-associated desmosomal mutation carriers. *J Am Coll Cardiol.* 2013;62(19):1761-1769.

R1 R2 R3 R4 R5 R6 R7 R8 R9 R10 R11 R12 R13 R14 R15 R16 R17 R18 R19 R20 R21 R22 R23 R24 R25 R26 R27 R28 R29 R30 R31 R32 R33 R34 R35 R36 R37 R38 R39

18. Bhonsale A, James CA, Tichnell C, et al. Incidence and predictors of implantable cardioverter-defibrillator therapy in patients with arrhythmogenic right ventricular dysplasia/cardiomyopathy undergoing implantable cardioverter-defibrillator implantation for primary prevention. *J Am Coll Cardiol.* 2011;58(14):1485-1496.
19. James CA, Bhonsale A, Tichnell C, et al. Exercise increases age-related penetrance and arrhythmic risk in arrhythmogenic right ventricular dysplasia/cardiomyopathy-associated desmosomal mutation carriers. *J Am Coll Cardiol.* 2013;62(14):1290-1297.
20. Sawant AC, Bhonsale A, Te Riele AS, et al. Exercise has a Disproportionate Role in the Pathogenesis of Arrhythmogenic Right Ventricular Dysplasia/Cardiomyopathy in Patients Without Desmosomal Mutations. *J Am Heart Assoc.* 2014;3(6).
21. Hulot JS, Jouven X, Empana JP, Frank R, Fontaine G. Natural history and risk stratification of arrhythmogenic right ventricular dysplasia/cardiomyopathy. *Circulation.* 2004;110(14):1879-1884.
22. Nava A, Bauce B, Basso C, et al. Clinical profile and long-term follow-up of 37 families with arrhythmogenic right ventricular cardiomyopathy. *J Am Coll Cardiol.* 2000;36(7):2226-2233.
23. Tedford RJ, James C, Judge DP, et al. Cardiac transplantation in arrhythmogenic right ventricular dysplasia/cardiomyopathy. *J Am Coll Cardiol.* 2012;59(3):289-290.
24. Aneq MA, Lindstrom L, Fluur C, Nylander E. Long-term follow-up in arrhythmogenic right ventricular cardiomyopathy using tissue Doppler imaging. *Scand Cardiovasc J.* 2008;42(6):368-374.
25. Saguner AM, Vecchiati A, Baldinger SH, et al. Different Prognostic Value of Functional Right Ventricular Parameters in Arrhythmogenic Right Ventricular Cardiomyopathy/Dysplasia. *Circ Cardiovasc Imaging.* 2014.
26. Piccini JP, Nasir K, Bomma C, et al. Electrocardiographic findings over time in arrhythmogenic right ventricular dysplasia/cardiomyopathy. *Am J Cardiol.* 2005;96(1):122-126.
27. Jaoude SA, Leclercq JF, Coumel P. Progressive ECG changes in arrhythmogenic right ventricular disease. Evidence for an evolving disease. *Eur Heart J.* 1996;17(11):1717-1722.
28. Saguner AM, Ganahl S, Kraus A, et al. Electrocardiographic features of disease progression in arrhythmogenic right ventricular cardiomyopathy/dysplasia. *BMC Cardiovasc Disord.* 2015;15:4.
29. Folino AF, Bauce B, Frigo G, Nava A. Long-term follow-up of the signal-averaged ECG in arrhythmogenic right ventricular cardiomyopathy: correlation with arrhythmic events and echocardiographic findings. *Europace.* 2006;8(6):423-429.
30. Lemola K, Brunckhorst C, Helfenstein U, Oechslin E, Jenni R, Duru F. Predictors of adverse outcome in patients with arrhythmogenic right ventricular dysplasia/cardiomyopathy: long term experience of a tertiary care centre. *Heart.* 2005;91(9):1167-1172.
31. Asimaki A, Tandri H, Duffy ER, et al. Altered desmosomal proteins in granulomatous myocarditis and potential pathogenic links to arrhythmogenic right ventricular cardiomyopathy. *Circ Arrhythm Electrophysiol.* 2011;4(5):743-752.
32. Te Riele ASJM, James CA, Sawant AC, et al. Arrhythmogenic Right Ventricular Dysplasia/Cardiomyopathy in the Pediatric PopulationClinical Characterization and Comparison With Adult-Onset Disease. *JACC: Clinical Electrophysiology.* 2015;1(6):551-560.
33. Bhonsale A, Te Riele AS, Sawant AC, et al. Clinical Presentation, Cardiac Phenotype and Long Term Prognosis of Patients With Late Onset Arrhythmogenic Right Ventricular Dysplasia/Cardiomyopathy *Abstracts - American Heart Association 2015 - Arrhythmias and Electrophysiology Session Title: Arrhythmias and Electrophysiology VI* 2015.
34. Lipshultz SE, Orav EJ, Wilkinson JD, et al. Risk stratification at diagnosis for children with hypertrophic cardiomyopathy: an analysis of data from the Pediatric Cardiomyopathy Registry. *Lancet.* 2013;382(9908):1889-1897.

SUPPLEMENTARY FILES

Supplementary Table 1. Electrocardiographic and arrhythmic definitions:

Epsilon wave	Distinct waves of small amplitude within the ST segment in the right precordial leads and are distinct from the QRS complex.
Terminal activation duration	The longest value in V_1–V_3, from the nadir of the S wave to the end of all depolarization deflections. Considered abnormal when ≥55 msec.
Right bundle branch block	QRSd ≥0.12 s, secondary R wave in right precordial leads, and wide S wave in leads I and V_6.
Sustained ventricular tachycardia	Ventricular tachycardia which lasts 30 seconds or more, or less than 30 s when terminated electrically or pharmacologically

Supplementary Table 2. Overview of mutations represented in the study population

Gene	Nucleotide change	Protein change	Probands (N=)	Family Members N=	Total
PKP2 (44)	c. 1211-1212insT	p. Val406SerfsX4	3	4	7
	c. 1307_1315delins8	p. Leu436HisfsX11	1	0	1
	c. 1369_1372delCAAA	p. Gln457X	1	1	2
	c. 148_151delACAG	p. Thr50SerfsX61	3	0	3
	c. 1613G>A	p. Trp538X	1	0	1
	c. 1643delG	p. Gly548ValfsX15	0	1	1
	c. 1848C>A	p. Tyr616X	1	0	1
	c. 2013delC	p. Lys672ArgfsX12	1	1	2
	c. 2146-1G>C	Abnormal splice product	3	2	5
	c. 2197_2202delinsG	p. His733AlafsX8	0	1	1
	c. 235C>T	p. Arg79X	1	3	4
	c. 2386T>C	p. Cys796Arg	3	2	5
	c. 2489+4A>C	Abnormal splice product	3	1	4
	c. 397C>T	p. Gln133X	1	2	3
	c. 917-918delCC	p. Pro318GlnfsX29	0	1	1
	deletion exon 1-14		1	1	2
	deletion exon 1-4		1	0	1
***DSG2* (3)**	c. 137G>A	p. Arg46Gln	1	0	1
	c. 874C>T	p. Arg292Cys	1	0	1
	c. 918 G->A,146 G->A *	W306X, R49H	1	0	1
DSC2 (1)	c. 608G>A	p. Arg203His	1	0	1
***DSP* (2)**	c.1060_1061delCT	p.Leu354AlafsX15	1	0	1
	c. 1264G>A	p. Glu 422Lys	1	0	1
***PLN* (14)**	**c.** 40_42delAGA	R14del	**14**	**0**	**14**

* = 1 proband was found to be digenic heterozygote. *PKP2* = plakophilin 2, *DSP* = desmoplakin, *DSG2* = desmoglein 2, *DSC2* = desmocollin 2

CHAPTER 8

Implementation of Echocardiographic Deformation Imaging for Optimal Assessment of Structural Disease Progression in Early ARVC

Thomas P Mast, Maarten J Cramer, Jeroen F van der Heijden,
Pieter A Doevendans, Arco J Tekse

Submitted

ABSTRACT

Introduction: Arrhythmogenic right ventricular cardiomyopathy (ARVC) is an inherited cardiomyopathy characterized by both electrical and structural abnormalities. Remarkably, structural disease progression (RV dilatation and dysfunction) is uncommon during the early disease stages while progression of electrical abnormalities is frequently seen. We hypothesize that current imaging techniques lack the sensitivity to detect subtle functional abnormalities. Echocardiographic deformation imaging might bridge the gap between electrical progression and the apparent lack of structural progression in early ARVC.

Methods/Results: Eighty-four subjects underwent serial evaluation (mean follow-up: 4.3±2.4 years) including electrocardiography (ECG), Holter-monitoring, and cardiac imaging (including RV deformation imaging) according to Task Force diagnostic criteria (TFC). At first evaluation, 50 patients fulfilled TFC for definite diagnosis (64% probands, 84% mutation carrier), and 34 first-degree relatives (74% mutation carrier) not fulfilling diagnostic TFC without diagnosis (early ARVC). In definite ARVC patients, conventional measurements showed signs of structural disease progression: RV outflow tract dimension: from 17.6±3.3 mm/m^2 to 18.8±4.9 mm/m^2 (P=.049), RV peak velocity: from 9.5±2.2cm/s to 9.0±2.6cm/s (P=.011), and left ventricular ejection fraction from 54.9±8.9% to 50.9±8.9% (P=.001) Deformation imaging detected additional increasing mechanical dysfunction in all RV segments. In early ARVC, all conventional structural parameters were comparable between baseline and follow-up, while deformation imaging showed signs of progressive RV mechanical dysfunction: post-systolic index increased, basal: from 22 [42] to 30 [80] (P=.049), and increased duration to onset shortening, mid: from: 61 [52] to 77 [80] (P=.004).

Conclusion: Echocardiographic deformation imaging reveals progressive local RV mechanical dysfunction during the early stages of ARVC. While conventional imaging approaches do detect global structural progression in definite ARVC patients, these techniques seem to lack the sensitivity to detect local signs of structural disease progression in early ARVC. Deformation imaging resolves the apparent discrepancy between the rate of electrical progression and structural progression in early ARVC.

INTRODUCTION

Arrhythmogenic right ventricular cardiomyopathy (ARVC) is an inherited cardiomyopathy clinically characterized by ventricular arrhythmias and predominantly right ventricular (RV) dysfunction.[1] This condition is histopathological characterized by fibro-fatty replacement of the myocardium, which results in detectable electrical and structural abnormalities during cardiac evaluation.[2] Family members are at risk of developing ARVC due to the familial and genetic character of this disease, and for that reason serial cardiac evaluation is advised.[3-5] Recently, several large studies were conducted to optimize ARVC family screening protocols resulting in improved knowledge of how ARVC develops during the early disease stages.[6-10] These studies found that structural disease progression seems uncommon compared to electrical progression in early ARVC.[6-10]

It is currently unclear why this discrepancy exists between electrical disease progression and structural disease progression in early ARVC. Current conventional imaging diagnostic approaches, as mentioned in the Task Force criteria (TFC), might not be able to detect the occurrence of subtle abnormalities and might suffer from low sensitivity.[3] This might be the main explanation that structural progression is rarely seen in early ARVC.[3,11] This is supported by a recent study which showed that local mechanical dysfunction detected by echocardiographic RV deformation imaging is already present in absence of established structural disease criteria.[12] This technique might bridge the gap between the rate of structural progression and electrical progression in early ARVC.

Accurate assessment of structural disease progression might be clinical important for risk stratification.[5,10] We aimed to investigate whether echocardiographic RV deformation imaging is able to detect progressive RV mechanical dysfunction as expression of structural disease progression during the early ARVC stages.

METHODS

Study population

This study was conducted between 2006-2016 in the University Medical Center Utrecht in The Netherlands and was approved by the local institutional ethics review board. During this period, 161 subjects underwent echocardiography including RV deformation imaging as part of their clinical work-up for ARVC. This included known definite ARVC patients during their clinical follow-up, and family members that underwent diagnostic cardiac evaluation for ARVC. A total of 84 subjects (age≥18 years) underwent a second cardiac evaluation including RV deformation imaging, this cohort comprised our study population (**Figure 1**).

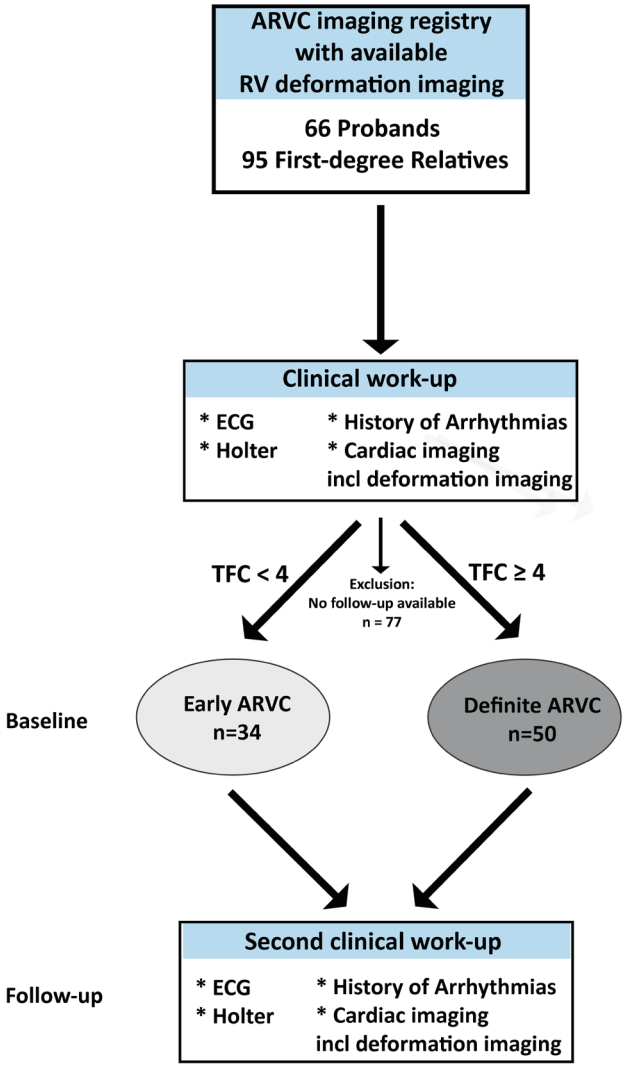

Figure 1. Study design
Abbreviations: ARVC = arrhythmogenic right ventricular cardiomyopathy; RV = right ventricle; ECG = electrocardiography; TFC = task force criteria

Standard serial evaluation

All subjects underwent diagnostic clinical work-up according to the 2010 Task Force criteria at baseline and follow-up.[3] Standard 12-lead electrocardiography (ECG) was performed to detect repolarization abnormalities (precordial T-wave inversions) and depolarization abnormalities (epsilon waves and terminal activation duration (TAD) >55ms in right precordial leads (V_1-V_3).[3] For definitions of ECG parameters, see *supplementary table 1.* Holter monitoring

was performed for premature ventricular complexes (PVC) count per 24 hours and (non-) sustained ventricular tachycardia.[3] History of (non)-sustained ventricular arrhythmias with left bundle branch block morphology were taken into account as described in the TFC.[3] Cardiac imaging was performed by both echocardiography and cardiac magnetic resonance (CMR) according to previously published protocols.[13,14] Echocardiographic exams were analyzed for RV regional wall motion abnormalities (akinesia, dyskinesia, and aneurysm). RV outflow tract (RVOT) dimension was measured in the parasternal long- and short axis view (PLAX/PSAX), and RV systolic function was assessed by RV fractional area change (RV-FAC) as mentioned in the TFC.[3,13] In addition, RV systolic function was also assessed by RV systolic peak annular velocity (S') and tricuspid annular plane systolic excursion (TAPSE),[13,15] LV systolic function by LV ejection fraction (LVEF) by Simpson biplane method.[16] CMR studies were analyzed for fulfillment of TFC defined as RV regional wall motion abnormalities (akinesia, dyskinesia, and aneurysm) combined with RV dilatation by RV end-diastolic volume (RV-EDV) and RV systolic function by RV ejection fraction (RVEF).[3] Late gadolinium (LGE) was used to detect areas with late enhancement to assess myocardial fibrosis.[14]

Echocardiographic deformation imaging

All subjects underwent echocardiographic RV deformation imaging in addition to standard clinical work-up at baseline and follow-up. We previously published our protocol regarding echocardiographic image acquisition and post-processing to perform 2D-speckle tracking.[17] In brief, narrow-focused 2D images of the RV free wall were acquired with Vivid 7 or Vivid E9 (General Electric, Milwaukee, MN). Sector width was adjusted to optimize the frame rate, frame rates between 55-110 fps were allowed for post processing. Off-line analysis was performed by commercially available software: EchoPAC PC version 12, GE Vingmed Ultrasound AS. After manual tracking of the RV free wall, the software automatically divides the RV free wall into three segments: basal, mid, and apical regions. RV outflow tract spectral Doppler signal was used for timing of the pulmonary valve opening and closure (PVO/PVC). The following deformation parameters were analyzed: time to onset shortening,[12,18] systolic peak strain value,[12,19,20] and post-systolic index.[12,21] For definitions of the deformation imaging parameters used in this study, see *supplementary figure 1***.** All deformation analyses were performed blinded for clinical data.

Assessment of structural disease progression

Structural disease progression was assessed by comparing both conventional echocardiographic measurements and deformation imaging derived parameters between baseline and follow-up. Analysis for structural disease progression was performed separately for two groups: 1) *definite ARVC patients*: subjects fulfilling TFC for definite diagnosis (TFC≥4) at baseline and, 2) *early ARVC*: subjects without fulfilling diagnostic criteria (TFC<4) at baseline. (**Figure 1**)

R1 R2 R3 R4 R5 R6 R7 R8 R9 R10 R11 R12 R13 R14 R15 R16 R17 R18 R19 R20 R21 R22 R23 R24 R25 R26 R27 R28 R29 R30 R31 R32 R33 R34 R35 R36 R37 R38 R39

Statistical analysis

Differentiation between normally and non-normally distributed data was assessed by the Shapiro-Wilk test. Continuous data were presented as mean ± standard deviation (SD) in case of normally distributed data, or median [inter-quartile range] in case of non-normally distributed data. Categorical variables were presented as numbers (percentages), n/N (%). Comparison of continuous data between groups was performed by independent Student's *t*-test or Mann-Whitney-U test, and categorical data were compared by the Fisher-exact test. The paired Student's *t*-test or Wilcoxon Signed rank test was used to evaluate differences in continuous variables between baseline and last follow-up. McNemar's test without Yates' correction for continuity was used for paired proportional data. A P-value < 0.05 was considered significant. All calculations were performed by a commercially available software package: IBM SPSS Statistics for Windows, Version 21.0.

RESULTS

Study population at first evaluation

The final study population consisted of 84 subjects and baseline characteristics are shown **Table 1**. At baseline evaluation, 50 subjects fulfilled ARVC diagnosis after clinical work-up, 32 (64%), probands and 33 (66%) males. The remaining 34 early ARVC subjects were first-degree relatives not fulfilling ARVC diagnosis (15 (44%) males). Patients with definite ARVC were significantly older compared to the early ARVC subjects, 46.6±15.3 year vs. 28.4±14.1 years (P<.001)

Definite ARVC patients showed more signs of ARVC phenotypic expression by TFC compared to early ARVC subjects. RV end-diastolic dimension was significantly enlarged in this group, RV-EDV: 125.1±36.6 ml/m^2 versus 96.8±9.5 ml/m^2 (P<.001). RV systolic function was significantly reduced, RVEF 38.4±9.6 % vs. 53.4±6.7 % (P<.001), and RV-FAC: 33.8±8.6 % vs 45.4±5.8 % (P<.001). Other conventional quantitative measurements specified for definite ARVC patients and early ARVC subjects are provided in **Table 1**.

During first evaluation, deformation imaging derived parameters differed between definite ARVC patients and early ARVC subjects (**Table 1**). Marked differences were seen in the RV basal and RV mid area, the mean systolic peak strain in the RV basal area was half the value in definite ARVC patients compared to early ARVC: -10.6±8.4 % vs. -21.1±6.5%, (P<.001). In this region we also observed more post-systolic shortening: 22 [42] % vs. 1 [13] (P<.001), and longer duration of time to onset shortening: 139 [121] ms vs. 92 [83] ms (P=.002). In the RV apical region, systolic peak strain was lower compared to early ARVC, other deformation imaging parameters were comparable. For comparison of the conventional and deformation imaging derived quantitative parameters between our study population and healthy controls, normal values are provided in *Supplementary Table 2*.

Table 1. Clinical characteristics at baseline evaluation

	Definite ARVC (N=50)	Early ARVC (N=34)	P-Value
Age	46.6±15.3	28.4±4.1	<.001
Probands	32 (64)	0 (0)	<.001
Males	33 (66)	15 (44)	.072
Pathogenic mutation: *PKP2/DSG2/PLN*	29/3/10 (58/6/20)	19/3/3 (56/9/9)	.396
Follow-up duration (y)	4.7 ± 2.5	3.8±2.2	.111
ICD	24 (48)	0 (0)	<.001
Task Force Criteria (major or minor)			
Structural TFC	42 (84)	0 (0)	<.001
Depolarization TFC	35 (70)	7 (21)	<.001
Repolarization TFC	40 (80)	0 (0)	<.001
Arrhythmic TFC	47 (94)	3 (9)	<.001
Family TFC	37 (74)	34 (100)	.001
CMR			
RV wall motion abnormality	30/40 (75)	1 (3)	<.001
RV-EDV (ml/m^2)	125.1 ± 36.6	96.8 ± 9.5	<.001
RVEF (%)	38.4 ± 9.6	53.4 ± 6.7	<.001
LVEF (%)	53.9 ± 11.9	57.3 ± 6.3	.174
LGE	22/40 (55)	0 (0)	<.001
Echocardiography			
RV wall motion abnormality	45 (90)	1 (3)	
RVOT-PLAX (mm/m^2)	17.6 ± 3.3	14.8 ± 2.5	<.001
RVOT-PSAX (mm/m^2)	18.4 ± 3.2	15.7 ± 2.8	<.001
RV-FAC (%)	33.8 ± 8.6	45.4 ± 5.8	<.001
TAPSE (mm)	18.2 ± 3.7	22.9 ± 2.9	<.001
RV peak annular velocity (S') (cm/s)	9.5 ± 2.2	12.9 ± 2.1	<.001
LVEF (%)	54.9 ± 8.9	58.7 ± 5.6	.025
Echocardiographic deformation imaging			
RV basal			
Time to onset shortening (ms)	139 [121]	92 [83]	.002
Systolic peak strain (%)	-10.6 ± 8.4	-21.1 ± 6.5	<.001
Post-systolic index (%)	22 [42]	1 [13]	<.001
RV mid			
Time to onset shortening (ms)	61 [52]	40 [39]	.023
Systolic peak strain (%)	-17.1 ± 6.5	-26.7 ± 6.4	<.001
Post-systolic index (%)	3 [11]	0 [3]	.001
RV apex			
Time to onset shortening (ms)	40 [48]	38 [37]	.174
Systolic peak strain (%)	-21.7 ± 6.5	-29.3 ± 5.4	<.001
Post-systolic index (%)	0 [3]	0 [1]	.238

Values are presented as n/N (%), mean ± standard deviations, or median [inter-quartile ranges]. * CMR was limited available in definite ARVC patients (40 at baseline, 8 at follow-up). *Abbreviations*: ARVC = arrhythmogenic right ventricular cardiomyopathy; RV = right ventricle; LV = left ventricle; EF = ejection fraction; *PKP2* = Plakophillin-2; *DSG2* = Desmoglein-2; *PLN* = Phospholamban; ICD = implantable cardioverter defibrillator; CMR = cardiac magnetic resonance imaging; LGE = late gadolinium enhancement; EDV = end-diastolic volume; RVOT = right ventricular outflow tract; PSAX/PLAX = parasternal short/long axis view; FAC = fractional area change; TAPSE = tricuspid annular plane systolic excursion

R1 R2 R3 R4 R5 R6 R7 R8 R9 R10 R11 R12 R13 R14 R15 R16 R17 R18 R19 R20 R21 R22 R23 R24 R25 R26 R27 R28 R29 R30 R31 R32 R33 R34 R35 R36 R37 R38 R39

Structural disease progression by conventional imaging

Patients that fulfilled definite ARVC diagnosis during first evaluation underwent a second evaluation after a mean follow up duration of 4.7±2.5 years (**Table 2**). Mean RVOT dimension measured in the PLAX view increased over time, 17.6±3.3 mm/m^2 to 18.8±4.9 mm/m^2 (P=.049). Mean RV systolic function measurements decreased during follow-up, which reached significance for RV peak annular velocity, 9.5±2.2 cm/s to 9.0±2.6 cm/s (P=.011). A significant decrease in LV systolic function was seen, LVEF decreased from 54.9±8.9 % to 50.9±8.9 %, (P=.001).

Table 2. Disease progression by fulfillment of Task Force criteria and conventional imaging

	Definite ARVC (n=50)		**P-value**	**Early ARVC (n=34)**		**P-value**
	Baseline	**Follow-up**		**Baseline**	**Follow-up**	
Age (y)	46.6 ± 15.3	51.2 ± 16.2	<.001	28.4 ± 14.1	32.1 ± 14.8	<.001
ICD	24 (48)	40 (80)	<.001	0 (0)	3 (9)	.248
Task Force Criteria						
Structural TFC	42 (84)	44 (88)	.157	0 (0)	3 (9)	.083
Depolarization TFC	35 (70)	39 (78)	.046	7 (21)	11(32)	.046
Repolarization TFC	40 (80)	40 (80)	NS	0 (0)	3 (9)	.083
Arrhythmic TFC	47 (94)	47 (94)	NS	3 (9)	9 (26)	.014
CMR*						
RV wall motion abnormality	30/40 (75)	NA	-	1 (3)	4 (12)	.083
RV-EDV (ml/m^2)	125.1 ± 36.6	NA	-	100.2 ± 7.9	100.5 ± 11.4	.909
RVEF (%)	38.4 ± 9.6	NA	-	52.1 ± 6.0	54.5±6.3	.224
LVEF (%)	53.9 ± 11.9	NA	-	58.0 ± 5.9	56.4 ± 3.9	.236
LGE	22/40 (55)	NA	-	0 (0)	1 (3)	1.00
Echocardiography						
RV wall motion abnormality	45 (90)	45 (90)	NS	1 (3)	3 (9)	.157
RVOT-PLAX (mm/m^2)	17.6 ± 3.3	18.8 ± 4.9	.049	14.8 ± 2.5	15.0 ± 2.4	.574
RVOT-PSAX (mm/m^2)	18.4 ± 3.2	18.8 ± 4.7	.644	15.7 ± 2.8	15.7 ± 2.4	.745
RV-FAC (%)	33.8 ± 8.6	32.0 ± 9.3	.247	45.4 ± 5.8	47.4 ± 5.9	.162
TAPSE (mm)	18.2 ± 3.7	17.6 ± 4.5	.376	22.9 ± 2.9	22.6 ± 2.9	.596
RV peak velocity (cm/s)	9.5 ± 2.2	9.0 ± 2.6	.011	12.9 ± 2.1	12.4 ± 1.7	.225
LVEF (%)	54.9 ± 8.9	50.9 ± 8.9	.001	58.7 ± 5.6	57.8 ± 4.8	.313

Values are presented as n/N (%), mean ± standard deviations, or median [inter-quartile ranges]. * CMR was limited available in definite ARVC patients (40 at baseline, 8 at follow-up). *Abbreviations:* ARVC = arrhythmogenic right ventricular cardiomyopathy; RV = right ventricle; LV = left ventricle; EF = ejection fraction; ICD = implantable cardioverter defibrillator; CMR = cardiac magnetic resonance imaging; LGE = late gadolinium enhancement; EDV = end-diastolic volume; RVOT = right ventricular outflow tract; PSAX/PLAX = parasternal short/long axis view; FAC = fractional area change; TAPSE = tricuspid annular plane systolic excursion; NA = not available

Early ARVC subjects underwent a second evaluation after 3.8±2.2 year. Disease progression by fulfillment of TFC was found in 9 subjects (26%), all showing signs of electrical disease progression (new fulfillment of depolarization, repolarization, or arrhythmic TFC which was absent at baseline). Three subjects (9%) showed structural progression by fulfillment of structural TFC on top of electrical progression (**Table 2**). All mean values of RV dimension and RV systolic function measured by conventional echocardiography and CMR were found to be comparable at second evaluation with respect to baseline values. LVEF, as indicator of LV systolic function, was also comparable between baseline and follow-up.

Structural disease progression by echocardiographic RV deformation imaging

Table 3 provides an overview of the changes in deformation imaging parameters during follow-up. In definite ARVC patients, we observed increased RV mechanical dysfunction in the basal segment. In this segment, systolic peak strain significantly decreased from-10.6±8.4 % to -7.7±7.8 % (P<.001), and the post-systolic index increased from 22 [42] to 30 [80] (P=.026). In the RV mid segment, systolic peak strain significantly decreased from-17.1 ±6.5 % to -14.1±7.8 % (P<.001), and time to onset shortening increased from 61 [52] ms to 77 [80] ms (P=.004). In the apical segment, the systolic peak strain significantly decreased from -22.2±5.9 % to -20.7±6.7 % (P<.001) and time to onset shortening increased from 40 [48] ms to 48 [65] ms (P=.012). **Figure 2** shows a typical example of structural progression by RV deformation imaging in a definite ARVC patient.

Table 3. Disease progression by deformation imaging

	Early ARVC (n=34)		P-value	Definite ARVC (n=50)		P-value
Basal						
Time to onset (ms)	92 [83]	96 [72]	.985	139 [121]	169 [115]	.066
Systolic peak strain (%)	-21.1±6.5	-20.4±6.4	.410	-10.6 ± 8.4	-7.7 ± 7.8	<.001
Post-systolic index (%)	1 [13]	8 [14]	.049	22 [42]	30 [80]	.026
Mid						
Time to onset (ms)	40 [39]	55 [38]	.004	61 [52]	77 [80]	.004
Systolic peak strain (%)	-26.7±6.4	-25.5±5.7	.228	-17.1 ± 6.5	-14.1 ± 7.8	<.001
Post-systolic index (%)	0 [3]	0 [1]	.338	3 [11]	4 [17]	.286
Apex						
Time to onset (ms)	38 [37]	40 [32]	.179	40 [48]	48 [65]	.012
Systolic peak strain (%)	-29.3±5.4	-28.6±5.6	.288	-22.2 ± 6.5	-20.7±6.7	<.001
Post-systolic index (%)	0 [1]	0 [1]	.987	0 [3]	0 [2]	.827

Abbreviations: ARVC = arrhythmogenic right ventricular cardiomyopathy;

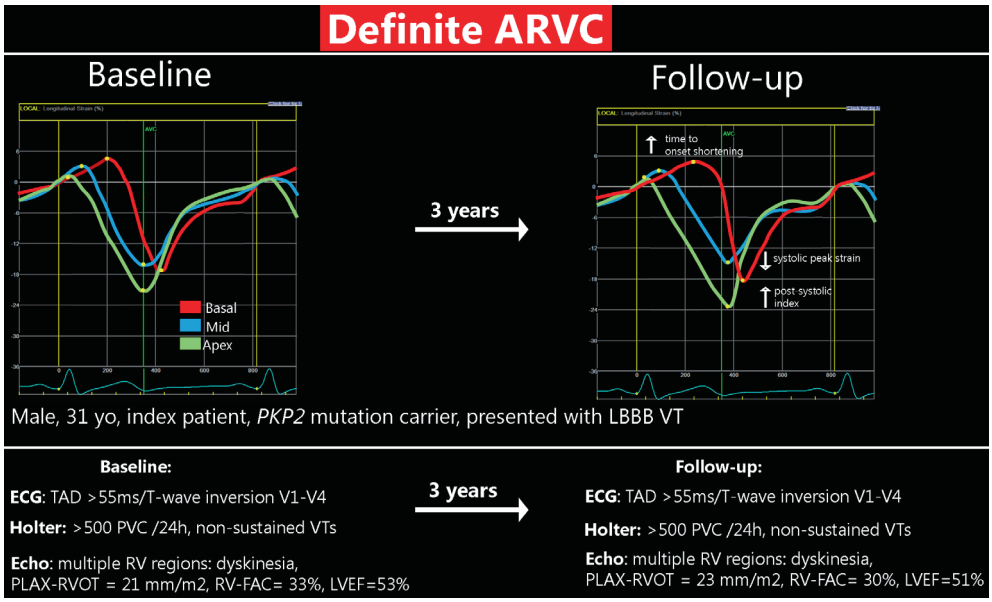

Figure 2. Structural progression by RV deformation imaging in definite ARVC
Upper left: RV deformation imaging results at baseline which showed abnormal deformation in the basal area: prolonged time to onset shortening, reduced systolic peak strain, and post-systolic shortening. The mid area shows only prolonged onset of shortening. *Upper right:* RV deformation imaging results at follow-up which showed signs of increased mechanical dysfunction in the RV basal area. *Lower left:* results from evaluation at baseline according to Task Force criteria (TFC). *Lower right:* results from evaluation according to TFC. *Abbreviations*: ARVC = arrhythmogenic right ventricular cardiomyopathy; RV = right ventricle; LV = left ventricle; EF = ejection fraction; *PKP2* = Plakophillin-2; RVOT = right ventricular outflow tract; PSAX/PLAX = parasternal short/long axis view; FAC = fractional area change

In early ARVC, echocardiographic deformation imaging was able to show differences in local mechanical function between first evaluation and second evaluation. In the basal segment, we observed an increase in post-systolic index from 1% [13] at baseline to 8% [14] at follow-up (P=.049). In the mid segment, time to onset shortening significantly increased from 44 [39] ms to 55 [38] ms (P=.004). In the apical segment, all deformation parameters were found comparable between baseline and follow-up. **Figure 3** shows an example of structural disease progression by RV deformation imaging in an early ARVC subject.

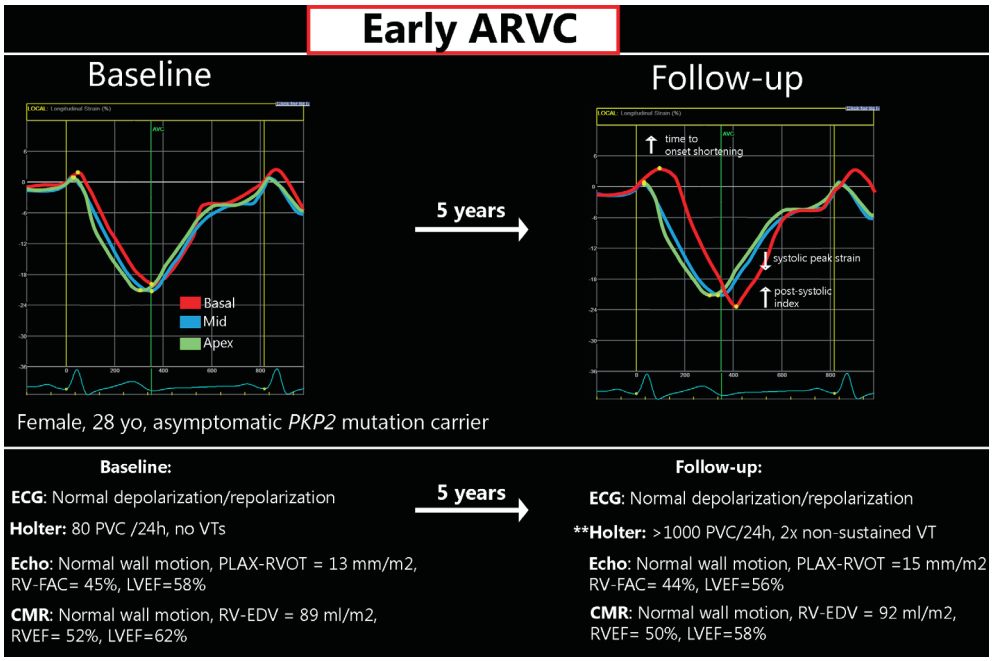

Figure 3. Structural progression by RV deformation imaging in early ARVC
Upper left: RV deformation imaging results at baseline which showed normal deformation in all segments. *Upper right:* RV deformation imaging results at follow-up which showed signs of increased mechanical dysfunction in the RV basal area. *Lower left:* results from evaluation at baseline according to Task Force criteria (TFC). *Lower right:* results from evaluation according to TFC. *Abbreviations*: ARVC = arrhythmogenic right ventricular cardiomyopathy; RV = right ventricle; LV = left ventricle; EF = ejection fraction; *PKP2* = Plakophillin-2; CMR = cardiac magnetic resonance imaging; PVC = premature ventricular complexes; RVOT = right ventricular outflow tract; PSAX/PLAX = parasternal short/long axis view; FAC = fractional area change; ** Holter monitoring showed >500 PVCs/24h which fulfilled a new minor arrhythmic Task force criteria

DISCUSSION

Up till now, several studies showed that structural disease progression is uncommon compared to electrical disease progression in early ARVC. However, these studies only used conventional imaging approaches according to the TFC to assess structural disease progression.[6-8,10] This is the first longitudinal study that includes repeated echocardiographic deformation imaging measurements to assess structural progression in ARVC. The main finding of the present study is that echocardiographic deformation imaging reveals progressive RV mechanical dysfunction in early ARVC subjects in the absence of structural progression based on conventional imaging approaches. These techniques seems to be unable to monitor the often subtle changes in structural disease during the early stages. Therefore, echocardiographic

deformation imaging might resolves the apparent discrepancy between the rate of electrical progression and structural progression as observed in early ARVC.

Structural and Electrical disease in ARVC

ARVC is characterized by progressive replacements of the RV myocardium by fibro-fatty tissue.[1,2] This histopathological substrate leads to both electrical abnormalities as well as structural abnormalities which will be detectable by different diagnostic modalities as the disease progresses.[3] Fibro-fatty tissue replacements of healthy myocardium results in structural alterations that will eventually lead to abnormal RV wall motion, global RV systolic dysfunction, and RV dilatation. Conventional imaging techniques, such as standard 2D-echocardiography and CMR are able to visualize structural RV abnormalities.[20,22] In addition, a valuable application of CMR is the characterization of tissue which enables the detection of fat and fibrosis in the RV.[22,23] Electrical abnormalities have their origin by the interference of the histopathological abnormalities on electrical myocardial conduction, seen as depolarization abnormalities on the ECG.[24] These alterations also lead to reentrant circuits which is a cause of the ventricular arrhythmias seen in ARVC.[25] The broad variety of diagnostic modalities in ARVC all aim to detect the same characteristic histopathological substrate, by measuring electrical expressions of the substrate, or by visualizing the structural alterations itself.[2] Therefore, it is debatable to what extent the imbalance between structural progression and electrical progression in early ARVC, as observed in previous studies, is actually based on a pathophysiological process and not a lack of sensitivity of our current imaging techniques.[6,7,10]

Disease progression by TFC

In contrast to the numerous studies with focus on defining the genetic basis of ARVC as well as optimizing arrhythmic risk stratification, only a few studies have focused on structural disease progression itself.[26-29] Nevertheless, ARVC is generally considered as a progressive disease, notable by the fact that symptoms are usually not present during early childhood, and heart failure occurs in end-stages of the disease.[4] The few previous studies available showed that both electrical and structural abnormalities may increase during follow-up in definite ARVC patients.[26-29] On the other hand, early ARVC is characterized by hardly any structural progression while electrical disease progression is much more common.[6,7,10] It is important to notice that these studies defined disease progression by the development of a new TFC, possibly neglecting subtle changes in functional/mechanical abnormalities. In the present study, we confirmed the finding that the development of electrical TFC is much more common compared to structural disease progression by TFC in early ARVC subjects. In the present study, approximately a quarter of the early ARVC subjects showed signs of electrical disease progression, compared to the 9% of the subjects showing structural disease progression.

RV deformation imaging detects extensive structural disease progression in definite ARVC

In the present study, we were able to show that definite ARVC patients underwent progressive contractile dysfunction, as an expression of disease progression, in all RV segments measured by deformation imaging. A decline in myocardial function is detected as a decrease in systolic peak strain, an increase in post-systolic index, and an increase in time to onset shortening. In a recent study, we showed that these abnormal deformation characteristics are most likely the result of an underlying mechanical substrate consisting of hypocontractility (myocardial cell loss) and increased passive wall stiffness (replacement fibrosis), and not solely due to electrical abnormalities.[12] This supports our idea that the increasing mechanical dysfunction as observed in this study is an expression structural disease expression. Due to the increasing amount of this pathological substrate in a considerable larger part of the RV free wall (with a gradient from base to apex), we also observed a decline in global systolic function by conventional structural parameters.

RV deformation imaging detects local structural disease progression in early ARVC

The most interesting finding in our study is that echocardiographic deformation imaging is capable of unmasking local structural disease progression in early ARVC subjects. A major advantage of echocardiographic deformation imaging is the ability to measure local quantitative myocardial function instead of the conventional measurements of global myocardial function.[17,20] This is important in ARVC which is known to show a high degree of regional heterogeneity in disease expressivity.[1,2,30] The subtricuspid area seems to act as a hotspot region where the first sign of disease often appears.[12,21,30] Previous studies, including several performed at our center, showed that echocardiographic deformation imaging is capable to quantify local mechanical dysfunction in this specific area, even in absence of abnormalities detected by conventional imaging.[12,18,21,31,32] In the present study we showed that post-systolic shortening increases in the subtricuspid area during follow-up as well as the time to onset shortening in the RV mid segment. Therefore, our results suggest the presence of common structural disease progression in early ARVC, abnormalities become more pronounced in the subtricuspid region and seem to spread towards the apex during follow up. Conventional techniques were unable to show structural progression in early ARVC subjects. Apparently, the increasing local structural abnormalities do not (yet) give rise to a measurable global structural dysfunction by conventional imaging techniques. The current results extends our previous findings that echocardiographic RV deformation imaging is capable to detect local mechanical dysfunction prior to conventional imaging approaches.[12,18,21,31] The optimal assessment of structural disease progression by this technique could be of important clinical value. The presence of structural disease is known to be associated with arrhythmic outcome in early ARVC.[5,7,10] Therefore, the assessment of the rate of structural progression by deformation imaging could be of importance in risk stratification and optimizing family

R1 R2 R3 R4 R5 R6 R7 R8 R9 R10 R11 R12 R13 R14 R15 R16 R17 R18 R19 R20 R21 R22 R23 R24 R25 R26 R27 R28 R29 R30 R31 R32 R33 R34 R35 R36 R37 R38 R39

screening interval. Finally, this technique could be used to identify modifiers of structural disease and determine the effectiveness of future therapeutic interventions.

Limitations

This study was designed to determine if echocardiographic deformation imaging is capable to detect progressive functional abnormalities during the early ARVC stages. Although our results are promising, we were unable to determine the association between progressive deformation abnormalities and electrical disease progression due to the small size of this study. The presence of extensive structural abnormalities are known to be important for risk stratification in ARVC.[5,10,28] However, it is currently unclear whether subjects showing structural disease progression by deformation imaging are at increased arrhythmic risk, and this should be the focus of future studies.

Conclusion

Echocardiographic deformation imaging reveals structural disease progression not only in ARVC patients, but also in early ARVC. The progression of these regional disease abnormalities are not detected by conventional imaging approaches. Echocardiographic deformation imaging improves the ability of non-invasive imaging to detect subtle functional abnormalities. Our results challenges the existence of the gap between common electrical disease progression and uncommon structural progression in early ARVC. During serial evaluation of ARVC patients and their relatives this technique seems a valuable tool to track structural disease progression. The prognostic implications of worsening of deformation parameters in this specific cohort remains to be investigated.

REFERENCES

1. Marcus FI, Fontaine GH, Guiraudon G, et al. Right ventricular dysplasia: a report of 24 adult cases. *Circulation.* 1982;65(2):384-398.
2. Basso C, Corrado D, Marcus FI, Nava A, Thiene G. Arrhythmogenic right ventricular cardiomyopathy. *Lancet.* 2009;373(9671):1289-1300.
3. Marcus FI, McKenna WJ, Sherrill D, et al. Diagnosis of arrhythmogenic right ventricular cardiomyopathy/dysplasia: proposed modification of the task force criteria. *Circulation.* 2010;121(13):1533-1541.
4. Groeneweg JA, Bhonsale A, James CA, et al. Clinical Presentation, Long-Term Follow-Up, and Outcomes of 1001 Arrhythmogenic Right Ventricular Dysplasia/Cardiomyopathy Patients and Family Members. *Circ Cardiovasc Genet.* 2015;8(3):437-446.
5. Corrado D, Wichter T, Link MS, et al. Treatment of Arrhythmogenic Right Ventricular Cardiomyopathy/Dysplasia: An International Task Force Consensus Statement. *Circulation.* 2015;132(5):441-453.
6. te Riele AS, James CA, Rastegar N, et al. Yield of serial evaluation in at-risk family members of patients with ARVD/C. *J Am Coll Cardiol.* 2014;64(3):293-301.
7. Te Riele AS, James CA, Groeneweg JA, et al. Approach to family screening in arrhythmogenic right ventricular dysplasia/cardiomyopathy. *Eur Heart J.* 2016;37(9):755-763.
8. Protonotarios N, Anastasakis A, Antoniades L, et al. Arrhythmogenic right ventricular cardiomyopathy/dysplasia on the basis of the revised diagnostic criteria in affected families with desmosomal mutations. *Eur Heart J.* 2011;32(9):1097-1104.
9. Gomes J, Finlay M, Ahmed AK, et al. Electrophysiological abnormalities precede overt structural changes in arrhythmogenic right ventricular cardiomyopathy due to mutations in desmoplakin-A combined murine and human study. *Eur Heart J.* 2012;33(15):1942-1953.
10. Te Riele AS, Bhonsale A, James CA, et al. Incremental value of cardiac magnetic resonance imaging in arrhythmic risk stratification of arrhythmogenic right ventricular dysplasia/cardiomyopathy-associated desmosomal mutation carriers. *J Am Coll Cardiol.* 2013;62(19):1761-1769.
11. Borgquist R, Haugaa KH, Gilljam T, et al. The diagnostic performance of imaging methods in ARVC using the 2010 Task Force criteria. *Eur Heart J Cardiovasc Imaging.* 2014;15(11):1219-1225.
12. Mast TP, Teske AJ, Walmsley J, et al. Right ventricular deformation imaging and computer simulation for electromechanical substrate characterization in arrhythmogenic right ventricular cardiomyopathy (ARVC). *J Am Coll Cardiol.* 2016 Nov 15;68(20):2185-2197.
13. Mast TP, Teske AJ, Doevendans PA, Cramer MJ. Current and future role of echocardiography in arrhythmogenic right ventricular dysplasia/cardiomyopathy. *Cardiol J.* 2015;22(4):362-374.
14. Te Riele AS, Tandri H, Bluemke DA. Arrhythmogenic right ventricular cardiomyopathy (ARVC): cardiovascular magnetic resonance update. *J Cardiovasc Magn Reson.* 2014;16:50.
15. Rudski LG, Lai WW, Afilalo J, et al. Guidelines for the echocardiographic assessment of the right heart in adults: a report from the American Society of Echocardiography endorsed by the European Association of Echocardiography, a registered branch of the European Society of Cardiology, and the Canadian Society of Echocardiography. *J Am Soc Echocardiogr.* 2010;23(7):685-713.
16. Lang RM, Badano LP, Mor-Avi V, et al. Recommendations for cardiac chamber quantification by echocardiography in adults: an update from the American Society of Echocardiography and the European Association of Cardiovascular Imaging. *J Am Soc Echocardiogr.* 2015;28(1):1-39 e14.
17. Teske AJ, De Boeck BW, Melman PG, Sieswerda GT, Doevendans PA, Cramer MJ. Echocardiographic quantification of myocardial function using tissue deformation imaging, a guide to image acquisition and analysis using tissue Doppler and speckle tracking. *Cardiovasc Ultrasound.* 2007;5:27.

18. Mast TP, Teske AJ, Te Riele AS, et al. Prolonged Electromechanical Interval Unmasks Arrhythmogenic Right Ventricular Dysplasia/Cardiomyopathy in the Subclinical Stage. *J Cardiovasc Electrophysiol.* 2016;27(3):303-314.
19. Prakasa KR, Wang J, Tandri H, et al. Utility of tissue Doppler and strain echocardiography in arrhythmogenic right ventricular dysplasia/cardiomyopathy. *Am J Cardiol.* 2007;100(3):507-512.
20. Teske AJ, Cox MG, De Boeck BW, Doevendans PA, Hauer RN, Cramer MJ. Echocardiographic tissue deformation imaging quantifies abnormal regional right ventricular function in arrhythmogenic right ventricular dysplasia/cardiomyopathy. *J Am Soc Echocardiogr.* 2009;22(8):920-927.
21. Teske AJ, Cox MG, Te Riele AS, et al. Early detection of regional functional abnormalities in asymptomatic ARVD/C gene carriers. *J Am Soc Echocardiogr.* 2012;25(9):997-1006.
22. Te Riele AS, Tandri H, Sanborn DM, Bluemke DA. Noninvasive Multimodality Imaging in ARVD/C. *JACC Cardiovasc Imaging.* 2015;8(5):597-611.
23. Tandri H, Friedrich MG, Calkins H, Bluemke DA. MRI of arrhythmogenic right ventricular cardiomyopathy/dysplasia. *J Cardiovasc Magn Reson.* 2004;6(2):557-563.
24. Tanawuttiwat T, Te Riele AS, Philips B, et al. Electroanatomic Correlates of Depolarization Abnormalities in Arrhythmogenic Right Ventricular Dysplasia/Cardiomyopathy. *J Cardiovasc Electrophysiol.* 2016;27(4):443-452.
25. Haqqani HM, Tschabrunn CM, Betensky BP, et al. Layered activation of epicardial scar in arrhythmogenic right ventricular dysplasia: possible substrate for confined epicardial circuits. *Circ Arrhythm Electrophysiol.* 2012;5(4):796-803.
26. Saguner AM, Ganahl S, Kraus A, et al. Electrocardiographic features of disease progression in arrhythmogenic right ventricular cardiomyopathy/dysplasia. *BMC Cardiovasc Disord.* 2015;15:4.
27. Nava A, Bauce B, Basso C, et al. Clinical profile and long-term follow-up of 37 families with arrhythmogenic right ventricular cardiomyopathy. *J Am Coll Cardiol.* 2000;36(7):2226-2233.
28. Saguner AM, Vecchiati A, Baldinger SH, et al. Different Prognostic Value of Functional Right Ventricular Parameters in Arrhythmogenic Right Ventricular Cardiomyopathy/Dysplasia. *Circ Cardiovasc Imaging.* 2014.
29. Mast TP, James CA, Calkins H, et al. Structural Progression in Arrhythmogenic Right Ventricular Dysplasia/Cardiomyopathy. *JAMA Cardiol.* In Press. 2017
30. Te Riele AS, James CA, Philips B, et al. Mutation-positive arrhythmogenic right ventricular dysplasia/cardiomyopathy: the triangle of dysplasia displaced. *J Cardiovasc Electrophysiol.* 2013;24(12):1311-1320.
31. Mast TP, Teske AJ, vd Heijden JF, et al. Left Ventricular Involvement in Arrhythmogenic Right Ventricular Dysplasia/Cardiomyopathy Assessed by Echocardiography Predicts Adverse Clinical Outcome. *J Am Soc Echocardiogr.* 2015;28(9):1103-1113.
32. Sarvari SI, Haugaa KH, Anfinsen OG, et al. Right ventricular mechanical dispersion is related to malignant arrhythmias: a study of patients with arrhythmogenic right ventricular cardiomyopathy and subclinical right ventricular dysfunction. *Eur Heart J.* 2011;32(9):1089-1096.

SUPPLEMENTARY FILES

Supplementary table 1.

Electrocardiographic definitions	
Epsilon waves	Distinct waves of small amplitude within the ST segment in the right precordial leads and are distinct from the QRS complex.
Terminal activation duration	The longest value in V_1–V_3, from the nadir of the S wave to the end of all depolarization deflections. Considered abnormal when ≥55 msec.
T-wave inversion	T-wave was considered inverted if the voltage was ≥0.1 mV

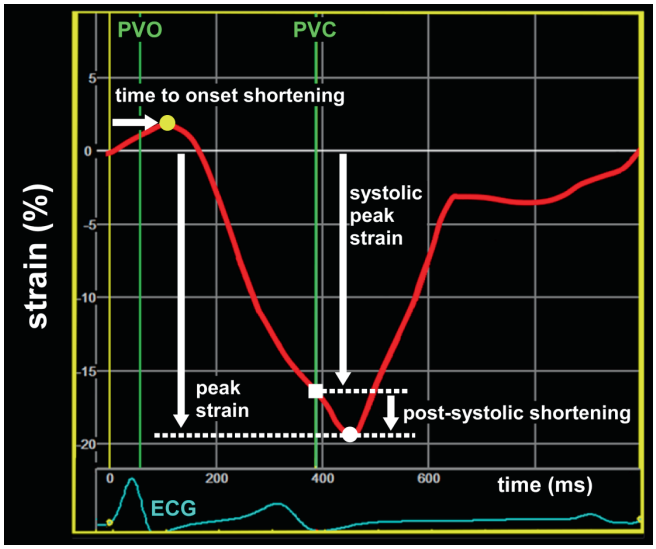

Supplementary figure 1

Deformation imaging definitions	
Time to onset shortening	time between onset-QRS and onset of mechanical shortening
Systolic peak strain	maximal negative value between pulmonary valve opening (PVO) and closure (PVC). In case of positive strain during systole, the value at PVC was taken
Peak strain	maximal negative value during entire cardiac cycle.
Post-systolic index	$100 * \frac{\text{peak strain} - \text{systolic peak strain}}{\text{peak strain}}$

R1 R2 R3 R4 R5 R6 R7 R8 R9 R10 R11 R12 R13 R14 R15 R16 R17 R18 R19 R20 R21 R22 R23 R24 R25 R26 R27 R28 R29 R30 R31 R32 R33 R34 R35 R36 R37 R38 R39

Supplementary table 2. Normal values

	Mean (95CI) / ±SD or median [IQR]		Reference
CMR			
RV-EDV (ml/m^2)	Males: 91 ± 15	Females: 80 ± 16	[1]
RVEF (%)	Males: 62 ± 5	Females: 61 ± 5	[1]
LVEF (%)	Males: 66 ± 4.5	Females: 67 ± 4.6	[1]
Echocardiography			
RVOT-PLAX (mm/m^2)	14.1 ± 2.2		[2]
RVOT-PSAX (mm/m^2)	15.4 ± 2.3		[2]
RV-FAC (%)	49 (47-51)		[2]
TAPSE (mm)	23 (22-24)		[3]
RV peak velocity (cm/s)	15 (14-15)		[3]
LVEF (%)	Males: 62 ± 5	Females: 64 ± 5	[4]
Deformation imaging*			
Basal			
Time to onset (ms)	56 ± 29		[5]
Systolic peak strain (%)	-25.4 ± 5.5		[2]
Mid			
Time to onset (ms)	39 ± 23		[5]
Systolic peak strain (%)	-29.7 ± 3.6		[2]
Apex			
Time to onset (ms)	34 ± 22		[5]
Systolic peak strain (%)	-31.9 ± 3.0		[2]

* Post-systolic shortening is not listed as normal value as it is a pathological sign in the RV.
Abbreviations: = 95 CI = 95% confidence interval; SD = standard deviation; IQR = interquartile ranges; right ventricle; LV = left ventricle; EF = ejection fraction; CMR = cardiac magnetic resonance imaging; EDV = end-diastolic volume; RVOT = right ventricular outflow tract; PSAX/PLAX = parasternal short/long axis view; FAC = fractional area change; TAPSE = tricuspid annular plane systolic excursion; NA = not available

Normal values are derived from:

1. Kawel-Boehm N, Maceira A, Valsangiacomo-Buechel ER, et al. Normal values for cardiovascular magnetic resonance in adults and children. *J Cardiovasc Magn Reson.* 2015;17:29.
2. Teske AJ, Cox MG, De Boeck BW, Doevendans PA, Hauer RN, Cramer MJ. Echocardiographic tissue deformation imaging quantifies abnormal regional right ventricular function in arrhythmogenic right ventricular dysplasia/cardiomyopathy. *J Am Soc Echocardiogr.* 2009;22(8):920-927.
3. Rudski LG, Lai WW, Afilalo J, et al. Guidelines for the echocardiographic assessment of the right heart in adults: a report from the American Society of Echocardiography endorsed by the European Association of Echocardiography, a registered branch of the European Society of Cardiology, and the Canadian Society of Echocardiography. *J Am Soc Echocardiogr.* 2010;23(7):685-713.
4. Lang RM, Badano LP, Mor-Avi V, et al. Recommendations for cardiac chamber quantification by echocardiography in adults: an update from the American Society of Echocardiography and the European Association of Cardiovascular Imaging. *J Am Soc Echocardiogr.* 2015;28(1):1-39 e14.
5. Mast TP, Teske AJ, Te Riele AS, et al. Prolonged Electromechanical Interval Unmasks Arrhythmogenic Right Ventricular Dysplasia/Cardiomyopathy in the Subclinical Stage. *J Cardiovasc Electrophysiol.* 2016;27(3):303-314.

DISCUSSION

CHAPTER 9

Moving From Multimodality Diagnostic Tests Toward Multimodality Risk Stratification in ARVC

Arco J Teske, **Thomas P Mast**

Editorial in:
JACC Cardiovasc Imaging. 2016 Oct 14

R1
R2
R3
R4
R5
R6
R7
R8
R9
R10
R11
R12
R13
R14
R15
R16
R17
R18
R19
R20
R21
R22
R23
R24
R25
R26
R27
R28
R29
R30
R31
R32
R33
R34
R35
R36
R37
R38
R39

Arrhythmogenic right ventricular cardiomyopathy (ARVC) is probably, within the field of cardiology, the single most complex disease to diagnose. It is required that we follow the recommendations stated in the 2010 Task Force criteria (TFC), obtaining points on structural, histological, electrocardiographic, arrhythmic, and genetic features of the diseases (1). Even when we know the patient carries a disease-causing mutation, he/she might have definite, possible, or borderline ARVC depending on how many abnormalities have been identified. Indeed, this disease is notorious for its reduced penetrance and variable disease expressivity, even within families carrying an identical pathogenic mutation in a desmosomal gene (2,3). ARVC is known to be associated with potential life-threatening arrhythmias, and this remains a major concern for both cardiologists and the individual patient (4). Nevertheless, it has been shown that the outcome is favorable after diagnostic criteria are met and treatment according to guidelines is initiated (4). Reported mortality rates vary between 0.08% and 3.6%/year after the diagnosis has been made (excluding sudden cardiac death victims) (5). In the past decades, major advances have been made in defining the genetic basis of ARVC (3,6). These advances have helped to identify a large group of family members who share the same genetic background and are therefore at risk for adverse arrhythmic outcome. Identifying predictors for ventricular arrhythmias during the early ARVC stages has been a focus for research (7–10). It seems that the presence of both electrical and structural abnormalities, as defined by the 2010 TFC, provides sufficient prognostic value in this group (8). However, because our methods for detecting pathology, particularly in the field of cardiac imaging, are improving, we are confronted by subtle phenotypic expressions of this disease in early ARVC that are currently of unknown significance (9,11). The clinical challenge in caring for the individual patient now primarily lies in the early ARVC stages without overt phenotypic expression, and the question remains: which individuals benefit the most from life-style modifications, treatment with antiarrhythmic medications, and implantable cardioverter-defibrillators? The ultimate goal for practicing cardiologists is to provide a specific, tailored approach to each patient with ARVC, such as exists in patients with HCM (12). This would guide our efforts toward those patients who would benefit most while safely implementing a "watchful waiting" strategy in low-risk patients. New cardiac imaging techniques that identify subtle pathology could be of incremental value in the clinical challenge of developing tailor-made strategies during early ARVC.

In this issue of iJACC, Leren *et al.* (13) investigated this clinically relevant problem using a multimodality approach. In this study, they aimed to establish the incremental value of a parameter called mechanical dispersion, assessed by echocardiographic deformation imaging, which is a functional representation of disease expression. Sarvari *et al.* (10) have previously shown that this parameter is related to ventricular arrhythmias in patients with ARVC.

Leren *et al.* (13) included a total of 162 individuals: 89 patients who met the ARVC diagnosis (classified as "overt AVRC") and 73 individuals with "early ARVC" (predominantly family members of patients with ARVC with confirmed pathogenic mutations that did not fulfill the ARVC diagnosis). The cross-sectional study was performed in a single center (13). Arrhythmic events (AE) were obtained retrospectively at inclusion, and were defined as documented nonsustained or sustained ventricular tachycardia, syncope, or aborted cardiac arrest. Finally, the authors aimed to identify markers of ARVC disease on the electrocardiogram (ECG) (as stated in the TFC) and echocardiography (right ventricular [RV] dimensions, right-left ventricular function, and deformation parameters including mechanical dispersion), which showed an association with previous arrhythmic events. In the period prior to inclusion, AE occurred in over 50% of subjects. This was largely driven by the patients with overt AVRC, but nevertheless, AE also occurred in 21% of patients with early ARVC. In the patients with overt ARVC, almost all investigated parameters on imaging and ECG were significantly more affected in the AE group compared with those without AE. This substantiates the hypothesis that the more affected the heart, the higher the likelihood of AE. In the smaller cohort of patients with early ARVC, the event rate was lower and the AE were less severe. Only RV diameter, RV mechanical dispersion, and abnormalities on the saECG were associated with AE in the past. When combining these parameters,the association became even stronger (**Figure 1**).

Although this study provides us with very specific cut-off values and recommendations for clinical decision making, we would like to emphasize (while stressing the importance of the reported findings) that the retrospective design of this study limits the overall applicability. For example, the median time from first arrhythmic event to echocardiography, during which themarkers to predict arrhythmiaswere explored, was 0.27 years (interquartile range: 0.1 to 5.9 years). This basically implies that a correlation between the 2 is purely hypothetical and that the presence of mechanical dispersion or RVOT dilation does not directly imply a higher risk of AE on the basis of the findings of this retrospective analysis. Nevertheless, it is likely that these parameters are linked. Indeed, larger ventriclesmight experience more wall stress, and reduced function (including mechanical dispersion) is likely a result of a significant amount of myocardial fibrosis, both of which are substrates for AE.

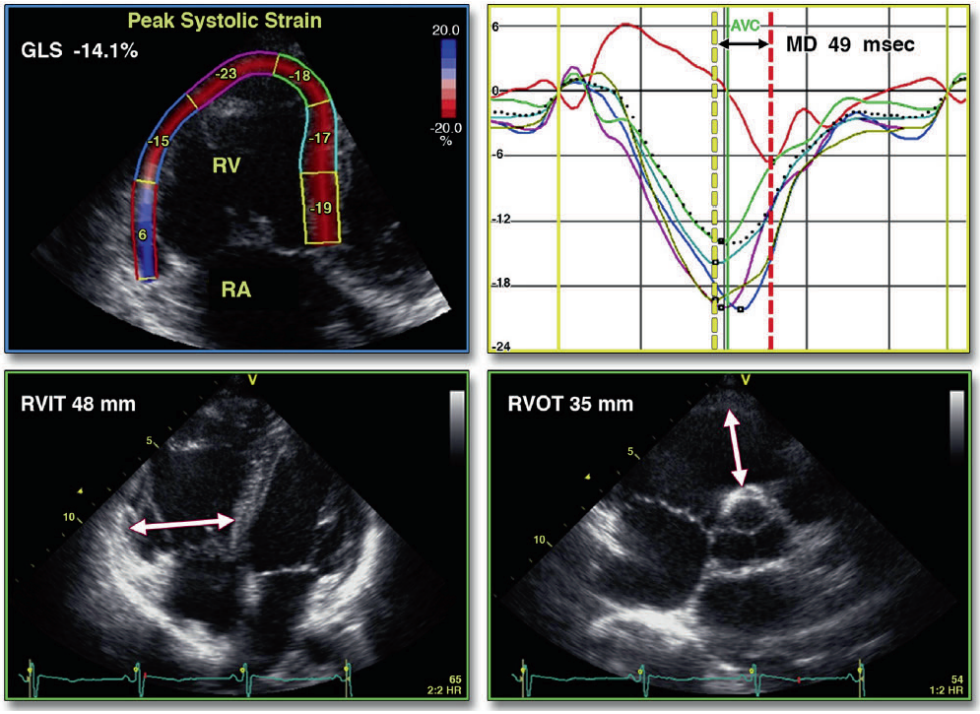

Figure 1. Proposed Echocardiogrpahic Measurements During Follow-up
Proposed parameters on echocardiography by Leren *et al.* (13) to evaluate the risk of AE during follow-up in a patient with arrhythmogenic right ventricular cardiomyopathy at our institution. (Top left) The reduced global longitudinal stain (GLS). (Top right) The prolonged mechanical dispersion (MD) of ≥37 ms. (Bottom) The dilation of the RVIT >40 mm and RVOT ≥34 mm. AVC = aortic valve closure; RA = right atrium; RV = right ventricle; RVIT/RVOT = right ventricular inflow/outflow tract.

How this can be used clinically and what the additional value over the current risk stratification is both remain to be determined (**Figure 2**), especially because positive and negative predictive values cannot be obtained from the current data. The precise role of CMR findings, although performed in most subjects, is also not evaluated in this study and might add important information about structural alterations (particularly in the left ventricle) that could contribute to arrhythmias in the near future (14).

Optimization of treatment and follow-up strategies in early ARVC remain interesting clinical challenges. In this light, mechanical dispersion deserves further validation. However, we currently do not know what causes these observed functional abnormalities, especially when considering the RV. Are we looking at the result of cardiomyocyte cell loss, fibrosis, delayed cell-to-cell communications by desmosome dysfunction, or perhaps a combination of these? One substrate might prove to be more arrhythmogenic than the other. We believe that this imaging technique will not reach its full potential until the underlying disease substrate causing specific deformation abnormalities is elucidated. After this insight is gained, we

potentially have a tool to characterize the affected myocardium. This would ideally lead to a better understanding of its dysfunction and consequently lead to improved risk prediction.
A multimodality approach, as suggested by these authors, definitely makes sense from a pathophysiological point of view, and this publication is not only novel but also very important from that perspective. If no single modality can reliably diagnose this condition, why would the progression of the disease and risk stratification be possible on a single modality? We firmly believe that this complex disease with its variable phenotypic expression requires a "complex" approach during follow-up. It would be extremely interesting to validate these findings in a prospective cohort and, preferably, in a larger and more heterogeneous population at different sites across the globe.

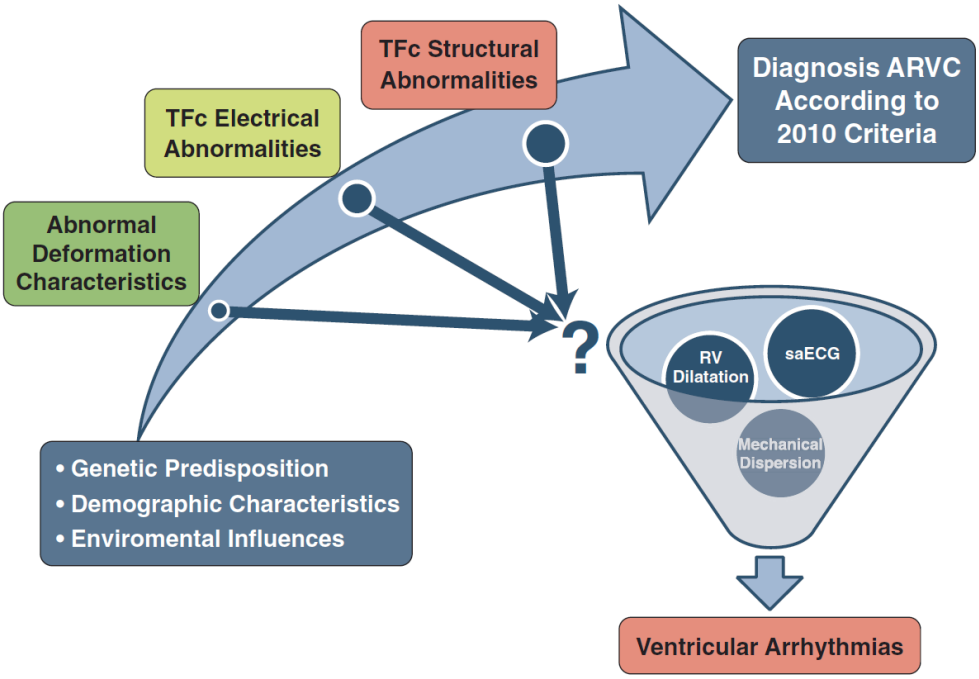

Figure 2. Multimodality Risk Stratification in ARVC
Theoretical disease progression in arrhythmogenic right ventricular cardiomyopathy (ARVC) from genetic predisposition to overt disease fulfilling the 2010 Task Force criteria (TFc). The investigation of exact place of the proposed parameters by Leren *et al.* (13) is the next step toward improving risk assessment. RV = right ventricle.

REFERENCES

1. Marcus FI, McKenna WJ, Sherrill D, et al. Diagnosis of arrhythmogenic right ventricular cardiomyopathy/dysplasia: proposed modification of the Task Force Criteria. *Eur Heart J* 2010;31: 806–14.
2. Dalal D, James C, Devanagondi R, et al. Penetrance of mutations in plakophilin-2 among families with arrhythmogenic right ventricular dysplasia/cardiomyopathy. *J Am Coll Cardiol* 2006;48:1416–24.
3. Bhonsale A, Groeneweg JA, James CA, et al. Impact of genotype on clinical course in arrhythmogenic right ventricular dysplasia/cardiomyopathy-associated mutation carriers. *Eur Heart J* 2015;36:847–55.
4. Groeneweg JA, Bhonsale A, James CA, et al. Clinical presentation, long-term follow-up, and outcomes of 1001 arrhythmogenic right ventricular dysplasia/cardiomyopathy patients and family members. *Circ Cardiovasc Genet* 2015;8:437–46.
5. Corrado D, Wichter T, Link MS, et al. Treatment of arrhythmogenic right ventricular cardiomyopathy/dysplasia: an International Task Force consensus statement. *Circulation* 2015;132:441–53.
6. McKoy G, Protonotarios N, Crosby A, et al. Identification of a deletion in plakoglobin in arrhythmogenic right ventricular cardiomyopathy with palmoplantar keratoderma and woolly hair (Naxos disease). *Lancet* 2000;355:2119–24.
7. Te Riele AS, James CA, Rastegar N, et al. Yield of serial evaluation in at-risk family members of patients with ARVD/C. *J Am Coll Cardiol* 2014;64:293–301.
8. Te Riele AS, James CA, Groeneweg JA, et al. Approach to family screening in arrhythmogenic right ventricular dysplasia/cardiomyopathy. *Eur Heart J* 2016;37:755–63.
9. Mast TP, Teske AJ, Te Riele AS, et al. Prolonged electromechanical interval unmasks arrhythmogenic right ventricular dysplasia/cardiomyopathy in the subclinical stage. *J Cardiovasc Electrophysiol* 2016;27:303–14.
10. Sarvari SI, Haugaa KH, Anfinsen OG, et al. Right ventricular mechanical dispersion is related to malignant arrhythmias: a study of patients with arrhythmogenic right ventricular cardiomyopathy and subclinical right ventricular dysfunction. *Eur Heart J* 2011;32:1089–96.
11. Teske AJ, Cox MG, Te Riele AS, et al. Early detection of regional functional abnormalities in asymptomatic ARVD/C gene carriers. *J Am Soc Echocardiogr* 2012;25: 997–1006.
12. Elliott PM, Anastasakis A, Borger MA, et al. 2014 ESC guidelines on diagnosis and management of hypertrophic cardiomyopathy: the Task Force for the Diagnosis and Management of Hypertrophic Cardiomyopathy of the European Society of Cardiology (ESC). *Eur Heart J* 2014;35: 2733–79.
13. Leren IS, Saberniak J, Haland TF, Edvardsen T, Haugaa KH. Echocardiography combined with ECGs improve identification of arrhythmic events in early ARVC. *J Am Coll Cardiol Img* 2016;9:XX–XXX.
14. Te Riele AS, Bhonsale A, James CA, et al. Incremental value of cardiac magnetic resonance imaging in arrhythmic risk stratification of arrhythmogenic right ventricular dysplasia/cardiomyopathy-associated desmosomal mutation carriers. *J Am Coll Cardiol* 2013;62:1761–9.

CHAPTER 10

General Discussion and Future Perspectives

R1
R2
R3
R4
R5
R6
R7
R8
R9
R10
R11
R12
R13
R14
R15
R16
R17
R18
R19
R20
R21
R22
R23
R24
R25
R26
R27
R28
R29
R30
R31
R32
R33
R34
R35
R36
R37
R38
R39

INTRODUCTION

In this thesis we addressed two main questions:

1) Is echocardiographic deformation imaging of incremental value in *early disease detection* of ARVC?
2) How to assess *structural disease progression* in ARVC?

To address these questions we divided this thesis into three parts. In ***Part I*** we described the current diagnostic and prognostic value of echocardiography in ARVC. Furthermore, we explored the potential value of new echocardiographic techniques such as deformation imaging and 3D-echcardiography. In ***Part II,*** we explored the role of echocardiographic deformation imaging in early ARVC disease detection. Finally, the capability of echocardiography to assess structural disease progression in ARVC was studied in ***Part III***.

Part I. Current and Future role of Echocardiography in Arrhythmogenic Right Ventricular Cardiomyopathy

In ***chapter 2,*** we discussed the current and future role of echocardiography in ARVC. We searched the literature for the diagnostic and prognostic value of both conventional echocardiography and new echocardiographic applications in ARVC. An important part of the diagnostic Task Force criteria (TFC) is the assessment of structural and functional right ventricular (RV) alterations by non-invasive cardiac imaging, and conventional echocardiography is an established imaging modality for that purpose.[1] The echocardiographic TFC requires visual regional wall motion analysis (akinesia, dyskinesia, or aneurysm) in combination with measurements of the RV (right ventricle) outflow tract dimension and RV systolic function. For almost a decade, we performed dedicated echocardiographic examinations in ARVC patients and in ARVC screening according to an in-house developed standardized RV protocol in our echocardiography lab. Included in this chapter is a description of our protocol including the specific echocardiographic RV views for optimal visual RV assessment and examples of the conventional functional RV measurements. In addition to the conventional approaches, we provided an overview of the novel echocardiographic applications: three-dimensional right ventricular (3D-RV) imaging and echocardiographic RV deformation imaging. Current literature suggest that especially the latter could be of incremental value in early diagnosis and risk stratification of ARVC due to its ability to quantify subtle RV regional wall motion abnormalities, and assess RV mechanical dyssynchrony. Several RV deformation parameters are discussed in this chapter such as: systolic peak strain, systolic strain-rate, post-systolic shortening, and mechanical dispersion. We concluded that the previously published data on RV deformation imaging and ARVC are encouraging and warrants further research.

Part II. The Ongoing Quest for Early Disease Detection in ARVC

Activation delay in the subtricuspid area

In the second part, we aimed to address the question whether echocardiographic deformation imaging provides incremental clinical value in early detection of phenotypical expression of ARVC. Early ARVC is characterized by electrical abnormalities in the absence of overt structural abnormalities.[2,3] This is supported by animal experimental studies which showed that activation delay, due to sodium channel dysfunction, is present prior to histopathological alterations.[4] Therefore, in ***chapter 3***, we focused on a deformation parameter that might be closely related to this activation delay. We defined a new echocardiographic deformation parameter: the electromechanical interval (EMI), that describes the interval between the onset of the QRS complex (electrical activation) to the onset of local myocardial shortening. We presumed that this parameter is a surrogate of electrical activation delay due to the electromechanical contraction coupling.[5] Therefore, our hypothesis was that this parameter might be able to identify signs of local activation delay in ARVC. We studied this parameter in 44 definite ARVC patients carrying a desmosomal mutation, 31 asymptomatic desmosomal mutation carriers, and 30 healthy individuals. The analysis of this parameter was feasible in almost all subjects and cut-off values for prolonged EMI were based on results of the control group. Both definite ARVC patients and asymptomatic mutation carriers showed signs of prolonged EMI in the subtricuspid area (77% vs. 45%, respectively). In early ARVC, the presence of prolonged EMI, as surrogate for activation delay, was correlated to arrhythmic outcome (premature ventricular complexes count/non-sustained ventricular tachycardias (VTs) during follow-up. These results suggests that echocardiographic deformation imaging is able to demonstrate early signs of activation delay in the subtricuspid area, even in family members without any established disease phenotypic expression. This new approach is mainly build on the well-established assumption of early disease expression in ARVC: that the subtricuspid area is the first affected region,[6] and activation delay (or electrical disease) is present prior to overt structural abnormalities.[2-4,7] The results of this study were in concordance with this established framework for early disease detection in ARVC.

What is the underlying substrate of abnormal subtricuspid deformation?

In ARVC, multiple echocardiographic deformation imaging parameters distinguishing normal deformation and abnormal deformation were described at the first part of this thesis. An overview of these parameters is provided in ***Chapter 2***. In our experience, these parameters are often present in combination with each other. Therefore, we developed a new pattern-based approach for the classification of subtricuspid deformation, which is described in ***chapter 4***. This approach combines multiple parameters instead of the use of an individual deformation parameter which makes it more robust and reduces inter-operator variability.

We defined three distinct RV deformation patterns varying from normal deformation (Type-I), to mild abnormal deformation (Type-II), and severe abnormal local deformation (Type-III) (**Figure 1**).

We investigated whether these patterns were correlated to ARVC disease severity. Therefore, we included a broad spectrum of desmosomal mutation carriers: 48 with overt structural disease, 15 with only electrical disease without structural abnormalities, and 21 subclinical staged mutation carriers without showing any established disease expression at all. We found that the structural stage was characterized by the presence of severe abnormal subtricuspid deformation (Type-III in 69%), the electrical stage showed predominantly mild abnormal deformation in 67%, while 27% showed severe abnormal deformation. A remarkable finding was that 48% of the mutation carriers in the subclinical stage showed also mild abnormal deformation (Type-II) in the subtricuspid area. This study showed, in line with the previous chapter, that RV deformation imaging was able to detect ARVC disease prior to any established conventional diagnostic approach.

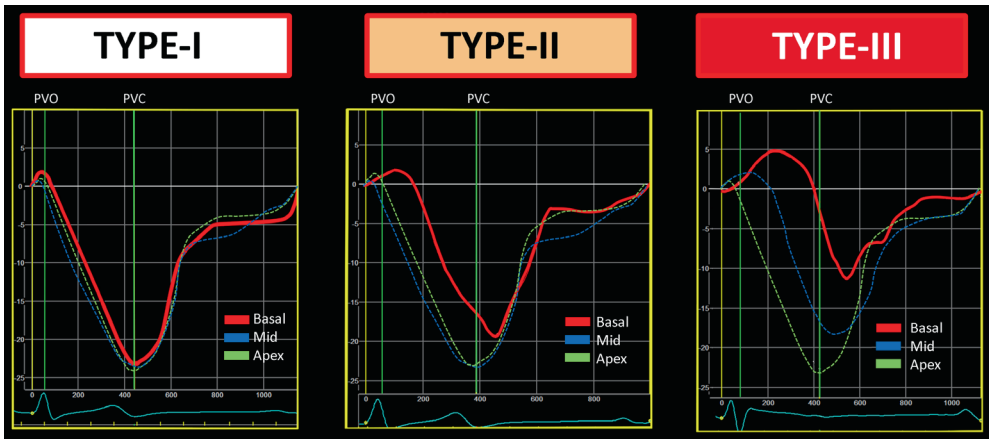

Figure 1. Three distinct RV deformation patterns
Three distinct RV deformation patterns as observed in ARVC. **Type-I** represent normal deformation, **Type-II** shows delayed onset shortening, decreased systolic peak strain, and post-systolic shortening. **Type-III** shows systolic stretching, severely decreased systolic peaks strain values, and large post-systolic shortening. *Abbreviations*: RV = right ventricle; PVO/PVC = pulmonary valve opening/closure

The abnormal deformation patterns consisted of three specific abnormal features in different degrees: 1) delayed onset of shortening, 2) decreased systolic peak strain, and 3) presence of post-systolic shortening. While the association between delayed onset of shortening and electrical activation delay might be easily substantiated,[5] it was definitely not certain what mechanism explained the full shape of the abnormal deformation patterns. Therefore, our second aim described in **Chapter 4** was to characterize the underlying disease substrate causing these abnormal deformation patterns. We hypothesized that, based on the strong

evidence that electrical abnormalities precede structural abnormalities in early ARVC, the mild abnormal deformation pattern (Type-II) as seen in the early clinical stages (subclinical stage and electrical stage) was caused by electrical activation delay. Severe abnormal deformation pattern (type-III), as seen particularly in the structural stage, would then be caused by a predominantly mechanical substrate. A computer model *(CircAdapt)* was used to simulate local deformation patterns by altering the local properties of the myocardium to gain insight in the underlying substrate.[8-10] Three major pathophysiological determinants were tested as potential parts of the pathological substrate: 1) electrical activation delay, 2) hypocontractility (e.g. due to myocardial cell loss), and 3) passive wall stiffness (e.g. due to replacement fibrosis). An unexpected finding was that both abnormal deformation patterns (Type-II/Type-III) were modeled by a mechanical substrate consisting of hypocontractility and increased passive wall stiffness. Remarkably, activation delay did not seem to be an important contributor to the abnormal deformation patterns. Our study suggested that local mechanical dysfunction does appear very early in the disease course, even before both detectable structural abnormalities and electrical abnormalities as described in the 2010 TFC. While this study shows that RV deformation patterns in the subtricuspid area are of incremental value in early disease detection, our data challenges the current clinical stage definitions. If a local mechanical substrate consisting of hypocontractility and passive wall stiffness is present in the electrical and subclinical stage, the stage classification might be inadequate.

Regarding this topic, it is important to notice that our results do not discard the current numerous experimental evidence that early remodeling of the sodium channel precede histopathological alteration in ARVC.[3,4,11] However, it is debatable to what extent the imbalance between structural disease and electrical disease in early ARVC, as observed in previous clinical studies, is based on the same pathophysiological process.[2,3,7,12,13]

The local mechanical substrate in the subtricuspid area is not detected by either the conventional ECG or conventional imaging approaches. A possible explanation for the latter is that the local mechanical dysfunction does not give rise to visual wall motion abnormalities and/or global dysfunction. Another explanation is that the simulated mechanical substrate consisting of hypocontractility and passive wall stiffness should not be interpreted as myocardial cell loss and replacement fibrosis. Perhaps another, yet to be determined, substrate is causing (or contributing to) these abnormal deformation patterns, e.g. alterations in intracellular calcium handling which is known to have an influence on both myocardial contraction and relaxation.[14,15]

Our results also suggest that the conventional surface ECG lacks sufficient sensitivity to detect the pathological substrate in the subtricuspid area. This seems to be supported by an electrophysiological study in which the surface ECG showed a poor correlation with RV abnormalities during electro-anatomic mapping in an ARVC cohort.[16]

A mechanical substrate in the subtricuspid area precede disease progression in early ARVC

Chapter 5 build on the findings of the prior chapter by exploring the clinical value of the presence of abnormal deformation patterns during ARVC family screening in a Dutch multi-center setting. We hypothesized that abnormal deformation precede disease progression in early ARVC as described in the 2010 TFC. First, we included 109 first-degree relatives of ARVC patients without any structural TFC to study early ARVC. Again, we observed a high incidence of abnormal deformation patterns (predominantly Type-II) in the early subclinical and electrical TFC stage. A subgroup underwent a second evaluation after 4 years according to the diagnostic TFC after 4 years. We found that normal deformation patterns at baseline was associated to an absence of disease progression in 96% of the family members after 4 years of follow-up. While current guidelines suggest that every family member should be evaluated every 2-3 years [17], our results suggest that an absence of a local subtricuspid mechanical substrate ensures no established disease progression by TFC during 4 years of follow-up. Based on this results, we propose that these relatives could safely benefit from a lower-frequency follow-up interval of 4-5 years.

Left ventricular involvement in ARVC

Echocardiographic deformation imaging is also capable of assessing regional wall motion of the left ventricle (LV).[18] Historically, ARVC is described as a cardiomyopathy predominantly involving the RV.[19] However, accumulating evidence suggest that LV involvement might be more common than initially thought.[6,20] The clinical importance for adverse outcome of LV involvement in ARVC was previously suggested, which makes it an important clinical research topic.[21,22] In ***chapter 6***, we investigated the presence of LV involvement, measured by echocardiographic deformation imaging in 38 definite ARVC patients, 16 asymptomatic mutation carriers, and 55 healthy controls. Cut-off values were based on healthy controls. We used a combination of systolic peak strain and post-systolic shortening to identify regions with LV pathology. Abnormal deformation in the LV was present in 68% of the ARVC patients and 25% of the relatives. These abnormalities were predominantly found in the posterolateral LV region in concordance with a large previous study using CMR and electrophysiological study.[6] We followed these subjects for 6 years: 20 (53%) ARVC patients experienced adverse cardiac events during follow-up while no events occurred in relatives. The clinical importance of LV dysfunction was clear, since global LV dysfunction (by LVEF<50%) was significantly associated to arrhythmic outcome during follow-up. Furthermore, we found that LV posterolateral involvement detected by deformation imaging was also associated to adverse outcome in ARVC. Moreover, the presence of this regional LV pathology detected by deformation imaging was of superior predictive value compared to global LV dysfunction by conventional echocardiography.

The quest for early disease detection in ARVC continues

The studies in ***Part II*** showed that echocardiographic deformation imaging is capable to detect early abnormalities in the subtricuspid area prior to any established non-invasive conventional technique as defined by TFC (**Figure 2**). The proposed pattern-based approach is a reliable tool to detect early disease expression which could be used to during family screening with a very high reproducibility.

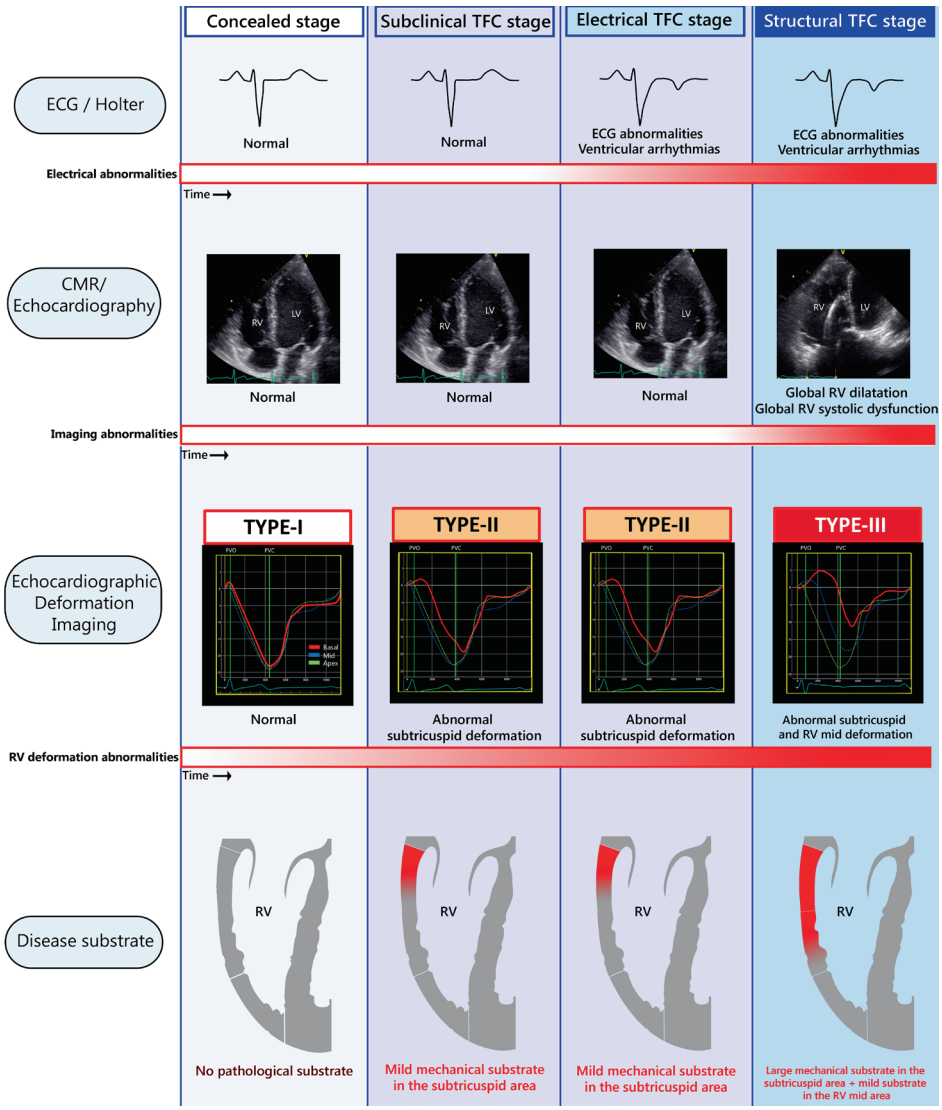

Figure 2. Clinical stages of ARVC with respect to the underlying substrate
Abbreviations: TFC = task force criteria; ECG = electrocardiography; CMR = cardiac magnetic resonance imaging; RV = right ventricle; PVO/PVC = pulmonary vale opening/closure

Part II shed light on the pathological disease substrate underlying the RV deformation graphs. We showed that, in contrast to current opinion, the early disease stages are characterized by subtricuspid mechanical dysfunction. Therefore, the current established disease stage definition seems to be inadequate. Our study implies that RV deformation imaging in combination with computer modeling could reveal interesting new information on ARVC disease mechanism in future studies. While the current framework of early disease detection in ARVC emphasizes the importance of electrical abnormalities for early detection, our studies suggest that mechanical dysfunction might be present earlier compared to electrical disease. Another cornerstone of early detection in ARVC is that the subtricuspid area is the first affected region in ARVC. Our studies definitely supports this idea and the subtricuspid area should be considered as the hotspot region of ARVC more than ever.[6,23]

While echocardiographic deformation imaging has high potential for early diagnosis, we could not yet demonstrate that the presence of abnormal deformation predicts the occurrence of life-threatening ventricular arrhythmias. Recently, a large study (designed for optimizing family screening protocols) found that the cumulative 5-year probability of first sustained ventricular arrhythmia in family members was only 4% and all fulfilled structural TFC at baseline.[12] In our studies, we predominately focused on earlier staged relatives without overt structural disease and this could be one of the explanation that we did not observe any sustained arrhythmias during follow-up.[7,12] Therefore, the prognostic role of RV deformation imaging in early ARVC is still not clear and the follow up duration of our studies might not be long enough. The same holds true for the prognostic value of LV involvement detected by deformation imaging. Although we found that the presence of LV involvement in the posterolateral region was an independent predictor for adverse outcome, the majority of the patients had already suffered from a sustained ventricular arrhythmia at baseline. In addition, no relatives with LV involvement suffered from first ventricular arrhythmia during the six year follow-up. Therefore, it is currently unclear what the prognostic value of deformation imaging is. We also touched upon this topic in ***Chapter 9*** as part of an editorial on echocardiographic deformation imaging for risk prediction in early ARVC.[24] Future studies with longer follow-up duration may shed light on the definite role of echocardiographic deformation imaging in risk prediction.

Part III. Towards optimal assessment of structural disease progression in ARVC

The understanding of structural disease progression is one of the last clinical frontiers in ARVC. Previous studies suggest that only a minority of ARVC patients develop heart failure due to progressive structural dysfunction.[25] The individual rate of structural disease progression is characterized by high variability, as some patients needs heart transplantation during their clinical course, while some retain at a relatively normal biventricular function (**Figure 3**).[25,26] Several reasons for the variability in structural disease progression are previously proposed. A

well-established disease modifier is exercise, which behaves in a dose-dependent relationship with the ARVC phenotype and might be an important contributor to progressive structural dysfunction.[27-30] Another hypothesis is that an episode of inflammation may give rise to an accelerating phase of structural disease progression.[31] Optimal assessment of structural disease progression is important in order to determine the effectiveness of therapeutic interventions such as life-style changes, heart failure medication, and future experimental therapies that aimed to alter the disease course in ARVC. In ***Part III***, we aimed to explore the individual disease progression as well as to define the optimal assessment of structural disease progression in both advanced and early ARVC.

In ***chapter 7***, we performed serial conventional echocardiography in a Trans-Atlantic study in 85 definite ARVC patients. After more than 6 years of follow-up we observed increased structural dysfunction reflected by increasing RV size, decreasing RV systolic function, and decreasing LV systolic function. We observed that structural progression was characterized by marked inter-patient variability. It is currently unknown what the cause of the high inter-patient variability is. Structural disease progression might act in a step-wise behavior instead of a continuous linear process, which could be an explanation for our findings. Since structural disease progression seems to be detectable after 6-years of follow-up in overt ARVC patients, we also conclude that conventional echocardiography is capable to study potential modifiers of disease progression, and evaluate therapeutic strategies in future large studies.

Previous studies showed that structural progression is rarely detected by conventional imaging approaches in early ARVC.[2,3,7,12] Conventional echocardiography and CMR seem unsuitable to measure subtle structural disease progression in subject during the early disease stages. In ***chapter 8*** we investigated the capability of RV deformation imaging to measure structural progression in early ARVC. We included 50 definite ARVC patients and 34 first degree relative without ARVC diagnosis. Conventional echocardiography was capable to show signs of structural disease progression in definite ARVC, in line with our results in the previous chapter. In this overt disease group, RV deformation imaging was also able to show clear structural disease progression in all the lateral RV free wall segments. In contrary, conventional echocardiography and CMR failed to identify any structural disease progression in these early ARVC stages, while deformation imaging importantly showed signs of increasing local mechanical dysfunction. Therefore, echocardiographic deformation imaging seems to be more sensitive in measuring structural disease progression during early ARVC comparing to conventional techniques.

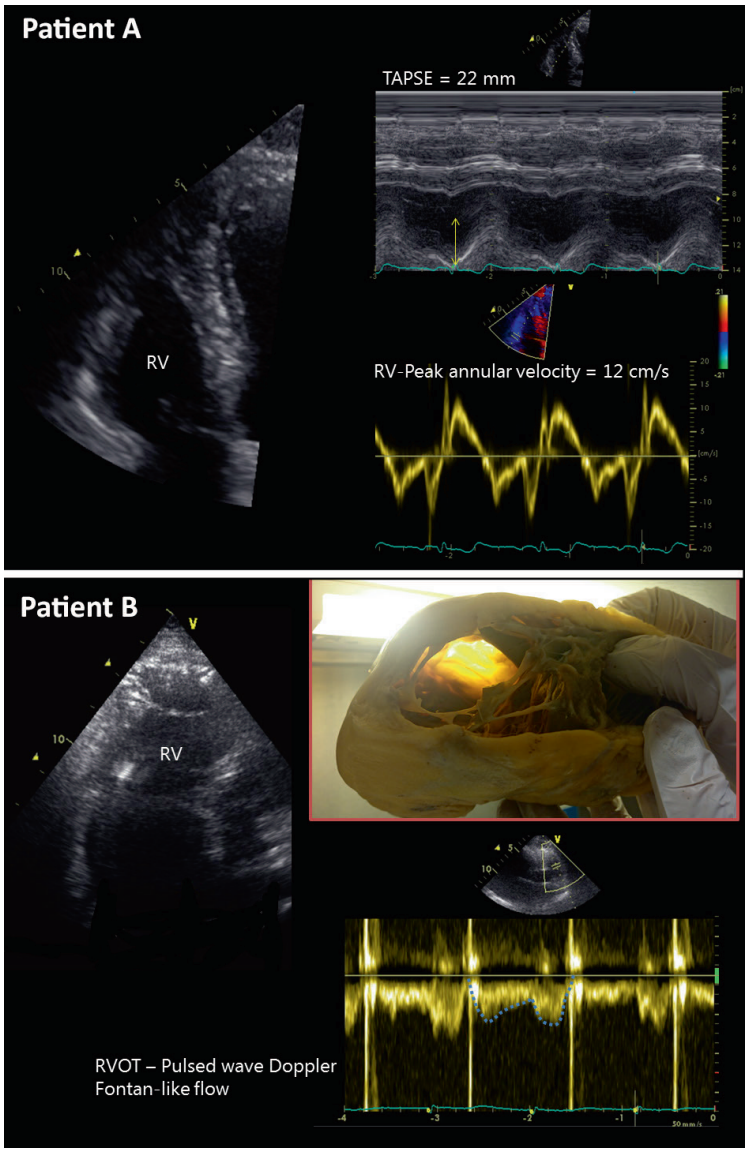

Figure 3. Structural progression is characterized by high inter patient variability
Upper: **ARVC patient A** is a 66 years old male diagnosed with ARVC approximately twenty years ago based on LBBB VT with superior axis and ECG abnormalities. 2D-echocardiogram shows a RV with normal dimensions and normal RV systolic function.
Lower: **ARVC patient B** is a 25 years old female diagnosed with ARVC five years ago based on VTs with multiple morphologies. 2D-echocardiogram showed a severely dilated RV. The pulsed wave Doppler in the RV outflow tract shows a Fontan-like signal due to a nearly absence of systolic RV function. The patient developed refractory heart failure and underwent a heart transplantation in our hospital. The explanted heart showed signs of extensive transmural replacement fibrosis and a remarkable thin RV free wall. *Abbreviations:* ARVC = arrhythmogenic right ventricular cardiomyopathy; LBBB = left bundle branch block; VT = ventricular tachycardia; RV = right ventricle

The assessment of structural disease progression is still in need for further optimization and validation. For conventional echocardiography, a large amount of parameters are described for the functional assessment of the RV. For the individual patient, it is currently unclear which parameter is the most reliable to measure structural disease progression during serial evaluation. Further validation is also still needed for deformation imaging derived parameters with respect to measuring structural disease progression. For example, values of systolic peak strain, the most commonly used deformation parameter, is affected by alteration in pre- and afterload which is a potential problem during the serial evaluation of patients. Therefore, we think that a similar pattern-based approach as provided in *part II* might be also of additional value in the assessment of structural progression. A pattern-based approach might be less vulnerable to false-negative and false-positive findings and this seems an important next step for the identification of structural disease progression on an individual level.

Closing remarks

Echocardiographic deformation imaging definitely has potential to enter the field of clinical decision making in ARVC. Its ability to study local RV pathology has major incremental advantages in addition to conventional approaches. Future studies are necessary to reveal the true clinical value of this technique. The next step to make this promising technique widely-accepted in ARVC is by leaving the single-nation, the single-center, and the single-vendor setting of research which characterized research on echocardiographic deformation imaging during the last decades.

REFERENCES

1. Marcus FI, McKenna WJ, Sherrill D, et al. Diagnosis of arrhythmogenic right ventricular cardiomyopathy/dysplasia: proposed modification of the task force criteria. *Circulation.* 2010;121(13):1533-1541.
2. te Riele AS, James CA, Rastegar N, et al. Yield of serial evaluation in at-risk family members of patients with ARVD/C. *J Am Coll Cardiol.* 2014;64(3):293-301.
3. Gomes J, Finlay M, Ahmed AK, et al. Electrophysiological abnormalities precede overt structural changes in arrhythmogenic right ventricular cardiomyopathy due to mutations in desmoplakin-A combined murine and human study. *Eur Heart J.* 2012;33(15):1942-1953.
4. Cerrone M, Noorman M, Lin X, et al. Sodium current deficit and arrhythmogenesis in a murine model of plakophilin-2 haploinsufficiency. *Cardiovasc Res.* 2012;95(4):460-468.
5. Prinzen FW, Vernooy K, De Boeck BW, Delhaas T. Mechano-energetics of the asynchronous and resynchronized heart. *Heart Fail Rev.* 2011;16(3):215-224.
6. Te Riele AS, James CA, Philips B, et al. Mutation-positive arrhythmogenic right ventricular dysplasia/cardiomyopathy: the triangle of dysplasia displaced. *J Cardiovasc Electrophysiol.* 2013;24(12):1311-1320.
7. Te Riele AS, Bhonsale A, James CA, et al. Incremental value of cardiac magnetic resonance imaging in arrhythmic risk stratification of arrhythmogenic right ventricular dysplasia/cardiomyopathy-associated desmosomal mutation carriers. *J Am Coll Cardiol.* 2013;62(19):1761-1769.
8. Arts T, Delhaas T, Bovendeerd P, Verbeek X, Prinzen FW. Adaptation to mechanical load determines shape and properties of heart and circulation: the CircAdapt model. *Am J Physiol Heart Circ Physiol.* 2005;288(4):H1943-1954.
9. Walmsley J, Arts T, Derval N, et al. Fast Simulation of Mechanical Heterogeneity in the Electrically Asynchronous Heart Using the MultiPatch Module. *PLoS Comput Biol.* 2015;11(7):e1004284.
10. Lumens J, Delhaas T, Kirn B, Arts T. Three-wall segment (TriSeg) model describing mechanics and hemodynamics of ventricular interaction. *Ann Biomed Eng.* 2009;37(11):2234-2255.
11. Rizzo S, Lodder EM, Verkerk AO, et al. Intercalated disc abnormalities, reduced Na(+) current density, and conduction slowing in desmoglein-2 mutant mice prior to cardiomyopathic changes. *Cardiovasc Res.* 2012;95(4):409-418.
12. Te Riele AS, James CA, Groeneweg JA, et al. Approach to family screening in arrhythmogenic right ventricular dysplasia/cardiomyopathy. *Eur Heart J.* 2016;37(9):755-763.
13. Protonotarios N, Anastasakis A, Antoniades L, et al. Arrhythmogenic right ventricular cardiomyopathy/dysplasia on the basis of the revised diagnostic criteria in affected families with desmosomal mutations. *Eur Heart J.* 2011;32(9):1097-1104.
14. Kim C, Wong J, Wen J, et al. Studying arrhythmogenic right ventricular dysplasia with patient-specific iPSCs. *Nature.* 2013;494(7435):105-110.
15. Wen JY, Wei CY, Shah K, Wong J, Wang C, Chen HS. Maturation-Based Model of Arrhythmogenic Right Ventricular Dysplasia Using Patient-Specific Induced Pluripotent Stem Cells. *Circ J.* 2015;79(7):1402-1408.
16. Tandri H, Asimaki A, Abraham T, et al. Prolonged RV endocardial activation duration: a novel marker of arrhythmogenic right ventricular dysplasia/cardiomyopathy. *Heart Rhythm.* 2009;6(6):769-775.
17. Corrado D, Wichter T, Link MS, et al. Treatment of Arrhythmogenic Right Ventricular Cardiomyopathy/Dysplasia: An International Task Force Consensus Statement. *Circulation.* 2015;132(5):441-453.
18. Teske AJ, De Boeck BW, Melman PG, Sieswerda GT, Doevendans PA, Cramer MJ. Echocardiographic quantification of myocardial function using tissue deformation imaging, a guide to image acquisition and analysis using tissue Doppler and speckle tracking. *Cardiovasc Ultrasound.* 2007;5:27.

19. Marcus FI, Fontaine GH, Guiraudon G, et al. Right ventricular dysplasia: a report of 24 adult cases. *Circulation.* 1982;65(2):384-398.
20. Sen-Chowdhry S, Syrris P, Ward D, Asimaki A, Sevdalis E, McKenna WJ. Clinical and genetic characterization of families with arrhythmogenic right ventricular dysplasia/cardiomyopathy provides novel insights into patterns of disease expression. *Circulation.* 2007;115(13):1710-1720.
21. Lemola K, Brunckhorst C, Helfenstein U, Oechslin E, Jenni R, Duru F. Predictors of adverse outcome in patients with arrhythmogenic right ventricular dysplasia/cardiomyopathy: long term experience of a tertiary care centre. *Heart.* 2005;91(9):1167-1172.
22. Pinamonti B, Dragos AM, Pyxaras SA, et al. Prognostic predictors in arrhythmogenic right ventricular cardiomyopathy: results from a 10-year registry. *Eur Heart J.* 2011;32(9):1105-1113.
23. Te Riele AS, Bhonsale A, Burt JR, Zimmerman SL, Tandri H. Genotype-specific pattern of LV involvement in ARVD/C. *JACC Cardiovasc Imaging.* 2012;5(8):849-851.
24. Leren IS, Saberniak J, Haland TF, Edvardsen T, Haugaa KH. Echocardiography Combined with ECGs Improve Identification of Arrhythmic Events in Early ARVC. *J Am Coll Cardio Img.* 2016;in press(in press):in press.
25. Groeneweg JA, Bhonsale A, James CA, et al. Clinical Presentation, Long-Term Follow-Up, and Outcomes of 1001 Arrhythmogenic Right Ventricular Dysplasia/Cardiomyopathy Patients and Family Members. *Circ Cardiovasc Genet.* 2015;8(3):437-446.
26. Tedford RJ, James C, Judge DP, et al. Cardiac transplantation in arrhythmogenic right ventricular dysplasia/cardiomyopathy. *J Am Coll Cardiol.* 2012;59(3):289-290.
27. Sawant AC, Bhonsale A, Te Riele AS, et al. Exercise has a Disproportionate Role in the Pathogenesis of Arrhythmogenic Right Ventricular Dysplasia/Cardiomyopathy in Patients Without Desmosomal Mutations. *J Am Heart Assoc.* 2014;3(6).
28. Sawant AC, Te Riele AS, Tichnell C, et al. Safety of American Heart Association-recommended minimum exercise for desmosomal mutation carriers. *Heart Rhythm.* 2016;13(1):199-207.
29. James CA, Bhonsale A, Tichnell C, et al. Exercise increases age-related penetrance and arrhythmic risk in arrhythmogenic right ventricular dysplasia/cardiomyopathy-associated desmosomal mutation carriers. *J Am Coll Cardiol.* 2013;62(14):1290-1297.
30. Heidbuchel H, La Gerche A. The right heart in athletes. Evidence for exercise-induced arrhythmogenic right ventricular cardiomyopathy. *Herzschrittmacherther Elektrophysiol.* 2012;23(2):82-86.
31. Asimaki A, Tandri H, Duffy ER, et al. Altered desmosomal proteins in granulomatous myocarditis and potential pathogenic links to arrhythmogenic right ventricular cardiomyopathy. *Circ Arrhythm Electrophysiol.* 2011;4(5):743-752.

APPENDIX

Nederlandse samenvatting

Contributing Authors

Curriculum Vitae

List of Publications

Dankwoord / Acknowledgments

R1
R2
R3
R4
R5
R6
R7
R8
R9
R10
R11
R12
R13
R14
R15
R16
R17
R18
R19
R20
R21
R22
R23
R24
R25
R26
R27
R28
R29
R30
R31
R32
R33
R34
R35
R36
R37
R38
R39

NEDERLANDSTALIGE SAMENVATTING

ARVC

Aritmogene rechter ventrikel cardiomyopathie (ARVC) is een relatief zeldzame hartspieraandoening die bij ongeveer 1:5000 mensen voorkomt. De ziekte wordt klinisch gekenmerkt door in potentie levensbedreigende kamerritmestoornissen en op langer termijn een verminderde pompfunctie. ARVC is in veel gevallen een familiaire aandoening. Op dit moment kan in meer dan de helft van de patiënten een genetische mutatie worden aangetoond die ten grondslag ligt aan dit ziektebeeld. De genen die betrokken zijn bij ARVC coderen vrijwel allemaal voor eiwitten die een belangrijke rol spelen in de functie en opbouw van het desmosoom. Desmosomen zijn de eiwitcomplexen die zorgen voor de mechanische verbindingen tussen twee hartspiercellen. Door mutaties in de desmosomale genen kan de uiteindelijke structuur en functie van het desmosoom dusdanig worden veranderd dat er desmosomale dysfunctie optreedt. De klassieke pathofysiologisch gedachte is dat de verminderde mechanische verbinding tussen myocardcellen leidt tot het afsterven van myocardcellen met vervolgens een vervanging van het hartweefsel met fibrose en vet. Echter laten recente onderzoeken zien dat het pathofysiologisch proces reikt tot buiten het desmosoom.

ARVC begint in specifieke regio's van de rechter kamer (RV) en verspreidt zich steeds verder over zowel de rechter als ook de linker kamer (LV). De veranderingen van het hartweefsel geven een verhoogd risico op het ontstaan van kamerritmestoornissen en plotse hartdood. In een later stadium kan een dusdanig groot gebied van hartspiersweefsel zijn vervangen door fibrose en vet dat er hartfalen (pompfalen) kan ontstaan, deze uiting van ernstige ziekteprogressie treedt echter maar in een klein gedeelte van de patiënten op.

De afgelopen jaren zijn er veel vorderingen geboekt om het genetisch substraat achter ARVC verder te ontrafelen. Dit heeft er toe geleidt dat er veel familieleden van ARVC patiënten zijn geïdentificeerd die met hun dragerschap van dezelfde genetische mutatie een zeker risico lopen dit ziektebeeld ook te ontwikkelen, dit risico bedraagt ongeveer één op de drie. Dit geeft een klinische uitdaging aan de behandelend cardioloog. De vraag welk familielid de ziekte gaat ontwikkelen is namelijk van groot klinisch belang. Het zo optimaal mogelijk identificeren van de eerste tekenen van ARVC leidt namelijk tot tijdig en optimaal behandelen van deze individuen. De achterliggende onderzoeksvraag daarbij is: hoe kan men de ziekte in een zo vroeg mogelijk stadium detecteren?

Echocardiografische deformatie beeldvorming

Echocardiografische deformatie beeldvorming (of: echocardiographic deformation imaging) is een toepassing van de echocardiografie die tracht regionale wandbeweging te kwantificeren door de gehele cardiale cyclus heen. Gedurende de contractiefase (systole)

van het hart verkort en verdikt het hartspierweefsel waardoor het bloed de grote vaten ingepompt wordt. Tijdens de vullingsfase (diastole) rekt het hart weer op naar zijn initiële afmetingen. Gedurende de hartcyclus verandert het hartweefsel dus van vorm (deformatie). Met echocardiografische deformatie beeldvorming is deze deformatie per verschillende regio te visualiseren en te kwantificeren.
In de vroege fase van ARVC kunnen er mogelijk subtiele afwijkingen in de deformatie van de RV ontstaan die bij de visuele beoordeling onopgemerkt zouden blijven. Hierdoor zou deze techniek van toegevoegde waarde kunnen zijn bij het zo vroeg mogelijk detecteren van ARVC. Deze hoofdvraagstelling is onderzocht in dit proefschrift.

Proefschrift

In **hoofdstuk 1** wordt een uitgebreide introductie van het onderwerp gegeven waarbij de vraagstelling geponeerd wordt die getracht is in dit proefschrift te beantwoorden. In **hoofdstuk 2** wordt de rol van de echocardiografie, inclusief echocardiografische deformatie beeldvorming, binnen ARVC beschreven zoals tijdens de start van dit proefschrift (3 jaar geleden) bekend was.

De rol van deformatie beeldvorming in vroeg-detectie van ARVC

In **hoofdstuk 3** wordt een nieuwe parameter geïntroduceerd die de tijd beschrijft tussen elektrisch activatie van het hart en de start van de regionale verkorting. In ARVC patiënten bleek deze tijd verlengd ten opzichte van gezonde personen. In genetisch aangedane familieleden zonder verdere uitingen van ARVC bleek deze parameter in ongeveer 50% ook al verlengd in een specifieke regio van de RV, het subtricuspide gebied. Deze parameter stelde ons in staat een zeer vroege uiting van de ziekte te herkennen. Deze parameter werkte tevens voorspellend voor toekomstige ziekteprogressie in deze groep.
In **hoofdstuk 4** hebben we deze parameter geïntegreerd met twee andere deformatie verschijnselen: piek-systolische deformatie (strain) en het optreden van post-systolische verkorting. We werkten de hypothesen uit dat deze deformatie verschijnselen vaak samen voorkomen en kenmerkende algehele deformatiepatronen veroorzaken. We definieerde drie deformatie patronen die goed correleerde met oplopende ernst van ziekte. Tevens maakte we gebruik van een computer model die het onderliggende substraat onthulde dat ten grondslag ligt aan deze patronen. In wederom ongeveer de helft van de familieleden met een genetische aanleg voor ARVC maar zonder enige klacht dan wel abnormaliteiten via andere diagnostische onderzoeken kon een afwijkend deformatiepatroon worden aangetoond. Het pathologische substraat bestond uit verminderde contractiliteit van het weefsel (hypocontractiliteit) en een verhoogde passieve stijfheid van het weefsel. Dit substraat was enigzins een verrassing, daar resultaten van eerdere onderzoeken met name in de richting wees van elektrische vertraging als veroorzaker van vroege abnormaliteiten in ARVC.

In **hoofdstuk 5** staat beschreven dat de deformatiepatronen een voorspellende waarde op ziekte progressie heeft tijdens follow-up. In andere woorden, de aan- of afwezigheid van afwijkende deformatiepatronen voorspelt wie verdere ziekte-uitingen krijgen en wie onaangedaan blijft. In dit hoofdstuk werken we toe naar een individuele op maat gemaakte follow-up strategie waarbij individuen met een normale deformatie minder vaak vervolgd zouden mogen worden en personen met een afwijkende deformatiepatroon juist frequenter. De LV afwijkingen bij ARVC werden van oudsher beschreven als laat in het ziektebeeld optredend. Omdat echocardiografische deformatie imaging een gevoelige methode is voor het opsporen van afwijkingen hebben wij deze techniek gebruikt om afwijkingen in deze kamer op te sporen. De resultaten van deze studie staan beschreven in **hoofdstuk 6**. Wij vonden dat LV afwijkingen vaak voorkwam in ARVC patiënten en ook in niet aangedane familieleden. Kortom, de afwijkingen in de LV bij ARVC dienen zeker niet als een laat fenomeen te worden beschouwd. Daarnaast bleek de aanwezigheid van deze subtiele LV afwijkingen ook een voorspellende waarde voor toekomstige ritmestoornissen en het optreden van hartfalen in ARVC patiënten.

De rol van echocardiografie in het detecteren van ziekteprogressie van ARVC

ARVC wordt beschouwd als een progressieve aandoening, met de jaren nemen de hartspierweefselveranderingen steeds meer toe. Over het gedrag van deze progressie is relatief weinig bekend. In **hoofdstuk 7** hebben wij gekeken of conventionele echotechnieken in staat zijn deze progressie te kunnen meten. Deze resultaten van deze studie lieten inderdaad zien dat er progressieve achteruitgang was met grote verschillen tussen de verschillende ARVC patiënten (niet-uniforme progressie). In **hoofdstuk 8** hebben wij tevens deformatie beeldvorming ingezet om progressie te bestuderen. Deze techniek liet dezelfde resultaten zien als conventioneel echo bij ARVC patiënten. Echter, een belangrijke bevinding was dat er ook in familieleden ziekteprogressie waarneembaar was waar die met conventionele technieken gemist zou zijn.

Hoofdstuk 9 en 10 worden de resultaten van dit proefschrift bediscussieerd en proberen we de toekomstige rol van echocardiografische deformatie beeldvorming binnen ARVC te definiëren.

Conclusie

Echocardiografische deformatie beeldvorming heeft de potentie om een belangrijke rol te spelen in de (poli)klinische beslissingen rondom ARVC patiënten en de familieleden. De voordelen van deze techniek om op lokaal niveau subtiele afwijkingen op te sporen is een goede aanvulling op de reeds bestaande technieken. De resultaten van dit proefschrift hebben deze techniek weer een stap dichterbij de kliniek gebracht. Verdere studies blijven echter nodig om de definitieve positie van deze techniek te bepalen.

R1
R2
R3
R4
R5
R6
R7
R8
R9
R10
R11
R12
R13
R14
R15
R16
R17
R18
R19
R20
R21
R22
R23
R24
R25
R26
R27
R28
R29
R30
R31
R32
R33
R34
R35
R36
R37
R38
R39

CONTRIBUTING AUTHORS

Theodore P Abraham
Department of Medicine, Division of Cardiology, Johns Hopkins University School of Medicine, Baltimore, Maryland, USA

Folkert W Asselbergs
Department of Medicine, Division of Cardiology, University Medical Center Utrecht, Utrecht, the Netherlands
Durrer Center for Cardiovascular Research, ICIN-Netherlands Heart Institute, Utrecht, the Netherlands
Institute of Cardiovascular Science, Faculty of Population Health Sciences, University College London, London, United Kingdom

Jacques M de Bakker
Department of Medical Physiology and Cardiology, University Medical Center Utrecht, the Netherlands
Department of Experimental Cardiology, Heart Center, Academic Medical Center, Amsterdam, the Netherlands
ICIN-Netherlands Heart Institute, Utrecht, the Netherlands

Maarten P van den Berg
University of Groningen, University Medical Center Groningen, Department of Cardiology, Groningen, the Netherlands

Berto J Bouma
Division of Cardiology, Academic Medical Center Amsterdam, Amsterdam, the Netherlands

Hugh Calkins
Department of Medicine, Division of Cardiology, Johns Hopkins University School of Medicine, Baltimore, Maryland, USA

Maarten J Cramer
Department of Medicine, Division of Cardiology, University Medical Center Utrecht, Utrecht, the Netherlands

Tammo Delhaas
Department of Biomedical Engineering, Cardiovascular Research Institute Maastricht (CARIM), Maastricht University, Maastricht, the Netherlands

Pieter A Doevendans
Department of Medicine, Division of Cardiology, University Medical Center Utrecht, Utrecht, the Netherlands

Dennis Dooijes
Department of Medical Genetics, University Medical Center Utrecht, Utrecht, the Netherlands

René van Es
Department of Medicine, Division of Cardiology, University Medical Center Utrecht, Utrecht, the Netherlands

Judith A Groeneweg
Department of Medicine, Division of Cardiology, University Medical Center Utrecht, Utrecht, the Netherlands

Richard N Hauer
ICIN – Netherlands Heart Institute, Utrecht, the Netherlands
Department of Medicine, Division of Cardiology, University Medical Center Utrecht, Utrecht, the Netherlands

Jeroen F van der Heijden
Department of Medicine, Division of Cardiology, University Medical Center Utrecht, Utrecht, the Netherlands

Cynthia A James
Department of Medicine, Division of Cardiology, Johns Hopkins University School of Medicine, Baltimore, Maryland, USA

Daniel P Judge
Department of Medicine, Division of Cardiology, Johns Hopkins University School of Medicine, Baltimore, Maryland, USA

Peter Loh
Department of Medicine, Division of Cardiology, University Medical Center Utrecht, Utrecht, the Netherlands

Joost Lumens
Department of Biomedical Engineering, Cardiovascular Research Institute Maastricht (CARIM), Maastricht University, Maastricht, the Netherlands; IHU Liryc, Electrophysiology and Heart Modeling Institute, Fondation Bordeaux Université, Bordeaux, France.

Brittney Murray
Department of Medicine, Division of Cardiology, Johns Hopkins University School of Medicine, Baltimore, Maryland, USA

Frits W Prinzen
Department of Physiology, Cardiovascular Research Institute Maastricht (CARIM), Maastricht University, Maastricht, the Netherlands

Anneline SJM Te Riele
Department of Medicine, Division of Cardiology, University Medical Center Utrecht, Utrecht, the Netherlands
Department of Medicine, Division of Cardiology, Johns Hopkins University School of Medicine, Baltimore, Maryland, USA
Netherlands Heart Institute, Utrecht, the Netherlands

Stuart D Russell
Department of Medicine, Division of Cardiology, Johns Hopkins University School of Medicine, Baltimore, Maryland, USA

Karim Taha
University of Amsterdam, Amsterdam, the Netherlands

Harikrishna Tandri
Department of Medicine, Division of Cardiology, Johns Hopkins University School of Medicine, Baltimore, Maryland, USA

Ryan J Tedford
Department of Medicine, Division of Cardiology, Johns Hopkins University School of Medicine, Baltimore, Maryland, USA

Arco J Teske
Department of Medicine, Division of Cardiology, University Medical Center Utrecht, Utrecht, the Netherlands

Crystal Tichnell
Department of Medicine, Division of Cardiology, Johns Hopkins University School of Medicine, Baltimore, Maryland, USA

Toon A van Veen
Department of Medical Physiology, University Medical Center Utrecht, Utrecht, the Netherlands

Birgitta K Velthuis
Department of Radiology, University Medical Center Utrecht, Utrecht, the Netherlands

John Walmsley
Department of Biomedical Engineering, Cardiovascular Research Institute Maastricht (CARIM), Maastricht University, Maastricht, the Netherlands;

CURRICULUM VITAE

Thomas Mast was born in Utrecht on September 26th to Gijs Mast and Hannah Vos. He grew up in Vianen with two older brothers: Bastiaan and Joost. During his childhood he played field hockey and played the piano. After graduating from Luzac College Utrecht in 2005, he started medical school at the University of Utrecht and obtained his Bachelor degree in 2010. During his medical education, Thomas became interested in cardiology and worked as a student under supervision of Dr. A.J. Six on developing the HEART score. During his final clinical rotation at the cardiology department in Amersfoort under supervision of Dr. P.J. Senden in 2013, he met Dr. A.J. Teske who introduced him into the world of echocardiographic deformation imaging. Thomas obtained his M.D. degree in 2013 and in the same year he started his PhD on the topic of deformation imaging and ARVC under supervision of Prof. dr. P.A.F.M. Doevendans, Dr. M.J.M. Cramer, and Dr. A.J. Teske. During his PhD he joined the ARVD/C research group at the Johns Hopkins University in Baltimore, USA for three months. In 2017, Thomas started his residency in cardiology under supervision of Dr. J.M. van Dantzig and Prof. dr. N.H. Pijls at the Catharina Hospital Eindhoven in 2017. Thomas lives together with his girlfriend Iris ter Horst. In his spare time, he likes to go running. He runs over 2000 km per year and finished multiple (ultra)marathons.

R1
R2
R3
R4
R5
R6
R7
R8
R9
R10
R11
R12
R13
R14
R15
R16
R17
R18
R19
R20
R21
R22
R23
R24
R25
R26
R27
R28
R29
R30
R31
R32
R33
R34
R35
R36
R37
R38
R39

LIST OF PUBLICATIONS

Structural Progression in Arrhythmogenic Right Ventricular Dysplasia/Cardiomyopathy
Mast TP, James CA, Calkins H, Teske AJ, Tichnell C, Murray B, Loh P, Russell SD, Velthuis BK, Judge DP, Dooijes D, Tedford RJ, Heijden van der JF, Tandri H, Hauer RN, Abraham TP, Doevendans, PA, Te Riele AS, Cramer MJ.
JAMA Cardiol 2017 Accepted

Right Ventricular Imaging and Computer Simulation for Electromechanical Substrate Characterization in Arrhythmogenic Right Ventricular Cardiomyopathy.
Mast TP, Teske AJ, Walmsley J, vd Heijden JF, Es van R, Prinzen FW, Delhaas T, v Veen TA, Loh P, Doevendans PA, Cramer MJ, Lumens J.
J Am Coll Cardiol. 2016;68(20):2185-2197

Moving From Multimodality Diagnostic Tests Toward Multimodality Risk Stratification in ARVC.
Teske AJ, **Mast TP**.
JACC Cardiovasc Imaging. 2016 Oct 14

Clinical characterization and risk stratification of patients with arrhythmogenic right ventricular dysplasia/cardiomyopathy ≥50 years of age.
van der Pols MJ, **Mast TP**, Loh P, van der Heijden JF, Cramer MJ, Hauer RN, Te Riele AS.
Neth Heart J. 2016 Aug 31

Influence of Genotype on Structural Atrial Abnormalities and Atrial Fibrillation or Flutter in Arrhythmogenic Right Ventricular Dysplasia/Cardiomyopathy.
Bourfiss M, Te Riele AS, **Mast TP**, Cramer MJ, Vd Heijden JF, v Veen TA, Loh P, Dooijes D, Hauer RN, Velthuis BK.
J Cardiovasc Electrophysiol. 2016 Oct 6.

Arrhythmogenic Right Ventricular Dysplasia/Cardiomyopathy in the Pediatric Population Clinical Characterization and Comparison With Adult-Onset Disease.
Te Riele AS, James CA, Sawant AC, Bhonsale A, Groeneweg JA, **Mast TP**, Murray B, Tichnell C, Dooijes D, van Tintelen JP, Judge DP, vd Heijden JF, Crosson J, Hauer RN, Calkins H, Tandri H
JACC: Clinical Electrophysiology. 2016;1(6)551-60

Echo response and clinical outcome in CRT patients.
van ‘t Sant J, **Mast TP**, Bos MM, Ter Horst IA, van Everdingen WM, Meine M, Cramer MJ.
Neth Heart J. 2016 Jan;24

R1 R2 R3 R4 R5 R6 R7 R8 R9 R10 R11 R12 R13 R14 R15 R16 R17 R18 R19 R20 R21 R22 R23 R24 R25 R26 R27 R28 R29 R30 R31 R32 R33 R34 R35 R36 R37 R38 R39

Prolonged electro-mechanical interval umasks arrhythmogenic right ventricular dysplasia/cardiomyopathy in the subclinical stage.
Mast TP, Teske AJ, Te Riele AS, Groeneweg JA, Heijden vd JF, Velthuis BK Loh P, Doevendans PA, Veen v TA, Dooijes D, De Bakker JM, Hauer RN, Cramer MJ.
J Cardiovasc Electrophysiol. 2015 Nov 20

Cardiac MRI in Diagnosis, Clinical Management and Prognosis of Arrhythmogenic Right Ventricular Dysplasia/Cardiomyopathy. 1st Edition Abidov A, Oliva I, Marcus F. Book Chapter 11: Echocardiographic Applications in Diagnosis and Management of Patients with ARVC
Mast TP, Teske AJ, Doevendans PA, Cramer MJ. ISBN: 9780128012833, *Elsevier, Academic Press, 2015*

Left ventricular involvement in arrhythmogenic right ventricular dysplasia/cardiomyopathy assessed by echocardiography predicts adverse clinical outcome.
Mast TP, Teske AJ, Vd Heijden JF, Groeneweg JA, Te Riele AS, Velthuis BK, Hauer RN, Doevendans PA, Cramer MJ.
J Am Soc Echocardiogr. 2015 Sep;28(9):1103-1113

Volumetric Response beyond Six Months of Cardiac Resynchronization Therapy and Clinical Outcome.
van 't Sant J, Fiolet AT, ter Horst IA, Cramer MJ, Mastenbroek MH, van Everdingen WM, **Mast TP**, Doevendans PA, Versteeg H, Meine M.
PLoS One. 2015 May 1;10(5)

Current and future role of echocardiography in arrhythmogenic right ventricular dysplasia/cardiomyopathy. **Mast TP**, Teske AJ, Doevendans PA, Cramer MJ.
Cardiol J. 2015;22(4):362-74

Measurements of electrical and mechanical dyssynchrony are both essential to improve prediction of CRT response.
Van't Sant J, Ter Horst IA, Wijers SC, **Mast TP**, Leenders GE, Doevendans PA, Cramer MJ, Meine M.
J Electrocardiol. 2015 Jul-Aug;48(4):601-8

A prospective validation of the HEART score for chest pain patients at the emergency department.
Backus BE, Six AJ, Kelder JC, Bosschaert MA, Mast EG, Mosterd A, Veldkamp RF, Wardeh AJ, Tio R, Braam R, Monnink SH, van Tooren R, **Mast TP**, van den Akker F, Cramer MJ, Poldervaart JM, Hoes AW, Doevendans PA.
Int J Cardiol. 2013 Oct 3;168(3):2153-8

Chest pain in the emergency room: a multicenter validation of the HEART Score.
Backus BE, Six AJ, Kelder JC, **Mast TP**, van den Akker F, Mast EG, Monnink SH, van Tooren RM, Doevendans PA.
***Crit Pathw Cardiol. 2010 Sep*;9(3):164-9.**

R1
R2
R3
R4
R5
R6
R7
R8
R9
R10
R11
R12
R13
R14
R15
R16
R17
R18
R19
R20
R21
R22
R23
R24
R25
R26
R27
R28
R29
R30
R31
R32
R33
R34
R35
R36
R37
R38
R39

R1
R2
R3
R4
R5
R6
R7
R8
R9
R10
R11
R12
R13
R14
R15
R16
R17
R18
R19
R20
R21
R22
R23
R24
R25
R26
R27
R28
R29
R30
R31
R32
R33
R34
R35
R36
R37
R38
R39

DANKWOORD / ACKNOWLEDGMENTS

Na drie jaar onderzoek maak ik de balans op en kom ik tot de conclusie dat de totstandkoming van dit proefschrift allerminst een individuele prestatie is geweest. Ik wil graag alle mensen die direct of indirect aan dit proefschrift hebben bijgedragen bedanken. Enkele personen wil ik in het bijzonder noemen:

Mijn promotor: **Prof. dr. P.A.F.M. Doevendans**, Pieter, ik ken niemand die met zo weinig woorden zoveel duidelijk kan maken (OK PD). Onze gesprekken heb ik altijd als kristalhelder en constructief ervaren. Ik ben je zeer dankbaar dat ik dit promotietraject onder jouw leiding heb mogen uitvoeren. Hoop dat we elkaar nog vaak treffen in de toekomst.

Mijn copromotoren:
Dr. M.J.M. Cramer en Dr. A.J. Teske, Maarten-Jan en Arco, we hebben een hoop meegemaakt deze drie jaar. Maarten-Jan heeft bij de start enkele maligniteit onder de duim gekregen wat een bewonderenswaardig gevecht was. Daarnaast heeft hij een echtscheidingsconvenant getekend wat best een kluif was, ik citeer: “ik ben langer aan het proberen te scheiden dan ik uiteindelijk getrouwd ben geweest”, ik zelf had hier en daar ook wat strubbelingen op het relationele vlak, en Arco, de enige stabiele factor van ons drieën heeft in plaats van één vrouw nu drie vrouwen thuis. De één wat kleiner dan de ander. Tussen deze gebeurtenissen door hebben we ook met zijn drieën ook nog dit boekje geschreven.
Maarten-Jan, zonder jouw enthousiasme en netwerkcapaciteiten had dit boekje de dikte gehad van het Donald-Duck weekblad. Met het energieniveau van een kerncentrale was jij de drijvende kracht achter dit proefschrift. In al die jaren ben ik je steeds meer gaan beschouwen als een vriend. Ik wens je alle goeds toe in grote gezondheid. Dank voor alles!
Arco, op de kop af 4 jaar geleden hebben wij elkaar ontmoet in Amersfoort, ik als semi-arts, jij als AOIS. Je hebt mij weggetrokken voor de poorten van de stamcellen waar ik je uiteraard zeer dankbaar voor ben. Door jouw onuitputtelijke koker van nieuwe ideeën en kennis is mijn promotietraject afgerond binnen de afgesproken tijd met een substantieel aantal hoofdstukken. Jouw koersvastheid is bewonderingswaardig, een stabiel en rustig baken die voor mij onmisbaar was tijdens deze periode. Hartelijk dank!

Dr. J.F. van der Heijden, Jeroen, ik wil graag bij deze benadrukken dat al mijn onderzoek en van al mijn voorgangers alleen maar kon bestaan door de goed geoliede (poli)klinische ARVC patiëntenzorg die jij onderhoudt. Ik ben je daar zeer dankbaar voor.

Dr. A.S. te Riele, Anneline, Annie, onze levens zijn al lang verstrengeld met elkaar; dezelfde dag jarig, ouders met dezelfde achtergrond, allebei een hockeyverleden, dezelfde

studentenvereniging, allebei geneeskunde, allebei cardiologie, allebei een PhD in het UMCU, allebei op ARVC. Alleen jij komt uit Brabant, ik niet. Al probeer ik dit met mijn huidige baan wel op te poetsen. Door jouw nogal bewonderingswaardig werkzaamheden tijdens je PhD in Baltimore kon ik daar ook een kwartaal aan de slag waarvoor ik je nogmaals wil bedanken. Ik weet zeker dat we qua research nog veel van je gaan horen. Ik ben blij dat ik er vanaf de start bij heb kunnen zijn. Ik denk dat gezien de toekomst we nooit meer echt van elkaar af komen en dat is eigenlijk ook maar gezellig ook.

Prof. dr. R.N. Hauer, Richard, hartelijk dank voor uw inzet tijdens mijn promotietraject. Met name tijdens mijn eerste jaar heeft u mij letterlijk wegwijs gemaakt in de wereld van de aritmogene cardiomyopathie. Die tijd heeft een solide basis gevormd voor alle projecten daarna. Ik kijk terug op een inspirerende samenwerking en ik hoop dat het Nederlandse ARVC onderzoek een waardige toekomst krijgt met de kwaliteit zoals u dat ooit geïnitieerd heeft.

Dr. J. Lumens, Joost, ik kan me goed herinneren dat je even bij mijn poster kwam kijken in Boston en dat we toen eigenlijk binnen 10 minuten een samenwerking hadden beklonken, de globale methodiek, en de mogelijke conclusies stonden al klaar. Onze samenwerking is de klap op de vuurpijl geworden van mijn promotie maar tevens voor de ARVC echoprogramma waar MJ en Arco al 10 jaar aan werken. Zonder jouw kennis op het gebied van de cardiomechanica was dit nooit en te nimmer gelukt. Ik hoop dat de samenwerking tussen Utrecht en de Maastrichtse groep (**Prof. Frits Prinzen, John Walmsley, Tammo Delhaas**) nog lang vruchtbaar blijft.

Special thanks to **Dr. Hugh Calkins, Cindy James, Dr. Ted Abraham, Crystal Tichnell, and Brittney Murray** at the Johns Hopkins Hospital in Baltimore. I felt very welcome during my stay and it was very inspiring to work with you. The tremendous amount of dedication from you all to the ARVD program ensures that your center will be the leading party in ARVD research for the upcoming years. Thank you for the opportunity to be a part of it!

Dr. T.A. van Veen, Toon, nooit gedacht dat ik samen met mijn Camel-rokende werkgroep begeleider nog samen zou publiceren. Dank voor al je input op het gebied van de fysiologie.

Dr. J.P. van Tintelen, Peter, dank voor je altijd hartelijke ontvangst in Amsterdam.

Prof. Dr. M.P. van den Berg, Maarten, dank voor het deelnemen in mijn beoordelingscommissie en de altijd fijne ontvangst in ‘t hoge Noorden.

Dr. B.K. Velthuis, Birgitta, dank voor je betrokkenheid bij mijn projecten vanuit de radiologie.

De leescommissie: **Prof dr. Marc Vos, Prof. dr. Folkert Asselbergs, Prof. Dr. Steven Chamuleau, Prof. Dr. Tim Leiner, en Prof Dr. Maarten van den Berg** wil ik bij deze bedanken voor het beoordelen van mijn proefschrift.

Mijn tweede huis tijdens deze jaren was uiteraard "**de Villa**". Een krappe warme ruimte met 10 man/vrouw achter een heet beeldscherm die SPSS proberen op te starten. Tel daarbij op dat er steevast twee mensen met een denkbeeldige monocle heel pedant en heel hardop een echo zitten te beoordelen. Een ietwat corpulente man met een technische achtergrond staat gelijktijdig zijn golfswing te oefenen. Een lange man met een flinke aortadiameter ratelt wat: "hier wordt pappa niet vrolijk van." Vaak waren het wel de enige lichtpuntjes van de dag. Een paar mensen moet ik daarvan even in het bijzonder noemen:

Remco Grobben, Corrie, Korrieaantje. Onze gelijkgestemdheid is bijzonder te noemen. Ik ken weinig mensen die flauwekul vertellen net zo belangrijk vindt als ik zelf. Lekker klagen op van alles en nog wat hebben wij tot de corebusiness van de Villa gemaakt. Jij kon ook als enige de PhD titel echt goed op zijn waarden schatten ("het tien-vinger criterium"). Het was een mooie tijd met een grande finale op de Bahama's. Eigenlijk moeten we bij deze ook de kostenplaats B911 bedanken voor de oneindige steun die tot dat festijn heeft geleid.

René van Es, Ronnie, Vanessa. De TG'er, je was altijd ijzersterk in de Villa. Onze vele uren MatLab zal ik nooit meer vergeten, ik op het krukje, jij achter de knoppen. Jij bent de ruggengraat van de villa en het ziet er naar uit dat je de komende jaren daar nog wel de baas kan spelen. Maar let op: kan wel is "heel taai" worden. Dank vriend!

Einar, zelden zo'n fijne Noor ontmoet. Je aanwezigheid in de Villa gaf het laatste jaar van mijn promotie een glanzend einde. Niet in de laatste plaats door je Einarretjes: je was er vol van overtuigd dat "Arcometeenc" Arco's volledige voornaam was, je hebt ooit uren patiëntendatabase uit de Hix-Zandbak gegenereerd, en **Ronald Groenemeijer** meermaals om de Paint Plug-in gevraagd, echt prachtig. We zullen elkaar zeker nog vaak zien. Succes in de kliniek, maar met name natuurlijk met de zoektocht naar de ware Dørinde.

Dirk van Osch, Durka-Durka, De Kaasschaaf, je hebt vele bijnamen met een oorsprong die het daglicht niet kunnen verdragen. Gigantisch snel gepromoveerd, maar een onuitwisbare indruk achter gelaten. Dan te bedenken dat bij elke hartslag het endotheel uit zijn vaatwand klappert is het een wonder te noemen dat de man nog leeft.

Bas van Klarenbosch, met trots kan ik zeggen dat de eerste zoon van Arco reeds geboren is. Weinigen krijgen zulke glunderende oogjes als er in Xcelera een sneeuwstorm wordt

geopend. Veel succes met je nieuwe huis, de marathon en natuurlijk je promotietraject. Met je begeleiding zit het in ieder geval, thuis heb je Kelly, hier heb je Arco. Ik spreek uit ervaring, er kan niks mis gaan.

Cheyenne, laten we eerlijk zijn, je hebt gewoon een moeilijke voornaam. Uiteindelijk is je naam door mijn toedoen verbasterd naar de klanken van een zachtjes opengaande slecht geoliede deur. We hebben goede 3 jaren gehad waarvoor zeer dank!

Mira-Mira, de vrouw die de stamcel echt groot gaat maken, maar dan wel waarschijnlijk in Duitsland. Ciao-Ciao!

Thijs, de man met een zwervend bestaan tussen CART-TECH, de Villa, en de waterkraan. Veel succes met je verdere promotie!

Buiten de Villa waren er ook pareltjes
Cas Teunissen, Casius, we zijn tegelijkertijd begonnen en bijna tegelijkertijd geëindigd, alleen jij bent ondertussen ook volleerd EFO-loog wat zeer knap is. Zonder jou waren het zeker minder mooie jaren geweest, niet in de laatste plaats door onze Thombocor bijeenkomsten. We zullen elkaar hopelijk nog veel blijven zien.

Wouter van Everdingen, de Tor, de mede-Speckle-Tracker van de groep. Je beheerst de techniek zo goed dat je er acuut sportarts door geworden bent. Dat zegt veel denk ik. Memorabel zijn je klaagzangen over van alles en nog wat, **De Commentator** is veruit je beste bijnaam. Veel succes met de sportgeneeskunde, ik heb al kunnen genieten van je kwaliteiten, binnen een week heb je mij genezen van een achillespeesblessure. Dank en ik zie je op Strava!

Peter-Paul, Peppie, ondanks dat je natuurlijk een likker 1e klas bent mag ik je erg graag. Maar dat jij nog een tong hebt is wel een wonder te noemen. Veel succes met de opleiding en hopelijk tot snel!
En dank ook bij deze aan de overige (oud-)collega's: **Ing-Han (奇特), Sanne, Gijs, Vivan, Frebus, Jetske, Roos, Judith, Marloes, Freek, Bart, Laurens, Arian, Lena, Martine, Rik,** en natuurlijk niet te vergeten **Fatih Güçlü**.

Heel wat studenten hebben mij geholpen de afgelopen jaren waarvoor hartelijk dank: **Karim Taha, Menco Niemeijer, Sarah Verhemel, Babs van Gageldonck en Feddo Kirkels.**

Ook de dames van het EFO-secretariaat bedankt, met name: **Cornelie, Linda, Joyce en Veronique.**

En uiteraard de dames van de hartfunctie, alwaar ik eigenlijk al 10 jaar onder werk: **Corien, Angelique, Karin, Museyen, Liesbeth, Jeanette, Sergio, Ineke, Milou, Annemarie, en alle Elly's (ik zal zeker onbedoeld enkele namen zijn vergeten….)**.

Dank ook voor de **vrienden** die hun aandacht mij significant zagen slinken de afgelopen drie jaar:

Jaarclub: **Beuf, Jean, Biba, Binnie, Jonkie, Crow, Dommel, Rein en Lord Forrest.**
Studievrienden: **Matthys, Matthijs, Mark, Wouter, Teun en Guus.**
Dit boekje is de reden waardoor ik vaak moest afzeggen. Het moeten dus nu wel betere tijden worden.

Mijn **familie**:

Mijn moeder, **Hannah**, dank voor je nimmer aflatende steun en interesse in mijn werk de afgelopen jaren.
Voor mijn vader, **Gijs**, geldt hetzelfde, daarbij speciale dank ook voor je goede adviezen die het bij mij nooit hebben gehaald. Ik quote vrijelijk: "Ik zou als ik jou was nooit medicijnen gaan studeren" of "Ik raad je aan om in ieder geval nooit cardioloog te worden" of "Ik zou zelf nooit gaan promoveren, die S is van slim, die zou ik er nooit zomaar af laten halen" en "Echo is een geloof, ik dacht dat je atheïst was."

Mijn paranimfen en broers **Bastiaan en Joost**, **Kastanje en Jopie**, maar ook behorend tot mijn beste vrienden. Ik hoop nadat deze poppenkast voorbij is we weer snel op Duitsland weekend kunnen gaan.

Richt ik mij als laatste nog tot twee zeer belangrijke personen:

Pieter, Pierre, je werd geboren toen ik een tijdje in Amerika zat, dat is jammer, het scheen dat je toen al een sterke indruk maakte. Wel wat klein, maar daar zullen we aan moeten wennen in de familie. We delen dezelfde passie voor bananen en de ukelele. Het kan niet anders dan dat je puik kereltje wordt.

En als laatste, **Iris Alice Hermien ter Horst**. Zoals MJ veelvuldig heeft geschreeuwd: "Mast, dit is de leukste en meest inspirerende tijd van je leven!". Nu was 3 jaar lang Science snuiven op een congres, 3 jaar lang dagelijks zeer inspirerende meetings bijwonen en 3 jaar lang SPSS tabellen tot de nok vullen met data en net zo lang kneden tot de p-waarden onder de 0,05 duikelen natuurlijk heel erg leuk, maar het leukste aspect van het werk was uiteraard Iris. Ik

R1
R2
R3
R4
R5
R6
R7
R8
R9
R10
R11
R12
R13
R14
R15
R16
R17
R18
R19
R20
R21
R22
R23
R24
R25
R26
R27
R28
R29
R30
R31
R32
R33
R34
R35
R36
R37
R38
R39

neem aan dat Maarten-Jan dit dan ook bedoelde. Ik ben erg blij dat jij mijn kamergenoot bent geworden en het is mijn bedoeling dat je dit ook blijft. Nog nooit heb ik mij zo op mijn gemak gevoeld bij iemand en ik hoop dat we nog heel lang, heel gelukkig samen blijven.

Thomas Mast
28 november 2016